MODELLING AND OPTIMISATION OF INTENSIFIED EXTRACTION IN SMALL CHANNELS FOR SPENT NUCLEAR FUEL REPROCESSING

Davide Bascone

A dissertation submitted in partial fulfilment
for the award of the degree of

DOCTOR OF PHILOSOPHY

Chemical Engineering

Faculty of Engineering Sciences

University College London

October 2018

Declaration of Authorship

I, Davide Bascone, confirm that the work presented in this thesis is my own. Where information has been derived from other sources, I confirm that this has been indicated in the thesis.

_____

Davide Bascone

Abstract

Nuclear energy is considered an option for future power supply. Spent Nuclear Fuel (SNF) reprocessing is essential to reduce the volume of nuclear wastes and to recover reusable materials, such as uranium and plutonium. Nowadays, all the commercial plants rely on the Plutonium Uranium Reduction Extraction (PUREX) process, an over 60-year old process. In the present work, a mathematical model for liquid-liquid extraction in small channels has been developed. The model is suitable for SNF reprocessing. Calculations of thermodynamics, hydrodynamics, pressure drop and nuclear criticality are included in the model. Several components and redox reactions, between the various oxidation states of U, Pu and Np, have been considered. Also, to increase the throughput and provide a good flow distribution within the channels, the design of a comb-like manifold has been included into the calculations. The resulting model, posed as optimisation problem, is a mixed-integer differential optimisation problem. The goal is to develop a methodology that allows to explore alternative flowsheets for the nuclear fuel cycle, using the small-scale extractor.

Different case studies have been investigated. Firstly, the "codecontamination" section of the PUREX process has been investigated to demonstrate the applicability of the model. Secondly, a novel codecontamination section has been investigated to compare the small-scale extractor and the two main conventional technologies, *i.e.* pulsed column and mixer-settler. Finally, an alternative flowsheet has been proposed, using the small-scale extractors. This process has been obtained using a superstructure optimisation approach. The flowsheet produces a mixed uranium/plutonium oxide, to preclude the risk of nuclear proliferation.

The mathematical model, despite its size and complexity, has been successfully solved in a short computational time. Results have shown that intensified extraction in small channel can provide to several benefits over the conventional

technologies, in particular in terms of solvent degradation and mass transfer.

Impact statement

The development of new nuclear fuel cycles is fundamental for future electricity production from nuclear source, as the environmental impact of the nuclear wastes can be reduced and reusable materials, such as uranium and plutonium, can be recovered. Today, all spent nuclear fuel reprocessing plants use the PUREX process and conventional solvent extraction technologies, which have several drawbacks.

In this thesis, a mathematical model for liquid-liquid extraction in small extractors is developed. It allows to investigate alternative flowsheets for spent nuclear fuel reprocessing, using the novel technology. A superstructure is proposed to identify an alternative process for future spent nuclear fuel reprocessing. Although the model is suitable for nuclear application, model and methodology can be applied to other applications, such as petrochemical industry, hydrometallurgy and pharmaceutical industry. The use of the small-scale technology would be beneficial in the nuclear industry, in particular to reduce the equipment footprint and to improve safety considerations. The model developed in this work can be the starting point for more detailed and customised tools, useful for the early stage design and to investigate different scenarios. It can be validated from experimental data and some correlations can be modified to increase reliability and robustness of the model.

From an academic point of view, the methodology developed in this work can be exploited to investigate new applications of the small-scale contactor. Novel solvents and components can be investigated. New thermodynamic and hydrodynamic equations can be integrated and novel models can be proposed. Several types of manifolds and phase separators can be investigated, so that their impact on the process may be analysed and their practicability evaluated. The model could be coupled with a more detailed and computational expensive model, such as a computational fluid dynamics model, to gain a better understanding of the

physical phenomena that occurs during the process (flow distribution, mixing, extraction, separation of the two phases), allowing the achievement of more reliable correlations. Finally, with the increasing computing power, complex superstructure flowsheets may be investigated to identify the optimal process design for the required targets. The combination of different technologies can be investigated, as well as multi-objective optimisation problems.

Acknowledgements

Last but not least, I want to thank my partner Mary for her unconditional support and encouragement, my little children Gabriele and Viola for recharging my batteries everyday with their love and finally my parents for their continued support.

Contents

Publications   146

References   147

Appendix: GAMS code used in Section 6.3   165

List of Figures

List of Tables

List of symbols

Nomenclature

Symbols	Description	Units
a	Interfacial area	$\text{m}^2\ \text{m}^{-3}$
A	Cross sectional area	m^2
	pulse amplitude	m
$ACapEx$	Annualised capital cost	£ y^{-1}
$B(d)$	Rate of birth of drops of diameter d	$\text{m}^{-1}\text{s}^{-1}$
B^2	Buckling	m^{-2}
Bo	Bond number $(\frac{D^2\Delta\rho}{\gamma})$	
C	Concentration	Mol m^{-3}
C_a	Cost of agitator	£
C_{pl}	Cost of platform and ladders	£
C_t	Cost of trays	£
C_v^h	Cost of horizontal vessel	£
C_v^v	Cost of vertical vessel	£
Ca	Capillarity number $(\frac{v\mu}{\gamma})$	
$CapEx$	Capital cost	£

D	Diameter	m
	Distribution coefficient	
$D(d)$	Rate of death of drops of diameter d	$\text{m}^{-1}\text{s}^{-1}$
d_{32}	Sauter mean diameter	m
$\mathscr{D}$	Diffusion coefficient	$\text{m}^2\,\text{s}^{-1}$
E	Extraction	
	Axial dispersion coefficient	$\text{m}^2\,\text{s}^{-1}$
f	pulse frequency	Hz
F	TBP fraction in organic phase	
F_d	flow maldistribution	
g	Gravitational acceleration (9.81)	$\text{m}\,\text{s}^{-2}$
ΔH	Plate spacing	m
L	Length	m
k	multiplication factor	
k_L	Mass transfer coefficient	$\text{m}\,\text{s}^{-1}$
K	Pseudo-equilibrium constant	(units depend on the reaction)
K_r	Resistant coefficient	
m	Distribution coefficient	
M^2	Migration area	m^2
MW	Molecular weight	$\text{g}\,\text{Mol}^{-1}$
N	Number of stages (unless otherwise specified)	

N_p	Power number	
	Number of perforated plates	
N_{oc}	Number of transfer units	
N_{rev}	Impeller speed	rpm
Pe	Peclet number $\left(\frac{vL}{\mathscr{D}}\right)$	
$OpEx$	Operating cost	£ y^{-1}
P	Power	W
$P(d)$	Volume fraction of drops of diameter d	m^{-1}s^{-1}
ΔP	Pressure drop	kPa
q	Aqueous to organic flow ratio	
r	hydraulic resistance ratio	
R	Reaction rate	Mol m^{-3} s^{-1}
	dispersed to continuous flow ratio	
Re	Reynolds number $\left(\frac{\rho vD}{\mu}\right)$	
Sc	Schmidt number $\left(\frac{\mu}{\rho\mathscr{D}}\right)$	
Sh	Sherwood number $\left(\frac{Kd_{32}}{\mathscr{D}}\right)$	
t	Time	s
T	Temperature	K
TAC	Total annualised cost	£ y^{-1}
v	Superficial velocity	m s^{-1}
V	Volume	m^3
$\dot{V}$	Volume flowrate	m^3 s^{-1}

W	Width	m
We	Weber number $\left(\frac{(N_{rev}/60)^2 D_i^3 \rho_c}{\gamma}\right)$	
x	Molar fraction in aq. phase	
y	Molar fraction in org. phase	

Greek Symbols

α	aqueous phase fraction	
γ	Interfacial tension	N m^{-1}
δ	Liquid film thickness	m
ϵ	plate free area fraction	
ϵ_g	gas phase volume fraction	
θ	Contact angle	$^\circ$
Θ	Correction factor for a	
λ	Lagrange multiplier	
λ_{NC}	Non-circularity coefficient	
μ	Viscosity	Pa s
ν	Stoichiometric coefficient	
ρ	Mass density	kg m^{-3}
τ	Residence time	s
	Temperature-dependent function	
φ	Phase holdup (volume fraction)	

Subscripts/Superscripts

aq	Aqueous phase	

back	Back extraction (stripping, scrubbing)
c	Continuous phase
ch	Channel
d	Dispersed phase
	Drop
eff	Effective
eq	Equilibrium
extr	Extraction
fr	Frictional
free	Free movement of drops
h	Hole
H	Hydraulic
i	Generic index
	Impeller
in	Inlet
int	Interfacial
j	Generic index
jet	Jetting movement of drops
k	Generic index
loc	Local
mix	Mixture
	Mixer

o	Overall
org	Organic phase
out	Outlet
set	Settler
t	Terminal
tot	Total
UC	Unit Cell
∞	Infinite

Acronysms

AHA	Acetohydroxamic Acid
BB	Branch and Bound
CFD	Computational Fluid Dynamics
COEX	Combined Extraction
CSEX	Cs EXtraction
DF	Decontamination Factor
DIAMEX	Diamide EXtraction
HAN	Hydroxylamine nitrate
HLW	High Level Waste
IL	Ionic Liquids
LP	Linear Programming
LWR	Light Water Reactor
MA	Minor Actinide

MILP	Mixed Integer Linear Programming
MINLP	Mixed Integer Nonlinear Programming
MOX	Mixed Oxide
MTHM	Metric Tons of Heavy Metals
NLP	Nonlinear Programming
NPEX	Neptunium Plutonium Extraction
PHWR	Pressurised Heavy Water Reactor
PUREX	Plutonium Uranium Reduction Extraction
QP	Quadratic Programming
REDOX	Reduction Oxidation
SANEX	Selective Actinide Extraction
SESAME	Selective Extraction and Separation of Americium by Means of Electrolysis
SQP	Sequential Quadratic Programming
SREX	Sr Extraction
TBP	Tributhyl Phosphate
THORP	Thermal Oxide Reprocessing Plant
TRUEX	Transuranic Element Extraction
UREX	Uranium Extraction

Chapter 1

Introduction & Background

1.1 Introduction

The nuclear energy is one the most reliable options for future electricity generation, while the use of fossil fuel should be restricted to limit CO_2 emissions. However, hazardous material is generated and requires proper treatment and disposal. The Spent Nuclear Fuel (SNF) composition depends on the type of fuel, enrichment and reactor. As shown in Figure 1.1.1, the irradiated fuel consists of, approximately, 96% uranium and 1% plutonium [1]. These are reusable materials, as they may be used as Mixed Oxide (MOX) fuel in suitable nuclear reactor.

The reprocessing of SNF would also allow to achieve:

- a reduction of the volume of High Level Wastes (HLW);

- a further $\approx 25\%$ of energy from the original uranium;

- reduction of the long-term radiotoxicity of HLW [2].

For SNF reprocessing, today all the commercial plants rely on the PUREX (Plutonium Uranium Extraction) process, a method to recover uranium and plutonium by liquid-liquid extraction operations [3, 4, 5]. It is generally based on two liquid-liquid extraction cycles: the first one includes codecontamination and U/Pu partitioning sections, whilst the second one includes U and Pu purifications cycles. A sketch of the PUREX process is shown in Figure 1.1.2. There can be a third cycle for further purification sections. However, the process is very old and
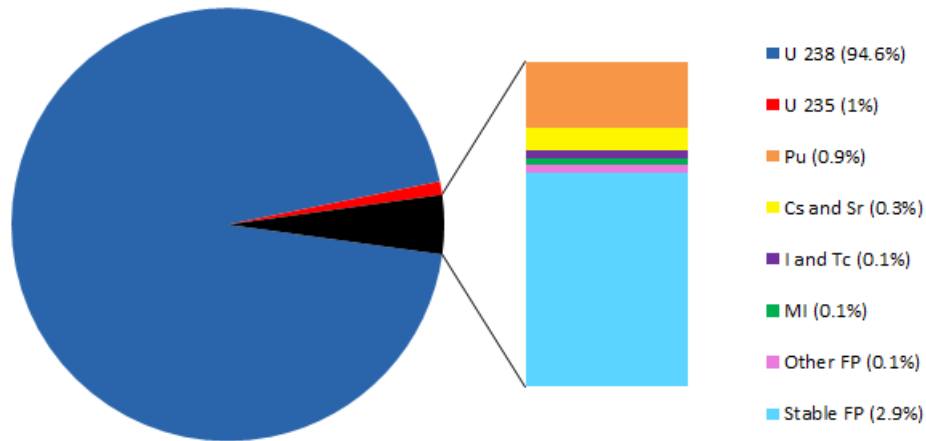
Figure 1.1.1: Typical spent nuclear fuel composition.

has several disadvantages. With the PUREX process, a nuclear proliferation risk exists: pure Pu is produced, which is suitable for military purpose. The conventional liquid-liquid extraction technologies cause solvent degradation, require large volume and may have nuclear criticality issues.
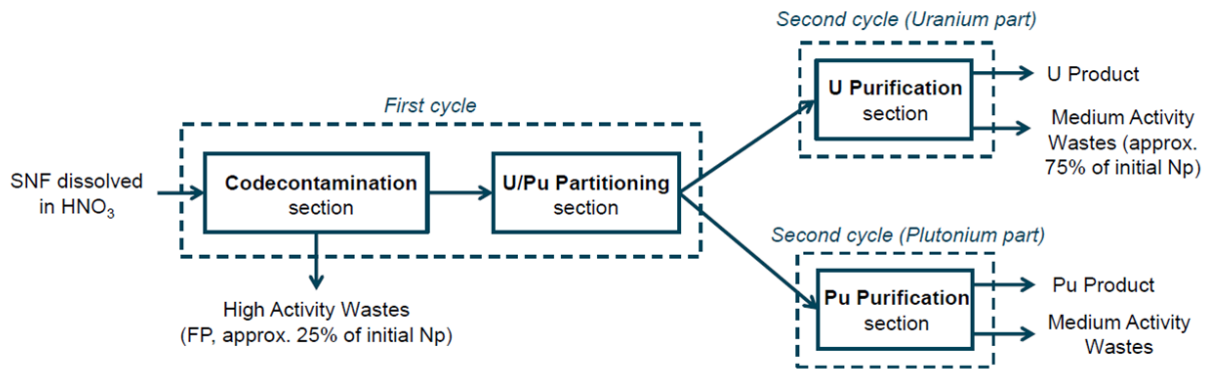
Figure 1.1.2: Sketch of the PUREX process, with focus on feed and main products. For the sake of simplicity, only the four main sections are shown. Codecontamination and U/Pu partitioning sections involve, in the modern PUREX process, twelve liquid-liquid extraction operations in total [6]. The second cycles, i.e. U and Pu purification cycles, involve two liquid-liquid extraction operations for each cycle [6].

A potential alternative to the conventional solvent extraction technologies is the intensified extraction in small channels. In the last decades the concept of process intensification has attracted the attention of the researchers. The idea is to decrease size and cost, without reducing the performance. This can be the case of liquid-liquid extraction in small-scale contactors, where the mass transfer is, in fact, enhanced. Other benefits may be the easy control of hydrodynamics and the volume reduction, which may be particularly advantageous in the nuclear industry considering the hazardous materials involved and the risk of nuclear criticality.

In this work, a mathematical model for a multi-component liquid-liquid extraction in small channels, suitable for SNF reprocessing, has been developed. Redox reactions, pressure drops and manifold design are included in the calculations. The resulting model, formulated as an optimisation problem, is a mixed integer differential optimisation problem, converted to an mixed integer nonlinear problem through discretisation. The size of the model is potentially large, as this depends on the granularity of the discretisation used. The model allows to explore alternative flowsheets for future SNF reprocessing using small channels.

Case studies have been investigated to demonstrate the applicability of the model and to allow comparison with the main conventional technologies. Finally, a superstructure flowsheet has been investigated, using the novel technology. The optimal process has been identified, according to economic criteria and precluding the nuclear proliferation risk.

1.2   Objectives

The goal of this PhD programme is to develop a methodology for the design and optimisation of alternative flowsheets for SNF reprocessing, using the novel small-scale technology. A mathematical model to design liquid-liquid extraction in small-scale contactors will be developed and alternative flowsheets for SNF reprocessing will be investigated, according to criteria such as economics and nuclear proliferation.

This work is part of the PACIFIC project (Providing A nuclear fuel Cycle In the UK For Implementing Carbon reduction), a multi-disciplinary programme which aims to support future nuclear fuel cycles in the United Kingdom, funded by the EPSRC.

1.3 Spent Nuclear Fuel Reprocessing

Currently, the PUREX process is used mainly for reprocessing of Light Water Reactor (LWR) irradiated fuel, as shown in Table 1.3.1.

The modern PUREX process, used in the La Hague and Rokkosho plants, is described by Herbst [6] and illustrated in Figure 1.3.1 and 1.3.2. These plants slightly differ from the others, since they include Tc scrub and complementary extraction. The tri-n-butyl-phosphate (TBP) is used as solvent, diluted to 20-30% (v/v) with paraffinic diluent, because of its high density and viscosity. The PUREX process has been used since the 50s. Compared to the Reduction Oxidation (REDOX) process, the previous process for SNF reprocessing, PUREX leads to less HLW since HNO_3, which is used as salting and scrubbing agent, is evaporated [1]. Furthermore, TBP is less volatile and flammable than hexone, used in the REDOX process, and more chemically stable. TBP selectivity depends on the oxidation state of the actinide: it is high for the +6 (*e.g.* U as UO_2^{2+}) and +4 (Pu as Pu^{4+}), lower for 5+ (Np as NpO^{2+}) and practically zero for +3 and lower states [6].

Table 1.3.1: Commercial reprocessing plants in the world [7].

	Plant	Capacity [t/yr]
LWR Fuel:	France, La Hague (UP-2/-UP-3)	1,7000
	UK, Sellafield (THORP)	600
	Russia, Ozersk (Mayak)	400
	Japan, Rokkasho	800
	Total LWR approx.	3500
Other nuclear fuels:	UK, Sellafield (Magnox)	1500
	India, 4 plants (PHWR fuel)	330
	Japan, Tokai (MOX fuel)	40
	Total other approx.	1870
Total civil capacity		5370

The chemical equilibria for U and Pu, originally present in the nitrate media as respectively UO_2^{2+} and Pu^{4+}, are:

$$UO_2^{2+} + 2NO_3^- + 2TBP \rightleftharpoons [UO_2(NO_3)_2] \cdot 2TBP \qquad (1.3.1)$$

$$Pu^{4+} + 4NO_3^- + 2TBP \rightleftharpoons [Pu(NO_3)_4] \cdot 2TBP \qquad (1.3.2)$$
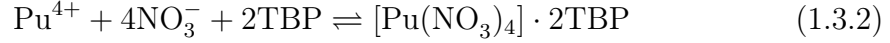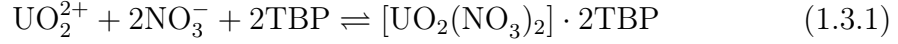
The distribution coefficient, which is the ratio between organic and aqueous concentration of the component at equilibrium, is significantly affected by the oxidation state of the component. For instance, Pu(IV) and Np(VI) are easily extractable (i.e. high distribution coefficient), contrarily to Pu(III) and Np(V), due to the TBP selectivity mentioned above. Distribution coefficients are also affected by the nitric acid concentration, for example an excess of NO_3^- shifts the equilibrium to the right in Eqs. 1.3.1 and 1.3.2. This phenomenon is known as the salting out effect [6]. The extraction of most of the components in the SNF is favoured by high HNO_3 concentrations, except for ruthenium. For this reason, the nitric acid concentration must be in a medium range to achieve a proper separation [8]. Other variables that have an important impact on distribution coefficients are TBP concentration and temperature, typically increased to back extract U and Pu.

Several developments of the PUREX process have been suggested, mostly to prevent nuclear proliferation and to reduce the radioactivity of nuclear wastes. Further objectives are the recovery of Np and other minor actinides and the minimisation of solvent degradation. Examples of advanced flowsheets are COEX (Combined Extraction), UREX (Uranium Extraction) and NPEX (Neptunium Plutonium Extraction) [6, 5, 9, 10].

The conventional liquid-liquid extraction technologies typically employed in the PUREX process are mixer-settler, pulsed column and centrifugal extractor. A brief description of these equipment is presented below.
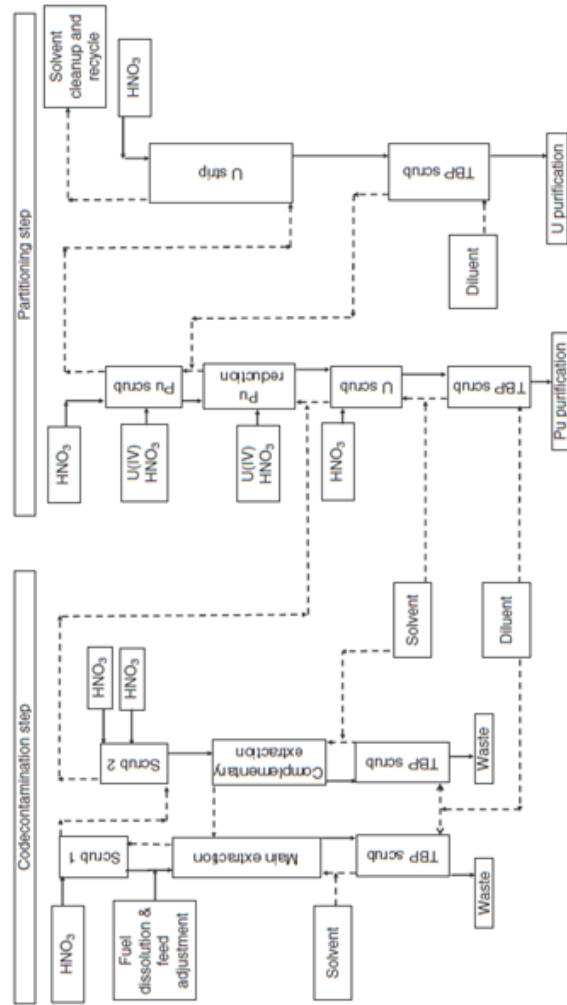
Figure 1.3.1: *Process flow diagram of the first extraction cycle of the modern PUREX process [6].*
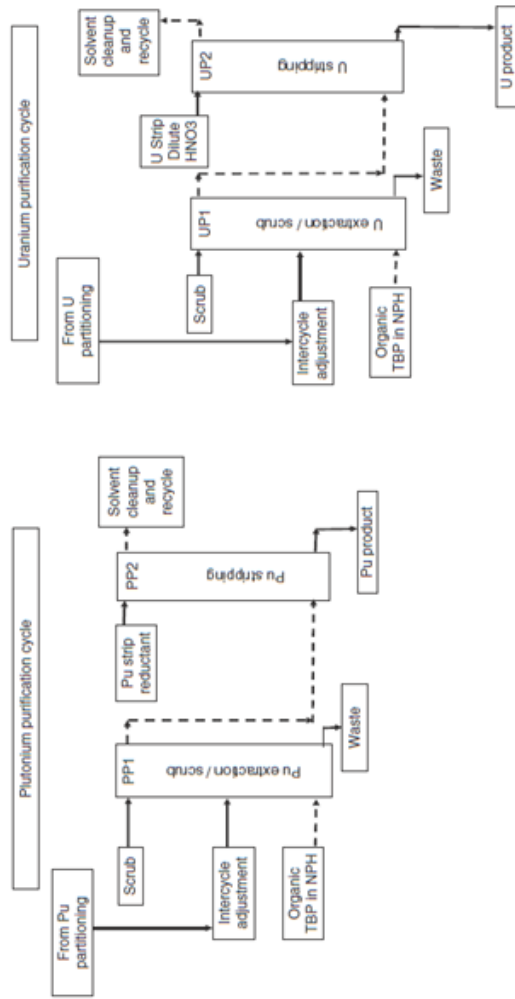
Figure 1.3.2: Process flow diagram of the second extraction cycles of the modern PUREX process [6].

1.3.1 Mixer-settler

The mixer-settler consists of two compartments: a small mixing chamber, where the two phases are mixed by an impeller, and a larger gravity settling chamber, where the two phases are separated by weirs. In counter-current processes, mixers and settlers are placed at alternating ends for each stage. A sketch of a mixer-settler bank is depicted in Figure 1.3.3.

Since the equilibrium concentration is typically reached, the mixer-settler is considered a stage wise contactor. It is widely employed in nuclear industry, mainly because of their simplicity. They do not require a flushing to be restarted after minor shutdowns and the long residence time facilitates operators in reacting in case of malfunctions [11]. However, since in these contactors the criticality safe is not achieved by geometry, they can be employed only in presence of diluted solution in fissile species. For this reason, mixer-settlers are employed in [3, 12]:

- UP-2 plant, La Hague (France), for U stripping in first extraction cycle, U purification cycles and solvent washing;

- UP-3 plant, La Hague (France), for U stripping in first extraction cycle, U/Pu partitioning, U purification cycles and solvent washing;

- THORP, Sellafield (UK), for U purification and solvent washing;

- Rokkasho plant (Japan), for both U and Pu purification cycles and solvent washing.

Further disadvantages of this device are represented by their volume and the long residence time, which causes solvent degradation.
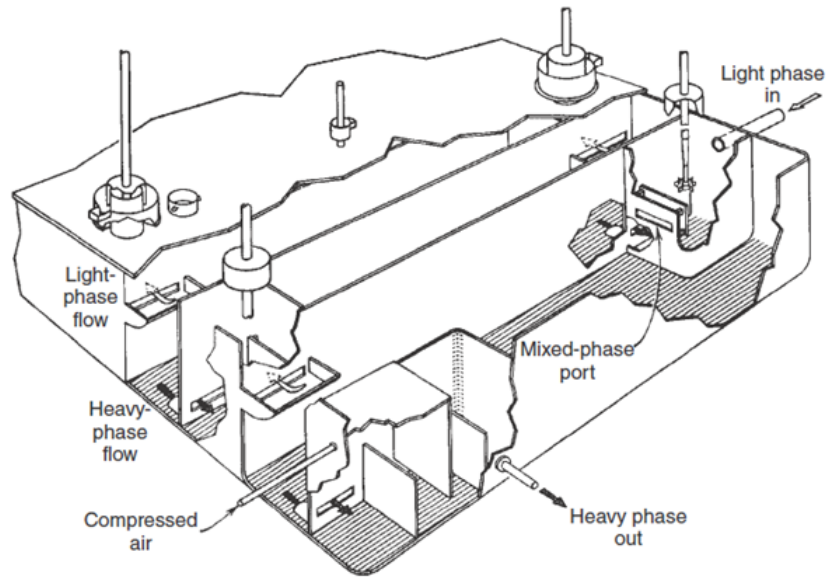
Figure 1.3.3: Schematic of a mixer-settler bank [11].

1.3.2 Pulsed column

Despite different types of extraction columns existing, only plate pulsed columns are used in the nuclear industry. They are differential contactors, as they do not have discrete stages and the concentration profile along the height is continuous.

A schematic of the pulsed column configuration is shown Figure 1.3.4. The two liquids are fed to the column counter-currently (aqueous solution at the top and organic solvent at the bottom). Through a series of plates, droplets formation and dispersion occur. These plates can be either perforated (THORP) or annular (La Hague plants), also called "disk and doughnut" plates. Plates are typically 2 inches spaced [13], and one theoretical stage is achieved in approximately 1 m. The pulsator, generally by injecting compressed air in a pulse leg, provides mechanical energy to the system, in order to reduce the droplet size and enhance the mass transfer.

Since the solids are directed with the dispersed phase, the extraction of U and Pu from the feed containing the dissolved irradiated fuel is accomplished dispersing the aqueous phase, in order to protect the organic solvent from any contamination, which is entrained by the dispersed phase [11]. Although their geometry leads

to criticality safety, special spiral spacers and tubes made of neutron absorbing material are employed.

Design of pulsed columns is carried out using standard algorithms. Scale up is difficult, since height is affected by liquid flow rate and column diameter [11].

Pulsed columns are generally 10-15 m high, therefore requiring a considerable amount of head space, but they do not require large floor space [11]. They imply a moderate solvent inventory. The residence time is long, with consequent solvent degradation, and the operation performance is not high if excessive phase ratios are used. They are employed when high fissile materials concentrations are involved, thus they are preferred in the codecontamination section. They are currently employed in [3]:

- UP-2 plant, La Hague (France), for codecontamination and U/Pu partitioning;

- UP-3 plant, La Hague (France), for codecontamination and Pu purification cycles;

- THORP, Sellafield (UK), for codecontamination and Pu purification cycles;

- Rokkasho plant (Japan), for codecontamination and Pu purification cycles.

More details on pulsed columns are provided by Arm [11] and Stevens [14].

From compressed air reservoir

Rotary pulse valve

Pneumacators for density measurement

To ventilation system

Top settler

Solvent outlet

Neutron absorbing tubes

Aqueous inlet

Feed distributor

Tie rod

Surface temperature probe guide tube

Neutron absorbing spiral spacer (located between each plate)

Perforated plate

Trend neutron monitor

Pneumacators for level and density measurement

Pulse limb

Bottom settler

Solvent inlet

Solvent/aqueous interface

Aqueous outlet

Figure 1.3.4: Schematic of a pulsed column [11].

1.3.3 Centrifugal extractor

A sketch of a centrifugal contactor is shown in Figure 1.3.5. Similarly to mixer-settlers, these extractors are stage-wise contactors and consist of two different compartments, for mixing and separation. They are also connected for counter-current processes in similar way. The main difference between these two devices is the phase separation, In centrifugal contactors a rotating rotor is employed (thousands of revolution per minute), leading to fast separation, efficient mixing and high single stage efficiency (higher than 95% [3]).

In order to minimise the wrong phase entrainment in the products, an optimum

between rotor speed must be found. Increasing the rotor speed leads to better separation but, as the droplet size decreases as rotor speed increase, very high velocities cause massive entrainment.
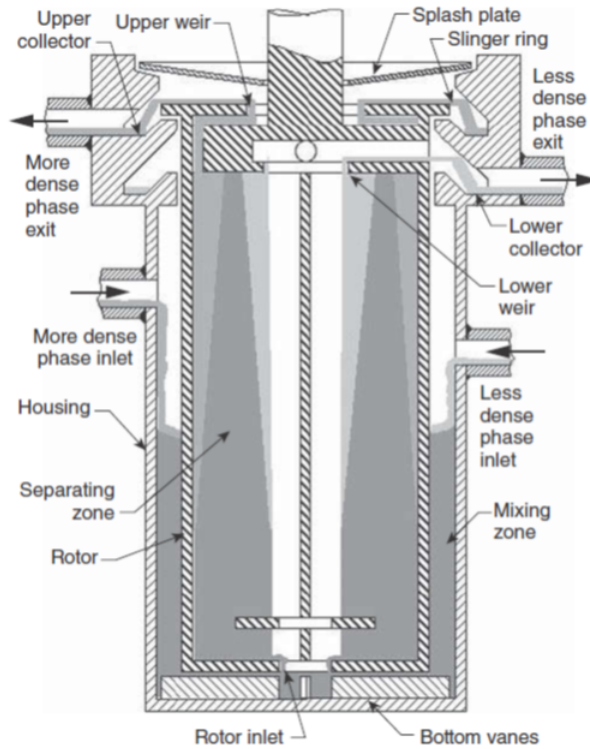
Figure 1.3.5: Schematic of an annular centrifugal contactor [11].

The most important advantages provided by this technology are the short liquid residence time and the small liquid hold-up, minimising the solvent degradation. However, a periodic maintenance for removal of the rotor and the motor is required.

Centrifugal contactors are ideal for the separation of solutions containing high concentration of fission products, since they are safe by the low liquid holdup [11]. However, their use has been limited. They were used in the decontamination process at the Savanna River F Canyon (US, shutdown in 2002) [15]. Since then, they are currently used only on laboratory scale and at the UP-2 plant in La Hague for the Pu purification cycle.

1.4   Intensified extraction

The concept of process intensification has been known in chemical engineering since the 80s. It was defined as "devising exceedingly compact plant which reduces both the main plant item and the installations costs" by Ramshaw [16]. The aim of the process intensification is to decrease the plant size and costs, but maintaining high performance and production capacity. Applications of microchannels are biochemical analysis, micro-power generation and micro-reactors [17].

The liquid-liquid extraction can significantly benefit from process intensification, especially for the nuclear industry, since:

- the mass transfer can be significantly improved;

- hydrodynamics can be easily controlled, to ensure high interfacial surface area and acceptable pressure drop;

- the volume of hazardous material can be reduced;

- lower cost can be achieved, in terms of both capital and operating costs;

- easier control of nuclear criticality is achieved, due to the high surface area to volume ratio (the neutrons have a greater possibility to escape) and the low liquid holdup involved;

- short residence time and therefore low solvent degradation, due to hydrolysis and radiolysis reactions, are achieved.

On the other hand, one of the most debatable points of the small-scale technologies is the scale out, since an impractical or unfavourable number of parallel devices may be required.

Intensified extraction in small or micro channels have been widely investigated in the last years [18, 19, 20, 21, 22]. In small channels different flow patterns can occur, depending on operating conditions, physical properties of fluids and channel (wettability), geometry of mixing junction and channel. Examples of flow patterns are drop flow, dispersed flow, quasi annular flow, segmented flow [22]. The latter flow pattern, which consists of dispersed plugs and continuous slugs, seems to improve mass transfer and it is considered the most attractive flow pattern [18, 23, 21, 24, 19, 20].

1.5 Nuclear Criticality Safety

Nuclear criticality has to be evaluated to design suitable equipment for nuclear applications. This analysis can be performed by estimating the effective multiplication factor k_{eff}, which is the ratio between the number of neutrons produced by fission in one neutron generation and the number of neutrons lost in the previous neutron generation (due to absorption and leakage):

$$k_{eff} = \frac{production\ rate}{absorption\ +\ leakage\ rate} \tag{1.5.1}$$

Hence, if $k_{eff}=1$ the system is critical, if $k_{eff} > 1$ it is supercritical and if $k_{eff} < 1$ it is subcritical. The effective multiplication factor should be rigorously calculated by codes that solve the time-dependent transport equation of the neutron flux. Examples of codes for nuclear criticality calculations are the KENO-Va code, a three dimensional multigroup Monte Carlo program developed by the Oak Ridge National Laboratory, and the MACPEX code, a one-dimensional model developed by Gonda *et al.* [25]. However, the latter can be used to predict the k_{eff} only in mixer-settlers, to be used in combination with the process calculation code.

1.6 Optimisation

In many engineering applications, optimisation is necessary when an efficient decision-making approach is required. In particular, in chemical engineering, optimisation is essential for experimental design, process synthesis retrofit, model development, parameter estimation, control and real-time optimisation, planning and integration of process operations into the supply chain for manufacturing and distribution [26].

Typically, it is possible to define a generic optimisation problem as follows:

$$\text{minimise} \quad f(x) \quad x \in R^n$$

$$\text{subject to} \quad c_i(x) = 0 \quad i \in E \quad \text{equality constraints}$$

$$i = 1, 2, \cdots, m'$$

$$c_j(x) \geq 0 \quad j \in I \quad \text{inequality constraints}$$

$$j = m' + 1, \cdots, m$$

where x is the independent variable, $f(x)$ the objective function and $c_j(x)$ the constraints.

When constraints and objective function which determine the feasible region are linear expressions, the problem is defined as a Linear Programming problem (LP). Similarly, when one of the previous expressions is nonlinear, then the problem is a Nonlinear Programming problem (NLP). Both of the previous problems involve only continuous variables. If integer variables are involved, then the problem is a Mixed Integer problem, which can be either linear (MILP) or nonlinear (MINLP).

If the solution is not restricted in R^n, the optimisation problem is called unconstrained and two conditions have to occur in the local minimum:

1. the gradient vector $(\partial f / \partial x_i)$ evaluated in the optimal solution x^* must be zero (the first order condition, necessary condition);

2. the Hessian matrix $(\partial^2 f / \partial x_i \partial x_j)$ evaluated in the optimal solution x^* must be positive definite, hence the function is convex (the second order condition, sufficient condition).

If the feasible region is constrained, then the first order condition for the local minimum becomes the so-called Kuhn-Tucker conditions:

$$\nabla L(x, \lambda) = 0 \tag{1.6.1}$$

$$c_i(x) = 0 \quad i \in E \tag{1.6.2}$$

$$c_j(x) \geq 0 \quad j \in I \tag{1.6.3}$$

$$\lambda_j \geq 0 \quad j \in I \tag{1.6.4}$$

$$\lambda_j c_j = 0 \quad \forall j \tag{1.6.5}$$

where L is the Lagrangian function $L(x, \lambda)$ defined as:

$$L(x, \lambda) = f(x) - \sum_{k=1}^{m} \lambda_k c_k(x) \qquad (1.6.6)$$

where λ is the Lagrange multiplier. Eq. 1.6.5 is called complementarity condition: if $c_i = 0$ then the constraint is active and $\lambda \geq 0$, else $\lambda = 0$ and the constraint is not active.

A more detailed description of the mathematical formulation of first and second order conditions, for constrained optimisation problems, is provided by Biegler [26].

Newton-type method is a popular algorithm for fast local optimisation, which has quadratic convergence rate and leads to inexpensive solution [26]. For unconstrained optimisation problems, Newton's method is derived applying the Taylor's theorem to a smooth function, at fixed value and direction. Constrained optimisation strongly relies on this method, as well. This method can fail if:

- the objective function is not smooth;

- the Hessian matrices have negative curvature (Newton steps with ascent directions, rather than descent);

- the initial point is far from the solution.

Sequential Quadratic Programming (SQP)-types methods are successful algorithms used for NLP constrainted optimisations. The SQP-method is an iterative procedure: for a given approximate solution x^k, the NPL is modelled by Quadratic Programming (QP) subproblems. The solution to the QP subproblem is used to contrast a new, better, iterate x^{k+1}. This construction iterates until the optimal solution x^* is identified. These methods could be considered as an extension of the Netwon's method and, similarly to them, they are fast but could be unsuccessful if iterate far from the solution. A detailed description of the Newton's and SQP algorithms can be found in [26].

1.7 Outline

The mathematical models of the current SNF reprocessing process and the relevant works on intensified extraction in small channels are discussed in Chapter

2. Also, a brief review of the flowsheets proposed in the literature for the next generations of PUREX processes is presented. In Chapter 3, the mathematical modelling of intensified extraction in small channels is described. The description of the mathematical models of conventional technologies, used to allow comparison, is presented in Chapter 4. A case study is discussed to compare novel and conventional technologies in Chapter 5. In Chapter 6 a combined U and Pu extraction process is proposed, using the small-scale extractors. This flowsheet has been obtained via a superstructure optimisation. Results, pros and cons of the process are discussed. Finally, in Chapter 7, the thesis concludes with a general overview of this work and future developments.

Chapter 2

Spent nuclear fuel reprocessing

The PUREX process has been investigated between since the 50s. Until the 80s, the matter of main concern was the thermodynamic behaviour of the system uranium-plutonium in nitric acid solution and TBP/dodecane. Also, the modelling of mixer-settlers was investigated, often assuming infinitely rapid mass transfer. Successively, mathematical models for pulsed columns, more complex than mixer-settlers, have been proposed. These works are summarised in Section 2.1.

To overcome the nuclear proliferation risk related to the PUREX process, designed for military purpose within the Manhattan Project, several new flowsheets have been proposed. The most promising processes are presented in Section 2.2.

Several disadvantages of the current SNF reprocessing process are due to the limits of the conventional solvent extraction equipment. The intensified extraction in small channels seems a promising alternative to the traditional ones. The interest in micro or small technologies has rapidly grown in the last years. Mass transfer, hydrodynamics and pressure drops in small-scale extractors have been investigated in the literature, as discussed in Section 2.3.

2.1 Modelling of PUREX process and solvent extraction technologies

The PUREX process is widely used in Europe and Asia for SNF reprocessing. Many authors have suggested models to predict the liquid-liquid extraction in the

PUREX process. Most of the works focused on the behaviour of the system U, Pu in nitric acid solution and a mixture TBP/paraffinic diluent. In the last 20 years, many authors have been investigating the behaviour of other components, such as Tc, Ru, Zr and Np. The latter has three and easily inter-convertible oxidation states that significantly affect Np extraction.

Many authors have modelled the behaviour of liquid-liquid extraction in conventional technologies, mostly pulsed columns and mixer-settlers. Pulsed columns today are always used for the codecontamination section [6]. Mixer-settlers are mostly used in the second cycle [3, 12]. The use of centrifugal contactor is limited despite it seems to be most promising technology among the conventional ones, this is probably due to their poor tolerance to solids and the maintenance required.

Below, the state of the art in the modelling of both PUREX process and the two main conventional technologies is presented. Furthermore, a short review of the relevant studies on intensified extractions is given.

2.1.1 Modelling of SNF extraction

Many authors have investigated the behaviour of the system U-Pu-HNO$_3$ in the two-phase system nitric acid solution-TBP/paraffinic diluent, to predict the extraction process. The most important model of the PUREX process is the one developed by Richardson and Swanson [27] in the 70s. Besides reactions 1.3.1 and 1.3.2, they assumed the following two forms of nitric acid in the organic phase:

$$H^+ + NO_3^- + TBP \rightleftharpoons [HNO_3] \cdot TBP \qquad (2.1.1)$$

$$H^+ + NO_3^- + 2TBP \rightleftharpoons [HNO_3] \cdot 2TBP \qquad (2.1.2)$$
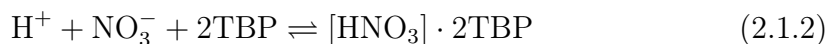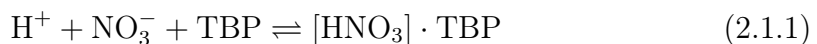
Richardson and Swanson investigated the effect of temperature, TBP concentration and ionic strength (*i.e.* the total nitrate concentration in the aqueous phase) on the thermodynamics of the system. They developed empirical correlations to estimate the distribution coefficients of U(VI), Pu(IV) and HNO$_3$. These equations will be shown in Chapter 3. Most of the authors that have proposed mathematical models to predict liquid-liquid extraction in conventional technologies, for SNF reprocessing, rely on the model developed by Richardson and Swanson to estimate the equilibrium concentrations of U, Pu and HNO$_3$ [28, 29, 27, 30, 31, 32, 33, 34, 35, 36, 37, 38].

As depicted in Figure 1.1.1, besides U and Pu, many other components are present in the SNF. To investigate alternative flowsheets for the nuclear fuel cycle, it is important to predict the behaviour of Zr, Ru and Tc, components which may require particular unit operations and operating conditions to be separated from U and Pu [6]. The thermodynamic behaviour of these component in the PUREX process have been studied in the literature. Distribution coefficients of Zr and Ru were calculated by Natarajan et al [39] as function of the ionic strength. Asakura *et al.* suggested empirical correlations to calculate the distribution coefficient of Tc, taking into account the effect of temperature and concentrations of U, Pu and Zr.

One of the most studied component of the SNF is Np, due to its complex behaviour in the system. Np can be present in nitric acid solution with three different and easily inter-convertible oxidation states, Np(IV), Np(V) and Np(VI), according to the following reactions:

$$NpO_2^+ + 0.5NO_3^- + 1.5H^+ \rightleftharpoons NpO_2^{2+} + 0.5HNO_2 + 0.5H_2O \qquad (2.1.3)$$

$$2NpO_2^+ + 4H^+ \rightleftharpoons Np^{4+} + NpO_2^{2+} + 2H_2O \qquad (2.1.4)$$
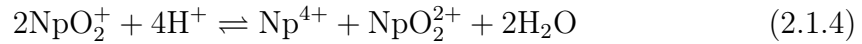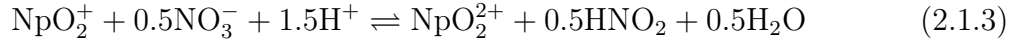
Benedict *et al.* investigated distribution coefficients of Np(IV) and Np(VI) [40], with Kumar and Koganti that recalculated the proposed parameters [41]. Np(V), contrarily to Np(IV) and Np(VI), is almost unextractable. Hence, it is necessary to consider the kinetic of reactions 2.1.3 and 2.1.4 in the PUREX process. Koltunov studied the kinetic of reaction 2.1.3, proposing a kinetic model which has been used by other authors [42]. Kumar and Koganti also proposed an alternative model to predict the distribution coefficients of Np(IV) and Np(VI), but for limited TBP concentrations [41]. They also developed similar correlations for U, nitric and nitrous acid [43, 44, 45].

Several redox reactions may occur in this system. Some of them are exploited to back extract Pu(IV) from organic phase, converting it to Pu(III), such as in the U/Pu partitioning section in the first cyle of the PUREX process. This reduction reaction is carried out using reductants such as hydroxylammine nitrate (HAN) and U(IV).

The Pu reduction can be hindered by the presence of nitrites, which catalyse the auto-oxidation of Pu(III) to Pu(IV). For this reason, a nitrite scavenger is used, typically hydrazine nitrate [6]. Tachimori and Gonda reported several expressions

to predict the kinetics of several reactions that can take place in the PUREX process, including nitrite scavenge by hydrazine and Pu(III) auto-oxidation [37, 36, 38, 46].

2.1.2   Modelling of mixer-settler

Mixer-settlers are generally simpler to model than pulsed columns. Between 1950 and 1980, many authors investigated this technology for SNF reprocessing [28, 29, 27, 30, 31, 32, 33]. The SEPHIS (Solvent Extraction Processes Having Interacting Solutes) code was widely used to predict the PUREX process using mixer-settlers. It is a steady-state and stage wise model, which considers U, Pu and HNO_3. Developments of this code were proposed in the 70s [31, 32, 33]. The concentrations in each stage were assumed equilibrium concentrations. Beyerlein *et al.* developed the PUBG code (Plutonium Uranium Beyerlein Geldard), assuming a deviations from mass transfer equilibrium conditions [34]. In the mixer, a short transient behaviour was assumed, compared with the one in the settler. Hence, the mass balances for the i component and phase k, in mixer and settler, becomes:

$$\text{Mixer:} \quad \dot{V}_k(C_{i,k}^{in} - C_{i,k}) - k_L a V_{mix}(C_{i,k} - C_{i,k}^{eq}) = 0 \qquad (2.1.5)$$

$$\text{Settler:} \quad \dot{V}_k(C_{i,k}^{in} - C_{i,k}) = \frac{d(V_{set}C_{i,k})}{dt} \qquad (2.1.6)$$

Perfect mixing and negligible mass transfer in the settler were assumed.

Similarly to the pulsed columns, many empirical correlations have been proposed to estimate hydrodynamic variables. For two-phase liquid systems in stirred vessel, a review of empirical correlations for the calculation of mass transfer coefficients was provided by Ghotli et al [47]. Many correlations for mass transfer and hydrodynamic variables can be found in the Perry's Chemical Engineering Handbook [48]. For the mass transfer coefficient in the continuous phase several correlations have been suggested, whilst only a few exist for the mass transfer coefficient in the dispersed phase, despite under agitation this seems to be the rate determining step [36].

Several empirical correlations have been proposed for the calculation of the Sauter diameter in stirred vessel, as well. A review of these correlations was done by Godfrey [49]. The stirred vessel is a commonly used equipment, also for gas-liquid and solid-liquid applications, hence a large number of models for

mass transfer and hydrodynamics have been developed. An overview of the main correlations suggested in the literature is given in Tables 2.1.1-2.1.2.

Table 2.1.1: Correlations for the mass transfer coefficient in agitated vessel [47]. Below, k_c is the mass transfer coefficient in the continuous phase, k_d in the dispersed phase.

Authors	Equation
Keey and Glen	$Sh = \frac{k_c D_I}{\mathscr{D}} = 8.92 \cdot 10^{-4} Re^{1.36} T^{-0.5} D_I^{-0.36} - 336$
Mok and Treybal	$k_c = 0.173 \frac{d}{t_f M} \left(\frac{\mu_d}{\rho_d \mathscr{D}}\right)^{1.115} \left(\frac{\Delta \rho g d^2}{\gamma g_c}\right)$
Chapman et al	$k_c = 0.13 \left(\frac{P \mu_c}{V_c \rho_c^2}\right)^{0.25} \left(\frac{\mu_c}{\rho_c \mathscr{D}}\right)^{2/3}$
Skelland and Lee	$\frac{k_c}{N_{rev} D}^{0.5} = 2.932 \cdot 10^{-7} \varphi^{-0.508} \left(\frac{D_I}{T}\right)$
Skelland and Moeti	$\frac{k_c d_p}{\mathscr{D}} = 1.237 \cdot 10^{-5} \left(\frac{\mu_c}{\rho_c \mathscr{D}}\right)^{1/3} Re^{2/3} \cdot$ $\left(\frac{D_I N_{rev}^2}{g}\right)^{5/12} \left(\frac{D_I}{d_p}\right)^2 \left(\frac{d_p}{T}\right)^{0.5} \left(\frac{\rho_d d_p^2 g}{\gamma}\right)^{5/4} \varphi^{-0.5}$
Treybal	$Sh_d = \frac{k_d d_{32}}{\mathscr{D}_d} = \frac{2\pi^2}{3}$
Aziz and Al Taweel	$k_d = 0.00375 v_t \left(\frac{\mu_C}{\mu_c + \mu_d}\right)$
Skelland and Xien	$k_d = \left(\frac{\mathscr{D}}{t_{F,95} - t_{t0}}\right)^{0.5} 5 \cdot 10^{-6} \varphi^{-0.0204} \left(\frac{D_I^2 N_{rev} \rho_M}{\mu_M}\right)^{1.14} \cdot \left(\frac{\rho_c}{\Delta \rho}\right)^{0.518}$ $\rho_M = \varphi \rho_d + (1 - \varphi) \rho_c$ $\mu_M = \frac{\mu_c}{1 - \varphi} \left(1 + \frac{1.5 \mu_d \varphi}{\mu_d + \mu_c}\right)$

Gonda *et al.* proposed a dynamic stage wise model for mixer-settlers [36, 38], suitable for PUREX process. They included several redox reactions in the model. The mass balance in the mixer is very similar to Eq. 2.1.5, but with the addition of a reaction term:

$$\dot{V}_k(C_{i,k}^{in} - C_{i,k}) + V_{mix} \sum R_{i,k} - k_L a V_{mix}(C_{i,k} - C_{i,k}^{eq}) = \frac{d(V_{mix} C_{i,k})}{dt} \qquad (2.1.7)$$

where $\sum R_{i,k}$ is the sum of all the chemical reactions involving the component i in phase k. Gonda *et al.* also suggested a correlation to estimate the mass

Table 2.1.2: Correlations for the Sauter droplet mean diameter in agitated vessels [50].

Authors	Equation
Vermeulen, Calderbank, Sprow	$d_{32}/D = C_1 We^{-0.6}$ $0.51 \leq C_1 \leq 0.53$
Shinar, Sprow	$d_{32}/D = C_2 \gamma D We^{-0.375}$ C_2=experimentally determinated
Calderbank	$d_{32}/D = 0.06(1 + 3.75\varphi)We^{-0.6}$ (4-blade)
	$d_{32}/D = 0.06(1 + 95\varphi)We^{-0.6}$ (6-blade)
Brown and Pitt	$d_{32}/D = 0.051(1 + 3.14\varphi)We^{-0.6}$
Mlynek and Resnik	$d_{32}/D = 0.058(1 + 5.4\varphi)We^{-0.6}$
Gharehbagh and Mousavian	$d_{32}/D = 0.081(1 + 4.47\varphi)We^{-0.6}$

transfer coefficient. However, they estimated the superficial velocity in the mixer by fitting the model to experimental data. This variable is otherwise difficult to evaluate in a stirred tank: it depends on impeller speed, flow rates, tank sizes and significant gradient velocity occurs. Therefore, this calculation is demanding and, in absence of experimental data, the application of the mass transfer model proposed by Gonda *et al.* may not challenging.

2.1.3   Modelling of pulsed colum

The mathematical modelling of pulsed columns is demanding, due to the complex hydrodynamics: droplets breakage and coalescence, axial back-mixing, dispersed phase holdup depending on both operating conditions and geometry.

A literature review on the modelling of extraction columns has been done by Mohanty [51]. He categorised the mathematical models in empirical, stagewise and differential models.

Empirical are the models typically proposed to predict hydrodynamic variables. Numerous authors have developed empirical correlations to calculate the dispersive axial coefficient, to describe the non-ideality of the plug flow in the column [52, 53, 37, 54]. Kumar and Hartland proposed correlations for hydrodynamics and mass transfer coefficient, regardless the packing type [55, 56, 57, 58]. A review on the correlations used for the estimation of hydrodynamic parameters in perforated

plate pulsed columns is given by Haverland and Slater [59]. In general, empirical models are often used to develop data-driven models in chemical engineering, when the theoretical estimation of some parameters is challenging.

Stagewise models are obtained assuming the column to be a series of stages, considered completely mixed. The stages are not necessarily real but they can be hypothetical. Steiner suggested the use of stagewise models for nonlinear equilibrium, *i.e.* when the distribution coefficient is calculated as function of the solute concentration [60].

Differential models come from differential mass balance equations for both phases. The dispersed phase can be considered either pseudo-homogeneous or discontinuous: the first assumption leads to a pseudo-homogeneous dispersion model where the system is represented as a continuum, whereas for the second one breakage and coalescence of the dispersed droplets must be considered, leading to a population balance dispersion model. Pseudo-homogeneous dispersion models have been often used in the literature [61, 62, 63, 64]. Typical boundary conditions are obtained through mass balances over a small region containing the entry points, considering dispersion and convection terms, and setting a zero slope at the exit [61, 62, 63, 64]:

$$\text{at } z = 0 \quad -\frac{dC_{i,c}}{dz} = Pe_c(C_{i,c}^{in} - C_{i,c}) \quad \text{and} \quad -\frac{dC_{i,d}}{dz} = 0 \tag{2.1.8}$$

$$\text{at } z = 1 \quad \frac{dC_{i,c}}{dz} = 0 \quad \text{and} \quad \frac{dC_{i,d}}{dz} = Pe_d(C_{i,d}^{in} - C_{i,d}) \tag{2.1.9}$$

where z is the dimensionless height (h/H, h sample height, H column height), $z = 0$ refers to the top of the columns, $z = 1$ to the bottom. These conditions are known as Danckwerts conditions [65], widely used for plug-flow with dispersion/reaction models.

Many authors proposed stagewise population balance model [66, 67, 68, 69]. Most of the authors proposed steady state models, despite the periodic pulsation may induce to opt for dynamic modelling. The models are summarized in Table 2.1.3.

Torab-Mostaedi *et al.* [61] proposed a differential pseudo-homogeneous dispersion model for perforated plate extraction columns, steady state model, using standard systems. The mass balance was modelled assuming plug-flow conditions.

24

Table 2.1.3: Basic categories of mathematical models for extraction columns [51, 60]

Model	Basic Equations
Empirical	for example $d_{32} = f(\text{phys. properties, geometry, oper. conditions})$
Stage-wise	$\frac{\partial C_c}{\partial t} = (\frac{N}{Pe_c} + 0.5)(C_{c,n+1} - C_{c,n}) + (\frac{N}{Pe_c} - 0.5)(C_{c,n-1} - C_{c,n}) - \frac{N_{oc}}{N}(C_{c,n} - C_{c,n}^{eq})$ $\frac{\partial C_d}{\partial t} = (\frac{N}{Pe_d} + 0.5)(C_{d,n-1} - C_{d,n}) + (\frac{N}{Pe_d} - 0.5)(C_{d,n+1} - C_{d,n}) - \frac{N_{oc}}{Nq}(C_{c,n} - C_{c,n}^{eq})$
Diff. homog. disp.	$\frac{\partial C_c}{\partial t} = v_c\frac{\partial C_c}{\partial z} + Pe_c\frac{\partial^2 C_c}{\partial z^2} + K_{oc}(C_c - C_c^{eq})$ $\frac{\partial C_d}{\partial t} = -v_d\frac{\partial C_d}{\partial z} + Pe_d\frac{\partial^2 C_d}{\partial z^2} - K_{oc}(C_c - C_c^{eq})$
Diff. popul. balance	$\frac{\partial P(d)}{\partial t} = -\frac{\partial[v(d)P(d)]}{\partial z} + \frac{\partial}{\partial z}[Pe_d\frac{\partial P(d)}{\partial z}] + B(d) - D(d)$

Hence, fluid velocity and concentrations are assumed constant at the same column cross section. The axial backmixing is described through the axial dispersion coefficient, as suggested by Miyauchi and Oya [70]. Boundary conditions are the Danckwerts conditions [65], see Eqs. 2.1.8-2.1.9. Torab-Mostaedi *et al.* estimated the axial coefficient of the continuous phase as proposed by Kumar and Hartland [55]. However, they have neglected the effect of the axial dispersion in the dispersed organic phase, therefore only three boundary conditions are required in this case. Holdup and Sauter mean drop diameter were experimentally measured. A correlation for the mass transfer coefficient was achieved by calibrating the model against pilot plant data.

Most of the liquid-liquid systems investigated in the literature are toluene-acetone-water and butyl acetate-acetone-water, the two standard European Federation of Chemical Engineering test systems [67, 62, 61, 71, 72, 68, 73, 74, 75, 64]. However, some authors have studied the system nitric acid solution - TBP/paraffinic diluent [76, 63] and several empirical correlations for hydrodynamic variables have been proposed [53]. Jiao et al [63] developed a pseudo homogeneous differential model for a 30% TBP in kerosene and a 3 M nitric acid solution in a perforated plate pulsed column. The mass transfer of HNO_3 was investigated, from continuous aqueous to dispersed organic phase. The mathematical model was developed similarly to Torab-Mostaedi *et al.*, the only difference is related to

the axial dispersion of the dispersed phase, which was not neglected by Jiao *et al.*. They evaluated the axial dispersion coefficients and the volumetric mass transfer coefficient from the experimental concentration profile, and the dispersed holdup as suggested by Tang *et al.* [77]. Jiao *et al.* assumed a constant distribution coefficient. In this case, the mass balance can be solved analytically. If the distribution coefficient is assumed as function of the solute concentration (nonlinear equilibrium), then the model must be solved numerically [60]. However, similarly to Torab-Mostaedi *et al.*, Jiao *et al.* solved the model applying the forth order explicit Rung-Kutta method.

Yu *et al.* [76] developed a stagewise backmixing model to investigate the mass transfer of HNO_3 in a perforated plate pulsed column, from continuous aqueous phase to dispersed organic phase (30% v/v TBP/kerosene). Backmixing parameters and mass transfer coefficient were evaluated from pilot plant data. The experimental mass transfer coefficients were compared to the mass transfer coefficients predicted by the single drop mass transfer method. Overall mass transfer coefficient was calculated considering the two mass transfer resistances in series:

$$k_L = \frac{1}{k_d} + \frac{1}{mk_c} \tag{2.1.10}$$

where the mass transfer coefficient of the dispersed phase was estimated by the simplified single turbulent circulating drop method, according to the Handlos-Baron correlation:

$$k_d = \frac{2.88 v_r}{768(1 + \mu_d/\mu_c)} \tag{2.1.11}$$

and the mass transfer coefficient of the continuous phase is calculated by the Garner equation:

$$Sh_d = \frac{k_c d_{32}}{\mathscr{D}_c} = 50 + 0.0085 Re Sc^{0.7} \tag{2.1.12}$$

Results showed that the mass transfer performance could be reasonably predicted by single turbulent circulating drop method.

Vassallo [53] studied the hydrodynamic of a perforated plate pulsed column using the system 30% TBP/ kerosene (dispersed phase) - 2 M nitric acid solution (continuous phase). In contrast to Yu *et al.*, Vassallo incorporated the effect of the dispersed phase holdup in the Sauter diameter correlation. They both obtained the same mathematical expression to predict the relative velocity. However, they

used different coefficients. Vassallo and Yu *et al.* considered a dispersed organic phase in an aqueous continuous phase, despite the opposite occurs in the first extraction step of the PUREX process.

All the mathematical models developed by the authors discussed above do not involve chemical reactions. This is not the case of the PUREX process, since a series of desired and undesired reactions occur. Despite the nuclear industry is one of the most important applications of extraction columns, few models for pulsed columns suitable for the PUREX have been proposed in the literature. Gonda and Matsuda developed a pseudo homogeneous differential model for the PUREX process in perforated plate pulsed column, the so-called PULCO code [37]. This is one of the most complex mathematical models for pulsed columns. It involves:

- dynamic model;

- multi-component extraction, including U(IV), U(VI), Pu(III), Pu(IV), HNO$_3$;

- redox reactions;

- extraction and stripping operations;

- empirical estimation of the mass transfer;

- empirical estimation of dispersed phase holdup for stainless steel and poly-tetrafluoroethylene (PTFE) plate;

- empirical estimation of the Sauter mean diameter for both phases;

- empirical estimation of the axial dispersion coefficient for both phases;

- distribution coefficients of U, Pu and HNO$_3$ according to Richardson and Swanson [78].

The model proposed to calculate the mass transfer coefficient is based on the boundary layer theory, the Handlos-Baron's theory and the penetration theory [79, 80]. These correlations are nonlinear functions of several parameters (pulsation intensity, droplets size, distribution coefficients, pH).

An exhaustive description on the computational procedures for extraction columns is presented by Steiner [60].

2.2 Future flowsheets for SNF reprocessing

The PUREX process has several drawbacks, such as nuclear proliferation and a large number of unit operations to separate U and Pu, which are mixed again for MOX fuel production. Also, due to the technologies used, solvent degradation occurs and a solvent cleanup and regeneration section is required. Many developments of the PUREX process have been proposed, however none of these processes has never been employed in industry. The goal of the next generations of these flowsheets is, mainly, the preclusion of nuclear proliferation risks. Further aims are the recovery of Np and minor actinides (MAs) and the minimisation of the solvent degradation. The choice of the flowsheet can depend, also, on the political strategies [6].

The main alternatives of the PUREX process are briefly discussed below. In all the following processes, the typical mixture TBP/paraffinic diluent is used as solvent.

2.2.1 COEX (Combined Extraction)

The aim of the COEX process is to simultaneously extract U and Pu. Possibly, some Np is extracted with Pu, as well. This process is designed to avoid pure Pu products and hence the nuclear proliferation risk. Contrary to the PUREX process, the U/Pu partitioning section is not required, reducing the investment cost. The design of this process was suggested through simulation tools and data validation at the La Hague plants (France) [6]. The first part of the process is identical to the first section of the PUREX process. A reducing agent is needed to strip Pu, exploiting the low affinity of Pu(III) with TBP. A final topping up of U is required to adjust the Pu/U ratio in the product.

2.2.2 UREX (Uranium Extraction)

The goal of the UREX process is to recover U (99.9% purity) and Tc (>95% purity) [5]. Pu is supposed to end up in the raffinate stream, together with Np, other MAs and fission products. Acetohydroxamic acid (AHA) is used to strip Np and Pu in aqueous phase [9, 10]. AHA is slightly extracted by TBP, which can be readily cleaned in a solvent regeneration section.

2.2.3 UREX+2

UREX+2 is a further evolution of the UREX process. Here U, Tc, Pu and Np are co-extracted early in the process, to simplify the next unit separations. An advantage is the lower amount of solvent required, due to the less extraction operations involved. U/Tc and Np/Pu streams are produced. Compared to the UREX process, the handling of the U/Tc and Np/Pu products is simpler, because of dose rates and shielding required [6]. Ionic exchange is used to separate U and Tc, whereas Pu and Np are efficiently recovered by reductive stripping (recovery, respectively, of 99.8% and 87.2% [6]).

2.2.4 NPEX (Neptunium Plutonium Extraction)

The objective of the NPEX process is to separate Np and Pu from the other MAs and fission products in the UREX raffinate. Nitric acid solution is evaporated and, then, Np and Pu extracted by TBP. AHA is used to strip Np and Pu, to achieve a mixed Np/Pu product [6]. A high extraction of Np is difficult to obtain, due to the difficult Np control. The extraction of Np can be completed in following processes. However, the nuclear proliferation risk is precluded.

2.2.5 Other processes

Many other developments of PUREX process have been proposed. For instance, DIAMEX (Diamide Extraction) and SANEX (Selective Actinide Extraction) have been suggested to recover other MAs (Am, Cm) from the high activity waste, TRUEX (Transranic element Extraction) to separate transuranic elements and lanthanides from the raffinate (in particular Zr). Other flowsheets are CSEX (Cs Extraction), SREX (Sr Extraction), SESAME (Selective Extraction and Separation of Americium by Means of Electrolysis) [6].

Furthermore, in the last years, several authors have investigated the use of new diluents for the nuclear fuel reprocessing, such as supercritical CO_2 [81, 82, 83] and ionic liquids [84, 24, 85, 86]. Also, new processes involving free HNO_3 solution (*e.g.* CARBEX, extraction in carbonate media [87]) and new technologies, such as micro or small devices for process intensification [84, 24, 88, 85], have been investigated.

2.3 Intensified extraction

Small-scale contactors have been widely investigated in the last decade [18, 19, 20, 21, 22]. Most of these works focus on the volumetric mass transfer coefficients, *i.e* the product between the mass transfer coefficient and the interfacial area, and numerous empirical and semi-empirical correlations have been proposed. As the gas-liquid operations have been intensively studied in the literature, a large number of correlations regards the Taylor flow, a gas-liquid flow pattern which consists of dispersed bubbles and liquid slugs. This flow pattern is similar to the segmented flow.

Numerous authors have investigated hydrodynamic characteristics, such as wall film thickness and plug size, important parameters to determine the interfacial area. Models have also been suggested for the estimation of the pressure drop within the micro or small channel.

2.3.1 Volumetric mass transfer coefficient

Several authors have studied the mass transfer in small channels. Tsaoulidis *et al.* [23, 21, 24], for segmented flow in small channels, calculated the volumetric mass transfer coefficient as follow:

$$k_L a = \frac{1}{\tau} \left(\frac{C_{eq} - C_{in}}{C_{eq} - C_{fin}} \right) \tag{2.3.1}$$

The equation above implies that an ideal plug flow model was assumed, no axial diffusion, constant volumetric mass transfer coefficient along the length of the channel.

Many authors have proposed empirical correlations to predict the mass transfer coefficient for two-phase flow in small channels, in particular for gas-liquid systems, mostly based on the penetration theory. A brief review of the main mass transfer models is presented by Tsaoulidis and Angeli [24]. Bercic and Pintar [89] did not incorporated in their model the contribution of the film around the channel wall (hence, a rapid saturation was assumed), but only the contribution of the caps. On the contrary, Vandu et al [90] considered only the contribute of the film. Van Baten and Krishna [91] and Irandoust and Anderson [92] included both contributions in their correlations. Kashid and Agar [20] correlated the overall

mass transfer coefficient to operating and geometrical variables. The mass transfer models mentioned above are summarised in Table 2.3.1.

Table 2.3.1: Correlations for the volumetric mass transfer coefficient in small channels

Authors	Equation
Bercic and Pintar. [89]	$k_L a = \dfrac{0.111 v_p^{1.19}}{\left[\left(1-\epsilon_d\right) L_{UC}\right]^{0.57}}$
Van Baten and Krishna [91]	$k_L a = k_{L,cap} a_{cap} + k_{L,film} a_{film}$ $k_{L,cap} a_{cap} = \dfrac{2^{1.5}}{\pi}\left(\dfrac{\mathscr{D}_c v_p}{D}\right)^{0.5}\dfrac{4}{L_{UC}}$ $k_{L,film} a_{film} = \dfrac{2}{\pi^{0.5}}\left(\dfrac{\mathscr{D}_c v_p}{L_{film}}\right)^{0.5}\dfrac{4 L_{film}}{L_{UC} D}$ for $Fo < 0.1$ $k_{L,film} a_{film} = 3.41\dfrac{\mathscr{D}_c}{\partial_{film}}\dfrac{4 L_{film}}{L_{UC} D}$ for $Fo > 0.1$ $Fo = \dfrac{\mathscr{D}_c L_{film}}{v_p \delta_{film}^2}$
Vandu *et al.* [90]	$k_L a = C\left(\dfrac{\mathscr{D}_c v_g}{L_{UC}}\right)^{0.5}\dfrac{1}{D}$ (C constant)
Kashid *et al.* [20]	$k_L a \dfrac{L}{v_{mix}} = a Ca^b Re^c\left(\dfrac{D}{L}\right)^d$ (a, b, c, d constants)
Tsaoulidis *et al.* [24]	$k_L a \dfrac{L}{v_{mix}} = 0.44 Ca^{-0.1} Re^{-0.65}\left(\dfrac{D}{L}\right)^{-0.1}$

2.3.2 Plug size

The interfacial area available for mass transport depends on the plug size. Several authors have suggested empirical correlations for the estimation of the plug size. Tsaoulidis [84] experimentally obtained plug length for IL-water and 30% TBP/IL-HNO$_3$ solution. Several operating conditions (velocity between 0.3 and 7 cm s^{-1}, organic fraction between 0.4 and 0.6) and geometries (channel diameter between 0.2 and 2 mm) were investigated. A good agreement between experimental and predicted data was found. A review of the main equations suggested in the literature to estimate the plug size can be seen in Table 2.3.2.

Table 2.3.2: Correlations for the plug size in small channels.

Authors	Equation	Flow
Leclercl *et al.* [93]	$\frac{L_b}{w_{gas}} = 1.03\frac{w_{gas}w_{liq}}{w_{chan}^2} + 2.17\frac{w_{gas}u_{gas}}{w_{liq}u_{liq}}$	Taylor
Xu *et al.* [94]	$L_p = 0.0116u_{slag}^{-0.32}D^{1.25}q^{0.89}$	segmented
Qian and Lawal [95]	$\frac{L_b}{D} = 1.637\epsilon_g^{-0.107}\left(1 - \epsilon_g\right)^{-1.05}Re^{-0.0075}Ca^{-0.0687}$	Taylor
Laborie *et al.* [96]	$\frac{L_b}{D} = 0.0878\frac{Re^{0.63}}{Bo^{1.26}}$	Taylor
Tsaoulidis [84]	$\frac{L_p}{D} = 0.1325\frac{Re_d q^{0.27}}{Ca_{mix}^{0.27}}\left(Re_c Re_{mix}\right)^{0.551}$	segmented

If the plug length is known, the interfacial area can be estimated according to Di Miceli *et al.*, considering two hemisferical caps [97]:

$$\text{if } Ca > 0.04 \quad a = \frac{\pi w_p(L_p - w_p) + \pi w_p^2}{L_{UC}w_{ch}^2} \tag{2.3.2}$$

$$\text{if } Ca < 0.04 \quad a = \frac{4w_p(L_p - w_p) + \pi w_p^2}{L_{UC}w_{ch}^2} \tag{2.3.3}$$

where w is the width, the subscript p refers to the plug, ch refers to the channel, usual meanings for the other symbols.

2.3.3 Liquid film thickness

Dore *et al.* investigated the hydrodynamic of dispersed plugs in microchannels, using the ionic liquid (IL)-water system. Hydrodynamic characteristics, such as length, velocity of the dispersed plug and film thickness of the continuous phase around the plug were experimentally observed varying the superficial velocity of the two-phase flow. They proposed a correlation to estimate the film thickness, based on the Irandout and Anderson model [92]. The equations suggested in the literature for the film thickness are summarised in Table 2.3.3.

2.3.4 Pressure drops

The prediction of the pressure drop is crucial to estimate the operating cost, which is the pumping cost. In the literature, pressure drop models for two-phase flow in small channels have been proposed. Jovanovic *et al.* [101] and Kashid and Agar

Table 2.3.3: Correlations for the wall film thickness in small channels.

Authors	Equation	Flow	Range of Ca number
Fairbrother and Stubbs [98]	$\delta = 0.5 Ca^{0.5} r$	Taylor	$7.5 \times 10^{-5} - 0.01$
Bretherton [99]	$\delta = 1.34 Ca^{2/3} r$	Taylor	Ca <0.003
Irandoust and Andersson [92]	$\delta = 0.36\left(1 - \exp\left(-3.1 Ca^{0.54}\right)\right)r$	gas-liq	$9.5 \times 10^{-4} - 1.9$
Aussillous and Quere [100]	$\delta = 1.34 Ca^{2/3} r$	Taylor	10^{-3}-1.4
Dore *et al.* [18]	$\delta = 0.30\left(1 - \exp\left(-6.9 Ca^{0.54}\right)\right)r$	liq-liq	$7 \times 10^{-3} - 0.16$

[19] assumed that the segmented flow consists of a series of unit cells (UC), *i.e.* a dispersed plug and a continuous slug. Kashid and Agar suggested the following equation:

$$\Delta P_{tot} = \frac{L}{L_{UC}}\Delta P_{fr} + \frac{2L - L_{UC}}{L_{UC}}\Delta P_{int} \qquad (2.3.4)$$

where ΔP_{fr} is the frictional pressure drop, calculated by the Hagen-Poiseuille equation, and ΔP_{int} the interfacial pressure drop. At low flow rates, where the film thickness is thin and almost stagnant, good agreement with experimental data was observed. At higher flow rates the film thickness increases and moves, causing additional frictional pressure drop [22].

Jovanovic *et al.*, in contrast to Kashid and Agar, considered the film thickness around the plugs, calculated according to Bretherton [99]. They proposed two models, the stagnant model and the moving one. However, since the film velocity was found to be negligible, the simpler stagnant model was suggested. In the latter, the frictional pressure drop is estimated by the Hagen-Poiseuille equation, whilst the interfacial pressure drop is calculated as:

$$\Delta P_{int} = 7.16(3Ca)^{2/3}\frac{\gamma}{D} \qquad (2.3.5)$$

Similarly to Kashid and Agar, good agreement with experimental data was found for low flow rates, whereas at high velocity the Bretherton model is not

valid [22].

The models developed by Jovanovic *et al.* and Kashid and Agar predict the pressure drop along the small channel. However, in order to reliably predict the pumping cost, pressure losses in mixing junction and splitting zone, for the two-phase separation, must be taken into account. Kashid and Agar provided experimental pressure drop in a Y-junction, but no models were proposed.

2.3.5 Other studies

Tsaoulidis [84], for a 30% TBP/IL-HNO$_3$ solution, proposed the following empirical correlation to estimate the plug velocity:

$$v_p = [3.55 \ln(D) + 32.3]v_{mix}^2 + 1.017v_{mix} \qquad (2.3.6)$$

This velocity is an indicator of residence time and mixing efficiency [84].

Tsaoulidis and Angeli developed a 2D axisymmetric model for the extraction of U(VI) in small channels. A computational fluid dynamics (CFD) model was implemented in COMSOL Multiphysics [102]. The mass transfer in a unit cell was simulated. The mathematical model consists of the Navier-Stokes equation (2.3.7), the continuity equation (2.3.8) and the convection-diffusion equation (2.3.9):

$$\rho(v \cdot \nabla)v = \nabla \cdot [-PI + \mu(\nabla v + (\nabla v)^T)] + F \qquad (2.3.7)$$

$$\rho \cdot \nabla v = 0 \qquad (2.3.8)$$

$$\frac{\partial C_i}{\partial t} + \nabla \cdot (\mathscr{D}_i \nabla C_i + vC_i) = 0 \qquad (2.3.9)$$

where I is the identity matrix, F the external forces applied to the fluid. Assumptions are laminar flow, no-slip condition at the wall, newtonian liquids, incompressible flow, moving channel at constant velocity (equal to the plug velocity) and constant plug shape. Firstly, Eqs. 2.3.7 and 2.3.8 were solved. Then, the convection-diffusion equation was solved. All the hydrodynamic data required, such as film thickness and plug length, had been obtained experimentally. Results predicted by the model were in good agreement with experimental data.

All the works described above focused of the mass transfer, hydrodynamics and pressure drop in a single channel. Several authors have investigated pressure drop

in manifolds with a large number of channels, to properly design distributors and collectors, which are essential to ensure good flow distribution and acceptable pressure drop [103, 104, 105, 106, 107, 108, 109]. A good manifold is crucial to "scale out", or "number up", the parallel channels, to increase the overall throughput for industrial application. Commenge *et al.* developed a methodology to design a comb-like flow network [108], based on a electrical resistance model. The methodology assumed isothermal and laminar flow ($Re < 2000$). However, there is a lack of information in the literature regarding flow networks for two-phase flows.

Another issue that requires further investigation is the separation of the two-phase flow at the end of the small channel. Scheiff *et al.* developed a model to design a two-phase separator at the end of the channel, using a mainstream and sidestream channel at the end of the small extractor [110]. The model, based on pressure drop calculations (see Eq. 2.3.4), exploits the different wettability of channels: hydrophilic sidestream channels were used to separate aqueous dispersed plugs from the organic continuous phase, whilst hydrophobic channels were used to separate organic dispersed plugs from the aqueous continuous phase. This method can be successfully employed to separate the two phases in a single channels. However, it may be not practical for a large number of channels arranged in a flow networks if significantly different flow rates within the parallel channels occur.

2.4   Overview

The PUREX process and the liquid-liquid extraction technologies typically employed in the nuclear industry have been widely investigated and modelled in the literature. To overcome the disadvantages of the current PUREX process, several alternatives for future SNF reprocessing have been suggested. The main goal is to preclude the risk of nuclear proliferation. Many drawbacks are related to the conventional solvent extraction technologies. The intensified extraction in small channels seems a promising alternative to the traditional equipment. The application of the small extractors to the nuclear industry may be beneficial to reduce solvent degradation, plant size and to achieve a better control of hydrodynamics. Liquid-liquid extraction in micro or small channels have been investigated in the literature. However, no mathematical models have been developed for the design and optimisation of alternative SNF reprocessing flowsheets using small channels.

In this thesis, a mathematical model of intensified extraction in small channels, suitable for SNF reprocessing, is developed. The model, presented in Chapter 3, will be used for optimisation-based design problems in Chapters 5 and 6.

Chapter 3

Modelling of intensified extraction

In this chapter, the mathematical modelling of intensified extraction in small channels is presented. Besides U and Pu, a large number of components present in the SNF is included in the physical system. Nitrous acid HNO_2, from HNO_3 degradation, is considered. Redox reaction between Np(IV), Np(V) and Np(VI) are included in the model. Typical solvent, a mixture TBP/paraffinic diluent, is used. This solvent has been preferred to promising alternatives, such as ionic liquid [84, 18, 21, 23, 22, 24], for the much larger amount of data in the literature, in particular thermodynamic data, and the higher U affinity. Pressure drop, economics, flow distribution and nuclear criticality calculations are implemented in the model. The resulting mathematical model, formulated as an optimisation problem, is a mixed integer differential problem, converted to an mixed integer nonlinear problem through discretisation. Integer variables are related to the number of stages and the number of elements of each level of the manifold. The model has been implemented in the General Algebraic Modeling System (GAMS) [111].

The mathematical modelling, which allows to design and optimise liquid-liquid extraction processes using the small contactors, is novel. The model will be used to explore future processes for SNF reprocessing using the small-scale technology.

This chapter is structured as follows. Section 3.1 provides details of the mathematical relationships used to describe the chemistry of the PUREX process. Correlations used to predict distribution coefficients and redox reactions are illustrated. In Section 3.2 the assumptions for the mass balance, mass transfer, pressure drop and flow network calculations are described. Details on the solver and solution

procedure are shown in Section 3.3. In Section 3.4 a case study is investigated to demonstrate the applicability of the model. An overview of the mathematical model developed in this chapter is presented in Section 3.5.

3.1 Chemistry

The physical system included in the model consists of U(VI), Pu(IV), Zr, Ru, Tc, Np(IV), Np(V) and Np(VI) dissolved in a HNO_3 solution. HNO_2, which is a degradation product of HNO_3, is also considered and included in the system to simulate HNO_3 radiolysis. Below, all the mathematical expressions to predict thermodynamics variables and reaction rates are presented.

3.1.1 Distribution coefficients

If the concentration of a solute is very small, then the relationship between organic and aqueous concentrations at equilibrium can be assumed linear (constant distribution coefficient). This linear trend occurs because the concentration of the solvent is large, if compared to the one of the solute, and the capability of the solvent to extract the solute is not affected since there is still a large amount of unbounded solvent, available for the solute extraction. This is not the case of industrial processes like the PUREX process, where the concentration of the metals is high, in particular of U. Increasing the metal concentration, the amount of solvent available for extraction decreases, therefore decreasing the distribution coefficient. The distribution coefficients are also affected by nitric acid concentration and temperature. The distribution coefficients of the components included in the model have been described as follows.

Uranium, plutonium and nitric acid

For the prediction of distribution coefficients of U, Pu and HNO_3 (see Eqs. 1.3.1–1.3.2 and 2.1.1–2.1.2), Richardson's correlations have been used [27]:

$$D_U = K_U[\text{TBP}]_{or}^2 \tag{3.1.1}$$

where $[\text{TBP}]_{or}$ is the free, *i.e.* unbounded, TBP concentration in the organic phase. The pseudo-equilibrium constant K_U is calculated by the following expression:

$$K_U = (3.7[\text{NO}_3^-]_{aq}^{1.57} + 1.4[\text{NO}_3^-]_{aq}^{3.9} + 0.011[\text{NO}_3^-]_{aq}^{7.3})(4F^{-0.17} - 3)e^{2500\tau} \quad (3.1.2)$$

where τ is the temperature-dependent function:

$$\tau = \frac{1}{T} - \frac{1}{298} \quad (3.1.3)$$

Distribution coefficients and pseudo-equilibrium constants of Pu and HNO_3 are:

$$D_{Pu} = K_{Pu}[\text{TBP}]_{or}^2 \quad (3.1.4)$$

$$K_{Pu} = K_U(0.20 + 0.55F^{1.25} + 0.0074[\text{NO}_3^-]_{aq}^2)(4F^{-0.17} - 3)e^{-200\tau} \quad (3.1.5)$$

$$D_{H1} = K_{H1}[\text{TBP}]_{or} \quad (3.1.6)$$

$$D_{H2} = K_{H2}[\text{TBP}]_{or}^2 \quad (3.1.7)$$

$$K_{H1} = (0.135[\text{NO}_3^-]_{aq}^{0.85} + 0.005[\text{NO}_3^-]_{aq}^{3.44})(1 - 0.54e^{-15F}e^{340\tau}) \quad (3.1.8)$$

$$K_{H1} = K_{H2} \quad (3.1.9)$$

where the subscripts $H1$ and $H2$ refer to the form of the nitric acid in the organic phase as illustrated, respectively, in Eq. 2.1.1 and Eq. 2.1.2.

Richardson's correlations have been used by many authors to model U and Pu extraction by TBP [28, 29, 27, 30, 31, 32, 33, 34, 38, 36, 37]. Kumar and Koganti suggested different models to predict extraction of U(VI) and HNO_3 [44, 43]. However, their models are only valid at room temperature and 30% TBP/kerosene (v/v). The temperature in the stripping operations is around 50°C, hence the models developed by Kumar and Koganti are not applicable in the back extraction operations. Also, varying TBP fraction will be investigated in this thesis.

Zirconium and ruthenium

Zirconium and ruthenium can be present in the nitric acid media in a variety of chemical forms [6]. They can be extracted by TBP, in particular at low acidity. Distribution coefficients of Zr and Ru have been calculated as proposed by Natarajan *et al.* [39], as a function of the ionic strength [39]:

$$D_{Zr} = K_{Zr}[\text{TBP}]_{or}^2 \quad (3.1.10)$$

$$D_{Ru} = K_{Ru}[\text{TBP}]_{or}^2 \quad (3.1.11)$$

where

$$\ln K_{Zr} = 0.2685[\text{NO}_3^-]_{aq}^2 - 0.6359[\text{NO}_3^-]_{aq} + 0.4853 \tag{3.1.12}$$

$$\ln K_{Zr} = -0.0691[\text{NO}_3^-]_{aq}^3 \, 0.8356[\text{NO}_3^-]_{aq}^2 - 2.3672[\text{NO}_3^-]_{aq} + 0.9165 \tag{3.1.13}$$

Limited data are available in the literature regarding the modelling of Zr and Ru extraction.

Technetium

During the dissolution, Tc is present as TcO_4^-. Its extraction is complex and can be represented by the following reactions [6]:

$$\text{H}^+ + \text{TcO}_4^- + 3\text{TBP} \rightleftharpoons \text{HTcO}_4 \cdot 3\text{TBP} \tag{3.1.14}$$

$$\text{UO}_2(\text{NO}_3)_2 \cdot 2\text{TBP} + \text{TcO}_4^- + 3\text{TBP} \rightleftharpoons [\text{UO}_2(\text{NO}_3)(\text{TcO}_4)] \cdot 2\text{TBP} \tag{3.1.15}$$

$$\text{M}(\text{NO}_3)_2 \cdot 2\text{TBP} + \text{TcO}_4^- + 3\text{TBP} \rightleftharpoons [\text{M}(\text{NO}_3)(\text{TcO}_4)] \cdot 2\text{TBP} \tag{3.1.16}$$
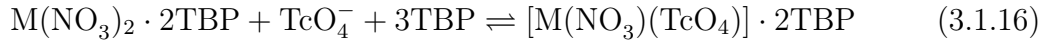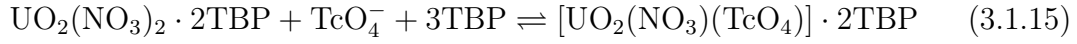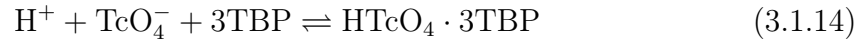
where M can be either Pu or Zr. The importance on the above reactions depends on the nitric acid concentration. The equilibrium phase behaviour of Tc is estimated as suggested by Asakura *et al.* [112], considering the influence of U, Pu, Zr concentrations and temperature:

$$D_{Tc} = D_{Tc,0} + D_{Tc,U} + D_{Tc,Pu} + D_{Tc,Zr} \tag{3.1.17}$$

$$D_{Tc,0} = 0.845[\text{TBP}]_{or}^{1.92e^{3300\tau}} \times \tag{3.1.18}$$

$$\times \frac{2.324[\text{NO}_3^-]_{aq}^{0.848e^{230\tau}} e^{8070\tau} e^{-350\tau}}{1 + 0.157[\text{NO}_3^-]_{aq}^{4.69e^{410\tau}} e^{324\tau} + 1.72[\text{NO}_3^-]_{aq}^{1.95e^{160\tau}} e^{3150\tau}} \tag{3.1.19}$$

$$D_{Tc,U} = 0.331 \frac{[\text{UO}_2^{2+}]_{or}}{[\text{UO}_2^{2+}]_{or} + [\text{Pu}^{4+}]_{or}} \{1 + 4.87[\text{NO}_3^-]_{aq}^{-1.343} e^{980\tau}\} e^{-1060\tau} \tag{3.1.20}$$

$$D_{Tc,Pu} = 3.31[\text{NO}_3^-]_{aq}^{-0.707} \frac{[\text{Pu}^{4+}]_{or}}{[\text{UO}_2^{2+}]_{or} + [\text{Pu}^{4+}]_{or}} e^{-1060\tau} \tag{3.1.21}$$

$$D_{Tc,Zr} = 1670[\text{Zr}]_{or}[\text{NO}_3^-]_{aq}^{-0.707} e^{2810\tau} \tag{3.1.22}$$

where τ, calculated by Eq. 3.1.3.

Similarly to Zr and Ru, limited information on the distribution coefficient of Tc can be found in the literature.

Neptunium

Np(IV) (as Np^{4+}) and Np(VI) (as NpO_2^{2+}) are easily extractable, according to the following reactions:

$$NpO_2^{2+} + 2NO_3^- + 2TBP \rightleftharpoons NpO_2(NO_3)_2 \cdot 2TBP \qquad (3.1.23)$$

$$Np^{4+} + 4NO_3^- + 2TBP \rightleftharpoons Np(NO_3)_4 \cdot 2TBP \qquad (3.1.24)$$
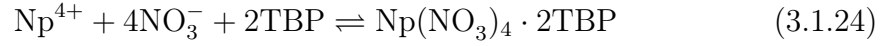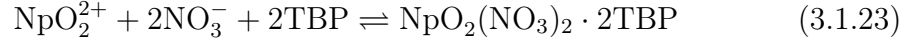
Their equilibrium behaviour has been described as suggested by Benedict *et al.* [40], but using the recalculated coefficients suggested by Kumar and Koganti for the same database of 88 experimental points [41]:

$$D_{Np(VI)} = 0.52768 D_U \qquad (3.1.25)$$

$$D_{Np(IV)} = 1.109 \cdot 10^{-7} e^{0.29623[NO_3^-]_{aq} + 0.041519T} D_U \qquad (3.1.26)$$

Kumar and Koganti [41] proposed another model to predict the distribution coefficients of Np(IV) and Np(VI). However, similarly to the case of U(VI), the model is valid only with a mixture 30% TBP/kerosene. Hence, the correlation by Benedict *et al.* has been used in this work.

Np(V), as NpO_2^+, is almost unextractable; therefore, a nominal value of 0.01 has been used for its distribution coefficient [42].

Nitrous acid

HNO_2 is a product from nitric acid radiolysis, which affects Np redox kinetics. A concentration of HNO_2 of 10^{-3} M has been included in the feed to simulate its generation [42]. It is extractable by TBP, according to the reactions:

$$H^+ + NO_2^- + TBP \rightleftharpoons HNO_2 \cdot TBP \qquad (3.1.27)$$
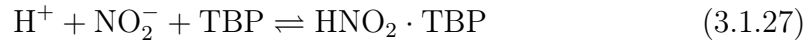
The correlations suggested by Uchiyama [113] have been used to describe the equilibrium of HNO_2:

$$D_{HNO_2} = 25[TBP]_{or} \qquad (3.1.28)$$

Kumar and Koganti suggested an empirical correlation to estimate the distribution coefficient of HNO_2 [45]. However it is only valid for a limited range of TBP concentration in the organic solvent.

3.1.2 Redox reactions

The Np control in the PUREX process is complex because its different oxidation states convert to each other while their thermodynamic behaviour is different. The kinetic of the reduction and oxidation reactions between Np(IV), Np(V) and Np(VI), as shown in Eqs. 2.1.3–2.1.4, have been described through the following reaction rates [42]:

$$-\frac{d[\text{NpO}_2^+]_{aq}}{dt} = 2.884 \times 10^{11} e^{-\frac{9922}{T}} [\text{NpO}_2^+]_{aq} [\text{HNO}_2]_{aq}^{0.5} [\text{H}^+]_{aq}^z [\text{NO}_3^-]_{aq}$$
$$+ 5.405 \times 10^{12} e^{-\frac{10031}{T}} [\text{NpO}_2^+]_{aq} [\text{HNO}_2]_{aq} [\text{H}^+]_{aq} \qquad (3.1.29)$$

$$-\frac{d[\text{NpO}_2^{2+}]_{aq}}{dt} = 2 \times 6.928 \times 10^{10} e^{-\frac{7505}{T}} [\text{NpO}_2^{2+}]_{aq} [\text{HNO}_2]_{aq} [\text{H}^+]_{aq}^{-1}$$
$$+ 2 \times 2.497 \times 10^{12} e^{-\frac{7806}{T}} [\text{NpO}_2^{2+}]_{aq} [\text{HNO}_2]_{aq}^{1.5} [\text{H}^+]_{aq}^{-0.5} [\text{NO}_3^-]_{aq}^{-0.5}$$
$$(3.1.30)$$

In Eq. 3.1.29, the most suitable value of the exponent z, for nitrous acid concentration of around 10^{-3} M, is 2 [114].

The kinetic law for Eq. 2.1.4 is taken from Tachimori [46]:

$$-\frac{d[\text{NpO}_2^+]_{aq}}{dt} = 4.1667 \times 10^{-2} [\text{NpO}_2^{2+}]_{aq}^2 [\text{H}^+]_{aq}^2 \qquad (3.1.31)$$

$$-\frac{d[\text{Np}^{4+}]_{aq}}{dt} = 1.3333 \times 10^{-5} [\text{Np}^{4+}]_{aq} [\text{NpO}_2^{2+}]_{aq} (2.16 + 12.5 [\text{NO}_3^-]_{aq}) \qquad (3.1.32)$$

The Np(V) oxidation in the organic phase has been considered, as well. However, contrarily to Eq. 2.1.3, it is assumed to be only a forward reaction from Np(V) to Np(VI) [42]:

$$-\frac{d[\text{NpO}_2^+]_{or}}{dt} = 1.952 \times 10^{11} e^{-\frac{9008}{T}} [\text{NpO}_2^+]_{or} [\text{HNO}_2]_{aq}^{0.5} [\text{H}^+]_{aq}^{0.5} [\text{H}_2\text{O}]_{or}^{-0.2} \qquad (3.1.33)$$

where water solubility in organic phase is assumed constant and equal to 0.42 M [42].

3.1.3 Nuclear criticality

To ensure safety with respect to nuclear criticality, the effective multiplication factor k_{eff} must be calculated. It is defined as the ratio between the number of

neutrons produced by fission in one neutron generation and the number of neutrons lost in the previous neutron generation (due to absorption and leakage, see Eq. 1.5.1). It should be rigorously calculated by codes that solves the time-dependent transport equation of the neutron flux. However, this type of equations is too computationally expensive and not suitable for the purpose of this work.

Here, the migration-area approximation has been used to calculate the effective multiplication factor k_{eff}, as follows [115]:

$$k_{eff} = \frac{k_{\infty}}{1 + M^2 \, B^2} \tag{3.1.34}$$

where migration area M^2 and infinite multiplication factor k_{∞} are parameters provided by nuclear handbooks, as a function of uranium and plutonium concentrations [115]. To simplify calculations, only values of M^2 and k_{∞} corresponding to the feed concentrations have been considered. This is the worst case, which involves the highest uranium and plutonium concentrations in the whole process. The buckling parameter B^2 depends on geometry. For a cylindrical shape channel, B^2 is given by:

$$B^2 = \left[\frac{2.405}{r + \delta}\right]^2 + \left[\frac{\pi}{L + 2\delta}\right]^2 \tag{3.1.35}$$

where δ is the extrapolation distance. This correlation does not take into account fission products and minor actinides, which are approximately 3% of the initial feed but highly active. Hence, minor actinides and fission products may affect the k_{eff}, resulting in underestimated k_{eff}. Further and more detailed calculations would be required, Eq. 3.1.35 can provide an approximated estimation of the nuclear criticality risk. However, due to the very small holdup and the high surface area to volume ratio, the expected k_{eff} in small channels using Eq. 3.1.35 is lower than 0.2 in the small extractors, and lower than 0.6 in the manifold distributors. Therefore, subcriticality is likely to be guaranteed, because of two reasons: the low values of k_{eff} and the geometry of the small channels, also compared to the geometry of centrifugal extractors, which ensures criticality safety.

3.2 Modelling of liquid-liquid extraction in small channels

Mass balance within the small channels is described assuming ideal plug flow, the mass transfer correlation is taken from literature. Similarly to numerous authors, steady state conditions have been considered. A multi-stage "pseudo" counter-current design is assumed. This configuration refers only to the pattern of the two streams outside the channels, as within the small contactor the flow can only be co-current. A co-current configuration is not practicable when high extraction efficiencies are required. A multi-stage cross-flow configuration, *i.e.* with a fresh nitric acid solution to each stage, will be investigated in Chapter 6. The possibility of fresh solvent in each stage will not be investigated, as the use of TBP, which is expensive, would be high. Manifolds are designed to "scale out" the channels and increase the overall throughput. The "scale-up" of the channels, above a certain value of diameter, is not beneficial: the advantages of the small-scale contactors, in terms of mass transfer and control of hydrodynamics, would be lost.

3.2.1 Mass balance

Ideal plug flow condition is assumed in the separation units, the small extractors. Therefore, the following simplifying assumptions have been incorporated:

- complete mixing along the radial direction;

- no velocity gradient along the radial direction;

- constant volumetric flow rates throughout the channel;

- no axial mixing.

The plug flow condition is widely used for the estimation of the mass transfer coefficient in this micro/small channels [21, 24]. The system is assumed homogeneous. It is a simplification of the system, to easily calculate the mass transfer coefficient from inlet and outlet concentrations. As segmented flow is studied in this work, in the real system there are dispersed plugs in a continuous phase. The regime is laminar, so the velocity has actually a parabolic profile. However, the

plug flow model can be used to accurately replicate the experiment's results. The radial gradients can be evaluated with more computational expensive models, such as CFD models, if the aim is to gain a detailed understanding of the physical and chemical phenomena occurring within the channel. However, this is beyond the goal of this work. The volume flow rate can be considered constant, the mass transfer does not affect it significantly. Axial diffusion can be neglected as the Peclet number, defined as $Pe = vL/\mathscr{D}$, is high, which makes the plug flow assumption particularly suitable to model these systems. A sketch of the plug flow model is shown in Figure 3.2.1.

Some analogies can be noted between small channels and extraction columns: both technologies are differential contactors, *i.e.* a concentration profile along the length and, typically, equilibrium concentration is not reached at the end of each stage (contrary to stage-wise contactors such as mixer-settlers and centrifugal contactors). In industry, extraction columns are often designed assuming a plug flow [116], although axial diffusion is considered since the Peclet number is not negligible.

In an infinitesimal volume element, the mass balance of the component i in the phase k, after the assumptions mentioned above, becomes:

$$\dot{V}_k C_k\Big|_L = k_L(C_{i,k} - C_{i,k}^{eq})A + \dot{V}_k C_{i,k}\Big|_{L+\delta L} + \sum R_{i,k}A\varphi_k\delta +$$
$$+ A\varphi_k\delta L\frac{\delta C_{i,k}}{\delta t} \tag{3.2.1}$$

$$\dot{V}_k C_k\Big|_L - C_{i,k}\Big|_{L+\delta L} = k_L(C_{i,k} - C_{i,k}^{eq})A + \sum R_{i,k}A\varphi_k\delta + A\varphi_k\delta L\frac{\delta C_{i,k}}{\delta t} \tag{3.2.2}$$

$$-v_k\frac{\delta C_{i,k}}{\delta L} = k_L\, a(C_{i,k} - C_{i,k}^{eq}) + \sum R_{i,k}\varphi_k + \varphi_k\frac{\delta C_{i,k}}{\delta t} \tag{3.2.3}$$

No process controls or transient operations are going to be investigated in this work, therefore the mass balance in small channels is modelled assuming steady state conditions. The aim is to optimise both design and operating variables for a liquid-liquid extraction process using small extractors, to investigate future SNF flowsheets. In process engineering, steady state process optimisations are often employed to design chemical processes [26]. Steady state models have been proposed in the literature to design equipment used in SNF reprocessing, such as extraction columns as suggested by Kumar and Hartland [116]. Also, at the Idaho National Engineering and Environmental Laboratory, steady-state simulations were carried
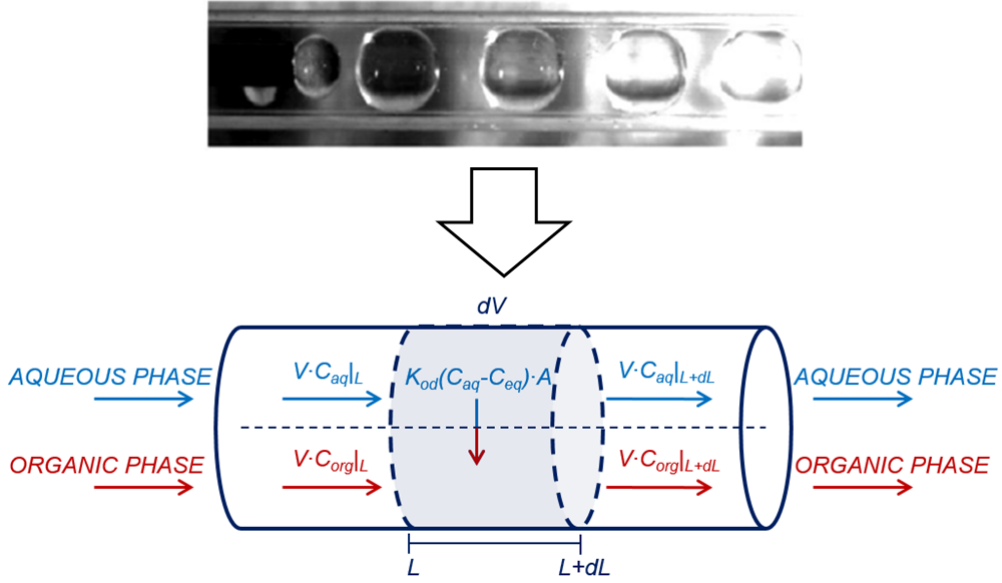
Figure 3.2.1: Schematic diagram of the plug flow model, assuming steady state. The mass balance of the solute, for each phase and over a volume element dV, is depicted. In the figure, mass transfer is assumed to occur from the aqueous to the organic phase. No reaction terms are considered in the sketch (e.g. for U and Pu). Image of segmented flow, at the top, taken from [84].

out to design and optimise centrifugal contactors for liquid-liquid extraction in a High Level Waste treatment facility [117]. Assuming steady state, Eq. 3.2.3 becomes:

$$v_k \frac{\delta C_{i,k}}{\delta L} + k_L a(C_{i,k} - C_{i,k}^{eq}) + \sum R_{i,k}\varphi_k = 0 \qquad (3.2.4)$$

The mass balance therefore consists of a convective term (first one from the left), a mass transfer term (second one) and a reactive term (third one).

The solubility of TBP in the aqueous phase is very low and the mass transfer of TBP from organic to aqueous phase can be neglected. The free TBP concentration, in the organic phase, can be calculated from the chemical reactions that occur in the extraction process:

$$[\text{TBP}] = [\text{TBP}]_0 - \sum \nu_i [\text{C}]_i^{org} \qquad (3.2.5)$$

where $[\text{TBP}]_0$ is the initial concentration of the fresh TBP, equal to $F \times \rho_{TBP}/MW_{TBP}$ (F is the TBP volume fraction, ρ mass density, MW molecular weight), $[\text{C}]_i^{org}$ is the concentration of the extracted component i in the organic phase. The parameter ν is the stoichiometric coefficient of the extracted component i in its extraction reaction. For example, according to Eqs. 1.3.1 and 1.3.2, ν is 2 for both U and Pu. All the stoichiometric coefficients are reported in Table 3.2.1. Some fission products exist in several forms and the stoichiometric coefficient may differ. However, considering their very small concentrations if compared to the TBP concentration, this difference has a negligible impact on the results.

Table 3.2.1: Stoichiometric coefficients for TBP mass balance (Eq. 3.2.5).

Component	Stoichiometric coefficient ν
U	2
Pu	2
HNO_3 (as in Eq. 2.1.1)	1
HNO_3 (as in Eq. 2.1.2)	2
Zr	2
Ru	2
Tc	3
Np(IV)	2
Np(V)	2
Np(VI)	2
HNO_2	2

For components not involved in any redox reaction, such as Zr or Ru, Eq 3.2.4 can be analytically solved as shown below:

$$-v_k \frac{dC_{i,k}}{dL} = k_L a (C_{i,k} - C_{i,k}^{eq}) \tag{3.2.6}$$

$$-v_k \int_{C_{i,k}^{in}}^{C_{i,k}(L)} \frac{dC}{C_{i,k} - C_{i,k}^{eq}} = \int_0^L k_L a dL \tag{3.2.7}$$

$$-v_k \ln\left(\frac{C_{i,k}(L) - C_{i,k}^{eq}}{C_{i,k}^{in} - C_{i,k}^{eq}} \right) = k_L a L \tag{3.2.8}$$

$$C_{i,k}(L) = C_{i,k}^{eq} - (C_{i,k}^{eq} - C_{i,k}^{in}) \exp(-k_L a \tau_k) \tag{3.2.9}$$

where the residence time τ in the phase k is:

$$\tau_k = \frac{L}{v_k} \tag{3.2.10}$$

However, due to the reaction term, Eq. 3.2.4 has been solved for all components numerically, converting the ordinary differential equation to a system of algebraic equations, using a uniform grid and by application of a fourth order Runge-Kutta method. The Runge-Kutta method has been used in the literature to solve plug flow in pulsed columns [63]. The granularity of the discretisation affects the size of the mathematical model. Eq. 3.2.9 was used to identify the optimal number of grid points, by comparing numerical and analytical solution while varying the number of grid points (excluding any chemical reaction).

3.2.2 Flow pattern configuration

A single stage is not sufficient to meet the industrial requirements in terms of separation efficiency. Therefore, a multi stage pseudo counter-current design has been considered. "Pseudo" since this counter-current flow configuration only applies to the flow arrangement outside the channels; within the channels, the flows are co-current, as depicted in Figure 3.2.2. This flow configuration requires significantly less fresh solvent than a cross-flow design for extraction operations, whilst a co-current configuration is not practical. A cross-flow design for back extraction, where the fresh stream is the aqueous one, will be investigated in Chapter 6. A similar counter-current configuration is used in the PUREX process with mixer-settler banks and centrifugal extractors. Within each stage the flow is distributed to a large number of channels using the distribution manifolds, as shown in Figure 3.2.4 and discussed in detail in Section 3.2.6. All the channels have been assumed equally sized, which simplifies maintenance operations.
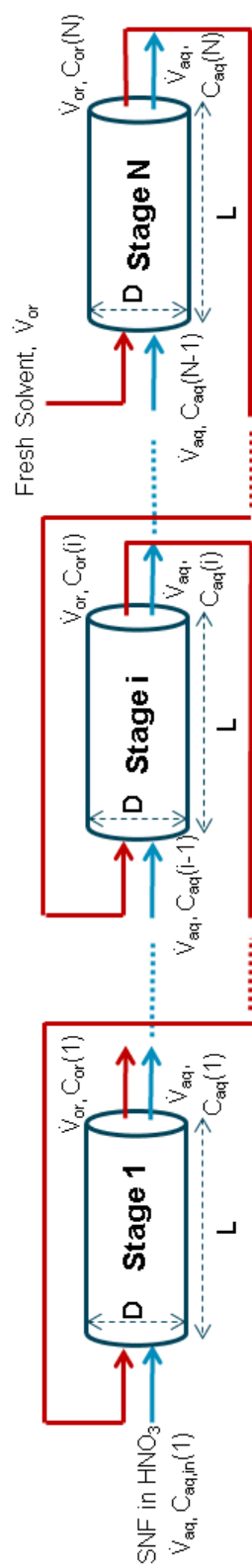
Figure 3.2.2: Schematic of the "pseudo" counter-current design. Only the first, a generic intermediate (i) and the final stages (N) are shown. Dotted lines are in placed of the remaining stages between the stages. The blue streams refer to the aqueous phase, red streams to the organic phase.

49

3.2.3 Mass transfer

The volumetric mass transfer coefficient $k_l a$ has been calculated as suggested by Kashid *et al.* [20], as a function of superficial velocity v, channel diameter D and length L:

$$k_L a = 0.88 \, \frac{v_{mix}}{L} \, Ca^{-0.09} \, Re_{mix}^{-0.09} \left(\frac{D}{L} \right)^{-0.1} \tag{3.2.11}$$

Reynolds and Capillary numbers have been calculated for the organic phase, which is the continuous phase in most of the investigated flowsheets in this thesis, rather than for the mixture. This assumption simplifies the calculations and does not affect the results. The viscosity, which is the most important difference between aqueous and organic phase, does not affect the $k_L a$, because of the same exponent (-0.09) for Ca and Re. The difference in the mass density between organic and aqueous phase has a negligible effect on $k_L a$. Using the density of the aqueous phase, a 2% difference in the $k_L a$ is achieved, however the density of the mixture is an average value between the aqueous and organic values, therefore the resulting difference in $k_L a$ is expected to be between 0 and 2%.

Eq. 3.2.11 seems to be the most suitable for the current work among all the empirical and semi-empirical correlations proposed in the literature. Tsaoulidis and Angeli showed that Eq. 3.2.11 exhibits a good agreement with experimental data of uranium extraction in small channels [24], although with a different solvent (TBP/IL) and hence with recalculated parameters.

Despite the volumetric mass transfer coefficient is experimentally measured assuming plug flow and constant $k_L a$ along the length, as can be noted from Eq. 3.2.11, the channel length affects the mass transfer coefficient: this is enhanced for short channel, due to the more intense internal circulation close to the mixing junction [24]. Hence, the resulting $k_L a$ is actually the average volumetric mass transfer coefficient $\overline{K_L \, a} = \int_0^L K_L a : dL / \int_0^L dL$.

Eq. 3.2.11 is nonlinear. This can cause numerical difficulties, especially in large model. Hence, for complex case studies, the linearisation of this equation can be beneficial. We will investigate this possibility in Chapter 6, due to the complexity of the case study.

The mass transfer model does not take into account variations in the phase flow ratio, which affects the interfacial area a and therefore the value of $k_L a$. Instead,

a correction factor Θ has been included in the model and multiplied to the $k_L a$,

$$\Theta = -0.511 \log\left(\frac{\dot{V}_d}{\dot{V}_c}\right) + 0.9702 \tag{3.2.12}$$

based on experimental data from Tsaoulidis *et al.* [21]. Experiments showed that increasing the dispersed (aqueous) to continuous flow rate ratio improves the liquid-liquid interfacial area and therefore the mass transport. Thus, the $k_L a$ calculated in this work for small channels is actually $k_L a = \Theta \times k_L a|_{Eq.3.2.11}$

It is worth noting that Kashid has correlated the mass transfer coefficient to the velocity of the mixture by a rearranged version of the Eq. 3.2.9. Hence, if the mass transfer coefficient from Eq. 3.2.11 is used in Eq. 3.2.9 (analytical solution of the mass balance), v_{mix} must be used in place of v_k in Eq. 3.2.10.

3.2.4 Pressure drop

To predict the pressure drop within the channel, the model developed by Kashid and Agar for two-phase liquid-liquid flows has been implemented [19]. They calculated the overall pressure drop as the sum of frictional losses and interfacial pressure drop (because of the dispersed phase):

$$\Delta P_{fr,aq} = \frac{8\mu_{aq}v_{mix}\alpha L_{UC}}{r^2} \tag{3.2.13}$$

$$\Delta P_{fr,org} = \frac{8\mu_{org}v_{mix}(1-\alpha)L_{UC}}{r^2} \tag{3.2.14}$$

$$\Delta P_{int} = \frac{2\gamma}{r}cos\theta \tag{3.2.15}$$

where α is the aqueous phase fraction, θ the contact angle, which has been assumed to be 70°, such as similar systems in PTFE channel [84].

An important impact on the overall pumping cost may be due to the singularity losses (such as an elbow, valve, tee, *etc.*). In particular, a significant contribute to the overall pressure drop is due to the presence of the mixing junction, where the two streams are mixed before entering the small-scale extractor. Singularity losses are often estimated using a resistance coefficient K_r [105, 109]:

$$\Delta P_{loc} = \frac{K_r \rho v^2}{2} \tag{3.2.16}$$

The total singularity loss is given by the sum of all singularity losses.

The resistance coefficient used in this work for the local pressure drop in the mixing junction is approximately equal to 4.8 (if SI units are used for velocity and mass density and pressure drop is expressed in kPa, as typically done). It has been obtained from the experimental data reported by Kashid *et al.* [19]. They measured the local pressure drop ΔP_{loc} in a Y-junction, 120°, for different superficial velocities, with microchannels (500 μm of diameter) and a segmented flow water-cyclohexane (physical properties similar to nitric acid solution and typical paraffinic diluent). This pressure loss is expected to be the prevalent one, which makes the value of the contact angle θ in Eq. 3.2.15 not crucial for pressure drop estimations.
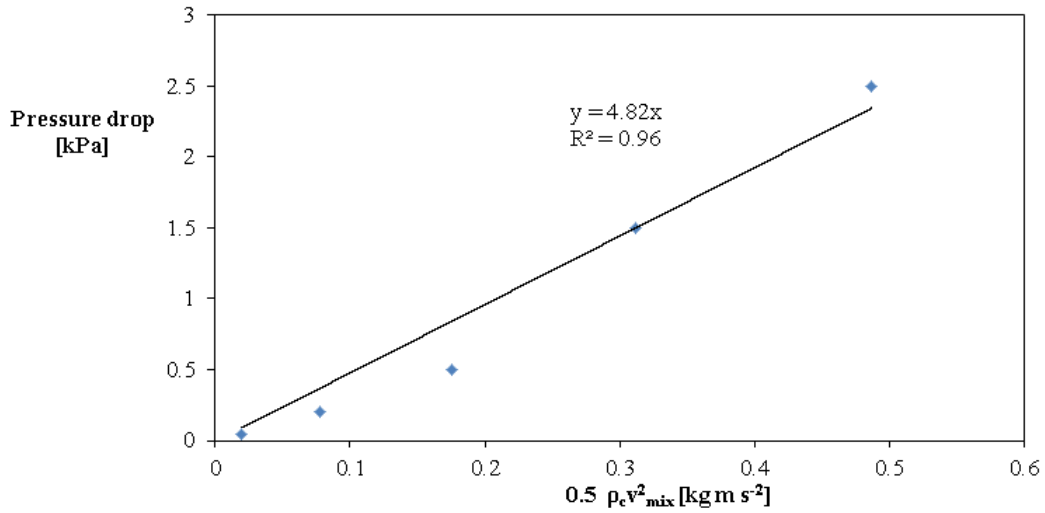
Figure 3.2.3: Singularity loss in the mixing junction plotted against $1/2\rho v_{mix}^2$, for the estimation of the resistant coefficient K_r .

3.2.5 Two-phase separation

The separation of the two phases at the end of the channel can be achieved by exploiting the difference in surface wettability between aqueous and organic phases. If the aqueous phase is dispersed, the flow splitter can consist of a hydrophobic mainstream branch and a hydrophilic sidestream branch (such as stainless steel

needles), and vice-versa if the aqueous phase is continuous (hydrophilic main-stream, hydrophobic sidestream). The cost of the separator may significantly affect the economics of the overall equipment. In this work, the model suggested by Scheiff *et al.* [110] has been used. The model, based on a pressure balance using the Hagen-Poiseuille equation (as Kashid and Agar, see Eqs. 3.2.13 and 3.2.14), allows to design the required mainstream and sidestream channels to separate the dispersed plugs from the continuou phase.

3.2.6 Flow distribution

The design of a flow network to distribute the flow rate in the parallel channels is important to ensure reasonable pressure drop and flow uniformity among the parallel small channels. Many authors have investigated flow networks for micro or small devices, and the comb-like network seems to be the most appropriate for the compact arrangement of small channels in a stack [103, 104, 105, 106, 107, 108, 109].

The methodology developed by Commenge *et al.* [108], based on a electrical resistances network model and laminar flow, has been used in this work. Due to the large number of parallel channels, a four-level structure has been considered (see Figure 3.2.4). The fourth level connects the different modules, the third level connects the different plates containing the small channels, whilst the second level connects the small extractors, which represent the first level. Mixing junctions are required at the beginning of the first level, as well as the separator at the end. The first level is shared between the two networks, one for each phase. For each level i, the hydraulic resistance R is defined as:

$$R_i = \frac{\Delta P_i}{\dot{V}_i} \qquad (3.2.17)$$

Assuming laminar flow, the Hagen-Poiseuille equation (Eqs. 3.2.13 and 3.2.14) can be used to predict the frictional pressure drop in levels 2, 3 and 4. Therefore, in the aforementioned levels, the hydraulic resistance of R_i, assuming non-circular channel, can be calculated as:

$$R = \frac{32\mu L_i \lambda_{NC}}{D_H^2} v \qquad (3.2.18)$$

where λ_{NC} is the non-circularity coefficient and D_H is the hydraulic diameter (for further details, see [105]). A square section is assumed, to simplify calculations.
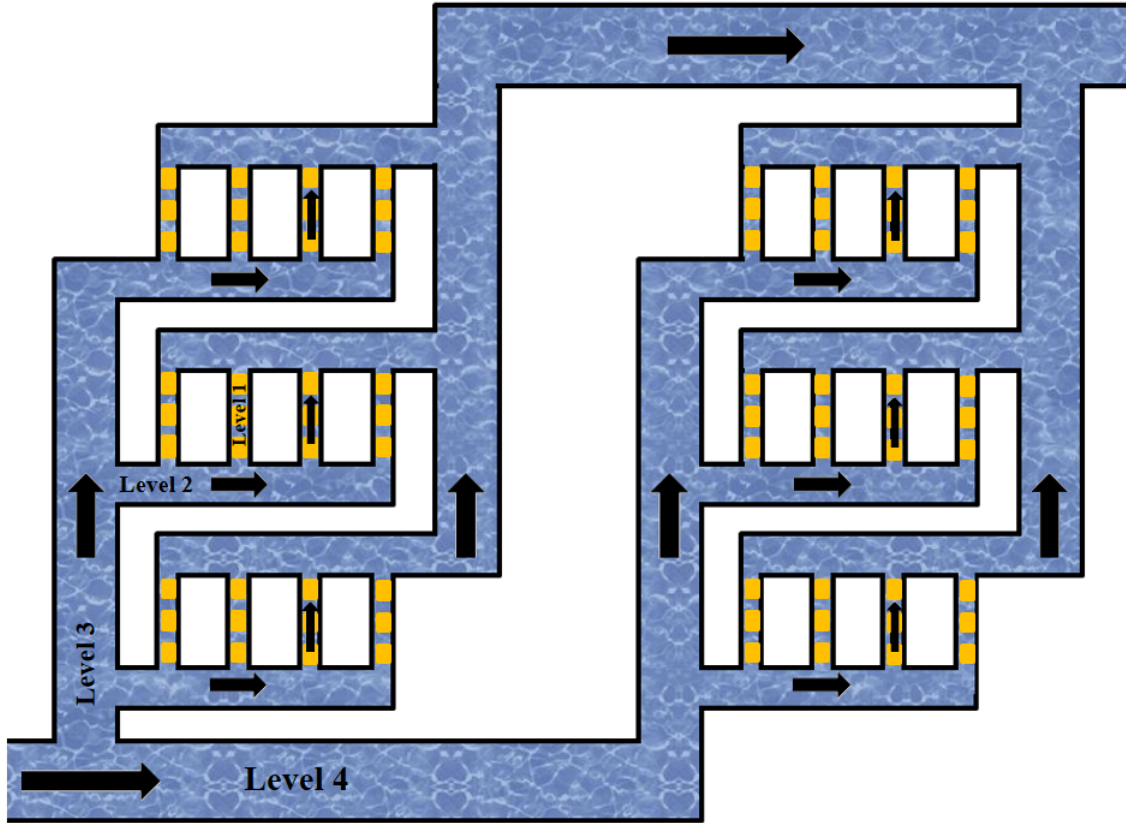
Figure 3.2.4: Schematic of a four-level network. In this sketch, one element in the level 4, two in the level 3, three in the level 2 and four in the level 1 are shown. The level 1 consists of the small extractors (yellow dispersed plugs are shown).

Exploiting the electrical circuit analogy, a network considering the system up to the nth level may be described by the equivalent hydraulic resistance $R_{1.n}$:

$$R_{1.n} = \frac{\sum_{i=1}^{i=n} \Delta P_i}{\dot{V}_n}$$

For instance, $R_{1.2}$ is the equivalent resistance of the sub-network involving a first and a second level, given by the ratio between the total ΔP in the first two levels the and volume flow rate entering the second level. Using the electrical analogy, the pressure drop can be easily calculated as the product of equivalent resistance and the volume flow rate (similarly to $V = R_{eq} \times I$ in the electrical

system). The flow distribution depends on the pressure drops within the network, and therefore on the hydraulic resistances.

The resistance ratio r is defined as the ratio between the equivalent resistance at one level and the resistance at the level above:

$$r = \frac{R_{1.n}}{R_{n+1}} \tag{3.2.19}$$

Many definitions are used in the literature to quantify flow maldistribution Fd. Commenge $et\ al.$ use the maximum flow difference to the average one [108]. The global flow maldistribution can be calculated as $Fd_{global} = 1-(1-Fd_1)(1-Fd_2)(1-Fd_3)$, where Fd_1, Fd_2 and Fd_3 are the flow maldistributions in their respective levels (level 4 is given by one only channel, see Figure 3.2.4). To simplify the calculations, the flow maldistribution is calculated by fitting the values provided by Commenge $et\ al.$ as a function of the number of channels and the resistance ratio, rather than solving mass and pressure balance for each node of the network and its loops (the number of nodes is not fixed but depends on the optimal design of the flow network). A parabolic equation $Fd(r, N) = a(r)N^2 + b(r)N$ is used, where N here is the number of elements in the sub level and $a(r)$ and $b(r)$ are nonlinear functions of the resistance ratio r.

Also, singularity losses in the manifolds, due to contraction, turning, splitting, combining and increase in the section area have been calculated using the resistance coefficients [105]. These further contributes to the overall pressure drop are used to calculate the total pressure drop in each level. However, apart from the first level where a significant pressure drop in the mixing zone occurs, these singularity losses are expected to be negligible if the Reynolds number is low.

3.2.7 Economics

The cost of channels has been formulated as linear function of diameter D and length L, hence $CapEx_{ch} = (k_1 \times D + k_2) \times L$, with k_1 and k_2 constants. D refers to the channel width for levels 2, 3 and 4. Cost for mixing junctions, considered fixed for each junction, is also included. The cost of manifolds is calculated, as a first estimation, as sum of channels cost and mixing junctions cost. A linear scaling factor is assumed [118]. Channels are assumed to be either hydrophobic, made of PTFE, or hydrophilic, made of stainless steel. PTFE has been investigated and

used for spent nuclear reprocessing, specifically for sieve plates in pulsed columns [38, 119, 120], as well as stainless steel. All the costs are taken from CM Scientific Laboratory Supplies [121], which provides transparent fluoropolymer and stainless steel channels for laboratory use. The cost of the polymeric channels has been multiplied by a material factor of 0.1, to convert the price in nontransparent polymer such as PTFE, taking into account typical market prices. The material factor is also used to predict more reasonable values for the comparison with traditional technologies, which is one of the goals of this work, as we will see in the Chapter 5.

The operating expenditure is the cost for pumping power $P = \dot{V}\Delta P_{tot}/\eta$ where η, the pump efficiency, is assumed to be 0.8. The cost of 1 kWh is assumed £0.10. The total pressure drop, ΔP, for pumping cost calculations includes:

- single phase frictional pressure drops in the distributing and collecting channels (i.e. levels 2, 3 and 4);

- singularity losses in the network, however they are expected to be negligible if laminar flow is established;

- the pressure drops in the mixing junction, this singularity loss is not negligible despite the laminar regime;

- the pressure drop of the two-phase flow in the extraction channel (level 1), given by frictional and interfacial pressure drops;

- the pressure drops in the mainstream and sidestream channels to achieve the phase separation.

3.2.8   Other equations

An important parameters in an extraction operation is the extraction E, defined as:

$$E = \frac{C_i^{in}(1) - C_i^{out}(N)}{C_i^{in}(1)} \qquad (3.2.20)$$

$$(3.2.21)$$

where $C_i^{in}(1)$ is the inlet concentration of the component i in the first stage, $C_i^{out}(N)$ is the outlet concentration in the last stage (N). In a SNF reprocessing plant, E must be higher than 99% for the components of interest (U, Pu). E will be used, in all the case studies investigated in this thesis, in the inequality constraints to set the minimum requirements of the process.

Another parameter that will be used is the decontamination factor DF, defined as the ratio between the amount of contaminant in the feed and the one in the product stream. The DF will describe the separation of minor actinides and fission products.

3.3 Implementation of the model and solution procedure

The mathematical model have been implemented in GAMS, a commercial software commonly used for mathematical programming and optimisation. It is based on an open structure which provides a wide portfolio with all the major commercial solvers [111]. GAMS does not support differential equations, so the discretisation method to solve to convert Eq. 3.2.4 into a set of algebraic equations has been implemented in the code. Below, details of solver and optimisation procedure used are described. Also, the nonlinear expression used to calculate the volumetric mass transfer coefficient has been reformulated.

3.3.1 Solver

Several integer variables have been used in the model: the number of stages, the on/off binary variables to select the stages, the number of elements in each level of the manifolds. Hence, a MINLP solver is required. Example of MINLP solvers available in GAMS are ALPHAECP, ANTIGONE, BARON, BONMIN, COUENNE, DICOPT, KNITRO, SBB, SCIP [111].

The SSB (Simple Branch and Bound), among all the solvers, has proven to be the most suitable for this model. It is a local optimiser, hence no global optimum can be guaranteed. The Branch-and-Bound (BB) is a general algorithm proposed for solving optimisation problems. "Branch" since a branching happens when a new

node is explored, "Bound" because upper and lower bounds on the best value of the current subproblem are estimated. The branch is discarded if, compared to the "incumbent" value (the optimal one so far), it does not produce a better solution. Hence, this method can be seen as a tree search, where each node represents a subproblem of the solution set. LP relaxation of subproblems (*i.e.* integer constraints are replaced by continuous constraints) are performed. Generally, if the problems is of limited size, the BB methods can find an optimal solution in reasonable time, it can otherwise be very time-consuming. However, it also depends on the initialisation. The SBB solver is based on a combination of one the NLP solvers supported by GAMS, such as CONOPT, Snopt and MINOS, and the Branch-and-Bound method. In this work, the CONOPT solver has been used as NLP solver. CONOPT, for complex and large models, uses inner Sequential Quadratic Programming iterations based on second derivatives. CONOPT is "well suited for models with very nonlinear constraints" [111].

In optimisation problems, the "quality" of the solution must be specified. This can be done providing a value for the "relative gap" ("OPTCR" in GAMS). This value is also known as termination criteria. For the estimation of this value, two numbers are important in the Branch-and-Bound algorithm: the "best integer", which is the incumbent (which satisfies all integer requirements), and the "best estimate". Hence, the OPTCR is the relative difference between "best integer"and "best estimate". In GAMS, the default value of the OPTCR is 0.1. In this work, a relative gap of 1% has been used, this means that the algorithm terminates if the OPTCR drops below 0.01, hence providing a "better" solution.

3.3.2 Solution procedure

Due to the large size and the nonlinearity of the mathematical model, convergence difficulties and/or long computational time may occur. Furthermore, one or more recycle streams are often included in the flowsheet and this complicates the calculations. A proper initialisation is necessary to solve the system. To achieve the initialisation and solve the problem, a three-stage approach has been used:

1. The recycle stream is disconnected and optimisations is carried out. A sequential modular approach is used. If a feasible solution is not found, some degrees of freedom are specified (such as the number of stages or the channel

diameter) and point 1 repeated. Results are used as initialisation at the next step.

2. The recycle stream is connected and the unit operations are simultaneously solved. Results are saved to provide estimates for the next step.

3. All the variables are now allowed to vary and the MINLP problem, initialised, is solved.

However, this approach is general and the optimisation procedure can slightly change depending on the case study. For example, if no feasible points are not found by the solver after point 3, it might be better to gradually free the variables previously specified in the point 1, rather then free them at the same time in the point 3.

3.3.3   Rearrangement of mass transfer equation

Some numerical difficulties have been encountered to solve Eq. 3.2.11 (mass transfer correlation). This is due to its high nonlinearity. Hence, Eq. 3.2.11 has been rearranged, reformulating it from $k_L a = f(\dot{V}, L, D)$ to $k_L a = f(\dot{V}) + f(L) + f(D)$. Avoiding multiplication between free variables will facilitate the calculations. Solving the Reynolds and Capillary numbers for the velocity v and substituting $v = 4\dot{V}/(\pi D^2)$, Eq. 3.2.11 can be reformulated as:

$$k_L a = 0.44 \frac{v_{mix}}{L} Ca^{-0.1} Re^{-0.65} \left(\frac{D}{L}\right)^{-0.1} \tag{3.3.1}$$

$$0.44 \frac{v_{mix}}{L} \frac{\mu v_{mix}}{\gamma}^{-0.1} \frac{\rho v_{mix} D}{\mu}^{-0.65} \left(\frac{D}{L}\right)^{-0.1} \tag{3.3.2}$$

$$0.44 \left(\frac{\mu}{\gamma}\right)^{-0.1} \left(\frac{\rho}{\mu}\right)^{-0.65} v_{mix}^{(1-0.1-0.65)} D^{(-0.65-0.1)} L^{(-1+0.1)} \tag{3.3.3}$$

$$0.44 \left(\frac{\mu}{\gamma}\right)^{-0.1} \left(\frac{\rho}{\mu}\right)^{-0.65} \left(\frac{4\dot{V}_{mix}}{\pi D^2}\right)^{0.25} D^{-0.75} L^{-0.9} \tag{3.3.4}$$

$$0.44 \left(\frac{\mu}{\gamma}\right)^{-0.1} \left(\frac{\rho}{\mu}\right)^{-0.65} \left(\frac{4\dot{V}_{mix}}{\pi}\right)^{0.25} D^{(-20.25-0.75)} L^{-0.9} \tag{3.3.5}$$

$$0.44 \left(\frac{\mu}{\gamma}\right)^{-0.1} \left(\frac{\rho}{\mu}\right)^{-0.65} \left(\frac{4}{\pi}\right)^{0.25} \dot{V}_{mix}^{0.25} D^{-1.25} L^{-0.9} \tag{3.3.6}$$

$$C\dot{V}_{mix}^{0.25} D^{-1.25} L^{-0.9} \tag{3.3.7}$$

where in C are included constants and physical properties.

The Eq. 3.3.7 can be written as sum of different contributes exploiting the logarithmic properties:

$$\log(k_L a) = \log(c) + 0.25 \log(\dot{V}_{mix}) - 1.25 \log(D) - 0.9 \log(L) \tag{3.3.8}$$

$$k_L a = 10^{\log(c) + 0.25 log(\dot{V}_{mix}) - 1.25 \log(D) - 0.9 \log(L)} \tag{3.3.9}$$

Although the mass transfer correlation is still nonlinear, power laws and multiplication between free variables have been replaced by a sum of logarithms of the single variables, hence distinguishing the contributes of D, L and $\dot{V}$. This rearrangement has facilitated the calculations.

3.3.4 Modelling methodology

The mathematical model, described in Section 3.2, has been implemented in the GAMS modelling system. As a large number of equations are required, the model has been built step by step. Each step has been solved. The results have been analysed for each step and have been used as initialisation for the next step, to facilitate the optimiser to solve the nonlinear mathematical system. Specifically, an eight-step approach has been used:

1. the system U/Pu/HNO$_3$-TBP has been considered; mass balance equations and empirical correlations for distribution coefficients and volumetric mass transfer coefficient have been implemented in the code;

2. the remaining components have been gradually added to the system, integrating the model with the necessary calculations for distribution coefficients;

3. estimation of pressure drops have been included in the model;

4. estimation of nuclear criticality and economics have been added to the model;

5. separator design has been considered;

6. manifold design has been included in the model;

7. chemical reactions have been gradually implemented in the model;

8. the mass balance equations to connect the process streams, according to the flowsheet investigated, have been included to the code.

3.4   Case study

A case study has been investigated to demonstrate the applicability of the mathematical model. In particular, the intensified extraction in small channels has been investigated for the first section of the PUREX process, the so-called "codecontamination" section (see Figure 1.3.1), where U and Pu are separated from the other components in the SNF. In the most modern flowsheets the codecontamination section consists of, mainly, four extraction steps [6]:

- main extraction (step 1), where U and Pu are separated from most of the other components in the SNF into an organic stream;

- Zr and Ru scrub (step 2), where a nitric acid solution is used to strip the extracted Zr and Ru (since U is also back extracted in this step, the aqueous stream is recycled to the main extraction step);

- Tc scrub (step 3), where a nitric acid solution is used to strip the extracted Tc from the organic stream, which is now ready for the U/Pu partitioning and purification cycles of U and Pu; and,

- complementary extraction (step 4), where fresh solvent is used to extract U and Pu stripped by the previous step, and the organic stream is recycled to the main extraction to increase the U recovery.

A sketch of the flowsheet is shown in Figure 3.4.1. The aim is to optimise the process, with regards to economic criteria, using the novel small-scale contactor. The objective is to minimise the Total Annualised Cost (TAC), which takes into account Operating Expenditure ($OpEx$) and Annualised Capital Expenditure ($ACapEx$) :

$$TAC = OpEx + ACapEx \qquad (3.4.1)$$

The decision variables are both design (i.e. diameter or width and length of each level in Figure 3.2.4, number of stages, number of extraction channels to increase throughput and their arrangement in the network) and operating variables
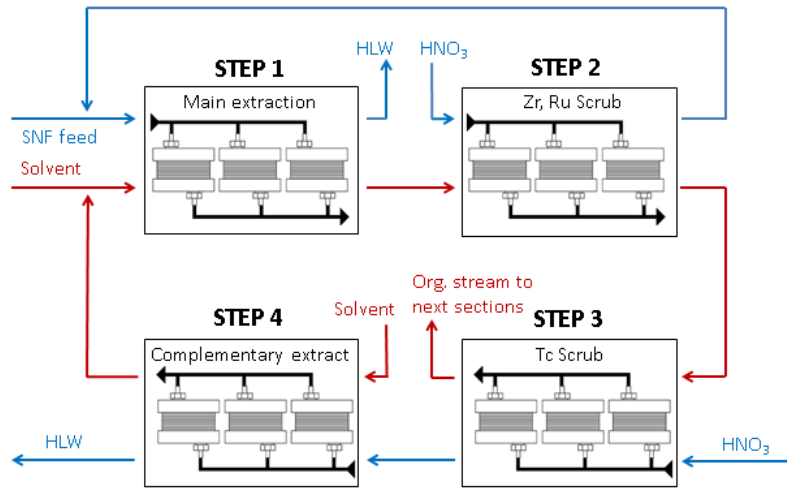
Figure 3.4.1: Schematic of the codecontamination flowsheet.

(HNO_3 concentration of all aqueous inlets, all flow rates except the aqueous feed). A summary of the optimisation problem is shown in Table 3.4.1.

Inputs of the problem are throughput, feed concentration, temperature and materials (see Table 3.4.2). The feed rate is 500 tons of heavy metals per year (MTHM y^{-1}). This throughput is an average one for SNF from Light Water Reactors (600 MTHM y^{-1} at THORP in Sellafied, UK, and 400 MTHM y^{-1} at Mayak in Russia, see Table 1.3.1). The feed concentration of the dissolved SNF in nitric acid solution is the typical one from a Light Water Reactor.

Typically, in liquid-liquid extraction operations, the continuous phase is the less expensive material, usually the aqueous phase, unless it is not convenient for other reasons. This is the case of the first extraction of SNF in the PUREX process: the aqueous feed is dispersed, instead of the organic one (the most expensive one), in order to protect the solvent from any contaminants, which will be entrained by the dispersed phase [11]. In the later steps of the flowsheet, the organic phase is typically dispersed. However, polymeric channels are more cost effective and, since in the scrubbing steps (2 and 3) the organic flow rate is expected to be significantly higher than the aqueous one, only polymeric (hydrophobic) channels have been investigated. When the organic to aqueous flow ratio is higher than one, the dispersion of the aqueous phase is advantageous as this leads to smaller

plugs and larger interfacial area.

Table 3.4.1: Optimisation problem definition, including assumptions, free variables, requirements and constraints.

Given:	Throughput, feed concentration, temperature, channel material,	
Optimise:	Design variables (number of stages, number of elements of manifold, diameter or width and length of each level), flow rates, HNO_3 inlet concentration in aqueous streams	
So as to minimise:	Annualised total cost	
Subject to:	Equality constraints:	Process model
	Inequality constraints:	$[U]_{aq,out}^{Step\ 1} \leq 1.68$ M
		$E_U \geq 0.99$
		$E_{Pu} \geq 0.99$
		Zr DF $\geq 10^4$
		Ru DF $\geq 10^4$
		Tc DF ≥ 50
		$k_{\text{eff}} \leq 0.95$
		$F_d^{\text{tot}} \leq 0.1$
		$Re \leq 2000$

The flowsheet shown in Figure 3.4.1 consists of approximately 365,000 equations, involving nonlinear equations and integer variables. Furthermore, there are two recycle streams. Hence, long computational times and convergence difficulties are expected. These difficulties are circumvented, to some degree, by adopting a sequential modular approach first, that provides the initialisation for solving the entire flowsheet simultaneously later (as mentioned in 3.3.2).

The mathematical model has been solved using the SBB solver. A termination tolerance of 1% has been used for the optimisation.

Table 3.4.2: Input parameters and flow pattern designs.

Parameter	Component/Step	Value
Feed concentration	U(VI)	1050.42
[Mol m^{-3}]	Pu(IV)	11.65
	Ru	7.59
	Zr	12.99
	Tc	2.77
	Np(V)	0.64
	HNO$_2$	1.00
Solvent concentration	TBP	1097.37
[Mol m^{-3}]		(=30% v/v)
Temperature [°C]	Steps 1, 2, 3, 4	25
Throughput [MTHM y^{-1}]	-	500
Channel material	Steps 1, 2, 3, 4	PTFE
Flow pattern design	Step 1, 2, 3, 4	Counter-current

3.4.1 Comments on model

The 4th order Runge-Kutta numerical method has been used to solve the differential mass balance equations (Eq. 3.2.4). Several attempts have been carried out to identify the appropriate number of grid points: coarser discretisation resulted in infeasible solutions, while 50 grid points were able to accurately reproduce the analytical solution (Eq. 3.2.4 can be analytically solved if no chemical reactions take place, *i.e.* for all components except neptunium).

For annualised cost, a payout time is to be set. Treybal investigated economic design of liquid liquid extraction, using mixer-settlers, up to a 5-year payout time [122]. Smith reported typical values of the latter between 5 and 10 years [123]. This process optimisation has been performed assuming a 5-year payout time. The optimisation problem has also been solved considering longer payout times, up to 10, and the optimal design has not been significantly affected.

Eq. 3.2.11 was developed for diameters varying from 0.5 to 1 mm [20], but it has been used in the literature to satisfactorily fit data up to a diameter of 2 mm

[24]. Hence, 0.5-2 mm has been used as range for the diameter.

The plug flow model satisfactorily describes the separation during segmented flow, because of the negligible axial dispersion. Hydrodynamics, in this orderly flow pattern, can be sufficiently predicted and therefore separation performance may be simply adjusted varying the flow rates within the channel or the length, to vary the residence time. Similarly, if redox kinetics are known, the Np behaviour may be easily predicted and its separation facilitated by the short residence time. The nature of the laminar flow pattern in small channels makes easier characterisation and modelling of the process, compared to the complex hydrodynamics and turbulent flows in the conventional technologies such as pulsed columns or mixer-settlers.

The typical concentration of TBP in the organic mixture has been considered, *i.e.* 30% v/v. However the model could also be employed to investigate higher TBP concentrations, improving extraction and reducing volumes of organic streams. The model could be also used with further components; in this case different distribution coefficients may need to be considered.

Regarding the robustness of the mathematical model, it is a large nonlinear model which includes integer variables and recycle streams, therefore a proper initialisation is required. The initialisation may significantly affect the optimal result. However, the latter point has not been addressed at this stage: the goal of this case study was to demonstrate the applicability of the model, rather than finding the optimal process design.

Below, the results of the case study described in Section 3.4 are discussed.

3.4.2 Results

An economic optimisation of the codecontamination section of the PUREX process has been performed. The minimum total annualised cost found is around £65,000 y^{-1}. Limited data on economics of conventional technologies are available in the literature, because of industrial confidentiality reasons. In first approximation, based on typical sizes of pulsed columns used in the PUREX process (12 m height, 0.3 m of diameter [6]), a preliminary comparison can be done. According to the correlation provided by Seider et al [124], the capital cost of a column of the aforementioned dimensions is around £200,000, so around £800,000 for four

columns. Without considering the operating costs, the total annualised cost using pulsed column is already higher than the one achieved using the small-scale contactors. However, this is a preliminary comparison based on typical data provided by the literature and other important aspects must be considered, such as size, solvent degradation, Np control, *etc.* A more detailed comparison with conventional technologies will be discussed in Chapter 5.

Table 3.4.3: *Optimal channel and manifold designs. The number of channels is intended for each stage. One distributing channel is required in level 4. The number of collecting channels is equal to the number of distributing channel. A sketch of the manifold achieved for step 1 is shown in Figure 3.4.2.*

| | No. stages | D [mm] | L [mm] | No. channels | No. distributing channels | | |
					Level 1	Level 2	Level 3
Step 1	4	2	100	5,280	48	11	10
Step 2	3	2	100	5,700	57	10	10
Step 3	3	2	100	4,264	41	13	8
Step 4	2	2	100	1,470	49	6	5

Table 3.4.4: *Optimal operating conditions. HNO$_3$ concentration in the feed before recycle is 2.5 M*

	Step 1	Step 2	Step 3	Step 4
$\dot{V}_{tot,aq}$ inlet [L h^{-1}]	512	289	207	207
$\dot{V}_{tot,or}$ inlet [L h^{-1}]	706	706	706	126
A/O ratio	0.7	0.4	0.3	1.6
[HNO$_3$]$_{aq}$ feed [M]	3.6 [1]	4.6	5.8	5.6

[1] Concentration after recycle

Operating cost is negligible, because of the very low pressure drops with optimal design and operating conditions. The main cause of pressure drop is associated with the mixing junctions, which can contribute by approximately 80% of the
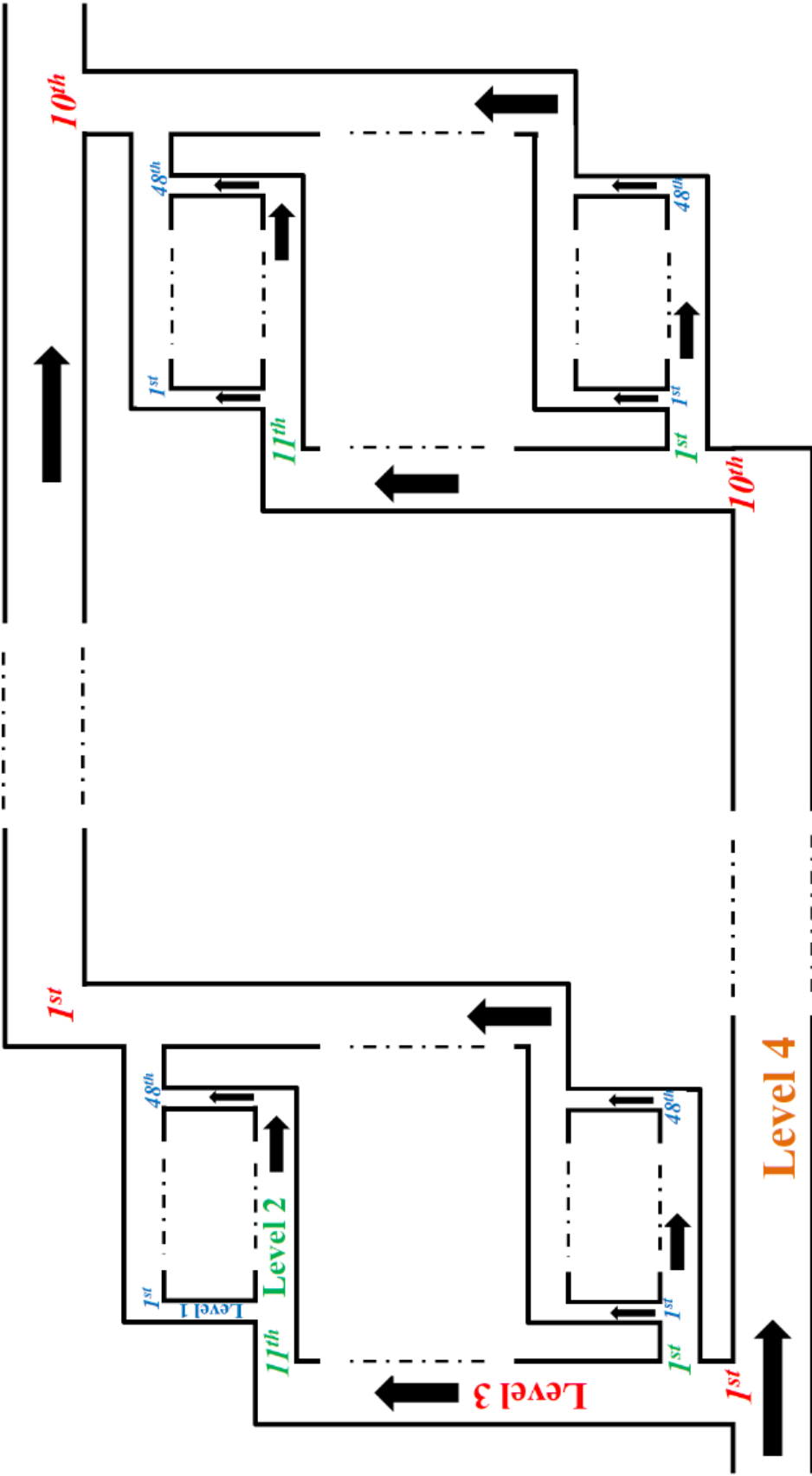
Figure 3.4.2: Schematic of the manifold design achieved for step 1 in the codecontamination section. Only the first and the last element in each level of the manifold are shown. The dot-dash lines indicates the intermediate elements in each level of the manifold. Level 4 (orange) consists of a single element. Level 3 (red) consists of 10 elements. Level 2 (green) consists of 11 elements. Level 1 (blue) consists of 48 elements. For step 1, a total of 8 manifolds is required (4 stages × 2 phases).

overall pressure drop. The design of the manifolds has a significant impact on the total capital cost: the manifolds constitute approximately 65% of the total cost. The cost for the two-phase separator itself is approximately 30%, whilst the cost of the small extractor channels is less than 5% of the overall cost.

The optimal design of both channel and flow network is shown in Table 3.4.3, the optimal operating conditions are depicted in Table 3.4.4. The diameter takes the maximum value of those considered to minimise the number of parallel units, the length tends to the lower bound to maximise the overall volumetric mass transfer coefficient (see Eq. 3.2.11), since most of the mass transfer occurs in the region close the mixing zone [24, 125].

The overall volumetric mass transfer coefficient is approximately 0.3 s^{-1} in all steps, higher than the same parameter reported in the literature for pulsed column operating with nitric acid solutions and TBP/paraffinic diluent [63, 126].

Nuclear criticality, due the large surface area to volume ratio provided by the small channels, does not appear to be an issue, with k_{eff} sufficiently far from unity. This result, if confirmed by more detailed criticality calculations, suggests that the use of small channels may be investigated as an alternative to pulsed columns where traditional mixer-settlers cannot be employed because of poor control of criticality.

An additional advantage of the use of small channels is the short residence times, of the order of seconds. Typical residence times for centrifugal contactors and pulsed columns are minutes, while for mixer-settlers they are hours [6]. The residence time may affect the solvent degradation and, hence, solvent regeneration in the PUREX process.

Furthermore, a short residence time may affect the Np recovery. The Np control in the PUREX process is complex since, as discussed in Section 3.1.2, Np exists in this system in three different oxidation states, with different equilibrium behaviours. The value of decontamination factors DF achieved in this flowsheet is around 30, *i.e.* only approximately 5% of the Np present in the aqueous feed ends up in the organic product, as already mentioned (instead of the 75% in the typical process [6]). The short residence time can explain this difference, since it does not allow high conversion from Np(V), unextractable, to Np(VI), very extractable. Np(IV) is also extractable, but its concentration seems to be negligible, according to the literature (negligible if HNO$_3$ concentration is lower than 4 M, small if it is lower than 8 M [127]).

Table 3.4.5: Outlet aqueous concentrations of metals, expressed as g L^{-1}.

	Step 1	Step 2	Step 3	Step 4
U(VI)	$4.00{\times}10^{-1}$	$1.86{\times}10$	$1.40{\times}10$	1.66
Pu(IV)	$5.37{\times}10^{-3}$	$2.33{\times}10^{-1}$	$1.47{\times}10^{-1}$	$1.74{\times}10^{-2}$
Zr	$5.16{\times}10^{-1}$	$7.93{\times}10^{-2}$	$7.71{\times}10^{-4}$	$5.85{\times}10^{-4}$
Ru	$3.35{\times}10^{-1}$	$5.30{\times}10^{-3}$	$6.64{\times}10^{-6}$	$6.56{\times}10^{-6}$
Tc	$9.75{\times}10^{-2}$	$3.52{\times}10^{-1}$	$4.74{\times}10^{-2}$	$4.61{\times}10^{-2}$
Np(IV)	$3.85{\times}10^{-8}$	$1.35{\times}10^{-7}$	$3.63{\times}10^{-8}$	$1.11{\times}10^{-8}$
Np(V)	$6.39{\times}10^{-2}$	$1.62{\times}10^{-3}$	$1.78{\times}10^{-5}$	$2.27{\times}10^{-5}$
Np(VI)	$1.66{\times}10^{-4}$	$7.98{\times}10^{-4}$	$5.51{\times}10^{-4}$	$7.80{\times}10^{-5}$

Another benefit of the small channels is the small volume of hazardous liquid involved. The extraction steps in the flowsheet investigated involve different liquid total volumes: approximately 220 L in step 1, 80 L in step 2, 110 L in step 3 and 15 L in step 4. These volumes may be further reduced by employing channel diameters above 2 mm; in this case, however, mass transfer coefficients may significantly decrease.

Predictions of separation performance and flow ratios seem reasonable: typical separation efficiency has been obtained [6], with flow ratio similar to the one used by Gonda and Miyachi for main extraction in pulsed column [37]. For the scrubbing steps, low aqueous to organic flow ratios are expected, to minimise back extraction of U and Pu. The optimal number of stages is greater when a larger amount of U and Pu must be extracted, as expected. These results may confirm the reliability of the benchmark equations integrated in the model, such as the Richardson's correlations for the modelling of the PUREX process [27]. The outlet concentrations of each component of the SNF in the aqueous and organic phases are shown, respectively, in Table 3.4.5 and Table 3.4.6. The uncertainty in some distribution coefficients could affect these results: the correlations used for Zr and Ru do not take into account the presence of U and Pu, but only depend on ionic strength. However, the concentration of U and Pu could affect the behaviour of Zr and Ru. Distribution coefficients of Np, in the model, are affected by concentrations of U and Pu, and not affected by Zr, Ru and Tc. Therefore,

Table 3.4.6: Outlet organic concentrations of metals, expressed as $g \ L^{-1}$.

	Step 1	Step 2	Step 3	Step 4
U(VI)	9.01×10	8.25×10	7.84×10	2.02×10
Pu(IV)	1.03	9.35×10^{-1}	8.92×10^{-1}	2.13×10^{-1}
Zr	3.27×10^{-2}	2.64×10^{-4}	3.75×10^{-5}	3.05×10^{-4}
Ru	2.17×10^{-3}	1.95×10^{-6}	0	1.25×10^{-7}
Tc	1.59×10^{-1}	1.56×10^{-2}	1.72×10^{-3}	2.01×10^{-3}
Np(IV)	8.77×10^{-8}	3.26×10^{-8}	2.19×10^{-8}	4.15×10^{-8}
Np(V)	6.63×10^{-4}	8.14×10^{-7}	1.45×10^{-8}	1.91×10^{-7}
Np(VI)	2.06×10^{-3}	1.74×10^{-3}	1.57×10^{-3}	7.69×10^{-4}

interactions between several components may not be taken into account. Also, the correlation used to predict the mass transfer coefficient, which is assumed to be the same for all components, has been developed for a different solute, hence the values of parameters in Eq. 3.2.11 may need to be recalculated with the current system. However, because of lack of information in the literature, original parameters have been used. These uncertainties could lead to an overestimation of the mass transfer, and hence to overestimated separation and underestimated dimensions.

3.5 Conclusions

A novel mathematical model of a multi-component liquid-liquid extraction in small channels for reprocessing of spent nuclear fuel has been developed. The design of distributors, collectors and two-phase separators has been included in this model. Redox reactions between the three existing oxidation states of Np in nitric acid solutions have been included, as well as an estimation of pressure drop and nuclear criticality. To demonstrate the potential use of this model, a case study of the code-contamination section of the PUREX process, has been addressed. The resulting design problem, a large scale nonlinear model (approximately 365,000 equations), has been formulated as a mixed-integer nonlinear programme and implemented in

the GAMS modelling system. The results show that the use of small-scale extraction technology may be advantageous in terms of residence time, plant size and neptunium control.

The mathematical model, despite the large size and the highly nonlinearity of some equations, has provided reasonable results and short computational time, when properly initialised. It combines the simplicity of a one-dimensional plug flow model and the reliability of well-known equations to deliver a tool for process design based on laboratory prototypes. It could also be the starting point for developing more detailed and customised models for liquid-liquid extraction in small channels, including different components and solvents.

If compared to the typical design of pulsed columns and mixer-settlers used in commercial reprocessing plants [11], intensified extraction in small channels may involve significant lower liquid volume and shorter residence time, leading to lower solvent degradation. However, in order to perform a more accurate comparison, the same case study must be evaluated for all technologies. In order to address this point, the modelling of the aforementioned conventional technologies is developed in Chapter 4. Then, a case study is investigated applying the three liquid-liquid extraction technologies in Chapter 5.

Chapter 4

Modelling of conventional technologies

In this chapter, the mathematical models used to investigate the conventional technologies is presented. The technologies considered are pulsed column and mixer-settlers. Centrifugal extractor, despite it seems to be the most promising technology among the conventional ones, has not been considered because of its very limited use in the nuclear industry. The modelling of these equipment is needed to allow comparison between novel and conventional technologies. Many models for mixer-settlers and pulsed columns have been suggested in the literature. Typically, U, Pu and HNO_3 have been investigated and the studies focus on mass transfer and redox reactions. In this thesis, besides these aspects, mass transfer of minor actinides and fission products is investigated, as well as a large number of chemical reactions, nuclear criticality safety and economics.

The mathematical modelling of mixer-settlers and pulsed columns is presented, respectively, in Section 4.1 and Section 4.2. Details of the calculation of mass balance, mass transfer and hydrodynamics are given. Finally, the mathematical modellings and their applications are discussed in Section 4.3.

4.1 Modelling of mixer-settler

Mixer-settlers have been widely modelled in the literature. Assuming homogeneous concentrations, this is the simplest equipment to model among all the liquid-liquid

extraction technologies. Hydrodynamic and mass transfer correlations are taken from the literature. Below, details on the assumptions and modelling of mixer-settler are given.

4.1.1 Mass balance

Similarly to the modelling of small extractors, steady state conditions are assumed. The two typical assumptions for this system have been assumed: complete mixing and no mass transfer in settlers. Also, the mixer has been modelled as a nonequilbrium stage. According to these assumptions, the mass balance model developed for the component i in the phase k in mixers and settlers is given by:

$$\text{mixer} \quad \dot{V}_k(C_{i,k}^{in} - C_{i,k}) + k_L a V_{mix}(C_{i,k} - C_{i,k}^{eq}) + \sum R_{i,k}\varphi_k V_{mix} = 0 \quad (4.1.1)$$

$$\text{settler} \quad \dot{V}_k(C_{i,k}^{in} - C_{i,k}) + \sum R_{i,k}\varphi_k V_{set} = 0 \quad (4.1.2)$$

In nuclear reprocessing plants, since numerous stage are required to achieved high separation efficiencies, mixer-settler banks are employed. For this reason, in this work mixer-settlers have been modelled considering a counter-current configuration, according to the mixer-settler banks, where the aqueous outlet from a settler is the inlet in the previous mixer, whilst the organic outlet is the inlet of the next mixer (see [11] for further details).

4.1.2 Mass transfer

According to Gonda *et al.* [36], the rate determining step in agitated vessel is the mass transfer in the dispersed phase, therefore the mass transfer coefficient in the continuous aqueous phase can be neglected. The correlation developed by Treybal has been used to approximately estimate the mass transfer coefficient k_L [128]. Treybal proposed, for drops with no internal circulation, to correlate the mass transfer coefficient with molecular diffusion:

$$Sh_d = \frac{K_L \, d_{32}}{\mathscr{D}_d} = \frac{2\pi^2}{3} \quad (4.1.3)$$

Gonda *et al.* [36] suggested an empirical correlation for the calculation of the mass transfer coefficient in mixer-settler. Although, for SNF reprocessing, their model

73

is probably more accurate than the one developed by Treybal, its application is challenging. In their model, the superficial velocity must be estimated by fitting the model to experimental data. Due to the lack of experimental data, the model proposed by Treybal has been preferred in this work.

4.1.3 Hydrodynamics

The interfacial area a is calculated as $a = 6\varphi/d_{32}$ (φ dispersed phase holdup). The Sauter mean diameter d_{32} has been calculated through the Calderbank equation for 4-blade impellers:

$$d_{32}/W = 0.06(1 + 3.75\varphi)\, We^{-0.6} \tag{4.1.4}$$

where W is the width of the vessel, We is the Weber number, defined as $\frac{(N_{rev}/60)^2 D_i^3 \rho_c}{\gamma}$, with N_{rev} the impeller speed expressed in rpm.

Eq. 4.1.4 describes the effect of the impeller speed and physical properties on the Sauter mean diameter and, then, on the volumetric mass transfer coefficient $k_L a$.

Settlers have been designed as suggested by the Coulson and Richardson's manual: the terminal (or raising) velocity of the dispersed droplets in the settler must be higher than the continuous phase velocity [129]. Terminal velocity v_t is calculated through the Stokes' law for laminar flow (low velocity in the settler):

$$v_t = \frac{g(\rho_c - \rho_d)\, d_{32}}{18\mu} \tag{4.1.5}$$

Continuous phase velocity is calculated referring to the area of the base of the settler (*i.e.*. $W \times L$, where L is the length of the settler).

4.1.4 Other equations

Furthermore, the following geometrical constraints have been implemented, based on designs of mixer-settler banks for SNF reprocessing [130, 131, 132, 133]:

- the impeller diameter D_i is lower than 50% of the mixer width;

- width and length of mixer are equal;

- mixer height greater or equal than mixer length;

- mixer width and settler width are equal;

- distance between operating height and height, for both mixer and settler, based on the average values in the literature (the liquid should not entirely fill the chambers);

- maximum ratio between operating height and width of mixer based on the average values in the literature;

- maximum ratio between mixer volume and settler volume based on the average values in the literature;

- settler length greater or equal than settler width.

The constraints above are necessary to achieve a reasonable geometry of the mixer-settlers bank. For example, since the settler is places behind the mixer, their widths must be the same; the impeller diameter must be in the typical range, since it affects the hydrodynamics and this is needed to rely on the empirical correlations used, taken from the literature for standard geometries; settler length must be larger than the settler width to avoid short and wide settlers (the dimension in the direction of the flow, *i.e.* the length, must be larger than the width).

The operating cost has been assumed to be the agitation cost, therefore the required power P is:

$$P = N_p \rho_c (N_{rev}/60)^3 D_i^5 \qquad (4.1.6)$$

N_P is the power number, approximately equal to 4 for the range of Reynolds numbers investigated in this study. It is worth noting that, for agitated systems, Re is calculated as $N_{rev} D_i^2 \rho_c / \mu_c$.

The capital cost of mixer-settler is, as first approximation, estimated as suggested by Seider *et al.* [124], summing costs of vessels (C_v^h) and agitators (C_a). The cost of the horizontal vessels is calculated as [124]:

$$C_v^h = \exp[8.717 - 0.2330 \log(W) + 0.04333 \log(W)^2] F_m^v MSI \qquad (4.1.7)$$

where W is the weight of the steel, expressed in lb. As can be seen in Eq. 4.1.7, the cost is multiplied by the "material" factor F_m^v, which is 2.1 for vessels of stainless steel (acid environment) [124]. However, other materials or linings could be used.

MSI is the Marshall & Swift Index 2015, assumed 1.52 (extrapolated value from values from 2002 to 2011, due to the lack of more recent data). For the calculation of the vessel weights, a thickness of 1.27 cm is assumed [134]. However, since in nuclear industry mixer-settler banks are used, several walls are in common between mixers and settlers. Therefore, the total weight W is lower than the product between the weight of a single stage and the number of stages (some walls are shared). This difference has been taken into account in the weight calculation.

The cost of the agitator is calculated as [135]:

$$C_a = C_A^{Ref}(P_a/P_a^{Ref})^{0.23}F_m^a MSI \tag{4.1.8}$$

where C_A^{Ref} is the cost of an agitator of reference, P_a the power required by the agitator of the mixer-settlers (expressed in hp), P_a^{Ref} the power of the agitator of reference, F_m^a for agitators is 2. The cost of the agitator of reference (2 hp) is taken from [124].

Chemistry (distribution coefficients, reaction rates) and nuclear criticality calculations have been calculated as described in Section 3.1. For the estimation of the effective multiplication factor, the buckling B^2 has been calculated assuming a parallelepiped shape (see [136] for further details).

4.2   Modelling of pulsed column

As discussed in Section 2.1.3, a large number of mathematical models for pulsed columns have been developed in the literature. The modelling of this technology is challenging. It is a differential contactor, so there is a gradient of concentration along the height, and it involves a complex hydrodynamics (for example, the dispersed phase holdup is not constant but function of geometry and operating conditions).

4.2.1   Mass balance

The types of model typically used to describe mass balance in extraction columns are shown in Table 2.1.3. Since the two-phase equilibria are nonlinear, *i.e.* the distribution coefficient is not constant, the stagewise mass balance model has been used, as suggested by Steiner [60]. Steady state conditions have been assumed,

including the effect of the pulsation into hydrodynamic correlations. Hence, assuming a stagewise back flow model, the resulting mass balance for the i component in the aqueous phase is given by:

$$\text{at bottom, stage 1} \quad (1+\alpha^{aq})(C_2^{i,aq} - C_1^{i,aq}) - \frac{N_{oc}}{N}(C_1^{i,aq} - C_{1,eq}^{i,aq})$$
$$+ \sum R_{i,aq}\varphi_{aq}V = 0 \tag{4.2.1}$$

$$\text{typical stage } n \quad (1+\alpha^{aq})(C_{n+1}^{i,aq} - C_n^{i,aq}) + \alpha^{aq}(C_{n-1}^{i,aq} - C_{i,aq}^{i,aq})+$$
$$- \frac{N_{oc}}{N}(C_n^{i,aqi} - C_{n,eq}^{i,aq}) + \sum R_{i,aq}\varphi_{aq}V = 0 \tag{4.2.2}$$

$$\text{at top, stage } N \quad C_{in}^{i,aq} + \alpha^{aq}C_{N-1}^{i,aq} - (1+\alpha^{aq})C_N^{i,aq}+$$
$$- \frac{N_{oc}}{N}(C_N^{i,aq} - C_{N,eq}^{i,aq}) + \sum R_{i,aq}\varphi_{aq}V = 0 \tag{4.2.3}$$

where α is N/Pe-0.5, N_{oc} is the number of transfer units ($= k_L a H/v$). The Peclet number Pe is calculated as $v\Delta H/E$, where ΔH is the plate spacing (5 cm, typical value [37, 116]), E is the axial dispersion coefficient. For the i component in the organic phase, the mass balance is:

$$\text{at bottom, stage 1} \quad C_{in}^{i,org} + \alpha^{org}C_2^{i,org} - (1+\alpha^{org})C_1^{i,org}+$$
$$+ \frac{N_{oc}}{qN}(C_1^{i,aq} - C_{1,eq}^{i,aq}) + \sum R_{i,org}\varphi_{org}V = 0 \tag{4.2.4}$$

$$\text{typical stage } n \quad (1+\alpha^{org})(C_{n-1}^{i,org} - C_n^{i,org}) + \alpha^{org}(C_{n+1}^{i,org} - C_n^{i,org})+$$
$$+ \frac{N_{oc}}{qN}(C_n^{i,aqi} - C_{n,eq}^{i,aq}) + \sum R_{i,org}\varphi_{org}V = 0 \tag{4.2.5}$$

$$\text{at top, stage } N \quad (1+\alpha^{org})(C_{N-1}^{i,org} - C_N^{i,org}) + \frac{N_{oc}}{qN}(C_N^{i,aq} - C_{N,eq}^{i,aq})$$
$$+ \sum R_{i,org}\varphi_{org}V = 0 \tag{4.2.6}$$

4.2.2 Mass transfer

Several models have been developed in the literature to estimate the mass transfer coefficient in extraction columns. Detailed correlations for mass transfer coefficient of U(VI), Pu(III), HNO_3, U(IV) and Pu(IV), for both extraction and stripping operations, have been developed by Gonda and Matsuda [37, 79]. According to

them, the mass transfer coefficient for U(VI) during extraction (from dispersed aqueous phase to continuous organic phase, falling drops) can be estimated as:

$$k_L^{extr} = 2.8 \times 10^7 (1/Pe)^{1.8} + \frac{3.55 \times 1014}{m}(1/Pe)^{2.95} \qquad (4.2.7)$$

where m is the distribution coefficient (here expressed with the symbol "m" instead of "D" to avoid confusion with the diameter), Pe calculated as in [79] using the terminal velocity. Different mass transfer correlations have been used for extraction and back extraction operation, as suggested by Gonda and Matsuda [37]. For the back extraction, two contributes have been assumed, the one related to the jetting movement of the drops pushed by the pulsation and the one related to the free movement of the falling/rising drops [37, 79]:

$$k_L^{back} = k_L^{back,jet} + k_L^{back,free} \qquad (4.2.8)$$

For U(VI), the two contributes above for mass transfer in back extraction have been calculated through the following relationships:

$$k_L^{back,jet} = 53t_0^{0.55} + 8.4 \times 10^2 [H^+]_{aq}^{-0.66} m t_0^{1.22} \qquad (4.2.9)$$

$$k_L^{back,free} = 3.94 \times 10^2 (1/Pe)^{0.786} + 1.74 \times 10^{-2} m (10^5/Pe)^{2.5} \qquad (4.2.10)$$

where t_0 is the time period for jetting, calculated as $t_0 = 1.18 v_h^{-1.23}$ (v_h is the drop velocity in nozzle). Similar expressions have been used for mass transfer of Pu(III), U(IV), Pu(IV) and HNO_3. The full set of equations can be found in [37, 79]. Hence, the calculation of the mass transfer coefficients in pulsed columns, through Eqs. 4.2.7-4.2.10, involve highly nonlinear equations and can be challenging.

For all the other metals (Np, Zr, Tc, Ru), due to the lack of information, the mass transfer calculated for U(VI) has been used. Mass transfer coefficient of HNO_3 has been used also for HNO_2. The correlations suggested by Gonda and Matsuda [37], described above, have been implemented in this work as, being specifically developed for the PUREX process in pulsed columns, they seem the most reliable among all the models suggested in the literature.

4.2.3 Hydrodynamics

The hydrodynamics is strongly affected by the geometry of the plates. Here, a perforated (or "sieve") plate is assumed. This type of plate is used in Sellafield,

78

and several correlations have been developed in the literature to calculate hydrodynamic variables. There are also modern plants that use the so called "annular" or "disk and doughnut" plates, but few models are available for this geometry.

Axial dispersion coefficient E in pulsed sieve plate columns, for the phase k, has been calculated as suggested by Gonda and Matsuda for the PUREX process [37]:

$$E_k = k_1 \left(\frac{\Delta H}{D}\right)^{2/3} \left(\frac{d_h}{\epsilon}\right) \left(Af\varphi_k + \frac{v_k}{2}\right) \tag{4.2.11}$$

where D is the column diameter, d_h is the hole diameter (typical value 0.3 cm [37, 116]), ϵ is the plate free area fraction (typical value 23% [37, 116]), A and f are respectively pulse amplitude and frequency. The parameter k_1 is 0.25 for organic continuous phase, 0.35 for aqueous dispersed phase, 0.55 for aqueous continuous phase and 0.60 for organic dispersed phase.

The interfacial area has been calculated as for mixer-settlers, $a = 6\varphi/d_d$. The drop diameter d_d is calculated as suggested by Gonda and Matsuda [37]:

$$d_d = (k_2 + 25.7v_d^{3.33})d_h^{0.7}\Delta H^{0.4}(Af)^{0.313} \tag{4.2.12}$$

where k_2 is equal to 0.093 for aqueous dispersed drops, 0.147 for organic dispersed drops.

In contrast to mixer-settlers, dispersed holdup phase is not constant but varies with column design and operating conditions. According to Gonda and Matsuda, it can be estimated as follows [37]:

$$\varphi_d = k_3 v_d^{1.03} D^{1.02}\Delta H^{-1.2}\epsilon^{-2.4}d_h^{0.89} \exp\left[0.70\left(\ln\frac{Af}{1.2}\right)\right] \tag{4.2.13}$$

where k_3 is 2.95×10^{-2} for PTFE perforated plates, 1.77×10^{-2} for stainless steel ones [37].

Condition of insufficient pulsation occurs if

$$2Af \leq v_d + v_c \tag{4.2.14}$$

The frequency corresponding to the maximum total throughput before flooding, is given by Berger and Walter [137]:

$$f_{max} = 0.4908 + 1.11 \times 10^2\gamma - 1.8 \times 10^3\gamma^2 - (3.44 \times 10^{-2} + 7.1\gamma)\ln R \tag{4.2.15}$$

where γ is the interfacial tension, R is the dispersed to continuous flow ratio. Conditions of insufficient pulsation and flooding have been included in the model. According to Haverland and Slater, the flooding is typically around 75% [59], so in this work it has been allowed to vary between 70% and 90%.

4.2.4 Other equations

To calculate the operating costs, the pumping power and the power requirements for pulse generations are considered. Static heads ΔP_{st} and pressure drops along the plates ΔP_p are taken into account for the pumping power required:

$$\Delta P_{st} = \rho g H \tag{4.2.16}$$

$$\Delta P_p = N_p \rho \frac{(1 - \epsilon^2)}{(0.72\epsilon^2)}((v + 2Af)^2 \tag{4.2.17}$$

where N_p is the number of perforated plates, $2Af$ is the mean pulsation velocity integrating $v_{pulse}(t) = \pi A f cos(2\pi f t)$ over a period of pulsation T. The power requirements for pulse generations has been calculated considering static head and pressure drop through plates, so similarly to Eqs. 4.2.16 and 4.2.17, as suggested by Jealous and Johnson [138].

Capital costs are calculated as suggested by Seider *et al.* [124], summing the cost of column (vertical vessel, C_v^v), platform and ladder (C_{pl}) and trays (C_t):

$$C_v^v = \exp[6.775 + 0.18255 \log(W) + 0.02297 \log(W)^2] F_m^v MSI \tag{4.2.18}$$

$$C_{pl} = 285.1 D^{0.73960} H^{0.70684} MSI \tag{4.2.19}$$

$$C_t = 369(1.401 + 0.724D) \exp(0.1739D) N_p MSI \tag{4.2.20}$$

where D and H must be expressed in ft.

A first design of the top and bottom settlers, assumed equally sized, is estimated. The diameter is calculated to allow the droplets to settle, similarly to settlers in Section 4.1. Costs of bottom and top settlers are added to the total cost.

Nuclear criticality is estimated similarly to small channels (cylindrical shape, see Eqs. 3.1.34-3.1.35).

4.3   Conclusions

The objective of this thesis is to develop a methodology for the design and optimisation of alternative flowsheets for SNF reprocessing, using the small-scale technology. The possibility of integrating novel and conventional technologies in the same process will be studied, as well as pros and cons of the novel technology when compared to the traditional ones. For this reason, the same case study must be investigated for all technologies and, hence, the mathematical modellings of the main conventional liquid-liquid extraction technologies are required. In this chapter, the mathematical modellings of mixer-settler and pulsed column, the most used equipment for liquid-liquid extraction in the PUREX process, have been described. Although these models have been widely investigated in the last years, no models suitable for SNF reprocessing, including all the components investigated in this work, have been reported in the literature. The models presented in this chapter will be used in Chapter 5 to compare novel and conventional technologies. The case study that will be investigated will also be used to evaluate the applicability of the models. The performance of the models will be discussed, although with less emphasis than the model of intensified extraction in small channels as this work mainly focuses on the novel small-scale technology, whilst mixer-settlers and pulsed columns are benchmark technologies.

Chapter 5

Comparison between technologies

The aim of this chapter is to compare the intensified extraction in small channels with the two main traditional liquid-liquid extraction technologies in the nuclear industry, mixer-settler and pulsed column. This step is important to evaluate the potential use of small-scale contactors for SNF reprocessing. A novel flowsheet for the codecontamination section of the PUREX process has been investigated as case study. A sketch of the flowsheet is shown in Figure 5.1.1. Design variables and operating conditions are optimised, according to economic criteria. The chemical engineering attributes of main interest in this field, *i.e.* cost, equipment size, solvent degradation, nuclear criticality, mass transfer coefficient, control of hydrodynamics and Np control are compared. The goals is to investigate the potential advantages of the the small-scale contactors over the conventional equipment, also with a view to potentially combining the different technologies for future SNF reprocessing flowsheets.

In Section 5.1, the case study is illustrated. The optimisation problems is described in Section 5.2, whilst in Section 5.3 details on the solution procedure are given. The benefits and drawbacks of the three extractors are presented in Section 5.4. In Section 5.5, the chapter concludes with a discussion on the performance of the different technologies.

5.1 Case study: alternative codecontamination section

In the conventional flowsheet for the codecontamination section of the modern PUREX process, a scrubbing step is used to separate Zr and Ru and another scrubbing step, with a significantly higher HNO_3 concentration, is used to remove Tc. The difference in HNO_3 concentration is due to thermodynamic reasons: back extraction of Ru and Zr is favoured at low HNO_3 concentration, whilst back extraction of Tc is favoured at high HNO_3 concentration.

In this case study, an alternative flowsheet for the codecontamination section is presented. Here, the two scrubbing sections are merged. The possibility of reducing the number of unit operations while achieving the minimum separation required,
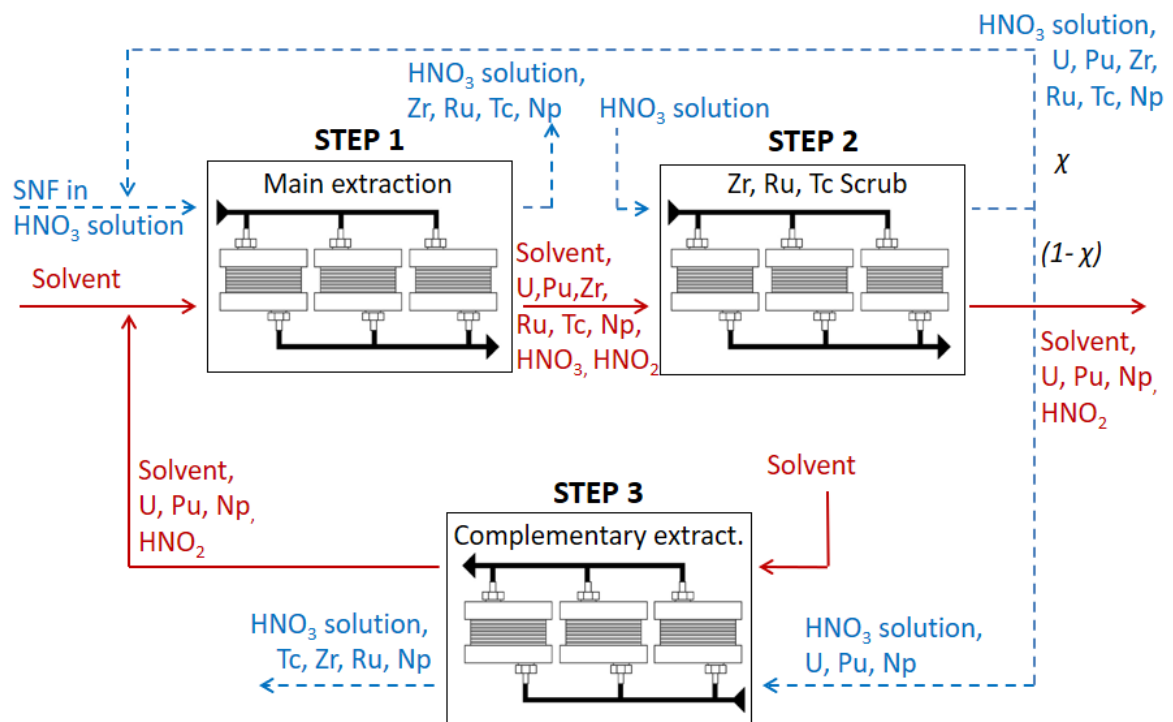
Figure 5.1.1: Schematic of the flowsheet for novel codecontamination section. Blue dashed line refers to aqueous stream. Red continuous line refers to organic streamn. No aqueous recycle from step 2 to step 1 if $\chi = 0$, no step 3 and organic recycle to step 1 if $\chi = 1$.

using a nitric acid solution of intermediate concentration and varying equipment design and operating conditions, is investigated. The process flow diagram is shown in Figure 5.1.1. The aqueous stream leaving the scrubbing step could be either recycled to the main extraction (step 1), fed to the complementary extraction (step 3) or split between these two steps. The design variable χ, which can vary between 0 and 1, describes the fraction of aqueous stream recycled to step 1, which is $\chi \dot{V}_{aq}$, whilst $(1 - \chi)\dot{V}_{aq}$ is the aqueous stream fed to step 3.

The total annualised cost is assumed as objective function, to minimise the overall cost. This objective function also incorporates information regarding size (capital costs) and usage of solvent (operating costs), other important criteria. Considering the large number of important criteria that must be taken into consideration, a multi-objective optimisation would be beneficial. However, the development of multi-objective optimisation model is complex and this is beyond the scope of this PhD programme. The considered capital costs consist of:

- costs of channels, manifolds and separators (mainstream and sidestram channels) for small channels [121];

- costs of vessels (for mixers and settlers) and agitators for mixer-settler [124, 135];

- costs of vessels (for column, bottom and top settlers), trays, platform and ladder for pulsed column [124, 138].

The operating costs consist of

- pumping costs for small channels;

- agitation costs for mixer-settler;

- pumping cost for pulsed column [138].

Several other costs, for both capital and operating expenditures, have not been included in the cost estimation for lack of data in the literature. In particular, the equipment used for SNF reprocessing may required specific instrumentation, devices and materials which are not considered by these calculations. These additional costs may significantly increase the overall cost, if compared to the cost

of equipment required for other liquid-liquid extraction processes. The comparison with actual economic data is challenging, due to the lack of information for reasons of commercial confidentiality. Although the results will be affected by the assumptions stated above, the methodology still allows the exploration of alternative process design.

5.2 Optimisation problem definition

The goal is to optimise the process shown in Figure 5.1.1 minimising the total annualised cost (TAC), which includes operating expenditure ($OpEx)$ and annualised capital expenditure ($ACapEx)$, as shown in Eq. 3.4.1. The process optimisation has been performed assuming a 5-year payout time. For this problem longer payout times, up to 10, are not expected to significantly affect the optimal design, similarly to the case study investigated in Chapter 3. This objective function is chosen since, for limited operating cost (as expected here), it leads also to smaller equipment footprint and safer design. Operating costs in this work do not involve losses of acid and solvent. Also, all the costs related to the solvent cleanup and regeneration section are not included in the calculations. These aspects must be taken into consideration in the comparison of the technologies, as well as all the other attributes of interest such as the separation performance, Np control, residence time, flexibility, nuclear criticality safety and mass transfer coefficients.

Free variables are all the design variables related to the geometry of the equipment, except the plate geometry of the pulsed column (in terms of plate spacing, holes diameter and plate free area fraction). For the small-scale contactor, these variables are length and width of each level of the flow network (diameter for the small extractors), number of stages and elements within each level. For mixer-settlers, the design variables are width, depth and length of mixers and settlers, diameter of the impeller, number of stages. For pulsed columns, the design variables are diameter and height, number of perforated plates. Further free variables are the ones regarding the operating conditions, hence the flow rate of all inlet streams except the feed, both aqueous and organic, as well as nitric acid concentration of the aqueous streams entering step 2. Also, the impeller speed is a free variable in the mixer-settler model, pulse frequency and amplitude in the pulsed column. Constraints such as minimal requirements for extraction (E) of U and

Pu, or decontamination factor (DF) of hazardous components such as Zr and Ru, are included in the optimisation problem. All the inequality constraints included in the optimisation problem are shown in Table 5.2.1.

Table 5.2.1: Inequality constraints of the optimisation problem.

Inequality constraints	Comment
$Rec_U \geq 0.99$	Minimum uranium recovery
$Rec_{Pu} \geq 0.99$	Minimum plutonium recovery
$[U]_{aq,out}^{Step1} \leq 1.68$ M	Maximum typical uranium concentration in HLW step 1
Zr DF $\geq 10^4$	Typical requirement [6]
Ru DF $\geq 10^4$	Typical requirement [6]
Tc DF ≥ 10	Typical requirement [6]
$k_{eff} \leq 0.95$	Nuclear criticality safety

The optimisation problem has been solved three times, one for each technology, to identify the potential advantages and disadvantages of each technology. Inputs of the problem are throughput, feed concentration, temperature and materials (see Table 5.2.2).

5.3 Optimisation procedure

The combination of the nonlinear models and the integer variables leads to the optimisation problem described as a mixed integer nonlinear programme. This problem is implemented and solved in GAMS [111]. The integer variables are the number of stages in models for intensified extraction in small channels and mixer-settlers, whilst in pulsed columns the integer variable represents the number of perforated plates. The optimisation problems defined for each of the three configurations have been solved using the SBB (Simple Branch and Bound) solver. The relative gap criterion (OPTCR) is 1%.

The optimisation model for the small-scale contactor is the largest, with approximately 270,000 equations, because of the 50 grid points used to convert the

Table 5.2.2: *Input parameters and flow pattern designs. SC=Small Channels, MS=Mixer-Settlers, PC=Pulsed Columns.*

Parameter	Component/Step	Value	Technology
Feed concentration	U(VI)	1050.42	SC, MS, PC
[Mol m^{-3}]	Pu(IV)	11.65	SC, MS, PC
	Ru	7.59	SC, MS, PC
	Zr	12.99	SC, MS, PC
	Tc	2.77	SC, MS, PC
	Np(V)	0.64	SC, MS, PC
	HNO$_2$	1.00	SC, MS, PC
Solvent concentration	TBP	1097.37	
[Mol m^{-3}]		(=30% v/v)	
Temperature [°C]	Steps 1, 2, 3	25	SC, MS, PC
Throughput [MTHM y^{-1}]	-	500	SC, MS, PC
Material	Steps 1, 2, 3	PTFE	SC
	Steps 1, 2, 3	Stainless steel	MS, PC
Plate geometry ($d_h,\epsilon,\Delta H$)	Steps 1, 2, 3	as given in sec. 4.2.3	PC
Flow pattern design	Step 1, 2, 3	counter-current	SC, MS

differential mass balance equation 3.2.4 to a set of algebraic equations. For the pulsed column alternative, there are approximately 20,000 equations due to the 50 theoretical stages, which must not be confused with the number of actual compartments (which vary with the height of the column and the number of plates). For the mixer-settler configuration, there are approximately 6,000 equations.

There are potentially two recycle streams, but the final number depends on the value of the recycle ratio χ. Hence, in particular for the model of small-scale contactors, long computational times and convergence difficulties are expected, as discussed in 3.3.2. To bypass these numerical difficulties, a sequential modular approach has been initially used for all liquid-liquid extraction technologies, that provides the initialisation for solving the entire flowsheet simultaneously later.

5.4 Results

The main results of the optimisation problems are summarised in Table 5.4.1. According to the models, the pulsed column is the most cost effective technology. The column height in the main extraction is significantly shorter than the typical value, as result of the operating conditions. To confirm the applicability of the pulsed column model, the single main extraction step has been investigated as case study to allow comparison with the typical design (12 m high by 0.3 m diameter, although the exact flow rates are not given [11]). No aqueous recycle has been used. The organic to aqueous flow ratio used is 2.5, an average value between the ones used in the literature [37?]. The design achieved is reasonable, 10 m high by 0.2 m diameter. This may confirm the reliability of the model, although unusual operating conditions, as the results of this optimisation problem, could have reduced the accuracy of some empirical correlations used (validity ranges were not provided by the authors).

The small contactor is the only one which makes use of the complementary extraction, step 3. The three most important advantages provided by the small-scale technology are related to the volumetric mass transfer coefficient $k_L a$, the neptunium separation and the residence time. The residence time has a direct effect on solvent degradation and hence on solvent regeneration and makeup costs.

The optimal design of intensified extraction in small channels is shown in Tables 5.4.2–5.4.4, whereas the designs of conventional technologies are illustrated

in Tables 5.4.5–5.4.7. A general comparison of all liquid-liquid extraction technologies, including centrifugal extractors, is shown in Table 5.4.8. In the latter, ratings for conventional technologies are taken from Law [3], except equipment operating cost and the last four rows where the ratings are based on the results obtained in this work. The ratings for small channels have been estimated assuming proportionality between the typical values of the attribute for the traditional technologies (provided by Arm *et al.* [11]), its rating (provided by Law), the value of the attribute of small channels achieved in this work and its rating. If values for conventional technologies are not provided by Arm *et al.*, the values obtained in this work are used. Where the attribute cannot be directly measured, such as ease of scale-up or process flexibility, a first estimation is provided by the author, referring to the ratings given by Law for the other equipment.

A more detailed comparison between technologies is discussed below.

Table 5.4.1: Comparison of small channels, pulsed columns and mixer-settlers.

Criteria	Small channels	Mixer-settler	Pulsed colum
Total annualised cost [$\pounds \text{y}^{-1} \times 10^3$]	40	58	27
Recycle ratio χ	0.71	1	1
Total solvent flow rate [L h^{-1}]	646	617	940
Total liquid volume [L]	289	350	239
Total residence time [min]	0.3	18.4	6.3
Np decontamination factor	30.5	3.4	1.7
Average $k_L a$ [s^{-1}]	0.35	0.19	0.11
Criticality safety: k_{eff}	0.4	0.7	0.6

5.4.1 Optimal flowsheet

Using the conventional technologies, the optimal flowsheet does not include step 3, *i.e.* $\chi = 1$. This choice reduces the total annualised cost for the conventional technologies.

With the small-scale contactor, the optimal value of χ is 0.71, therefore 29% of the aqueous stream leaving step 2 undergoes treatment in step 3. Using this technology, there is an approximately 3% difference in the total cost between the case with $\chi = 1$ and the optimal solution, i.e χ=0.71. When χ is 1 and step 3 is not included, the first step involves 5 stages and the second step 3 stages, whilst the optimal solution (χ=0.71) involves 4 stages in steps 1 and 2 but 1 stage in step 3, as shown in Table 5.4.4. Therefore, there is the same total number of stages in both cases for the first two steps, plus a small unit for step 3 (single stage) in the optimal flowsheet, similar overall cost and operating conditions and similar designs. The optimal solution (χ=0.71) involves slightly lower overall capital cost, mainly manifold cost, as a result of the 30% more cost effective manifold for step 1 (one stage less than the case with χ=1). These differences in the total annualised cost and process design show the benefits of the modular nature and hence the flexibility of the small-scale technology.

5.4.2   Economics

Pulsed columns were expected to be the least expensive conventional equipment [3]. The low cost of pulsed columns achieved in this work is due to the short height achieved, significantly shorter than the typical height reported in the literature for SNF reprocessing [11]. This is the result of the dilution of the feed with the aqueous stream leaving step 2 and the increased solvent flow rate (see Table 5.4.1), which improves extraction at the expense of a high usage of solvent and the related costs. These operating conditions lead to height and volume lower than expected. Also, costs of some equipment used for pulsed columns, such as neutron absorbers and pulsators, are not included in the calculation (due to the lack of data) and that would increase the cost of pulsed columns.

The operating cost of small channels, the pumping cost, is negligible compared to the annualised capital cost. The proper design of the manifolds reduces the pressure drop along distributors and collectors, minimising the pumping power required. Approximately 94% of the overall pressure drop in the small-scale technology occurs in the mixing junction at the entry of the small extractor (1$^{\text{st}}$ level of the manifold), where the two phases join. This result confirms the very small pressure drop achieved with the laminar flow in the distributors and collectors.

Compared to the operating costs required by conventional technologies, the resulting operating cost for small channels is one order of magnitude lower.

Table 5.4.2: Optimal design of flow network for intensified extraction in small channels. Steps: 1 = main extraction, 2 = scrubbing, 3 = complementary extraction.

Step	Phase	Scale	No. elements	Length [cm]	Diameter/ Width [cm]
1	aq.,org.	1	46	10.0	0.2
1	aq.	2	10	27.0	1.0
1	aq.	3	10	25.9	1.9
1	aq.	4	1	52.6	7.8
1	org.	2	10	27.0	1.1
1	org.	3	10	30.0	2.6
1	org.	4	1	70.4	9.5
2	aq.,org.	1	50	10.0	0.2
2	aq.	2	9	29.4	1.0
2	aq.	3	9	23.6	1.8
2	aq.	4	1	43.6	6.3
2	org.	2	9	29.4	1.1
2	org.	3	9	27.4	2.7
2	org.	4	1	64.8	9.5
3	aq.,org.	1	46	10.0	0.2
3	aq.	2	5	27.0	1.0
3	aq.	3	4	11.6	1.6
3	aq.	4	1	14.1	3.8
3	org.	2	5	27.0	1.1
3	org.	3	4	13.1	2.1
3	org.	4	1	19.1	4.7

5.4.3 Size

The size of equipment has a direct impact on safety as the amount of hazardous liquids present depends on the equipment volume. Furthermore, for equal flow rates, smaller sizes lead to shorter residence times and, hence, lower solvent degradation. The optimal design achieved with pulsed columns involves the lowest total liquid volume among all the alternatives considered, lower then small channels by approximately 15%, because of the reasons explained in Section 5.4.2. However, this volume is underestimated, as the column height provided by the calculations is the one to accommodate the trays, whilst the height required at the top and at the bottom of this height is neglected. On the contrary, the volume required by the small channels may be decreased with higher flow maldistribution (in the achieved design, the flow maldistribution is only 1%).

A lower volume of mixer-settlers, if compared to the one used in the nuclear industry [6], was expected. Mixer-settlers are used mostly in second cycles of liquid-liquid extractions where, together with small amount of contaminants, only either uranium or plutonium are present. Hence, there is no risk of nuclear criticality and a large mixer-settler banks can be used. Also, a large number of stages is used to achieve high purities. In this case study, high concentrations of uranium and plutonium are involved, apart from the fissile materials (which are not included in the nuclear criticality calculations), hence the typical design may not ensure subcriticality. Furthermore, high purities of U and Pu are not required in this flowsheet, hence a lower number of stages is reasonable.

The size of the extraction step using small-scale technology may be further decreased if higher TBP concentrations in the organic solvent were used. A high TBP concentration would improve extraction and reduce organic flow rates. The opposite trend is expected for back extraction: the aqueous flow rates required for scrubbing operations would increase. Therefore, a trade off for the TBP concentration must be found. The current TBP volume fraction in the organic solvent, which is 30%, is the typical one used in the nuclear industry to reduce density and viscosity of the organic phase. In small channels, contrary to conventional technologies, the separation does not rely on gravitational forces. Thus, higher TBP fractions could be investigated using small channels, with no separation issues. Hotokezaka *et al.* investigated U extraction using 100% TBP in microchannels

[139]. They used a 0.11 M U(VI) - 3 M HNO_3 aqueous solution. However, the effect of denser solvent in these systems, after a certain value of concentrations of the actinides in the feed, should be further investigated as phase inversion or third phase formation [140, 141] may occur.

Table 5.4.3: *Optimal design of phase separator for intensified extraction in small channels. Steps: 1 = main extraction, 2 = scrubbing, 3 = complementary extraction.*

Step	Stream	Length [cm]	Diameter [cm]	Material
1	Mainstream	2.8	0.2	PTFE
1	Sidestream	1.0	0.1	Stainless steel
2	Mainstream	2.6	0.2	PTFE
2	Sidestream	1.0	0.1	Stainless steel
3	Mainstream	2.7	0.2	PTFE
3	Sidestream	1.0	0.1	Stainless steel

5.4.4   Safety

In terms of nuclear criticality safety, the results confirm that the small-scale technology is safer than mixer-settlers and pulsed columns by geometry. Therefore, the use of small channels in the highly active section, in place of pulsed columns, can be a viable option for future SNF reprocessing. The low effective multiplication factor k_{eff} is due to the high surface area to volume ratio and the small liquid holdup in each small channel. The value of k_{eff} in small channels, which is 0.4, refers to the highest value achieved in the largest distributor (level 4). However, in pulsed columns, a neutron absorber can be used to reduce the risk of criticality. Mixer-settlers may be employed for low liquid holdup or diluted solutions, but more detailed investigations on nuclear criticality are required since only approximated calculations have been done and the method used does not take into account fission products and minor actinides.

Table 5.4.4: Optimal design of liquid-liquid extraction using small channels. Steps: 1 = main extraction, 2 = scrubbing, 3 = complementary extraction.

Variable	Step 1	Step 2	Step 3
No. stages	4	4	1
Aq. to org. flow ratio	0.65	0.41	0.60
[HNO$_3$] aqueous scrubbing stream [M]	N.A.	4.7	N.A.

5.4.5 Mass transfer and hydrodynamics

The volumetric mass transfer coefficient $k_L a$ achieved in small channels is three times greater than the one in the pulsed column and almost two times the one in mixer-settlers (see Table 5.4.1). This is not surprising, since the high mass (similarly heat) transfer coefficients is one of the main advantages of the small-scale processes. The $k_L a$ in the pulsed column, the only technology currently used when highly active material is involved, is the smallest between the three technologies, hence the application of small channels in that section would be of particular interest from an industrial point of view. Values of $k_L a$ achieved for the conventional technologies are of the same order of magnitude as those reported in the literature.

The hydrodynamics in small channels are easier to control and predict. A common flow pattern is plug or slug flow, which is relatively regular and the sizes of the plugs and slugs can be predicted reasonably well in the laminar flow conditions prevailing in the small channels [18]; prediction in good agreement with the experimental data can be developed [142]. Conversely, the turbulent two-phase flow in mixer-settlers and pulsed columns produces a dispersed droplet size distribution which may be affected by changes in geometry or operating conditions and, also, challenging to accurately predict because of droplet breakage and coalescence.

5.4.6 Np control

The control and separation of neptunium is improved using small channels because the residence times are short; this is a result of the efficient mass transfer.

Table 5.4.5: Optimal geometry of mixer-settlers. Steps: 1 = main extraction, 2 = scrubbing.

Step	Unit	Width [m]	Length [m]	Height [m]	Impeller diameter [m]
1	Mixer	0.23	0.23	0.23	0.15
1	Settler	0.23	0.90	0.23	N.A.
2	Mixer	0.20	0.20	0.20	0.13
2	Settler	0.20	0.80	0.20	N.A.

Table 5.4.6: Optimal design of liquid-liquid extraction using mixer-settlers. Steps: 1 = main extraction, 2 = scrubbing.

Variable	Step 1	Step 2
No. stages	4	3
Aq. to org. flow ratio	0.78	0.42
[HNO$_3$] aqueous scrubbing stream [M]	N.A.	5.2
Impeller speed [rpm]	200	200

The short residence time is not sufficient to allow high conversion of Np(V), un-extractable, to Np(VI), easily extractable. Formation of Np(IV), with these nitric acid concentrations, is negligible as expected [127]. The decontamination factor of Np, *i.e.* the ratio between the amount of Np in the feed and the one in the product stream (the organic stream outoing step 2) is around 30, which means that over 95% is removed with the high level wastes. Using conventional technologies, the decontamination factor for Np is between 1.7 (pulsed columns) and 3.4 (mixer-settlers), *i.e.* Np removal respectively of 40% and 70%. The presence of Np complicates the second section of the PUREX process, which could hence benefit from the employment of small channels.

5.4.7   Other results

One of the most important advantages of the small-scale technology is the low solvent degradation due to the short residence time of the two-phase flow in the contactor, approximately 5 seconds for each stage of each step. Consequently, the need of solvent makeup and the solvent regeneration costs are reduced. Solvent regeneration requires expensive evaporation and rectification operations [6].

Criticality, process volumes, costs, solvent exposure and the other aspects dis-

Table 5.4.7: *Optimal design of liquid-liquid extraction using perforated plate pulsed column. Steps: 1 = main extraction, 2 = scrubbing. Plate spacing = 0.05 m, plate free area = 23%, hole diameter 0.003 m.*

Variable	Step 1	Step 2
Height [m]	0.47	3.17
Diameter [m]	0.23	0.20
No. plates	9	61
Aq. to org. flow ratio	0.41	0.22
[HNO$_3$] aqueous scrubbing stream [M]	N.A.	4.5
Pulse frequency [s^{-1}]	0.67	0.55
Pulse amplitude [m]	1.77 $\times 10^{-2}$	0.89 $\times 10^{-2}$

cussed above are not the only factors to consider for the application of liquid-liquid extraction equipment in the nuclear industry. Process flexibility could benefit from using small channels: turndown in flow rate and change in the aqueous to organic flow ratio could be achieved by decreasing the number of parallel channels although the consequent possibility of flow maldistribution along the channels (*i.e.* non-uniform flow distribution in the channels) would need to be considered. An increase in the flow rates may lead to flow maldistribution. Small channels could be used in any section of the process, being safe from nuclear criticality by geometry.

To increase throughput scale up of the small-scale contactors by increasing the sizes of the channels can be considered. Above a certain size, however, the mass transfer coefficient could decrease and the resulting extraction will be less efficient. Scale-out, or numbering-up, is the use of more channels in parallel to achieve higher throughput. In scale-out, channel sizes are not modified. However, scale-out is limited by the design of the manifold: a very large and not practical number of channels may be required and high throughput could be difficult to achieve. Using small channels, scale-up and scale-out must be combined to increase throughput and ensure high separation performance.

Contrary to technologies with moving parts, such as mixer-settlers and centrifugal extractors, small channels could tolerate solids. The diameter of the channels, between 1 and 2 millimeters, are large enough to exlude the risk of occlusion.

These other characteristics, for both novel and conventional technologies, are compared in Table 5.4.8, along with the other main aspects.

Table 5.4.8: General comparison of small channels, mixer-settler, spulsed columns and centrifugal extractors. Ratings: 5 = superior, 4 = good, 3 = average, 2 = below average, 1 = poor. The ratings for the conventional technologies (except the last four rows) are taken from Law [3]. Process flexibility includes factors such as aqueous to organic flow ratio and turndown in flowrate. The long residence time is considered an advantage when it is required by the process kinetics, the short residence time is considered an advantage to limit the solvent degradation [3].

Attribute	Small channels	Mixer-settlers	Pulsed columns	Centrifugal Extractors
Long residence time	1	5	4	1
Short residence time	5	1	2	5
Building headroom	5	5	1	5
Floor space required	4	1	5	3
Ease of scale-up	1	3	3	5
Low hold-up volume	5	2	3	5
Equipment capital cost	4	4	5	4
Process flexibility	3	4	3	5
High throughput	1	2	5	5
Ability to tolerate solids	5	2	5	2
Np control	5	2	2	*
Control of hydrodynamics	5	2	2	*
Mass transfer	5	3	2	*
Nuclear criticality safety by geometry	5	1	4	5

* Data not reported by Law [3] and not investigated in this work for this technology.

5.5 Conclusions

A case study in spent nuclear fuel reprocessing has been presented to compare intensified extraction in small channels to conventional technologies, *i.e.* mixer-settlers and pulsed columns. To investigate the behaviour of the small-scale technology, the model developed in Chapter 3 has been used. Mathematical models

of pulsed columns and mixer-settlers have been described in Chapter 4. In this chapter, these models have been combined into a single process model allowing for the design of alternative configurations. The processing models are nonlinear and the design decisions include integer choices. Therefore, the optimisation-based design problem is described by a mixed integer nonlinear programme. Economics, mass transfer, size, solvent degradation, Np separation and nuclear criticality have been compared. The impact of the technology on the optimal flowsheet has been investigated through the recycle ratio design variable, χ, which could potentially lead to three different process configurations. This optimisation-based approach for process design and comparison, using both novel and conventional technologies, is novel.

It was found that pulsed column may be the most cost effective technology, at the cost of large solvent flow rate, the largest among all technologies. This low cost is also due to the large dilution of the feed with the aqueous stream recycled from step 2, which allows to reduce the column height. However, the cost of some equipment should be added.

The small channels can be less expensive than mixer-settler banks. However, the choices of materials and the design of manifolds are crucial. An important saving may be related to the significantly shorter residence time, which can decrease the solvent degradation and thus the solvent regeneration and cleanup costs. Another important consequence of the short residence time is Np separation: over 95% can be removed with small channels while 40% is removed with pulsed columns.

Small channels are safe in terms of criticality due to their geometry, resulting in small volume and a high surface area to volume ratio. Hence, their employment in the highly active section of the process, as an alternative to pulsed columns, should be considered more extensively. Small channels can be less expensive, lead to easier control of Np, exhibit lower solvent degradation and more efficient mass transfer.

To explore alternative flowsheets for SNF reprocessing, the combination of novel and conventional technologies must be evaluated. Considering the discussed benefits of small channels over the traditional equipment, the employment of conventional technologies is not advantageous in terms solvent usage (and inventory), solvent degradation, mass transfer coefficient, nuclear criticality safety, Np separation. The pulsed columns, compared to the case of small channels, allow a

30% reduction of the total annualised cost (costs of pulsator and other equipment excluded). This cost difference may be not important in relation to the facility cost. Pulsed columns require the largest flow rates and operating costs do not take into account losses of acid and solvent. Most importantly, the cost of the solvent regeneration section, which involves expensive operations such as evaporation and rectification, is not included in the calculations. The pulsed columns involve significantly higher residence times, then higher solvent degradation. Hence, considering the operating costs not estimated by the model, the solvent regeneration costs and the equipment not included in the pulsed column model, the process using small channels may actually be more cost effective. The Np separation using small channels is significantly better (DF almost 20 times higher). Volumetric mass transfer coefficients in small channels are three times higher than the one provided by pulsed columns. Taking all the above into consideration, the small channels are considered the most advantageous equipment. In Chapter 6, an alternative flowsheet for spent nuclear fuel reprocessing will be investigated using small channels.

Chapter 6

Alternative flowsheet for SNF reprocessing

In this chapter, an alternative process flow diagram for SNF reprocessing is proposed, based on a COEX process. The application of the novel small-scale technology is investigated, using the mathematical modelling developed in Chapter 3. Because of the several advantages provided by the small contractors over the conventional ones, as discussed in the Chapter 5, neither mixer-settlers nor pulsed columns are included in this flowsheet. The aim is to reduce the risk of nuclear proliferation, producing a mixed Pu/U oxide suitable for fabrication of Mixed Oxide (MOX) fuel instead of a pure Pu product, potentially suitable for military purpose. Another goal is to exploit the high mass transfer coefficients and good separation efficiency in small-scale contactors to reduce the number of unit operations required by the process, leading to a reduction of the plant size and cost.

The chapter is organised as follows. Section 6.1 introduces the goal of the COEX process and the main process flow diagram suggested by the literature. The potential advantages, compared with the current PUREX process, are discussed. In Section 6.2 a first design of a COEX process, exploiting the advantages of the novel technology, is investigated. The mathematical model developed in Chapter 3 needs to be integrated with new equations, to include further components in the physical system and to predict new phenomena, mostly redox reactions. Firstly, a preliminary design of a COEX process is investigated to demonstrate the applicability of the new relationships included in the model. This case study also

introduces the chemistry and unit operations required for this process when the small-scale extractors are used. Furthermore, the most suitable reducing agent for liquid-liquid extraction operations in small-channels is identified. No effect of input parameters or initialisation on the optimal flowsheet have been discussed at this stage. In Section 6.3, a flowsheet for a COEX process has been proposed as alternative process for future SNF reprocessing, employing the small-scale extractors. In contrast to the previous section, here pseudo counter-current and cross flow configurations are combined, to enhance the separation performance and reduce cost and size. Also, in this optimisation problem, TBP concentration in the organic solvent is allowed to vary. The optimal flowsheet has been identified using a superstructure optimisation approach. Finally, Section 6.4 presents an overview of of this chapter.

6.1   U/Pu Combined Extraction process: motivation and description

Several new flowsheets have been suggested in the literature as options for advanced SNF reprocessing. The main goal is to avoid pure Pu streams by either producing mixed Pu/U oxide or leaving some U and/or Np within the Pu streams [6], to preclude nuclear proliferation. Another objective is to separate minor actinides [6]. Some of these flowsheets are briefly described in 2.2.

After the codecontamination section, the PUREX process consists of:

- U/Pu partitioning, where U and Pu are separated using a Pu(IV) reductant;

- U purification, *i.e.* extraction and stripping operations to purify U from contaminants, in particular Tc and Np;

- Pu purification, similarly to the U purification section.

Therefore, products of the process are pure U and Pu streams. Pure Pu, for military purpose, was the goal of the PUREX process when it was developed within the Manhattan Project. Nowadays, Pu is used for MOX fuel fabrication. Pu and U oxides are mixed, after being separated and purified by 3, out of 4, sections of the process. Hence, the flowsheet seems counter-intuitive. One of the most interesting

alternatives to the PUREX process is the COEX (U and Pu Combined Extraction) process. The COEX process does not involve separation and purification of Pu. It has the same first section of PUREX process, the codecontamination section. The product stream of the codecontamination section, which is an organic phase containing U, Pu, HNO_3 and very small amounts of contaminants (Tc, Np, Zr and Ru) undergoes a first stripping step. This step is called "co-stripping", the goal is to strip simultaneously U and Pu from the organic stream. However, the Pu/U ratio in the organic stream leaving the codecontamination section is too low to produce suitable MOX fuel from this stream. Hence, the idea is to strip all Pu and only a small portion of U to achieve a suitable Pu/U ratio for MOX fuel fabrication, typically around 10% [143] (although it depends on the reactor type). This technique provides a better homogeneity of U/Pu distribution within the MOX fuel, compared to the current approach. To back extract all Pu and only a small fraction of U, the Pu oxidation states must be changed to exploit their different equilibrium behaviours. Pu is originally present in the mixture as Pu(IV), U as U(VI). A reducing agent is used to reduce Pu(IV) to Pu(III). Pu(III) is not very extractable, in contrast to Pu(IV) and U(VI), so it is simple to strip. Reductants suitable for the nuclear industry are hydroxylamine nitrate (HAN) and U(IV). Also, a nitrite scavenger is used to prevent the re-oxidation from Pu(III) to Pu(IV), which is autocatalytic in presence of nitrites. Typically, hydrazine nitrate $N_2H_4 \cdot HNO_3$ is used for this purpose [6].

The sketch of a simplified COEX process is shown in Figure 6.1.1 [6]. Steps 1-4 represent the typical codecontamination section, steps 5 is the Pu/U co-stripping step, where the reducing agent is used to strip all Pu and some U. Step 6 is needed for U stripping. Some contaminants are still present in the U product, hence a second cycle for U purification, which consists of steps 9 (U extraction) and 10 (U stripping), is required. The aqueous stream leaving step 5, loaded with U and Pu, is oxidised to convert U(IV) and Pu(III) in, respectively, U(VI) and Pu(IV), easier to extract in step 7. Step 8 is the final Pu/U stripping to produce the mixed Pu/U stream, which undergoes an adjustment step (topping up of U) to achieve the desired Pu/U ratio [6].

To sum up, the most important benefits of this flowsheet, when compared with the current PUREX process, are:

- no U/Pu partitioning section;

- no Pu purification section;

- no evaporation step;

- more cost effective (less unit operations required);

- better quality of MOX fuel;
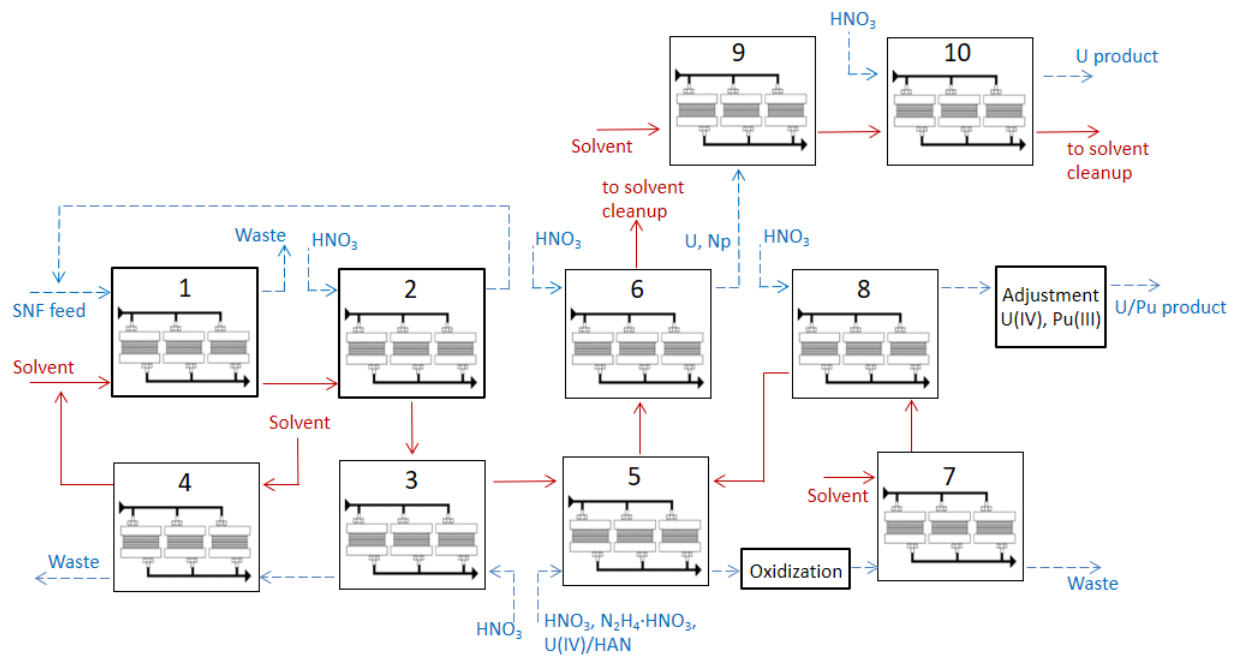
- no nuclear proliferation.

Figure 6.1.1: Sketch of a general COEX process [6]. Blue dashed lines refer to aqueous streams, red continuous lines refer to organic streams. Steps: main extraction (1), Zr and Ru scrubbing (2), Tc scrubbing (3), complementary extraction (4), Pu/U co-stripping (5), U stripping (6), Pu/U co-extraction (7), Pu/U stripping (8), U extraction (9), U stripping (10).

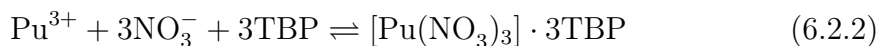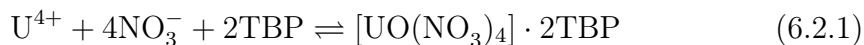## 6.2 Modelling and preliminary investigation of the COEX process

Further components, equilibrium relationships and chemical reactions must be included in the model to investigate a COEX process. In this section the integration of these phenomena, in the mathematical model developed in Chapter 3, is described. Then, a preliminary design of the COEX process is investigated. The aims are to introduce the COEX process using small channels and to test the suitability of the revised model for this process. Furthermore, the initialisation for a more challenging COEX process, that will be investigated in Section 6.3, is provided.

6.2.1 Integration of mathematical modelling

For a COEX process, the components to be added in the system are the following: the reducing agents HAN (*i.e.* NH_3OHNO_3) and U(IV), the reduced form of plutonium Pu(III), hydrazine nitrate $N_2H_4 \cdot HNO_3$ as nitrite scavenger. New mass transfer calculations and redox reaction must be included in the system. For example, Pu(IV) reduction plays a crucial role in the COEX process. Size and nonlinearity of the mathematical model will increase, and some simplifying assumptions are required to facilitate the calculations. Below, these aspects are discussed in detail.

Distribution coefficients

U(IV) and Pu(III), although their affinity with the solvent is not as high as for U(VI) and Pu(IV), are extractable by TBP, according to the following reactions:

$$U^{4+} + 4NO_3^- + 2TBP \rightleftharpoons [UO(NO_3)_4] \cdot 2TBP \tag{6.2.1}$$

$$Pu^{3+} + 3NO_3^- + 3TBP \rightleftharpoons [Pu(NO_3)_3] \cdot 3TBP \tag{6.2.2}$$

Distribution coefficients of U(IV) and Pu(III) have been estimated as suggested by Geldard *et al.* [144]:

$$D_{Pu(III)} = 1.138 \times 10^{-2} D_{U(VI)} \tag{6.2.3}$$

$$D_{U(IV)} = (0.0541 + 0.000658[NO_3^-]^2) D_{U(VI)} \tag{6.2.4}$$

105

Kumar and Koganti developed another method to estimate these distribution co-efficients [43, 145], but valid only for 30% TBP/dodecane and room temperature.

HAN and hydrazine nitrate are not extracted by the organic solvent [46]. They are only involved in chemical reactions.

Mass transfer

In Chapter 3, the volumetric mass transfer coefficient $k_L a$ was calculated by Eq. 3.2.11. In all previous case studies, the optimal values of diameter D and length L, both design variables, were respectively the upper (0.2 cm) and the lower (10 cm) bound. The superficial velocity v achieved has been, approximately, 0.02 m s^{-1} in most of the stages. Here, a first order Taylor series expansion has been used to linearise Eq. 3.2.11 around the aforementioned values of v and the upper bound for D, while L has been assumed to be at its lower bound. Hence, only variations of v and D are included in the calculation of $k_L a$. This linearisation simplifies the calculations. The effect of the upper bound of the diameter on the process design will be investigated at a later stage. It is crucial for small-scale contactors the possibility of increasing, simplifying the manifolds. On the contrary, the lower bound of the channel length is already considered a reasonable value as shortest length (in the literature, equal or greater lengths have been typically investigated [19, 20, 24, 146]). Furthermore, from an industrial point of view, it is more likely that the channel length will be increased, to provide further residence time (unless it is essential for Np control), rather than decreased, hence the investigation of shorter length in not essential at this stage. The resulting linearised equation of the $k_L a$, as function of only velocity v and diameter D, is given by:

$$
k_L a(v, D) = k_L a|_{Eq.3.2.11}(v_0, D_0) + \frac{\delta k_L a|_{Eq.3.2.11}}{\delta v}(v_0, D_0)(v - v_0) +
$$
$$
+ \frac{\delta k_L a|_{Eq.3.2.11}}{\delta D}(v_0, D_0)(D - D_0) \qquad (6.2.5)
$$

where v_0 is 0.02 m s^{-1}, D_0 is the upper bound used for the diameter. Eq. 6.2.5, compared to the nonlinear Eq. 3.2.11, provides small difference in the k_L for significant difference in velocity and diameter: for equal L, the linearised equation leads an overestimation in the $k_L a$ of approximately 4% if the velocity is halved and an underestimation of 4% if the diameter is halved.

Chemical reactions

In SNF reprocessing, a key role in the process is played by the reduction of Pu(IV) to Pu(III), using a reducing agent which inevitably affects U and Np oxidation states. Both typical reductants in the SNF reprocessing, U(IV) and HAN, have been considered. Hydrazine nitrate acts as weak reducing agent, as well. Therefore, several chemical reactions, mostly redox reactions, must be taken into consideration:

- Pu(IV) reduction by HAN, U(IV) and hydrazine;

- NO_2 scavenge by HAN and hydrazine nitrate;

- Np(VI) and Np(V) reduction by HAN, U(IV) and hydrazine;

- U(IV) auto-oxidation;

- Pu(III) auto-oxidation, catalysed by HNO_2.

In total, 12 chemical reactions have been implemented in the calculations, some of them in both aqueous and organic phases. These reactions and their rate laws are shown respectively in Table 6.2.1 and Table 6.2.2. Some of the chemical reactions occur in both aqueous and organic phase. In total, 12 chemical reactions have been implemented in the calculations.

Table 6.2.1: Chemical reactions included in the problem.

No.	Reaction	Phase
(6.2.6)	$2Pu^{4+} + 2NH_3OH^+ \rightarrow 2Pu^{3+} + N_2 + 2H_2O$	aq.
(6.2.7)	$2NH_3OH^+ + HNO_2 \rightarrow N_2O + 2H_2O + H^+$	aq.
(6.2.8)	$2NpO_2^{2+} + 2NH_3OH^+ \rightarrow 2NpO_2^+ + 4H^+ + N_2 + 2H_2O$	aq.
(6.2.9)	$2Pu^{4+} + U^{4+} + 2H_2O \rightarrow Pu^{3+} + UO_2^{2+} + 4H^+$	aq., org.
(6.2.10)	$2NpO_2^{2+} + U^{4+} + 2H_2O \rightarrow 2NpO_2^+ + UO_2^{2+} + 4H^+$	aq.
(6.2.11)	$2NpO_2^+ + U^{4+} + 4H^+ \rightarrow 2Np^{4+} + UO_2^{2+} + 2H_2O$	aq.
(6.2.12)	$2NpO_2^{2+} + 2N_2H_5^+ \rightarrow NpO_2^+ + N_2 + 2H^+ + 2NH_4$	aq.
(6.2.13)	$2Pu^{4+} + 2N_2H_5^+ \rightarrow 2Pu^{3+} + 2NH_4 + N_2 + 2H^+$	aq.
(6.2.14)	$HNO_2 + 2N_2H_5^+ \rightarrow HN_3 + H_2O + H^+$	aq.
(6.2.15)	$U^{4+} + NO_3^- + 2H_2O \rightarrow UO_2^{2+} + HNO_3 + H^+$	aq., org.
(6.2.16)	$3Pu^{3+} + H^+ + NO_3^- \rightarrow 3Pu^{4+} + NO + 2H_2O$	aq.

Table 6.2.2: Reaction rates used in the problem. Kinetic constants are given at $25^\circ C$. For different temperature, the values of the kinetic constants below are recalculated using the activation energy provided by the cited authors.

Ref. Reaction	Reaction rate R [Mol L^{-1}s^{-1}]	Phase	Ref.
6.2.6	$R = 1.22 \times 10^{-2} \frac{[\text{PU}^{4+}]^2}{[\text{PU}^{3+}]^2} \cdot \frac{[\text{NH}_3\text{OH}^+]^2}{[\text{H}^+]^4([\text{NO}_3^- +0.33]^2)}$	aq.	[46]
6.2.7	$R = 5.33[\text{H}]^+[\text{NH}_3\text{OH}^+] \cdot [\text{HNO}_2]$	aq.	[37]
6.2.8	$R = 1.54[2\text{NpO}_2^{2+}] \cdot [\text{NH}_3\text{OH}^+][\text{H}^+]^{-1}$	aq.	[46]
6.2.9	$R = 8.33 \times 10 \frac{[\text{PU}^{4+}]^2[\text{U}^{4+}]^2}{[\text{H}^+]+0.05^2}$	aq.	[46]
6.2.9	$R = 8.33 \times 10^{-2} \frac{[\text{PU}^{4+}]^2[\text{U}^{4+}]^2}{[\text{H}^+]+0.05^2}$	org.	[46]
6.2.10	$R = 1.17 \times 10^{-1}[2\text{NpO}_2^{2+}][\text{U}^{4+}]$	aq.	[46]
6.2.12	$R = 3.75 \times 10^{-2}[\text{NpO}_2^+][\text{U}^{4+}] \cdot (1.6[\text{H}^+]^{-2} + 1.42[\text{H}^+])$	aq.	[46]
6.2.11	$R = 1.38 \times 10^{-1}[\text{NpO}_2^{2+}] \cdot [\text{N}_2\text{H}_5^+][\text{H}^+]^{-1.3}$	aq.	[46]
6.2.13	$R = 6.33 \times 10^{-4} \frac{[\text{PU}^{4+}]^2[\text{N}_2\text{H}_5^+]^2}{[\text{H}^+]+0.35}$	aq.	[46]
6.2.14	$R = 6.17[\text{H}^+][\text{N}_2\text{H}_5^+][\text{HNO}_2]$	aq.	[37]
6.2.15	$R = 5.33[\text{U}^{4+}][\text{H}^+]^{2.7}[\text{HNO}_2]^{0.38}$	aq.	[37]
6.2.15	$R = 2.67 \times 10^{-4}[\text{U}^{4+}][\text{HNO}_2]^{0.49}$	org.	[37]
6.2.16	$R = 1.04 \times 10^{-1}[\text{Pu}^{3+}] \cdot [\text{HNO}_2]^{0.5}[\text{H}^+]^{0.5}[\text{NO}_3^-]^{0.4}$	aq.	[46]

Further assumptions

The additional equations have increased size and complexity of the mathematical model. To reduce the computational expense and solve the more challenging mathematical system, some simplifying assumptions have been necessary.

Firstly, since no comparison with conventional technologies is performed, the calculations for the design of the two-phase separator has been neglected; these calculations do not significantly affect the optimal design of the small channels and were required only for the purpose of overall comparison with traditional technologies. This assumption simplifies calculations.

Secondly, the nonlinear empirical relationship used to predict F_d (discussed in Section 3.2.6), to correlate F_d to the number of elements and the hydraulic resistance ratio r in each level of the manifold, have been replaced by two inequality constraints. The maximum number of elements in the first level of the manifold and the minimum resistance ratio between level 2 and level 1 have been set to,

respectively, 70 and 10^4. These two inequality constraints, in addition to a laminar regime ($Re \leq 2000$), are required to guarantee a flow maldistribution lower than approximately 10% [108] and replace the nonlinear empirical relationships described in Section 3.2.6.

6.2.2 Preliminary design of the COEX process using small channels

The small-scale contactors, providing high mass transfer coefficient and efficient decontamination, may be used to significantly reduce and simplify the COEX process proposed in the literature (see Figure 6.1.1). A reduction of the number of unit operations, for equal flow rates, would be advantageous in terms of sizes, safety, solvent degradation, economics. If a significant improvement of Np and Tc separations in the codecontamination section (steps 1-4 of Figure 6.1.1) can be achieve, the U purification cycle (steps 9-10) may be superfluous. Steps 7 and 8, which are a further cycle of extraction and stripping to purify the Pu/U product, may be unnecessary as well. Hence, using small channels and intensify the separation performance in the codecontamination section, the flowsheet shown in Figure 6.1.1 can be replaced by the flowsheet depicted in Fig 6.2.1. The codecontamination section investigated in the previous chapter, using a single scrubbing step of intermediate HNO_3 concentration, has been considered. The adjustment step shown in Figure 6.1.1 can be removed if the process is designed to provide a mixed oxide with the desired Pu/U concentration ratio.

Optimisation problem definition

Similarly to the previous chapters, the process has been optimised according to economic criteria, to minimise the total annualised cost (see Eq. 3.4.1). Design variables are geometrical variables (diameters, lengths, size of each level of the manifolds), number of stages, flow rates, concentrations of nitric acid solutions, hydrazine nitrate, reducing agent (HAN and U(IV), used alternatively).

For steps 1-3, the same inequality constraints of Chapter 5 have been used. In the rest of the flowsheet, further constraints have been added. Firstly, the Pu/U ratio in the organic stream leaving the co-stripping step (step 4 of Figure 6.2.1) has been set to 10%, which is an average ratio for Pu/U ratio in the MOX fuels
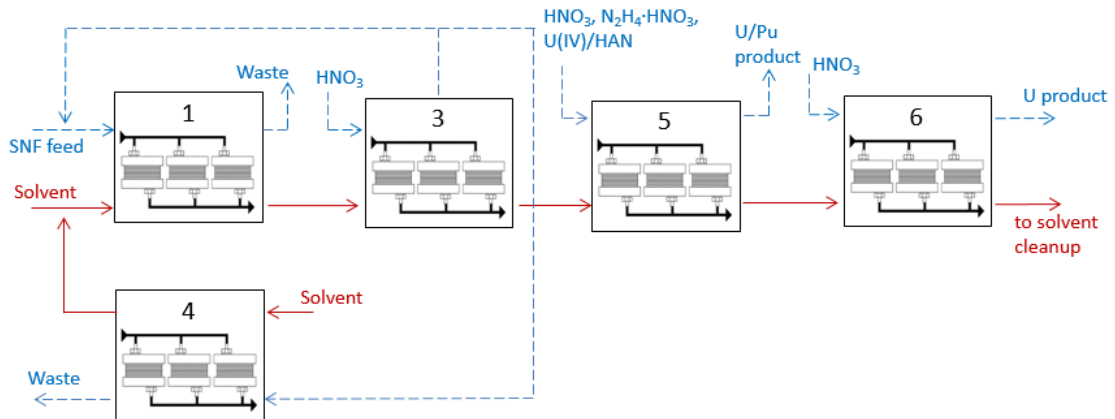
110

Figure 6.2.1: Sketch of a simplified COEX process [6]. Blue dashed lines refer to aqueous streams, continuous red lines refer to organic streams. Steps: main extraction (1), Zr and Ru scrubbing (2), Tc scrubbing (3), complementary extraction (4), Pu/U co-stripping (5), U stripping (6).

[143]. Secondly, Pu extraction and U back extraction equal or higher than 99%, respectively in step 5 and 6, have been included as requirement of the process.

In this optimisation problem, the results achieved in Chapter 5 with small channels have been used as initialisation. Same input parameters have been used, unless for step 5, where different temperature and channel material have been used. The temperature is set to 50°C, to favour back extraction. This is the typical temperature [6]. Low temperatures increases the required aqueous flow rates and costs. High temperatures may be unrealistic and leading to loss of acid and of/organic solvent due to evaporation. The channels are made of stainless steel, to disperse the organic flow rate, which is expected to be lower than the aqueous one. Therefore, it is preferred to disperse the organic phase, reducing the plug size and increase the superficial area. Steps 4 and 5 have been solved using a sequential modular approach first, then all unit operations have been simultaneously solved, as described in Section 3.3.2.

111

Results and discussions

The main results of this optimisation problem are summarised below. No different initialisations have been discussed. Also, the results achieved in steps 1-3 are very close to the ones achieved in Chapter 5 with small channels, thus they have not been reported here. A novel COEX process using small channels will be proposed and discussed in detail in Section 6.3.2, this is about a preliminary investigation to introduce the COEX process, to overview its chemistry and to provide initialisation for the next case study.

Optimal design   The optimal design and operating conditions of steps 1, 2 and 3 (see Figure 6.2.1) are close to the results achieved in the previous chapter, and will not be discussed in this section. This minimal difference is not surprising, as the results achieved in Chapter 5 for small channels have been used as initialisation and limited variations have been done in input parameters and constraints.

The results regarding steps 4 and 5 are shown in Table 6.2.3 and 6.2.4. As expected, a small aqueous flow rate is used in step 4 to strip Pu, whilst a very large aqueous flow rate is necessary to efficiently strip 99% of U(VI) in step 5. The affinity between TBP and U(VI) is high, so large aqueous to organic flow ratio are required. The nitric acid concentration of the acid solution used for the step 4 (co-stripping) is relatively low, around 0.4 M, to allow Pu stripping and extracting only a small fraction of U. The nitric acid concentration of the aqueous solution used for U tripping is very low, 0.01 M, the lower bound used for this variable.

Reductants and nitrite scavenger   Using small-scale contactors, U(IV) is a better reductant than HAN. The reason is related to the kinetics of the Pu(IV) reduction by HAN, which is not sufficiently fast to allow the stripping of 99% of Pu in the short residence time provided by the channels. The short residence time, an advantage of the small-scale contactor, implies the use of a strong reductant. U(IV) is a stronger and more effective reductant than HAN [6]. In the nuclear industry, HAN is used in the Pu purification section to avoid re-addition of U in the system. In this flowsheet, however, no pure Pu is produced, hence the addition of small amount of U(IV) is not counter-intuitive.

The short residence time makes negligible the oxidation of Pu(III) to Pu(IV) in presence of HNO_2 (see Eq. 6.2.16), which could complicate Pu stripping. Hence,

Table 6.2.3: Optimal design of flow network for intensified extraction in small channels. Steps: 4 = Pu/U co-stripping, 5 = U stripping, see Figure 6.2.1.

Step	Phase	Scale	No. elements	Length [cm]	Diameter/Width [cm]
4	aq.,org.	1	69	10	0.2
4	aq.	2	8	40.8	1.3
4	aq.	3	6	27.6	1.5
4	aq.	4	1	22.6	3.0
4	org.	2	8	40.8	2.7
4	org.	3	6	56.7	3.2
4	org.	4	1	48.5	6.7
5	aq.,org.	1	70	10	0.2
5	aq.	2	23	41.4	2.0
5	aq.	3	6	130.0	5.5
5	aq.	4	1	82.3	19.3
5	org.	2	23	41.4	1.7
5	org.	3	6	121.9	4.1
5	org.	4	1	61.7	6.7

Table 6.2.4: Optimal design of liquid-liquid extraction using small channels. Steps: 4 = Pu/U co-stripping, 5 = U stripping, see Figure 6.2.1.

Variable	Step 4	Step 5
No. stages	4	3
Aq. to org. flow ratio	0.18	2.02
[HNO$_3$] aqueous scrubbing stream [M]	0.36	0.01
[U(IV)] aqueous scrubbing stream [M]	2.39×10^{-2}	N.A.
[N$_2$H$_4$·HNO$_3$] aqueous scrubbing stream [M]	0	N.A.

no $N_2H_4\cdot HNO_3$ as nitrite scavenger is used by the process.

Further comments   The total annualised cost of the process is around £210,000 y^{-1}. Approximately 75% of this cost is due to the U stripping. The latter is the unit operation with the largest flow rates and the largest stack, to distribute the high flow rates in the large number of channels.

U stripping, as the aqueous flow rate is larger than the organic one, is the only unit operation where a dispersed organic phase is advantageous. Hence, the choice of stainless steel channels in this unit operation has proven to be reasonable. A continuous organic phase, with large dispersed aqueous plugs, as the aqueous flow rate is the largest flow, would have reduced interfacial area and mass transfer. For all the other steps, PTFE channels have been considered, to disperse the aqueous phase and increase the interfacial area when the aqueous flow rate is the smallest one. Stainless steel channels are more expensive than PTFE channels but, if the aqueous flow is the largest one, the use of polymeric channels would complicate the manifold design, resulting in more expensive and maybe not practicable manifolds (larger flow rates and more channels are required to overcome the reduction in the interfacial area).

The relationships used to estimate distribution coefficients of Zr and Ru do not take into account the effect of temperature; however, the concentration of these two components in the U stripping step is extremely low and their behaviour is negligible.

The purity of the U product is over 99.9%, hence the flowsheet and the inequality constraints used are sufficient to ensure a U product with high quality, according to the model. The purity of the Pu/U mixed product is around 99.85%, since the amount of Tc in this stream is still relatively high. A decontamination factor of 10 for Tc has been imposed as minimum requirement of the process, as this is the typical value achieved nowadays in the PUREX process [6]. However, if a purity greater or equal to 99.9% for the MOX product is required in this flowsheet, a better Tc separation must be achieved in steps 1-3, *i.e.* higher DF in the codecontamination section.

This flowsheet has several advantages over the current PUREX process. However, there are still options that may be worth exploring, in order to further improve the separation performance and reduce cost and size. This will be the goal of the

114

next section.

6.3 Superstructure optimisation of the COEX process

In this section, an alternative flowsheet for SNF reprocessing, based on a COEX process, is proposed. Similarly to the previous section, only the novel small-scale technology is used. Compared to the flowsheet investigated in Section 6.2, some potential improvements, such as different flow pattern configuration, are explored. Only one reducing agent, the suitable one identified in the previous section, is considered. Also, same channels materials have been assumed. The organic concentration in the solvent is not the traditional ones, but allowed to vary to investigate the optimal TBP concentration. An optimal flowsheet is then suggested via superstructure optimisation (see Figure 6.3.1), which embeds all the potential networks and alternative flowsheets of interest. The characteristics of the superstructure flowsheet are described in Section 6.3.1. The optimisation problem is defined in Section 6.3.2, whereas results are discussed in Section 6.3.3.

6.3.1 Superstructure flowsheet for the COEX process

A superstructure is a common and effective tool to formulate flowsheet synthesis problems, often as mixed-integer nonlinear programming problem [147, 148, 149, 150, 151, 152]. The superstructure incorporates all process design alternatives of interest, from which the best flowsheet can be identified. In the superstructure flowsheet studied in this section, except the three potential flowsheets determined by the value of χ (such as in sections 5.1 and 6.2.2), a large number of possible combinations of streams and hence flowsheets exist.

The main differences with the flowsheet investigated in Section 6.2 are:

1. possible flow splitters at the end of step 2;

2. interstage aqueous streams (fresh nitric acid solution) in step 4;

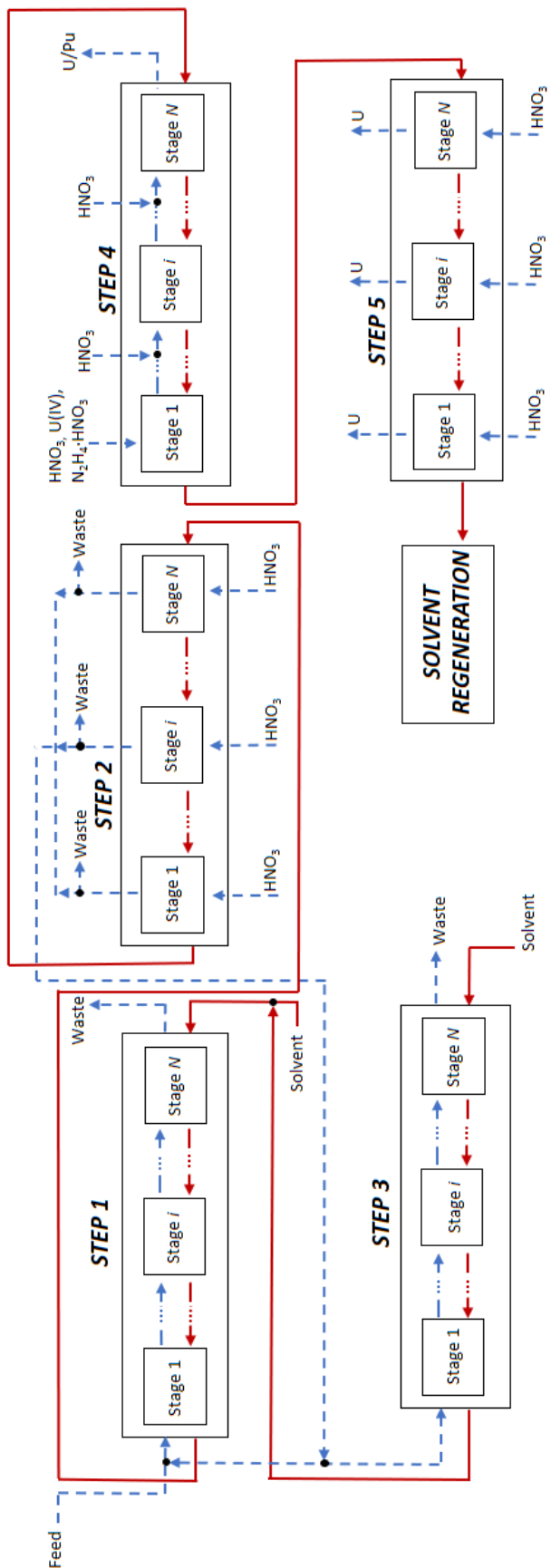3. pseudo cross-flow configuration in step 2 and 5.

Figure 6.3.1: *Flowsheet superstructure proposed for an alternative COEX process. The blue dashed streams refer to the aqueous phase, the red continuous streams refer to the organic phase. Within each step, only the 1st, the intermediate ith and the final Nth stages are shown. Black dots refer to the nodes, which acts as flow splitter if the streams are leaving, mixing junction if streams are incoming. Step 1 = main extraction, Step 2 = Zr, Ru and Tc scrubbing, Step 3 = complementary extraction, Step 4 = U/Pu co-stripping, Step 5 U stripping. Counter-current and cross flow configurations are shown.*

116

The points 1 and 2 described above, together with the value of the recycle ratio χ, can lead to a large number of potential flowsheets. The point 3 is the most important difference with the previous COEX flowsheet investigated. This choice can lead to different aqueous flow rates and stage designs, in terms of channels and manifolds design, within the different stages of the same unit operations. The pseudo cross-flow increases the size of the mathematical problem. The resulting superstructure flowsheet is depicted in Figure 6.3.1. The pseudo cross-flow, the interstage aqueous streams and the flows spitters are described below.

Pseudo cross-flow

Besides the geometry of channels, manifolds and number of stages, crucial decision variables are all flow rates and nitric acid concentrations, which significantly affect hydrodynamics, equilibria and mass transfer. In the previous case studies a pseudo counter-current flow configuration was considered, hence equal flow rates for each stage had been assumed. In the pseudo counter-current flow configuration, the nitric acid concentration in each stage is strongly affected by the value of the nitric acid concentration entering the first stage. It could be advantageous to use a different nitric acid solution for each stage. With this approach, significantly different values of HNO_3 concentration and aqueous flow rate could be explored, if necessary, at different stages of the same unit operation. HNO_3 can shift equilibria, and this flow configuration can be beneficial especially in the scrubbing section, where Ru and Zr can be easily stripped by diluted HNO_3 solution whilst Tc stripping requires concentrated HNO_3 solution. Also, the use of fresh nitric acid solution at each stage allows operation with larger driving forces for mass transport (the entering aqueous stream does not contain any metals). This design is applied to steps 2 and 5 of the flowsheet shown in Fig. 6.3.1.

This flow configuration increases the size of the model, since different flow rates and manifold designs must be allow even for the same stage.

Additional interstage streams

The Pu/U co-stripping, step 4, is different from the other scrubbing/stripping steps (2 and 5), because of the presence of the reductant in the inlet aqueous stream. Fresh HNO_3 solutions containing U(IV) cannot be fed to each stage in this unit

operation: the final U content in the Pu/U product would be too high, whilst with lower amount of fresh U(IV) per stage the reaction rate would not be high enough to complete Pu(IV) reduction into Pu(III). To investigate the possibility of different HNO_3 concentration and/or aqueous flow rate in this step, the use of fresh HNO_3 solution between the stages can be evaluated. In this way, the reductant can have the necessary residence time to allow Pu stripping with high efficiency, whilst the nitric acid solution and flow rates can be adjusted in some stages, if beneficial, to vary hydrodynamics, reaction kinetics and equilibrium relationships. However, flow rates and volumes would increase, hence no large additional amounts of HNO_3 solution are expected.

Additional flow splitters

A disadvantage of the pseudo cross flow configuration is the likely large overall aqueous stream leaving the unit operation. This aqueous stream is recycled from the scrubbing step (step 2 in Fig. 6.3.1) to the main extraction step (step 1), and also fed to the complementary extraction step (step 3). Hence, size and cost of steps 1 and 3 are affected by the large aqueous stream. Since the aim of this process is to recover U and Pu, whereas there is no interest in recovering minor actinides and fission products, a possible solution to reduce the total aqueous stream can be a partial discharge of the aqueous streams leaving the stages in step 2. This approach can be viable especially in the final stages, if the content of U and Pu in the final streams is very low.

6.3.2 Optimisation problem definition

The system involves 14 components: two forms of uranium, two forms of plutonium, two forms of neptunium, ruthenium, zirconium, technetium, two nitric acid complexes in the organic stream, nitrous acid, TBP, hydrazine nitrate. A total of 11 chemical reactions, mostly redox reactions, have been included (Eq. 2.1.3, which is a reversible reaction, and Eqs. 6.2.9-6.2.16). For this process, as discussed in Section 6.2.2, U(IV) is a better reductant than HAN. Hence, the latter has not been considered in this case study.

The process has been optimised according to economic criteria, to minimise the total annualised cost (see Eq. 3.4.1). A payout time of 5 years and a 5% interest

rate have been considered to calculate the annual costs. As for the previous case studies, the payout time, in a reasonable range, it is not expected to significantly affect the optimal design [153].

Decision variables are geometrical variables (channel diameters, lengths, size of each distributing channel in the manifolds), number of stages, flow rates, concentrations of nitric acid solutions, hydrazine nitrate and U(IV). In this case study, TBP fraction in the solvent is also an assumed decision variable. TBP is typically diluted to decrease viscosity and density, to separate the two phases exploiting gravitational forces (TBP and water have approximately the same mass density), as in conventional technologies. However, in small channels the separation is based on other principles, such as the wettability of the material, therefore the TBP fraction could be increased. High fraction of TBP enhances extraction, whilst low TBP fraction improves back extraction, so scrubbing and stripping.

The inequality constraints are described in Table 6.3.2. The first five con-

Table 6.3.1: Input parameters and flow pattern designs.

Parameter	Component/Step	Value
Feed concentration	U(VI)	1050.42
[Mol m^{-3}]	Pu(IV)	11.65
	Ru	7.59
	Zr	12.99
	Tc	2.77
	Np(V)	0.64
	HNO$_2$	1.00
Temperature [°C]	Steps 1, 2, 3, 4	25
	Step 5	50
Throughput [MTHM y^{-1}]	-	500
Channel material	Steps 1, 2, 3, 4	PTFE
	Step 5	stainless steel
Flow pattern design	Steps 1, 3, 4	counter-current
	Step 2, 5	cross flow

119

straints in the table, *i.e.* the one regarding U concentration in the aqueous stream leaving step 1, the recovery of U and Pu from step 1 to step 3, Zr and Ru decontamination factors are typical industrial requirements. Tc DF has been increased to 50, to allow higher purities of products (a typical value of this DF is 10 [6]). The effective multiplication factor k_{eff} has to be lower than 0.95 to ensure nuclear subcriticality. The inequality constraints related to the number of elements in the first level of the manifold (N_{level1}^{elem}) and to the resistance ratio between level 2 and level 1 (r_{level2}), in addition to the laminar regime ($Re \leq 2000$), are required to guarantee a flow maldistribution within the parallel channels lower than 10% [108], as described in Section 6.2.1. The last three inequality constraints in Table 6.3.2 are necessary to achieve high extraction efficiency of Pu and U in, respectively, step 4 and 5 ($\geq 99\%$).

Table 6.3.2: *Inequality constraints of the optimisation problem.*

Inequality constraints	Comment
$Rec_U^{Step1\text{-}3} \geq 0.99$	Minimum uranium recovery
$Rec_{Pu}^{Step1\text{-}3} \geq 0.99$	Minimum plutonium recovery
$[\text{U}]_{aq,out}^{Step1} \leq 1.68$ M	Maximum typical uranium concentration in HLW from step 1
Zr DF $\geq 10^4$	Typical requirement [6]
Ru DF $\geq 10^4$	Typical requirement [6]
Tc DF ≥ 50	Increased from typical requirement [6]
$E_{Pu}^{Step4} \geq 0.99$	Pu extraction efficiency required
$E_U^{Step5} \geq 0.99$	U extraction efficiency required
$[\text{Pu}]_{aq,out}^{Step\ 4} \backslash [\text{U}]_{aq,out}^{Step\ 4} = 0.1$	MOX concentration required
$k_{eff} \leq 0.95$	Nuclear subcriticality
$N_{level1}^{elem} \leq 70$	Requirement for good flow distribution
$r_{level2} \geq 1 \times 10^4$	Requirement for good flow distribution
$Re \leq 2000$	Laminar flow

A greater upper bound, compared to the previous case studies, has been used for the channel diameter, 2.5 mm rather than 2 mm. Despite most of the works

in the literature focuses on channel diameters between 0.5 and 2 mm, some authors investigated segmented flows in channels with diameter up to 3 mm, still achieving an advantageous mass transfer coefficient [154]. In a potential industrial application of this technology, it will be crucial to identify the largest diameter possible, to reduce the number of channels and simplify the manifold design. The effect of the diameter's upper bound on the process has been investigated in this paper. In particular, the goal is to explore the potential impact of a 25% increase in the channel diameter on the process design and performance. Although the mass transfer model used has never been validated for this value, the optimisation model can still provide valuable insight.

To reduce the computational expense to solve the more challenging mathematical system, due to the increase in the size and nonlinearity of the model, some simplifying assumptions have been necessary. Concentrations of Zr and Ru, considering the very high decontamination factors achieved in the first part of the flowsheet (steps 1-3), are expected to be extremely low in organic stream leaving step 4 (lower than 1×10^{-4} Mol m^{-3}) and can be neglected in step 5, to simplify the calculations. The formation of Np(IV) is negligible in the range of HNO$_3$ concentrations expected [127], the concentration of Np(IV) is then neglected here.

All the unit operations in Figure 6.3.1 are solved simultaneously. The overall number of equations is approximately 450,000; the integer variables are 47. The solver used for this optimisation problem is the SBB solver (maximum relative gap set to 1%). The other MINLP solvers have shown difficulties to find feasible solutions.

6.3.3 Results and discussions

The optimal flowsheet is shown in Figure 6.3.2. Compared to the current flowsheet for SNF reprocessing, this design improves the economics and safety of the process. No portions of the aqueous streams leaving step 2 are discharged, to meet the high requirements in terms of U and Pu recovery. Approximately 93% ($\chi = 0.934$) of the overall aqueous stream leaving step 2 is recycled to step 1 and 6% is fed to step 3. In the step 4, no further streams are used between stages, to minimise volumes and cost.

The overall total annualised cost has been around £173,000 per year, to which

the cost of separators should be added. Approximately, the 60% of the cost is due to step 5, which uses the most expensive material to disperse organic phase.

Compared to the flowsheet shown in Figure 6.2.1 and discussed in the paragraph 6.2.2, the cost reduction is approximately by 18%, and the separation performance of the process has been significantly improved (minimum Tc DF from 10 to 50, better quality of U and MOX products).

The optimal TBP fraction achieved is 34.2% (v/v), slightly above the typical value (30%). It is reasonable that the TBP fraction is still relatively low, since this flowsheet involves more back extraction steps than extraction steps, hence high TBP concentration would increase the cost of all scrubbing/stripping steps (the majority) and the overall annualised cost.

Whereas for steps 1, 3 and 4 a conventional counter-current configuration has been investigated, for steps 2 (Zr, Ru and Tc scrubbing) and 5 (U stripping) a pseudo cross flow, involving fresh nitric acid solution in each stage, has been investigated. Despite the scrubbing of Zr and Ru is favoured by lower nitric acid solution, the nitric acid solution of all the fresh aqueous streams obtained for step 2 is similar and relatively high: between 4.37 M and 4.49 M (see Table 6.3.4), similarly to Section 5.4. A sketch of the manifold design for the step 1 is shown in Fig. 6.3.3.

The choice of the material may significantly affect the design, as it is a cost minimisation problem and the operating cost is small. In particular, with a more expensive polymeric material, higher TBP fraction and/or lower aqueous to organic flow ratio may have been obtained to reduce the size of the step 1, which is the biggest equipment in the process using polymeric small extractors. All the results are further discussed below.

Solvent concentration

The optimal volumetric fraction of TBP in the organic phase, *i.e.* 34.2%, is slightly above the typical value (30%). Increasing further the TBP fraction, an increase of the overall cost would be due to the step 5 (U stripping). The latter is the most expensive unit operation, as it involves large flowrates and stainless steel channels are employed, to disperse the organic phase and reduce the number of channels required. Hence, this TBP concentration has been affected by the design
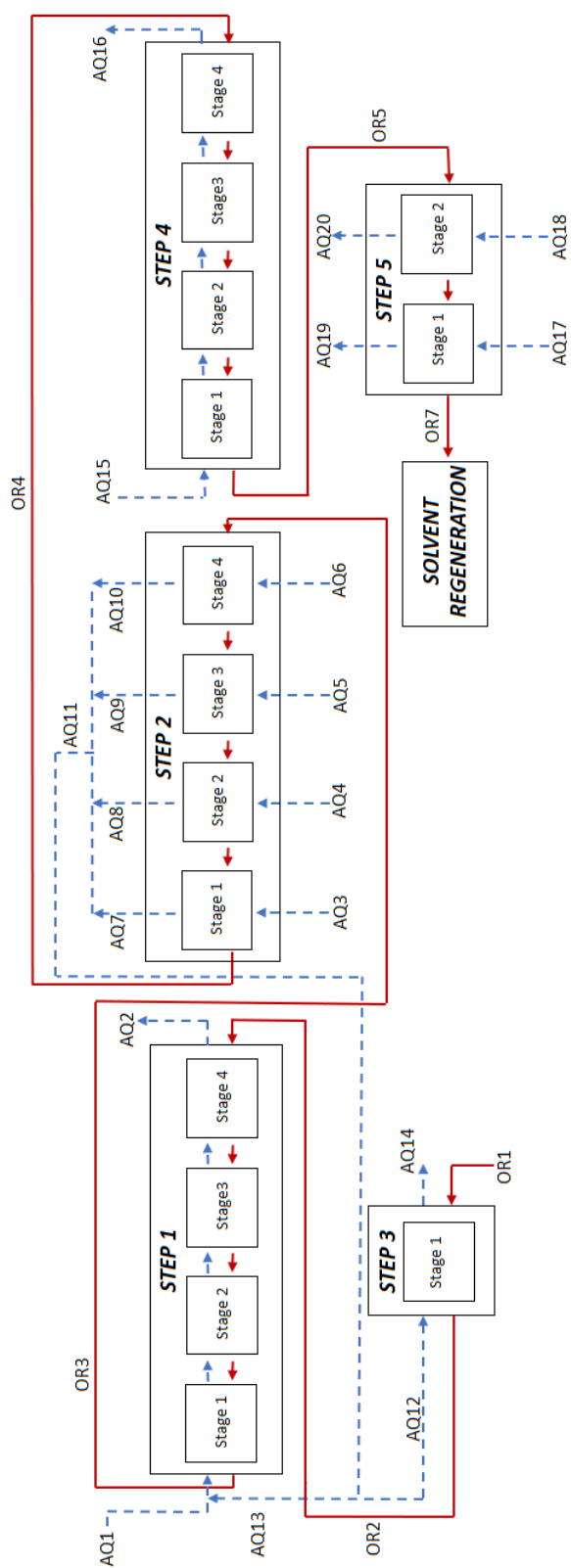
Figure 6.3.2: Flowsheet proposed for SNF reprocessing using small channels. The blue dashed (- -) streams refer to the aqueous phase, the red streams refer to the organic phase. Dash dot line (— · —) black lines identify the single unit operation (step). Step 1 = main extraction, Step 2 = Zr, Ru and Tc scrubbing, Step 3 = complementary extraction, Step 4 = U/Pu co-stripping, Step 5 U stripping. Counter-current and cross flow configurations are shown. Temperature is 25°C for steps 1, 2, 3 and 4, 50°C for step 5.

of flowsheet and the material chosen, which affects hydrodynamics and costs. With flowsheets involving more extraction steps or more cost effective materials for the U stripping, a further higher TBP fraction may prove to be beneficial.

Table 6.3.3: Separation performance of the flowsheet proposed.

Variable	Value	Comment
U Rec_{1-3}	99.22%	U recovery in codecontamination section (steps 1-3), larger than typical value
Pu Rec_{1-3}	99.00%	Pu recovery codecontamination section (steps 1-3), minimum requirement
Zr DF	1×10^4	Typical value in codecontamination section (steps 1-3), minimum requirement
Ru DF	4.39×10^6	Larger than typical value in codecontamination section (steps 1-3)
Tc DF	50.00	Larger than typical value in codecontamination section (steps 1-3)
Np DF	8.35	Larger than typical value in codecontamination section (steps 1-3)
U/Pu product purity	99.95%	Purity of MOX fuel (stream AQ16), molar basis
U product purity	99.98%	Purity of U product (mixing streams AQ19 and AQ20), molar basis

Design of pseudo cross flows

The HNO_3 concentration achieved for scrubbing solution, significantly larger than the typical HNO_3 concentration for Zr and Ru scrubbing, is needed to improve the Tc separation, which is favoured by high HNO_3 concentrations (typically a 10 M HNO_3 solution is used [6]), so an intermediate nitric acid concentration has been achieved. All the aqueous streams of fresh nitric acid solution required in this flowsheet, if compared to the aqueous flow rate achieved in the counter-current configuration investigated in sections 5.1 and 6.2.2, are decreased by approximately

Table 6.3.4: Optimal flow rates and concentrations (nitric acid, uranous cation and hydrazine nitrate) in the incoming streams. All of the following are decision variables in the optimisation problem, except flow rate of AQ1 (feed). Flow rates are expressed in L h^{-1}, all concentrations in Mol L^{-1}. Flow rates are assumed constant within all unit operations, for example AQ2=AQ1+AQ13, AQ3=AQ7, AQ11=AQ7+AQ8+AQ9+AQ10 and so on.

Stream	Flow rate	[HNO$_3$]	[U(IV)]	[N$_2$H$_4\cdot$HNO$_3$]
	L h^{-1}	Mol L^{-1}	Mol L^{-1}	Mol L^{-1}
AQ1	223.65*	2.50	-	-
AQ3	176.86	4.49	-	-
AQ4	165.43	4.49	-	-
AQ5	164.38	4.46	-	-
AQ6	162.44	4.37	-	-
AQ12	44.01	4.34	0	0
AQ13	625.10	4.45	0	0
AQ15	133.82	0.37	2.40×10^{-2}	0
AQ17	1725.82	0.01	-	-
AQ18	3115.84	0.01	-	-
OR1	590.88	-	-	-

*fixed by the given throughput for the case study

40%. This design decreases size and cost of step 2 and improves the separation. However, the flow rates fed to step 1 and 3 are larger than using the previous counter-current design, hence size and cost of steps 1 and 3 are increased.

The aqueous flow rates used for the U stripping, step 5, are significantly larger then the organic flow rate: the aqueous to organic flow ratio in these two stages are 2.9 in the first stage and 5.3 in the second one. The use of large aqueous flow rates was expected, to improve the back extraction by increasing the driving force. The HNO$_3$ concentration of the two fresh nitric acid solutions is very low, 0.01 M, which is the lower bound for this variable. No further lower bounds have been investigated. This value is very low and the acid concentration must be enough to allow U dissolution. The value of this concentration was expected, as scrubbing

is favoured by low HNO_3 concentration (high HNO_3 concentrations enhance U extraction, the so-called "salt effect", see Eq. 1.3.1). Also, this is the value of HNO_3 concentration used for this unit operation in industrial reprocessing plants [6].

Effect of the diameter

As already mentioned, the value of 2.5 mm has been used in this problem as an upper bound for the diameter. The optimisation problem has also been solved using 2 mm as an upper bound, to investigate the impact of this value on the main results.

In both cases, the optimal diameter has always been the upper bound.

A small reduction of the $k_L a$, approximately by 12% on average, has been observed as the diameter increases, as expected. However, the $k_L a$ is still higher than the ones achieved in the conventional technologies in Chapter 5.

The number of parallel small extractors required, increasing the diameter from 2 mm to 2.5, has been reduced on average by 30% for each stage, according to the increase of the cross sectional area (by 36% increasing from 2 mm to 2.5 mm of diameter). The total annualised cost, which is mainly the total annualised capital cost, has been reduced by approximately 20%, as the result of the reduction of the estimated costs for manifolds and stainless steel channels in step 5.

The organic flow rate in each unit operation, as the diameter increases from 2 mm to 2.5 mm, has been decreased by approximately 20% but with TBP fraction increased from 28.8%, to 34.2% ($\approx$ +20%). Hence, the amount of TBP used has been almost constant. To balance the lower mass transfer coefficients, with the largest diameter, the superficial velocity within the channels has been reduced by approximately 40% in steps 1 and 2, to allow higher residence times and improve extraction. The aqueous flow rates in step 1 and 2 are almost unchanged, contrary to the one in stage 3 (reduced by 27%), step 4 (reduced by 7%) and in step 5 (-15% in the first stage, +6% in the second one). The amount of aqueous stream recycled from step 2 to step 1 has not been markedly affected by the change in the channel diameter (91.7% recycled using a 2 mm diameter, 93.9% with 2.5 mm).

Performance separation of the process has been almost unchanged, the only difference is the decrease of Np DF from the case with D =2 mm (DF=14.81) to

Table 6.3.5: Outlet concentrations of components. All concentrations are expressed in Mol m^{-3}.

Component	Phase	Step 1	Step 2	Step 3	Step 4	Step 5
U(VI)	Aq.	2.04	63.24	2.21	113.65	44.71
U(VI)	Org.	466.09	394.48	4.55	370.07	3.71
Pu(IV)	Aq.	2.90×10^{-2}	0.80	3.21×10^{-2}	0.96	3.90×10^{-4}
Pu(IV)	Org.	5.27	4.37	5.70×10^{-2}	3.20×10^{-3}	2.64×10^{-5}
HNO$_3$	Aq.	3851.53	4343.10	1119.20	1870.04	14.65
HNO$_3$·TBP	Org.	235.72	351.97	127.76	26.65	0.28
HNO$_3$·2TBP	Org.	12.85	20.87	112.37	11.93	0.24
HNO$_2$	Aq.	0.65	2.43	7.03×10^{-2}	0.50	6.63×10^{-2}
HNO$_2$	Org.	5.50	2.75	0.18	2.63	2.09
Zr	Aq.	3.42	0.15	1.52×10^{-2}	2.09×10^{-3}	0
Zr	Org.	0.17	4.92×10^{-4}	9.90×10^{-3}	1.93×10^{-5}	0
Ru	Aq.	2.00	9.57×10^{-3}	1.78×10^{-3}	0	0
Ru	Org.	1.08×10^{-3}	6.55×10^{-7}	5.80×10^{-4}	0	0
Tc	Aq.	0.72	0.33	4.57×10^{-2}	4.33×10^{-2}	1.34×10^{-3}
Tc	Org.	0.38	2.10×10^{-2}	2.10×10^{-2}	1.11×10^{-3}	1.62×10^{-4}
Np(IV)	Aq.	0	0	0	0	0
Np(IV)	Org.	0	0	0	0	0
Np(V)	Aq.	0.14	1.47×10^{-3}	1.31×10^{-3}	1.50×10^{-4}	4.80×10^{-4}
Np(V)	Org.	1.62×10^{-3}	3.23×10^{-7}	1.27×10^{-5}	2.47×10^{-6}	9.56×10^{-7}
Np(VI)	Aq.	2.77×10^{-3}	9.28×10^{-3}	4.00×10^{-4}	1.64×10^{-2}	2.54×10^{-3}
Np(VI)	Org.	3.96×10^{-2}	2.90×10^{-2}	6.61×10^{-4}	2.50×10^{-2}	1.84×10^{-4}
U(IV)	Aq.	0	0	0	8.57	0.26
U(IV)	Org.	0	0	0	2.16	1.13×10^{-3}
Pu(III)	Aq.	0	0	0	11.26	4.91×10^{-3}
Pu(III)	Org.	0	0	0	4.05×10^{-2}	2.04×10^{-4}
N2H4·HNO$_3$	Aq.	0	0	0	0	0
N2H4·HNO$_3$	Org.	0	0	0	0	0
TBP	Aq.	0	0	0	0	0
TBP	Org.	34.10	53.80	888.67	446.06	1234.80

the case with D = 2.5 mm (DF=8.35). This change can be explained by to the longer residence time required in the case of larger diameters. With the larger residence time available, a higher amount of Np (V) can convert to Np(VI), which is extractable by TBP. However, this Np DF is still significantly higher than the one achieved with conventional technologies.

The linearisation of the mass transfer coefficient correlation, around the upper bound used for the diameter, was reasonable as the optimal diameters have always been the upper bound, as expected. Also, the channel length has been the lower bound, as expected.

Effect of initialisation

Three different initialisations have been used to evaluate their effect on the solution. The initialisations differed in the channel diameter and manifold design. A slight change, within the 3%, has been observed in the solutions obtained. The overall design has been almost unaffected (same number of stages, channels diameter and length). The only differences are one or two elements of difference in some levels of the comb-like manifolds and a slight difference in the TBP fraction. Only the best solution has been discussed.

Impact of input parameters and constraints

The materials do not affect only the costs of channels and manifolds, but also hydrodynamics and then the separation performance, because the dispersion of one phase depends on the wettability of the material used. If, for example, in step 5 (U stripping) a hydrophobic material is used for the small-scale extractors, then the aqueous phase will be dispersed and the organic one continuous. Since an aqueous to organic flow ratio greater than unity is required to back extract uranium, it is beneficial that the phase less present (in this case, the organic one) is dispersed, so that the plugs are smaller and the interfacial area is larger. Polymeric channels may also be investigated, but they probably lead to larger, more expensive and/or unpractical manifolds, because higher flow rates should be used to counterbalance the lower interfacial area. Hence, a reasonable choice may be the use of hydrophilic materials for the first 4 steps and of hydrophobic for the last one.

Table 6.3.6: *Optimal design of steps 1 (main extraction step), 2 (scrubbing), 3 (complementary extraction) and 4 (co-stripping). The number of elements in each level of the manifold is the same. Lengths, diameters and widths are expressed in cm.*

	Step 1	Step 2	Step 3	Step 4
No. of stages	4	4	1	4
1st level manifold:				
No. of elements	70	70	70	70
Length (aq./org.)	10.0	10.0	10.0	10.0
Diameter (aq./org.)	2.5×10^{-1}	2.5×10^{-1}	2.5×10^{-1}	2.5×10^{-1}
2nd level manifold:				
No. of elements	15	6	5	6
Length (aq.)	51.8	51.8	51.8	51.8
Width (aq.)	1.0	1.0	1.0	1.0
Length (org.)	51.8	51.8	51.8	51.8
Width (org.)	1.2	1.1	1.1	1.1
3rd level manifold:				
No. of elements	15	6	5	5
Length (aq.)	42.6	14.7	11.4	14.4
Width (aq.)	2.4	1.4	1.0	1.3
Length (org.)	48.7	16.8	13.1	16.5
Width (org.)	2.6	2.2	2.1	2.2
4th level manifold:				
No. of elements	1	1	1	1
Length (aq.)	99.5	21.0	11.6	15.7
Width (aq.)	2.4	1.4	1.2	1.3
Length (org.)	108.5	33.1	25.0	26.0
Width (org.)	2.6	2.2	2.1	2.2

The inequality constraints used for the decontamination factors in the separation process, in particular of Tc (more difficult than Zr and Ru to separate), affect the aqueous flow rates, especially in the first 3 steps. No minimim Np DF has been used. The Np separation achieved is already much better than the typical

Np separation achieved with conventional technologies in the current commercial plants. All these constraints are illustrated in Table 6.3.2. In general, the higher the minimum DF required, the larger are the flow rates, which leads to bigger and most expensive equipment. Minimum back extraction efficiency of steps 4 and 5 is set to 99%, which lead to products with purities shown in Table 6.3.3 ($\geq$99.95%). As for decontamination factors, higher values of separation efficiency would require larger flow rates, hence larger sizes and higher costs. However, the change in the overall design is expected to be minimal, since the addition of only few elements in the second and/or third levels of the manifolds can be sufficient to increase the flow rates.

The constraint to guarantee nuclear subcriticality does not affect the problem, as it is easily achieved and the value of k_{eff} is very far from the upper limit.

The imposed upper limit for the number of units in the first level of the manifold, *i.e.* 70, is the number of units provided with the solution. Hence, the flow maldistribution achieved in the manifolds will be close to the maximum maldistribution permitted, 10%, as the number of small extractors in the first level is pushed to the upper limit (above 70 channels, higher flow maldistribution are likely). This result is achieved to minimise size and cost. In the case studies investigated in sections 3.4 and 5.1, using empirical nonlinear correlations to calculate the flow maldistribution Fd, the number of units in the first levels was lower whilst the one in the second levels was higher, which led to more gradual ramification of the flow and small flow maldistribution (around 1%, significantly below the limit of 10%). Therefore, the replacement of the former nonlinear correlations to estimate Fd with the inequality constraints has facilitated the calculations and led to better solutions, at the cost of higher flow maldistribution (but still below the maximum vale permitted).

In the case studies investigated so far, the same throughput has been investigated. Below, the mathematical model is tested for a significantly lower throughput.

Table 6.3.7: Optimal design of step 5, U stripping, two stages. Lengths, diameters and widths are expressed in cm.

	Stage 1	Stage 2
1st level manifold:		
No. of elements	70	70
Length (aq./org.)	10.0	10.0
Diameter (aq./org.)	2.5×10^{-1}	2.5×10^{-1}
2nd level manifold:		
No. of elements	10	12
Length (aq.)	51.7	51.7
Width (aq.)	1.0	1.0
Length (org.)	51.7	51.7
Width (org.)	1.1	1.1
3rd level manifold:		
No. of elements	9	12
Length (aq.)	25.7	31.4
Width (aq.)	2.3	2.7
Length (org.)	29.4	35.9
Width (org.)	1.9	1.8
4th level manifold:		
No. of elements	1	1
Length (aq.)	55.4	88.6
Width (aq.)	2.3	2.9
Length (org.)	45.9	59.3
Width (org.)	1.9	2.0

Small flow rate

In this paragraph, the effect of a significantly different throughput is investigated. In particular, the superstructure flowsheet shown in Figure 6.3.2 has been solved assuming a throughput of 50 HMTM y^{-1}, decreased by 90% from the one used in the previous case studies.
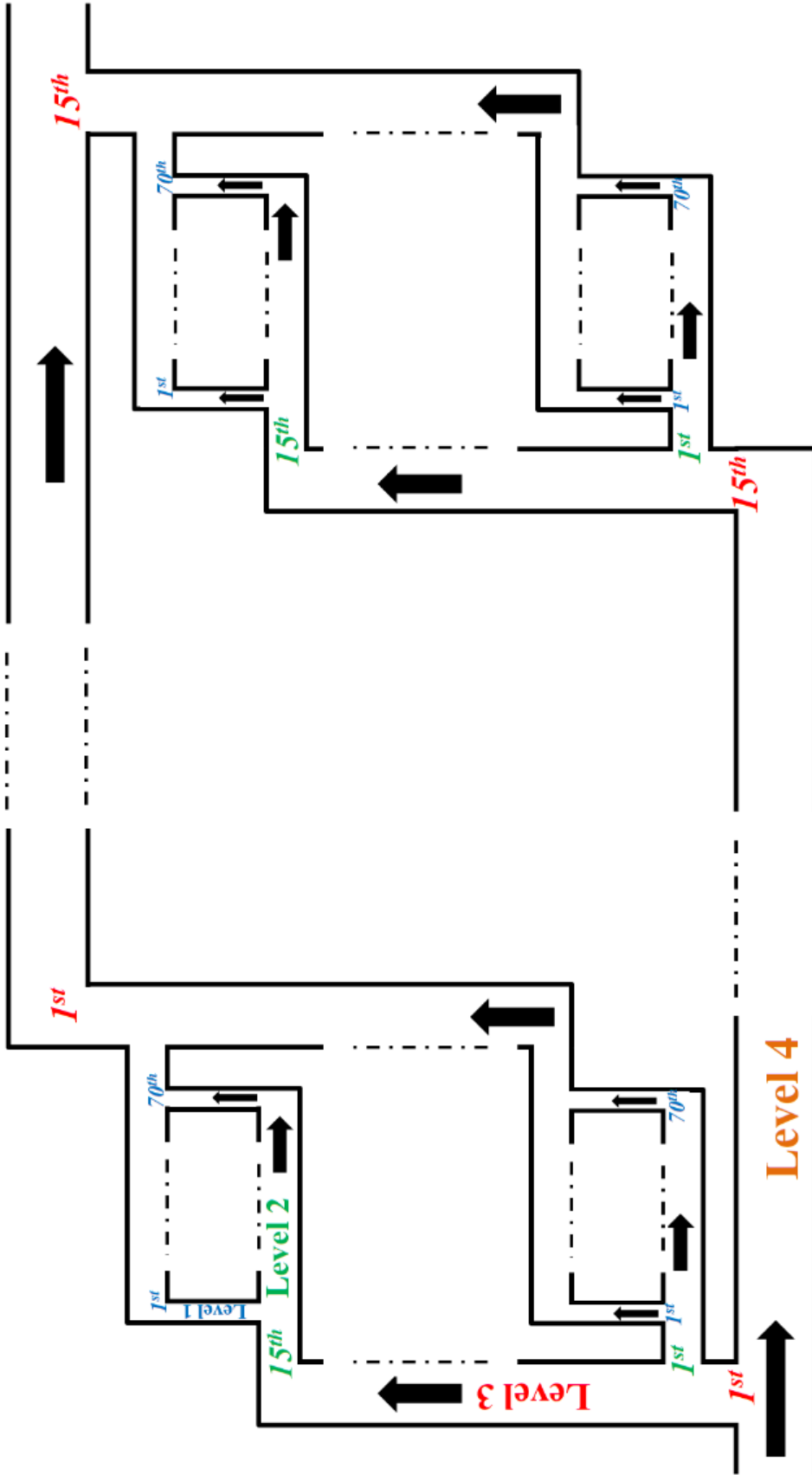
Figure 6.3.3: Schematic of the manifold design achieved for step 1 in the COEX process. Only the first and the last element in each level of the manifold are shown. The dot-dash lines indicates the intermediate elements in each level of the manifold. Level 4 (orange) consists of a single element. Level 3 (red) consists of 15 elements. Level 2 (green) consists of 15 elements. Level 1 (blue) consists of 70 elements. For step 1, a total of 8 manifolds is required (4 stages × 2 phases).

132

Table 6.3.8: *Optimal flow rates and concentrations of nitric acid and additional compounds of the incoming streams (case of 50 MTHM y^{-1}). Flow rates are expressed in L h^{-1}, all concentrations in Mol L^{-1}. Flow rates are assumed constant within all unit operations for example AQ2=AQ1+AQ13, AQ3=AQ7, AQ11=AQ7+AQ8+AQ9+AQ10 and so on.*

Stream	Flow rate	[HNO$_3$]	[U(IV)]	[N2H4·HNO$_3$]
AQ1	22.36[1]	2.50	-	-
AQ3	16.57	4.47	-	-
AQ4	16.49	4.46	-	-
AQ5	16.35	4.45	-	-
AQ6	17.26	4.35	-	-
AQ12	3.73	4.43	0	0
AQ13	62.93	4.43	0	0
AQ15	13.58	0.36	2.45×10^{-2}	0
AQ17	167.44	0.01	-	-
AQ18	335.67	0.01	-	-
OR1	63.98	-	-	-

[1]fixed by the given throughput for the case study

As expected, being the feed concentration unchanged, the number of stages has not been affected. Hydrodynamics, mass transfer and concentrations are approximately unvaried if compared to the previous case with larger throughput, thus they are not reported in this paragraph. The marked decrease in the feed rate has led to a reduction of all flow rates and a decrease in the number of parallel small extractors required. The reduction of the flow rates is almost linear with the throughput reduction. The flow rates are shown in Table 6.3.8, whilst the design of the manifolds can be seen in Table 6.3.9 and Table 6.3.10.

The problem has been solved by gradually decreasing the feed rate, to investigate the response of the model and facilitate the calculations. Decreasing the throughput, the reductions in the total annualised cost and in the number of parallel small channels are linear, as shown in Figure 6.3.4. These results confirm the modularity of the small technology and the ease of its design for varying flow rates,

Table 6.3.9: *Optimal design of steps 1 (main extraction step), 2 (scrubbing), 3 (comple-mentary extraction) and 4 (co-stripping). The number of elements in each level of the manifold is the same. Lengths, diameters and widths are expressed in cm.*

	Step 1	Step 2	Step 3	Step 4
No. of stages	4	4	1	4
1st level manifold:				
No. of elements	70	55	46	53
Length (aq.,org.)	10.0	10.0	10.0	10.0
Diameter (aq.,org.)	2.5×10^{-1}	2.5×10^{-1}	2.5×10^{-1}	2.5×10^{-1}
2nd level manifold:				
No. of elements	5	2	2	2
Length (aq.)	51.8	40.5	33.8	39.0
Width (aq.)	1.0	0.9	0.9	0.9
Length (org.)	51.8	40.5	33.8	39.0
Width (org.)	1.2	1.0	1.0	2.0
3rd level manifold:				
No. of elements	4	2	2	2
Length (aq.)	12.3	2.7	2.6	2.7
Width (aq.)	1.8	0.9	0.9	0.9
Length (org.)	14.1	3.1	2.9	3.0
Width (org.)	1.9	1.3	1.3	1.3
4th level manifold:				
No. of elements	1	1	1	1
Length (aq.)	15.8	2.7	2.6	2.7
Width (aq.)	1.8	1.1	0.9	0.9
Length (org.)	17.5	4.0	4.0	4.0
Width (org.)	1.9	1.8	1.3	1.3

simply by numbering up or down the small channels and modifying the manifolds accordingly. The reduction of the cost is mainly due to the simpler, smaller and then more cost effective manifolds required.

The separation performance of the process, in terms of extraction efficiencies

Table 6.3.10: Optimal design of step 5, U stripping, two stages. Length and width are expressed in cm.

	Stage 1	Stage 2
1st level manifold:		
No. of elements	70	68
Length (aq.,org.)	10.0	10.0
Diameter (aq.,org.)	2.5×10^{-1}	2.5×10^{-1}
2nd level manifold:		
No. of elements	3	4
Length (aq.)	51.7	50.2
Width (aq.)	1.0	0.9
Length (org.)	51.7	50.2
Width (org.)	1.1	1.1
3rd level manifold:		
No. of elements	3	4
Length (aq.)	5.7	8.5
Width (aq.)	1.4	1.6
Length (org.)	6.5	9.7
Width (org.)	1.3	1.3
4th level manifold:		
No. of elements	1	1
Length (aq.)	8.4	14.3
Width (aq.)	1.4	1.6
Length (org.)	8.0	11.6
Width (org.)	1.3	1.3

and decontamination factors, has been unvaried except for Ru DF (decreased by 10% but still a couple of orders of magnitude above the minimum requirement, Ru is practically zero in the products).
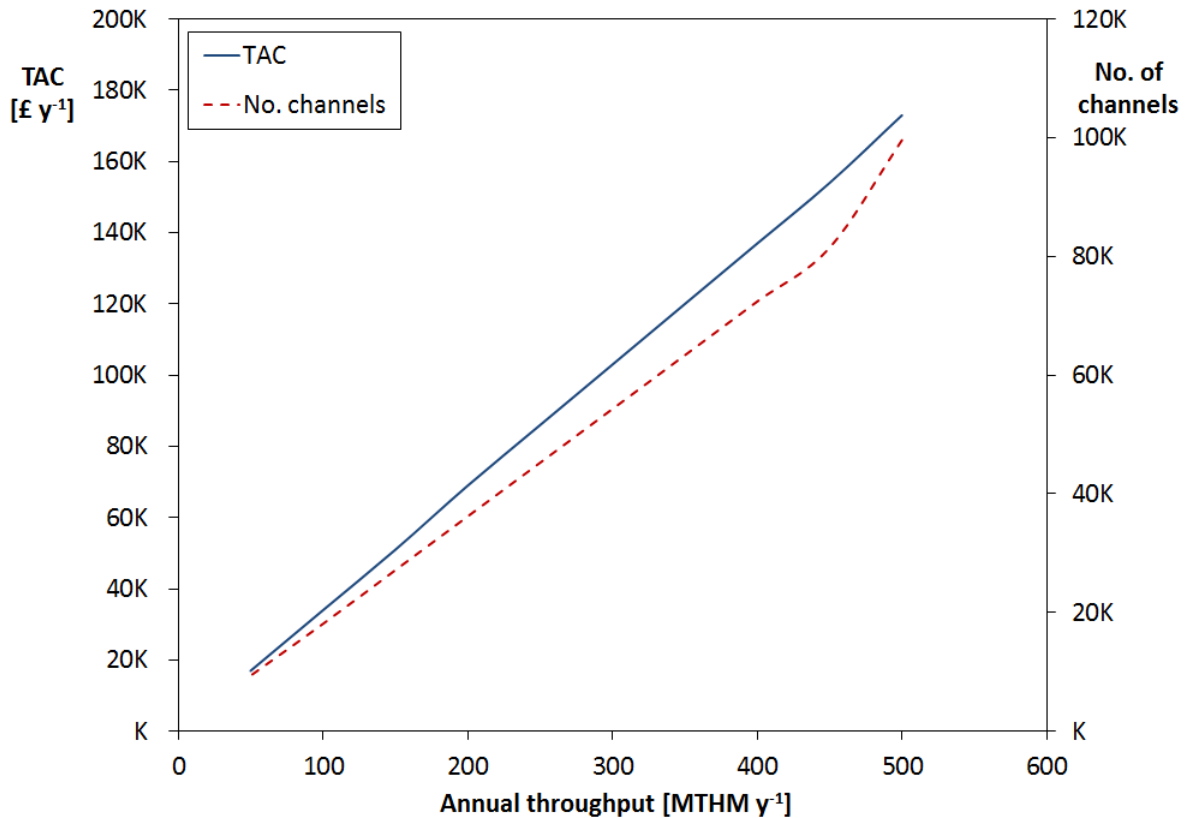
Figure 6.3.4: Impact of the annual throughput on the total annualised cost and number of parallel small channels required.

6.4 Conclusions

A superstructure flowsheet for the nuclear fuel cycle has been investigated. The application of the small-scale extractors, to overcome the disadvantages of the conventional technologies, has been studied. The systems involves a large number of species and chemical reactions, mostly redox reactions. Two different reducing agents, U(IV) and HAN, have been considered. Pseudo counter-current and cross flow configurations have been combined in the flowsheet. This is a novel flow configuration in SNF reprocessing.

The superstructure has been solved according to economic criteria. The best flowsheet identified is more cost effective than the current PUREX process and several advantages are provided by the use of small channels. Two products, ura-

nium oxide and a mixed uranium/plutonium oxide are achieved, hence precluding nuclear proliferation risks. Also, this flowsheet produces a perfectly homogeneous mixed Pu/U oxide, in contrast to the current MOX fuel fabrication technique. Less unit operations are involved, reducing capital and operational costs and with improvements in terms of safety and equipment footprint. This is a novel flowsheet for SNF reprocessing. Due to large size and nonlinearity of the mathematical model, an initialisation is required to solve the superstructure. How a significantly different initialisation (e.g. significantly different number of stages, flow rates and concentrations) can affect the optimal flowsheet is still an open question.

The results suggest that, using small-scale extractors, U(IV) is a more suitable reductant than HAN, because of the faster kinetics which allows to complete Pu reduction in the short residence times provided by small channels. Input parameters such as the channel material may affect the optimal flowsheet design. The feed rate linearly affects the number of parallel channels and the total annualised cost. The pseudo cross-flow in the scrubbing and stripping steps, although it increases the amount of nitric acid solution required, allows high decontamination from minor actinides and fission products. Increasing the diameter up to 2.5 mm, according to the model, may be beneficial to reduce the overall cost, because of the simpler manifolds, and can still provide high performance and higher volumetric mass transfer coefficients if compared to the conventional technologies.

Chapter 7

Conclusions and future developments

Besides the development of safer nuclear reactors, a more efficient and safer nuclear fuel cycle is fundamental for future power generation from nuclear source of energy.

The aim of this thesis was to develop a methodology that allows to explore the application of the small-scale extraction technology for spent nuclear fuel reprocessing flowsheets. A novel mathematical model have been developed for this purpose, relying on models available in the literature to estimate phenomena such as mass transfer or redox reactions. A comparison with conventional technologies has been investigated, and several advantages have been found. The design of a combined Pu/U extraction (COEX) process has been suggested through a superstructure optimisation approach, using the small-scale contactors. Below, a general discussion of this thesis and the potential future works are presented.

7.1 Overview of the thesis

The state of the art on the spent nuclear fuel reprocessing, with focus on both conventional liquid-liquid extractions technologies and next generations of PUREX reprocessing facilities, have been reviewed in Chapter 2. Furthermore, the relevant studies on intensified extraction in micro or small channels have been discussed.

A mathematical modelling of intensified liquid-liquid extraction in small-scale contactors has been developed in Chapter 3. The model, suitable for spent nu-

clear fuel reprocessing, includes the design of both flow network distribution and two-phase separator. Besides the mass transfer calculations, several chemical reactions, mostly redox reactions, have been considered. Calculations of pressure drop, economics and nuclear criticality have also been included in the model. The differential mass balance equations, the large number of components considered and the nonlinearity of numerous relationships increase the complexity of the mathematical model. The size of the model depends on the granularity of the discretisation used, to convert the differential mass balance equations into a set of algebraic equations. The development of a code that embeds all the aforementioned aspects in the modelling of the small extractors is novel. The model allows to define optimisation-based design problems by a mixer integer nonlinear programme and, hence, can be used to investigate new flowsheets for spent nuclear fuel reprocessing using the small-scale technology. The model has been implemented in the GAMS modelling system.

A case study have been investigated to demonstrate the applicability of the model. In particular, the use of the small-scale technology has been studied for the codecontamination section of the current PUREX process. A pseudo counter-current flow configuration has been assumed. The model has required a proper initialisation. The latter can be achieved solving the flowsheet through a sequential modular approach in a first stage. The computational time required was relatively short, between some minutes and a couple of hours (depending on the initialisation).

Another goal of this works was to compare intensified extraction in small channels with mixer-settlers and pulsed columns, which are nowadays the two main conventional liquid-liquid extraction technologies employed in the nuclear industry. Mathematical models of these two conventional technologies have been built for this purpose in Chapter 4. The novelty related to these models relies on the challenging physical system considered (12-component system, mass transfer/reaction model suitable for spent nuclear fuel reprocessing) and the variety of aspects included in the calculations, such as hydrodynamics, pressure drops, economics and nuclear criticality. The process design of these technologies and their comparison through optimisation-based design problems, for both small and conventional technologies, is novel.

A case study in spent nuclear fuel reprocessing has been investigated in Chap-

ter 5, to compare novel and conventional technologies. The models developed in the previous chapters have been combined into a single larger process model, allowing for the design of alternative configurations. The main aspects that have been compared are economics, mass transfer coefficient, liquid volume, residence time, Np separation and nuclear criticality safety. Results have shown that pulsed columns may be less expensive than small channels. However, the cost of several equipment required for the pulsed columns, not included in the model because of the lack of information in the literature, should be added. The choice of materials, manifold type and two-phase separator, issues which are currently being investigated, are crucial to estimate economics and applicability of the small channels. However, the intensified extraction has provided a large number of advantageous. The residence time can be significantly reduced using small channels, thus reducing solvent degradation and solvent regeneration costs. Furthermore, the short residence time leads to markedly improved Np separation. Regarding the nuclear criticality safety, the small channels are safe by geometry because of the small holdup of liquid involved and the high surface area to volume ratio. Hence, small channels may represent an alternative to the pulsed columns in the highly active section of the PUREX process.

In Chapter 6, an alternative flowsheet for spent nuclear fuel has been proposed, employing the small-scale extractor. The flowsheet has been obtained using a superstructure optimisation approach. The application of the small-scale technology allows for alternative and novel strategies for process configuration, where different stages and fresh streams at each stage may be investigated within the same unit operation. Furthermore, higher TBP concentration and hence novel solvents may be used. The flowsheet is based on a Pu/U Combined Extraction (COEX) process. The main goal of the process is to preclude the nuclear proliferation risk, which is the goal of the next generations of PUREX processes. There are several motives behind the choice of this type of flowsheet. A COEX process produces a U oxide and a mixed Pu/U oxide, suitable for Mixed Oxide (MOX) fuel fabrication. The MOX fuel achieved via this method has a better homogeneity of uranium/plutonium distribution than the MOX produced by the current fuel fabrication technique. The U/Pu partitioning section is not required, contrary to the PUREX process, therefore reducing the number of unit operations required by the process and resulting in a less expensive process. The mathematical model de-

scribed in Chapter 3 has been integrated with new components and correlations, in particular to predict the large number of potential redox reactions. Two reductants have been investigated: U(IV) and hydroxylammine nitrate (HAN). The resulting multi-component system involves 14 components (two forms of uranium, two forms of plutonium, two forms of neptunium, ruthenium, zirconium, technetium, two forms of nitric acid, nitrous acid, TBP, hydrazine nitrate as nitrite scavenger) and a total of 11 chemical reactions. TBP fraction in the organic solvent has been allowed to vary in the optimisation problem. "Pseudo" counter-current and cross flow configurations have been combined in the flowsheet. The overall number of equation is approximately 450,000, the integer variables are 47 (number of stages and number of elements in each level of the manifold). The best flowsheet identified by the superstructure optimisation has provided several advantages over the current process for SNF reprocessing. Specifically, compared to the conventional process and equipment used, the main benefits of the COEX process proposed using small channels are:

- no risk of nuclear proliferation;

- more cost effective process;

- reduced number of liquid-liquid extraction operations;

- smaller equipment footprint;

- improvements in terms of nuclear criticality safety;

- no evaporator, in contrast to the second cycle of the PUREX process;

- better Np control and separation;

- easier control of hydrodynamics;

- lower solvent degradation, with consequent less expensive solvent cleanup and regeneration section.

Due to size and nonlinearity of the model, a good initialisation is required. Few different initialisations have been investigated, with small difference on the objective function and process design. However, significantly different initialisations have not been found and hence not investigated.

Using small-scale contactors, U(IV) is a better reducing agent than HAN. The U(IV) has a faster kinetics, which allows complete Pu stripping in the short residence time. The pseudo cross-flow in the back extraction steps lead to high decontamination from Zr, Ru, Tc and Np. For Ru, Tc and Np decontamination factors higher than the typical ones have been achieved. According to the model, purities of U and mixed oxides Pu/U products are higher than 99.95%. The desired Pu/U ratio of the mixed oxide fuel, set to 10% (average value for MOX fuel), has been achieved through optimisation of design and operating variables, such as flow rates, HNO_3 and U(IV) concentrations in the entering aqueous flow rates.

If the channel diameter is increased to 2.5 mm, according to the model, the size of the stacks of channels and then the overall capital cost may be significantly reduced. Still advantageous volumetric mass transfer coefficients may be achieved, higher than the ones provided by conventional technologies. However, the mass transfer correlation used has not been tested with diameter larger than 2 mm and a more reliable mass transfer model may be needed.

The mathematical model of intensified extraction in small channels has been applied to case studies with some different input parameters. Different channels materials have been investigated (PTFE in Section 3.4, Section 5.1 and [153], PTFE and stainless steel in Section 6.2.2, Section 6.3 and [125, 155]). Two different temperatures have been used: 50°C for the U stripping, 25°C otherwise. Several inequality constraints have been added or modified from Chapters 3 and 5 to Chapter 6, such as increased Tc DF and constraints to ensure a good flow distribution. Different flowsheets have been investigated, as well as different flow pattern configuration and TBP concentrations. The effect of different upper bounds for the channel diameter, a crucial design variable, has been investigated. To further demonstrate the applicability of the model, the superstructure flowsheet investigated in Chapter 6 has also been solved for a small throughput, 50 MHTM y^{-1}, one tenth of the throughput used in the previous case studies. As expected, the same separation performance has been achieved decreasing linearly the number of parallel small-scale extractors required and varying the manifold design accordingly. The effect on hydrodynamics and concentration profiles has been negligible.

7.2 Future developments

The mathematical model developed in this thesis can be used as starting point for more detailed and customised models for liquid-liquid extraction in small channels. Further actinides and fission products may be included in the calculations and other mathematical relationships, to investigate further phenomena (depending on the application studied), can be integrated in the model, as done in Chapter 6. For example, the potential use of novel "green" solvents may be investigated, implementing physical properties and equilibrium relationships in the model. The resulting model can be validated by experimental data, and then used for the early stage design.

To increase the reliability of the current model, specific correlations to estimate mass transfer and thermodynamics would be beneficial. The range of applicability of these correlations has to be extended, in particular in terms of channel diameter as it is essential to investigate the largest diameter possible.

More detailed 2D numerical studies may be investigated, through the development of CFD models. These models, often computationally expensive, may be exploited to investigate the chemical/physical phenomena involved in a such complex system, *i.e.* a two-phase flow where mixing, mass transfer, chemical reactions and two-phase separation occur. Also, a CFD model can be useful to better understand the hydrodynamics in the manifolds for distribution and collection of the two phases, varying geometry and operating conditions. In general, this kind of models may be used to get the details which are difficult or impossible to measure experimentally. These data can be use to identify new empirical correlations to improve the model developed in this thesis.

Manifolds are essential to increase the throughput and meet the industrial requirements. Nowadays, the field of flow distribution networks is currently intensively investigated. In this work, a 4-level comb-like network has been assumed. The latter seems to be the most suitable design to arrange a large number of parallel small channels in a compact stack, but several other types of manifold exist and may be implemented. For example, the monolithic reactor type or the tree-like network may be investigated. Hydrodynamics, pressure drops and flow distribution are challenging to predict, experimental works (and CFD analysis, as already mentioned) will be essential to identify the optimal manifold.

Similarly to the manifold, the two-phase separator is still an issue to address, as well as the mixing of the two phase. For example, due to the large number of channels, the two-phase separation through a hydrophobic or hydrophilic sidestream needle may not be the best choice, and several type of coalescers are currently being studied. Experimental investigations to evaluate their applicability and reliability will be crucial. Then, these information can be used for the mathematical model of small channels. Distribution, mixing, separations and collection of the two phases are fundamental steps for future industrial applications of this small-scale technology.

The methodology developed in this work allows to investigate different scenarios and flowsheets for spent nuclear fuel reprocessing. The use of a flowsheet to selectively recover some contaminants (for example DIAMEX or SANEX process), after a main process for the spent nuclear fuel reprocessing (for example COEX or UREX) is worth being investigated. Coupling these flowsheets, it would be possible to significantly reduce volume and radiotoxicity of the nuclear wastes.

Optimal flowsheets can be found through superstructure optimisation. The possible combination of novel and conventional technologies may be investigated when the throughput is very large and unpractical manifold would be required. Also, the two most suitable flows configurations (cross flow, counter-current) may be integrated in the superstructure as alternative option for each unit operation, as well as different types of manifolds and separators, letting the optimiser explore all the configurations and identify the optimal design. Similarly, another degree of freedom may be the material of the small extractor, which determines which phase is dispersed, significantly affecting hydrodynamics and cost. The superstructure flowsheet may be optimised according to criteria different from economics and nuclear proliferation. Possible objective functions of interest can be the environmental impact. Also, decommissioning considerations may be evaluated. A multi-objective optimisations can prove to be useful.

However, numerical difficulties will be encountered. To solve this mathematical system in the near future, strategies such as simplifying assumptions, linearisation of several relationships, good initialisations and proper optimisation procedures will be essential. Hence, besides the study of the chemistry/physics of the problem, the development of techniques and approaches for initialisation and optimisation procedures requires further investigation.

144

The application of the model developed in this work is the nuclear fuel cycle. Therefore, components (spent nuclear fuel, TBP, nitric acid) and phenomena (mass transfer, redox reactions, nuclear criticality) are the typical ones in the nuclear industry. However, the methodology can be applied to investigate the use of intensified liquid-liquid extraction for any other applications, such as the petrochemical industry, hydrometallurgy and pharmaceutical industry.

Publications

List of peer-reviewed publications:

1. D. Bascone, P. Angeli, E. S. Fraga (2017), Mathematical modelling of intensified extraction for spent nuclear fuel reprocessing, in A. Espuña, M. Graells & L. Puigjaner (Editors), Proceedings of the 27th European Symposium on Computer Aided Process Engineering – ESCAPE 27, 356-360.

2. D.Bascone, P. Angeli, E. Fraga (2018), Mathematical modelling of intensified extraction for spent nuclear fuel reprocessing, Nuclear Engineering and Design, 332, 162-172.

3. D. Bascone, P. Angeli, E. S. Fraga (2018), Optimal design of a COEX process for spent nuclear fuel reprocessing using small channels, in M. R. Eden, M. Ierapetritou and G. P. Towler (Editors), Proceedings of the 13th International Symposium on Process Systems Engineering – PSE 2018, 2365-2371.

Publication in preparation:

1. D. Bascone, P. Angeli, E. S. Fraga (2018), Comparison between intensified extraction in small channels and conventional solvent extraction technologies (submitted)

2. D. Bascone, P. Angeli, E. S. Fraga (2018), Optimisation of a superstructure flowsheet for spent nuclear fuel reprocessing using small scale extractors.

List of conference presentations:

1. Modelling and optimisation of intensified extraction for the nuclear fuel cycle, poster presentation at ChemEngDay 2016, 31 March – 1 April 2016, Bath, United Kingdom.

2. Modelling and optimisation of intensified extraction for the nuclear fuel cycle, oral presentation at Universities Nuclear Technology Forum 2016, 5–7 April 2016, Sheffield, United Kingdom.

3. Modelling and design of intensified extraction for spent nuclear fuel reprocessing, oral presentation at International Workshop on Process Intensification 29–30 September 2016, Manchester, United Kingdom.

4. Modelling of multi-component liquid-liquid extraction in small channels for spent nuclear fuel reprocessing, oral presentation at Universities Nuclear Technology Forum 2017, 4–6 April 2017, Liverpool, United Kingdom.

5. Mathematical modelling and optimisation of multi-component liquid-liquid extraction in small channel, oral presentation at EGL Applied & Numerical Mathematics Workshop, 8–9 June 2017, London, United Kingdom.

6. Design of multi component liquid-liquid extraction in small channels for spent nuclear fuel reprocessing, poster presentation at PSE@ResearchDayUK, 27 June 2017, London, United Kingdom.

7. Mathematical modelling of intensified extraction for spent nuclear fuel reprocessing, oral presentation at the 27th European Symposium on Computer Aided Process Engineering, 1–5 October, Barcelona, Spain.

8. Mathematical modelling of intensified extraction for spent nuclear fuel reprocessing, oral and poster presentations at Annual Industrial Consortium Meeting, 7–8 December, London, United Kingdom.

9. Optimal design of a COEX process for spent nuclear fuel reprocessing using small channels, oral presentation at the 13th International Symposium on Process Systems Engineering, 1–5 July, San Diego, United States.

References

[1] T. A. Todd. Spent nuclear fuel reprocessing. In *Proc. of Nuclear Regulatory Commission Seminar*, 2008.

[2] IAEA. Spent fuel reprocessing options. In *IAEA-TECDOC-1587*, 2008.

[3] J. D. Law and T. A. Todd. Liquid-liquid extraction equipment. Technical Report INL/CON–08-15151, Idaho National Laboratory, United States, 2008.

[4] M. F. Simpson and J. D. Law. Nuclear fuel reprocessing. Technical report, Idaho National Laboratory, 2010.

[5] L. Borges Silverio and W. de Q. Lamas. An analysis of development and research on spent nuclear fuel reprocessing. *Energy Policy*, 39(1):281–289, January 2011.

[6] R. S. Herbst, P. Baron, and M. Nilsson. Standard and advanced separation: PUREX processes for nuclear fuel reprocessing. In K. L. Nash and G. J. Lumetta, editors, *Advanced Separation Techniques for Nuclear Fuel Reprocessing and Radioactive Waste Treatment*, Woodhead Publishing Series in Energy, pages 141–175. Woodhead Publishing, 2011.

[7] OECD/NEA. Nuclear energy data. 2007.

[8] E. R. Irish and W. H. Reas. The purex process : a solvent extraction reprocessing method for irradiated uranium. Technical report, Hanford Atomic Product Operation Richmond, 1975.

[9] R. J. Taylor, I. May, A. L. Wallwork, I. S. Denniss, N. J.l Hil, B. Ya. Galkin, B. Ya. Zilberman, and Yu. S. Fedorov. The applications of formo- and

aceto-hydroxamic acids in nuclear fuel reprocessing. *Journal of Alloys and Compounds*, 271-273:534 – 537, 1998.

[10] I. May, R. J. Taylor, I. S. Denniss, and A. L. Wallwork. Actinide complexation in the purex process. *Czechoslovak Journal of Physics*, 49(1):597–601, Jan 1999.

[11] S. Arm and C. Phillips. Chemical engineering for advanced aqueous radioactive materials separations. In K. L. Nash and G. J. Lumetta, editors, *Advanced Separation Techniques for Nuclear Fuel Reprocessing and Radioactive Waste Treatment*, Woodhead Publishing Series in Energy, pages 58–94. Woodhead Publishing, 2011.

[12] F. Drain, R. Vinoche, and J. Duhamet. 40 years of experience with liquid-liquid extraction equipment in the nuclear industry. In *Waste Management Conference 2003*, pages 23–27, Tucson, United States, February 2003.

[13] C. Phillips. Commissioning of the solvent extraction processes in the thermal oxide reprocessing plant. In *Solvent Extraction in the Process Industries*, pages 1463–1470. Elsevier Applied Science, 1993.

[14] G. W. Stevens. Packed columns. In J. C. Godfrey and M. J. Slater, editors, *Liquid-Liquid Equipment*, pages 227–246. John Wiley & Sons Ltd, 1994.

[15] L. P. Fernandez. Savannah river site canyons âĂŞ nimble behemoths of the atomic age. Westinghouse Savannah River Company, 2000.

[16] C. Ramshaw. Higee distillation-an example of process intensification. *Chem. Engr.*, 389:13–14, 1983.

[17] P. Angeli and A. Gavriilidis. Hydrodynamics of taylor flow in small channels: A review. *Proceedings of the Institution of Mechanical Engineers, Part C: Journal of Mechanical Engineering Science*, 222(5):737–751.

[18] V. Dore, D. Tsaoulidis, and P. Angeli. Mixing patterns in water plugs during water/ionic liquid segmented flow in microchannels. *Chemical Engineering Science*, 80:334–341, October 2012.

[19] M. N. Kashid and D. W. Agar. Hydrodynamics of liquid-liquid slug flow capillary microreactor: flow regimes, slug size and pressure drop. *Chemical Engineering Journal*, Vol. 131, 1-13, 2007.

[20] M. N. Kashid, A. Gupta, A. Renken, and L. Kiwi-Minsker. Numbering-up and mass transfer studies of liquidâĂŞliquid two-phase microstructured reactors. *Chemical Engineering Journal*, 158(2):233–240, April 2010.

[21] D. Tsaoulidis, V. Dore, P. Angeli, N. V. Plechkova, and K. R. Seddon. Dioxouranium(VI) extraction in microchannels using ionic liquids. *Chemical Engineering Journal*, 227:151–157, July 2013.

[22] D. Tsaoulidis, V. Dore, P. Angeli, N. V. Plechkova, and K. R. Seddon. Flow patterns and pressure drop of ionic liquidâĂŞwater two-phase flows in microchannels. *International Journal of Multiphase Flow*, 54:1–10, September 2013.

[23] D. Tsaoulidis, V. Dore, P. Angeli, N. V. Plechkova, and K. R. Seddon. Extraction of dioxouranium(VI) in small channels using ionic liquids. *Chemical Engineering Research and Design*, 91(4):681–687, April 2013.

[24] D. Tsaoulidis and P. Angeli. Effect of channel size on mass transfer during liquidâĂŞliquid plug flow in small scale extractors. *Chemical Engineering Journal*, 262:785–793, February 2015.

[25] K. Gonda, H Aoyagi, K. Nakano, and H. Kamikawa. Criticality calculation method for mixer-settlers. Technical report, International Nuclear Information System, 1980.

[26] L. T. Biegler. *Nonlinear programming : concepts, algorithms and applications to chemical processes*. MOS-SIAM series on optimization. Society for industrial and applied mathematics, Philadelphia, 2010.

[27] G. L. Richardson and J. L. Swanson. Plutonium partitioning in the purex process with hydrazine stabilized hydroxylamine nitrate. Technical report, Hanford Engineering Development Laboratory, 1975.

[28] R. Treybal. *Liquid Extraction.* McGraw Hill Book Company Inc., New York, 1963.

[29] W. O. Haas. *"Chemical Reprocessing of Reactor Fuel", Edited by J. F. Flagg.* Academic Press, New York, 1961.

[30] S. B. Watson and R. H. Rainey. Modifications of the sephis computer code for calculating the purex solvent extraction system. Technical report, Oak Ridge National Laboratory, 1975.

[31] A. D. Mitchell. A comparison between sephis-mod4 and previous models for the purex solvent exctraction system. Technical report, Oak Ridge National Laboratory, 1979.

[32] A. D. Mitchell. Sephis-mod4: A user's manual to a revised model of the purex solvent exctraction system. Technical report, Oak Ridge National Laboratory, 1979.

[33] W. C. Scotten. Solvex–a computer program for simulation of solvent extraction processes. Technical report, Savannah River Laboratory, 1975.

[34] A. L. Beyerlein, J. F. Geldard, and H. F. Chung. Deviations from mass transfer equilibrium and mathematical modeling of mixer-settler contactors. In *Measurement Technology for Safeguards and Materials Control*, 1980.

[35] W. S. Groenier, Mitchell A.D., and Jubin R.T. Computational techniques used in the development of co-processing flowsheets. In *Fast Reactor Fuel Reprocessing*, 1980.

[36] K. Gonda, S. Miyachi, and S. Fukuda. Mass Transfer Model of Purex Process in Mixer-Settlers. *Journal of Nuclear Science and Technology*, 23(5):472–474, 1986.

[37] K. Gonda and T. Matsuda. Solvent Extraction Calculation Model for Purex Process in Pulsed Sieve Plate Column. *Journal of Nuclear Science and Technology*, 23(10):883–895, 1986.

[38] K. Gonda, S. Miyachi, and S. Fukuda. Stage Efficiency for Mixer-Settlers Process with Chemical Reactions. *Journal of Nuclear Science and Technology*, 23(3):279–281, March 1986.

[39] R. Natarajan, N. K. Pandey, V. Vijayakumar, and R. V. Subbarao. Modeling and Simulation of Extraction Flowsheet for FBR Fuel Reprocessing. *Procedia Chemistry*, 7:302–308, 2012.

[40] M. Benedict, T. H. Pigford, and H. W. Levi. *Nuclear Chemical Engineering 2nd Edition*. McGraw Hill, New York, 1980.

[41] S. Kumar and S. B. Koganti. Modelling of np(iv) np(vi) distribution coefficients in 30% tbp/n-dodecane/nitric acid/water biphasic purex system. *Indian Journal of Chemical Technology*, 8(1):41–43, January 2001.

[42] C. Hongyan, R. J. Taylor, M. Jobson, and A. J. Masters. Simulation of neptunium extraction in an advanced purex process–model improvement. *Solvent Extraction and Ion Exchange*, 35(1):1–18, 2017.

[43] S. Kumar and S. B. Koganti. Empirical Modelling of U(IV) Distribution in Nitric Acid-Water-30%TBP/n-Dodecane Biphasic System in Presence of U(VI), Pu(III) and Hydrazine Nitrate. *Nuclear technology*, Vol. 123, No.1, 116-119, JulyâĂŹ98 (1998), 1998.

[44] S. Kumar and S. B. Koganti. Purex distribution modelling: Benchmarking of an empirical model for nitric acid extraction in biphasic system. *Indian Journal of Chemical Technology*, 5:368–370, November 2000.

[45] S. Kumar and S. B. Koganti. Modelling of distribution coefficients of nitrous acid in 15-30 vol.tbp/n-dodecane/nitric acid system. *Indian Journal of Chemical Technology*, 7(6):336–337, January 2000.

[46] S. Tachimori. Extra-m: A computing code system for analysis of the purex process with mixer settlers for reprocessing. Technical report, Japan Atomic Energy Research Institute, 1994.

[47] R. A. Ghotli, A. Abdul Raman Abdul, and Shaliza Ibrahim. Liquid-liquid mass transfer studies in various stirred vessel designs. *Reviews in Chemical Engineering*, 31(4):329–343, 2015.

[48] R. C. Perry and D. W. Green. *PerryâĂŹs Chemical EngineersâĂŹ Handbook, seventh ed.* McGraw-Hill,, 1999.

[49] J. C. Godfrey. Mixers. In J. C. Godfrey and M. J. Slater, editors, *Liquid-Liquid Equipment*, pages 363–410. John Wiley & Sons Ltd, 1994.

[50] F. S. Gharehbagh and S. M. A. Mousavian. Hydrodynamic characterization of mixer-settlers. *Journal of the Taiwan Institute of Chemical Engineers*, 40(3):302–312, May 2009.

[51] S. Mohanty. Modeling of liquid-liquid extraction column: a review. *Reviews in Chemical Engineering*, 16(4):199âĂŞ248, January 2000.

[52] T. Miyauchi and H. Oya. Longitudinal dispersion in pulsed perforated-plate columns. *AIChE Journal*, 11(3):395–402, May 1965.

[53] G. Vassallo, Research Commission of the European Communities. Directorate-General for Science, and Development. *The Hydrodynamic Behaviour of a Pulsed Column*. Nuclear science and technology. Commission of the European Communities, 1983.

[54] A. B. Jahya, G. W. Stevens, and H. R. C. Pratt. Pulsed discâĂŘandâĂŘ-doughnut column performance. *Solvent Extraction and Ion Exchange*, 27(1):63–82.

[55] A. Kumar and S. Hartland. Prediction of continuous-phase axial mixing coefficients in pulsed perforated-plate extraction columns. *Industrial & Engineering Chemistry Research*, 28(10):1507–1513, October 1989.

[56] A. Kumar and S. Hartland. Unified Correlations for the Prediction of Drop Size in LiquidâĹŠLiquid Extraction Columns. *Industrial & Engineering Chemistry Research*, 35(8):2682–2695, January 1996.

[57] A. Kumar and S. Hartland. Prediction of dispersed phase hold-up in pulsed perforated-plate extraction columns. *Chemical Engineering and Processing: Process Intensification*, 23(1):41–59, January 1988.

[58] A. Kumar and S. Hartland. Correlations for Prediction of Mass Transfer Coefficients in Single Drop Systems and Liquid–ŠLiquid Extraction Columns. *Chemical Engineering Research and Design*, 77(5):372–384, July 1999.

[59] H. Haverland and M. J. Slater. Pulsed sieve-plate columns. In J. C. Godfrey and M. J. Slater, editors, *Liquid-Liquid Equipment*, pages 277–306. John Wiley & Sons Ltd, 1994.

[60] L. Steiner. Computational procedure for column simulation and design. In J. C. Godfrey and M. J. Slater, editors, *Liquid-Liquid Equipment*, pages 116–135. John Wiley & Sons Ltd, 1994.

[61] M. Torab-Mostaedi, J. Safdari, and A. Ghaemi. Mass transfer coeficients in pulsed perforated-plate extraction columns. *Brazilian Journal of Chemical Engineering*, 27(2):243–251, June 2010.

[62] M. Torab-Mostaedi, A. Ghaemi, M. Asadollahzadeh, and P. Pejmanzad. Mass transfer performance in pulsed disc and doughnut extraction columns. *Brazilian Journal of Chemical Engineering*, 28(3):447–456, September 2011.

[63] C. Jiao, S. Ma, and Q. Song. Mass Transfer Characteristics in a Standard Pulsed Sieve-plate Extraction Column. *Energy Procedia*, 39:348–357, 2013.

[64] R. Teflanab, A. M. Ghoreishi, J. Safdari, and M. Torab-Mostaedi. Axial dispersion model in predictive mass transfer correlation for random pulsed packed column. *Chem. Ind. Chem. Q.*, 21(1):77–83, April 2014.

[65] P. V. Danckwerts. Continuous flow systems: Distribution of residence times. *Chemical Engineering Science*, 2(1):1 – 13, 1953.

[66] M. O. Garg and H. R. C. Pratt. Measurement and modelling of droplet coalescence and breakage in a pulsed-plate extraction column. *AIChE Journal*, 30(3):432–441.

[67] A. Zimmermann, C. Gourdon, X. Joulia, A. Gorak, and G. Casamatta. Simulation of a multicomponent extraction process by a nonequilibrium stage model incorporating a drop population model. *Computers & Chemical Engineering*, 16, Supplement 1:S403–S410, May 1992.

[68] S. Mohanty and A. Vogelpohl. A simplified hydrodynamic model for a pulsed sieve-plate extraction column. *Chemical Engineering and Processing: Process Intensification*, 36(5):385–395, September 1997.

[69] S. D. Al Khani, C. Gourdon, and G. Casamatta. Dynamic and steady-state simulation of hydrodynamics and mass transfer in liquidâĂŤliquid extraction column. *Chemical Engineering Science*, 44(6):1295–1305.

[70] T. Miyauchi and T. Vermeulen. Diffusion and Back-Flow Models for Two-Phase Axial Dispersion. *Industrial & Engineering Chemistry Fundamentals*, 2(4):304–310, November 1963.

[71] M. Torab-Mostaedi, J. Safdari, M. A. Moosavian, and M. G. Maragheh. Stage efficiency of hanson mixer-settler extraction column. *Chemical Engineering and Processing: Process Intensification*, 48(1):224–228.

[72] M. Torab-Mostaedi, S. J. Safdari, M. A. Moosavian, and M. Ghannadi Maragheh. Mass transfer coefficients in a hanson mixer-settler extraction column. *Brazilian Journal of Chemical Engineering*, 25(3):473–481.

[73] A. Safari, J. Safdari, H. Abolghasemi, M. Forughi, and M. Moghaddam. Axial mixing and mass transfer investigation in a pulsed packed liquidâĂŞliquid extraction column using plug flow and axial dispersion models. *Chemical Engineering Research and Design*, 90(2):193–200, February 2012.

[74] M. Jaradat, M. Attarakih, and H. J. Bart. Population Balance Modeling of Pulsed (Packed and Sieve-Plate) Extraction Columns: Coupled Hydrodynamic and Mass Transfer. *Industrial & Engineering Chemistry Research*, 50(24):14121–14135, December 2011.

[75] M. Jaradat, M. Attarakih, and H. J. Bart. Advanced prediction of pulsed (packed and sieve plate) extraction columns performance using population balance modelling. *Chemical Engineering Research and Design*, 89(12):2752–2760, December 2011.

[76] Q. Yu, F. Weiyang, and W. Jiading. A study on mass transfer in pulsed sieve plate extraction column. *Journal of Chemical Industry and Engineering (China)*, 4(2):218–228, 1989.

[77] X. Tang, G. Luo, and J. Wang. A dynamic forward mixing model for evaluating the mass transfer performances of an extraction column. *Chemical Engineering Science*, 59(21):4457–4466.

[78] G. L. Richardson. Effect of high solvent radiation exposure on tbp processing of spent lmfbr fuels. Technical report, Handford Engineering Development Lab., 1973.

[79] T. Matsuda and K. Gonda. Motion of Dispersed Drops and Mass Transfer in Pulsed Column. *Journal of Nuclear Science and Technology*, 23(7):633–642, 1986.

[80] T. Matsuda and K. Gonda. Mass Transfer Coefficients of Uranium and Plutonium across Aqueous/Organic Interfaces of Solvent Extraction. *Journal of Nuclear Science and Technology*, 23(6):529–539, 1986.

[81] A. Shadrin, A. Murzin, A. Lumpov, and V. Romanovsky. The possibility of reprocessing of spent nuclear fuel using supercritical fluids. *Solvent Extraction and Ion Exchange*, 26(6):797–806, November 2008.

[82] T. Shimada, S. Ogumo, N. Ishihara, Y. Kosaka, and Y. Mori. A study on the technique of spent fuel reprocessing with supercritical fluid direct extraction method (Super-DIREX method). *Journal of Nuclear Science and Technology*, 39(sup3):757–760, November 2002.

[83] M. D. Samsonov, T. I. Trofimov, S. E. Vinokurov, S. C. Lee, B. F. Myasoedov, and C. M. Wai. Dissolution of Actinide Oxides in Supercritical Fluid Carbon Dioxide, Containing Various Organic Ligands. *Journal of Nuclear Science and Technology*, 39(sup3):263–266, November 2002.

[84] D. Tsaoulidis. *Studies of intensified small-scale processes for liquid-liquid separations in spent nuclear fuel reprocessing*. PhD thesis, University College London, 2014.

[85] S. H. Ha, R. N. Menchavez, and Y. M. Koo. Reprocessing of spent nuclear waste using ionic liquids. *Korean Journal of Chemical Engineering*, 27(5):1360–1365, September 2010.

[86] A. Rout, K. A. Venkatesan, T. G. Srinivasan, and P. R. Vasudeva Rao. Tuning the extractive properties of purex solvent using room temperature ionic liquid. *Separation Science and Technology*, 48(17):2576–2581, November 2013.

[87] S. I. Stepanov, A. V. Boyarintsev, M. V. Vazhenkov, B. F. Myasoedov, E. O. Nazarov, A. M. Safiulina, I. G. Tananaev, Hen Vin So, A. M. Chekmarev, and A. Yu Civadze. CARBEX process, a new technology of reprocessing of spent nuclear fuel. *Russ J Gen Chem*, 81(9):1949–1959, October 2011.

[88] A. Gavriilidis, P. Angeli, E. Cao, K. Yeong, and Y. Wan. Technology and applications of microengineered reactors. *Chemical Engineering Research and Design*, 80(1):3 – 30, 2002. Process and Product Development.

[89] G. BercĚĞicĚĞ and A. Pintar. The role of gas bubbles and liquid slug lengths on mass transport in the taylor flow through capillaries. *Chemical Engineering Science*, 52(21):3709–3719, 1997.

[90] C. O. Vandu, H. Liu, and R. Krishna. Mass transfer from taylor bubbles rising in single capillaries. *Chemical Engineering Science*, 60(22):6430–6437, 2005.

[91] J. M. van Baten and R. Krishna. CFD simulations of mass transfer from taylor bubbles rising in circular capillaries. *Chemical Engineering Science*, 59(12):2535–2545, 2004.

[92] S. Irandoust and B. Andersson. Liquid film in taylor flow through a capillary. *Industrial & Engineering Chemistry Research*, 28(11):1684–1688, 1989.

[93] A. Leclerc, R. Philippe, V. Houzelot, D. Schweich, and C. de Bellefon. GasâĂŞliquid taylor flow in square micro-channels: New inlet geometries and interfacial area tuning. *Chemical Engineering Journal*, 165(1):290–300, 2010.

[94] B. Xu, W. Cai, X. Liu, and X. Zhang. Mass transfer behavior of liquidâĂŞliquid slug flow in circular cross-section microchannel. *Chemical Engineering Research and Design*, 91(7):1203–1211, 2013.

157

[95] D. Qian and A. Lawal. Numerical study on gas and liquid slugs for taylor flow in a t-junction microchannel. *Chemical Engineering Science*, 61(23):7609–7625, 2006.

[96] S. Laborie, C. Cabassud, L. Durand-Bourlier, and J. M. Lainé. Characterisation of gas–liquid two-phase flow inside capillaries. *Chemical Engineering Science*, 54(23):5723–5735, 1999.

[97] N. Di Miceli Raimondi, L. Prat, C. Gourdon, and P. Cognet. Direct numerical simulations of mass transfer in square microchannels for liquid–liquid slug flow. *Chemical Engineering Science*, 63(22):5522–5530.

[98] F. Fairbrother and A. E. Stubbs. 119. studies in electro-endosmosis. part VI. the "bubble-tube" method of measurement. *Journal of the Chemical Society (Resumed)*, (0):527–529, 1935.

[99] F. P. Bretherton. The motion of long bubbles in tubes. *Journal of Fluid Mechanics*, 10(2):166–188, 1961.

[100] P. Aussillous and D. Quere. Quick deposition of a fluid on the wall of a tube. *Physics of Fluids (1994-present)*, 12(10):2367–2371, 2000.

[101] J. Jovanović, W. Zhou, E. V. Rebrov, T. A. Nijhuis, V. Hessel, and J. C. Schouten. Liquid–liquid slug flow: Hydrodynamics and pressure drop. *Chemical Engineering Science*, 66(1):42–54, 2011.

[102] COMSOL, Inc. COMSOL Multiphysics Reference Manual, version 5.3, www.comsol.com.

[103] C. Amador, A. Gavriilidis, and P. Angeli. Flow distribution in different microreactor scale-out geometries and the effect of manufacturing tolerances and channel blockage. *Chemical Engineering Journal*, 101(1):379–390, 2004.

[104] Minqiang Pan, Yong Tang, Liang Pan, and Longsheng Lu. Optimal design of complex manifold geometries for uniform flow distribution between microchannels. *Chemical Engineering Journal*, 137(2):339–346, 2008.

[105] M. Pan, Y. Tang, H. Yu, and H. Chen. Modeling of velocity distribution among microchannels with triangle manifolds. *AIChE J.*, 55(8):1969–1982, 2009.

[106] M. Saber, J. M. Commenge, and L. Falk. Rapid design of channel multi-scale networks with minimum flow maldistribution. *Chemical Engineering and Processing: Process Intensification*, 48(3):723–733, 2009.

[107] M. Saber, J. M. Commenge, and L. Falk. Heat-transfer characteristics in multi-scale flow networks with parallel channels. *Chemical Engineering and Processing: Process Intensification*, 49(7):732–739, 2010.

[108] J. M. Commenge, M. Saber, and L. Falk. Methodology for multi-scale design of isothermal laminar flow networks. *Chemical Engineering Journal*, 173(2):541–551, 2011.

[109] M. Al-Rawashdeh, X. Nijhuis, E. V. Rebrov, V. Hessel, and J. C. Schouten. Design methodology for barrier-based two phase flow distributor. *AIChE J.*, 58(11):3482–3493, 2012.

[110] F. Scheiff, M. Mendorf, D. Agar, N. Reis, and M. Mackley. The separation of immiscible liquid slugs within plastic microchannels using a metallic hydrophilic sidestream. *Lab Chip*, 11(6):1022–1029, 2011.

[111] GAMS Development Corporation. General Algebraic Modeling System (GAMS) Release 24.2.1. Washington, DC, USA, 2013.

[112] T. Asakura, S. Hotoku, Y. Ban, M. Matsumura, and Y. Morita. Technetium separation for future reprocessing. *Journal of Nuclear and Radiochemical Sciences*, 6(3):271–274, December 2005.

[113] G. Uchiyama, S. Hotoku, and S. Fujine. Distribution of nitrous acid between tri-n-butyl phosphate/ n-dodecane and nitric acid. *Solvent Extraction and Ion Exchange*, 16(5):1177–1190, 1998.

[114] J. E. Birkett, M. J. Carrott, O. D. Fox, C. J. Jones, C. J. Maher, C. V. Robeu, R. J. Taylor, and D. A. Woodhead. Controlling neptunium and plutonium within single cycle solvent extraction flowsheets for advanced fuel cycles. *Journal of Nuclear Science and Technology*, 44(3):337–343, 2007.

[115] R. D. Carter, G. R. Kiel, and K. R. Ridgway. Criticality handbook vol. 1. Technical report, Atlantic Richfield Hanford Co. Report ARH-600, 1968.

[116] A. Kumar and S. Hartland. Computational Strategies for Sizing Liquid–Liquid Extractors. *Industrial & Engineering Chemistry Research*, 38(3):1040–1056, March 1999.

[117] T. T. Nichols, C. M. Barnes, L. Lauerhass, and D. D. Taylor. Selection of steady-state process simulation software to optimize treatment of radioactive and hazardous waste. Technical report, Idaho National Engineering and Environmental Laboratory, 2001.

[118] A. Tonkovich, D. Kuhlmann, A. Rogers, J. McDaniel, S. Fitzgerald, R. Arora, and T. Yuschak. Microchannel technology scale-up to commercial capacity. *Chemical Engineering Research and Design*, 83(A6):634–639, 2005.

[119] R.G. Geier and Hanford Atomic Products Operation. *Application of the pulse column to the Purex process*. Hanford Atomic Products Operation, 1957.

[120] R.B Geier and L.M Browne. Solvent extraction equipment evaluation study. part 1. review of the literature. Technical Report BNWL–2186(PT.1), Battelle Pacific Northwest Labs., Richland, Wash. (USA), January 1977.

[121] CM Scientific. http://www.cmscientific.com/. Accessed on 23/10/2017.

[122] Robert E. Treybal. The economic design of mixer-settler extractors. 5(4):474–482.

[123] R. Smith. *Chemical Process Design and Integration*. John Wiley & Sons Ltd, United Kingdom, 2005.

[124] W. D. Seider, J. D. Seader, and D. R. Lewin. *Product and process design principles: synthesis, analysis, and evaluation*. Wiley, New York, 2004.

[125] D. Bascone, P. Angeli, and E. S. Fraga. Mathematical modelling of intensified extraction for spent nuclear fuel reprocessing,). In *A. Espuña, M.*

Graells & L. Puigjaner (Editors), *Proceedings of the 27th European Symposium on Computer Aided Process Engineering – ESCAPE 27*, pages 355–360, Barcelona (Spain), 2017.

[126] Y. Qian, W. Y. Fei, and J. D. Wang. A study on mass transfer in pulsed sieve-plate extraction column. *Chin. J. Chem. Eng.*, 4(2):218–228, 1989.

[127] B. Guillaume, J. P. Moulin, and Ch. Maurice. Chemical properties of neptunium applied to neptunium management in extraction cycles of purex process. In *Extraction '84*, pages 31–45. Pergamon, 1984.

[128] B. Hanson. Process engineering and design for spent nuclear fuel reprocessing and recycling plants. In R. Taylor, editor, *Reprocessing and Recycling of Spent Nuclear Fuel*, Woodhead Publishing Series in Energy, pages 125 – 151. Woodhead Publishing, Oxford, 2015.

[129] R. K. Sinnott. *Coulson & Richardson's Chemical Engineering*. Chemical Engineering Design, vol. 6, fourth ed. Elsevier Butterworth-Heinemann, 2005.

[130] R. C. Cairns, J. R. May, M. G. Baillie, and M. S. Farrell. Conceptual design study of a low throughput reprocessing facility for nuclear fuel. Technical report, Australian Atomic Energy Commission, 1967.

[131] D. Royston and A. Burwell. The design and perfonrmance of pump-mix and gravity-flow mixer-settlers. Technical report, Australian Atomic Energy Commission, 1973.

[132] M. G. Baillie and R. C. Cairns. Development of a ten stage mixer settler. Technical report, Australian Atomic Energy Commission, 1958.

[133] P. G. Alfredson, B. G. Charlton, R. K. Ryan, and V. K. Vilkaitis. Development of processes for pilot plant production of purfied uranyl nitrate solutions. Technical report, Australian Atomic Energy Commission, 1975.

[134] S. D. Kahook. Neutronic analysis of the 1d and 1e banks reflux detection system. Technical report, Westinghouse Savannah River Company, 1999.

[135] D. E. Garrett. *Chemical Engineering Economics*. Springer Netherlands, New York, 1989.

[136] R. Fullwood. Lecture notes for nuclear criticality. Technical report, Brookhaven National Laboratory/Associated Universities, Inc., 1992.

[137] A. Kumar and S. Hartland. Empirical prediction of operating variables. In J. C. Godfrey and M. J. Slater, editors, *Liquid-Liquid Equipment*, pages 625–735. John Wiley & Sons Ltd, 1994.

[138] A. Carleton Jealous and Homer F. Johnson. Power Requirements for Pulse Generation in Pulse Columns. *Industrial & Engineering Chemistry*, 47(6):1159–1166, June 1955.

[139] Hiroyasu Hotokezaka, Manabu Tokeshi, Masayuki Harada, Takehiko Kitamori, and Yasuhisa Ikeda. Development of the innovative nuclide separation system for high-level radioactive waste using microchannel chipâĂŤextraction behavior of metal ions from aqueous phase to organic phase in microchannel [Progress in Nuclear Energy 47 (2005) 439âĂŞ447]. *Progress in Nuclear Energy*, 48(2):187, March 2006.

[140] R. Chiarizia, M. P. Jensen, M. Borkowski, J. R. Ferraro, P. Thiyagarajan, and K. C. Littrell. Third Phase Formation Revisited: The U(VI), HNO3âĂŞTBP, nâĂŘDodecane System. *Solvent Extraction and Ion Exchange*, 21(1):1–27, January 2003.

[141] M. Pelendritis. *Nuclear fuel waste extraction: Third phase revisited*. PhD thesis, Univerisity of Manchester, 2017.

[142] Dimitrios Tsaoulidis and Panagiota Angeli. Effect of channel size on liquid-liquid plug flow in small channels. *AIChE Journal*, 62(1):315–324, January 2016.

[143] World Nuclear Association. `https://http://www.world-nuclear.org//`. Accessed: 25/02/2018.

[144] J. F. Geldard, A. L. Beyerlein, and L. Phillips. Correlation functions for the distribution coefficients of u(iv) and pu(iii) ions between acqueous nitric acid and 30diluent. *Nuclear Technology*, 17(12):394–400, 1985.

[145] S. Kumar and S. B. Koganti. An Empirical Correlation for Pu(III) Distribution Coefficients in 30% TBP/nâĂŘDodecane PUREX System in the Presence of U(VI), U(IV), Pu(IV), Pu(III), and Hydrazine Nitrate. *Solvent Extraction and Ion Exchange*, 21(3):369–380, January 2003.

[146] M. N. Kashid, Y. M. Harshe, and D. W. Agar. Liquid-Liquid Slug Flow in a Capillary:âĂĽ An Alternative to Suspended Drop or Film Contactors. *Industrial & Engineering Chemistry Research*, 46(25):8420–8430, December 2007.

[147] Ignacio Grossmann and Carnegie Mellon University Engineering Design Research Center. MINLP optimization strategies and algorithms for process synthesis. *Department of Chemical Engineering*, January 1989.

[148] Mariano MartÃŋn and Ignacio E. Grossmann. Energy optimization of bioethanol production via hydrolysis of switchgrass. *AIChE Journal*, 58(5):1538–1549, May 2012.

[149] Mariano MartÃŋn and Ignacio E. Grossmann. ASI: Toward the optimal integrated production of biodiesel with internal recycling of methanol produced from glycerol. *Environmental Progress & Sustainable Energy*, 32(4):891–901, December 2013.

[150] Mariano MartÃŋn and Ignacio E. Grossmann. Optimal simultaneous production of i-butene and ethanol from switchgrass. *Biomass and Bioenergy*, 61:93–103, February 2014.

[151] Xiao Yang, Hong-Guang Dong, and Ignacio E. Grossmann. A framework for synthesizing the optimal separation process of azeotropic mixtures. *AIChE Journal*, 58(5):1487–1502, May 2012.

[152] Linlin Yang, Raquel Salcedo-Diaz, and Ignacio E. Grossmann. Water Network Optimization with Wastewater Regeneration Models. *Industrial & Engineering Chemistry Research*, 53(45):17680–17695, November 2014.

[153] Davide Bascone, Panagiota Angeli, and Eric S. Fraga. Mathematical modelling of intensified extraction for spent nuclear fuel reprocessing. *Nuclear Engineering and Design*, 332:162–172, June 2018.

[154] Nobuaki Aoki, Ryuichi Ando, and Kazuhiro Mae. GasâĹŠLiquidâĹŠLiquid Slug Flow for Improving LiquidâĹŠLiquid Extraction in Miniaturized Channels. *Industrial & Engineering Chemistry Research*, 50(8):4672–4677, April 2011.

[155] D. Bascone, P. Angeli, and E. S. Fraga. Optimal design of a coex process for spent nuclear fuel reprocessing using small channels. In *M. R. Eden, M. Ierapetritou and G. P. Towler (Editors), Proceedings of the 13th International Symposium on Process Systems Engineering – PSE 2018*, pages 2365–2371, San Diego (US), 2018.

Appendix

GAMS code used in Section 6.3

```
1 *SET
2 set h finite elements for length discretisation /1*50/
3 set scale scale for manifolding /1*4/
4 set SUBSET_scale(scale) /2*4/;
5 set k_man phases in manifolds /aq,org/
6 set sep phase separation /main, side/
7 set mater channel material - polymer or stainless steel /poly,SS/
8 set comp components /U_VI,Pu_IV,HNO3,HNO3_2,TBP, Zr, Ru, Tc, Np_V, Np_VI,
Np_»
IV, HNO2, U_IV, Pu_III, HAN, N2H5/
9 set step /main_extr_codec, scrub1_codec, comp_extr_codec,co_strip,u_strip/
10 set red reducing agents /HAN,U_IV/
11 set k phases /aq,org,mix/
12 set k2 phases /aq,org/
13 set j n stages max /1*6/;
14 set i phases for pressure drop calc. /disp,cont/
15 set iter for loops /1*9/
16
17 Parameter
18 F0 TBP fraction - when considered constant /0.3/
19 sf scaling factor /1000/
20 MW_TBP TBP molecular weight [g mole-1] /266/
21 rho_TBP TBP mass density [kg m-3] /973/
```

22 MW_av average MW metals[g mole-1]

23 int fractional interest rate /0.05/

24 n_y number of years for annualised cost /5/

25 T(step) temperature [K]

26 C0_aq(comp,step) U concentration in the aqueous feed [mol m-3]

27 C0_org(comp,step) Initial U concentration in the organic solvent [mol m-3]

28 mu_2(k2,step) viscosity - for [Pa s]

29 rho_2(k2,step) mass density [kg m-3]

30 Diff(k2,comp) diffusion coefficient [m2 s-1]

31 gamma interfacial tension [N m-1] /0.01/

32 tau_T(step) T correction factor Richardson correlation

33 mu(k,step) viscosity - only for IS model [Pa s]

34 rho(k,step) mass density - only for IS model [kg m-3]

35 ann_throughput annual throughput [tons metal year -1] /500/

36 Fm material factor - Stainless 316 from Seider /2.1/

37 USDoll_to_UKPou scaling factor US dollars to UK Pounds /0.6615/

38 MSI Marshall&Swift Chem Plant Index 2015 extrapolated from 2002-2011 values /»
1.52/

39 eta pump efficiency /0.8/

40 Energy_price cost of energy [£kWh-1] /0.1/

41 m3_to_gal /264.172/

42 kg_to_lb to convert kg to lb /2.20462/

43 vessel_exp exponent for horizontal vessel cost from Garret Chemical Engineeri»
ng Economics by Donald E. Garrett 1989 /.64/

44 vessel_cost1000lb horizontal vessel cost for 1000 lb from Seider 2004 [$] /10»
000/

45 TBP_sol TBP solubility in nitri acid solution - 25C 3 M HNO3 - [mg L-1] from »
Vladimirova 1991 using WebPlotDigitizer /175/

46 a1_Zr empirical costant for Zr distribution coeff - Natarajan et al 2012 /0»
.2682/

47 a2_Zr empirical costant for Zr distribution coeff - Natarajan et al 2012 /-0»
.6359/

48 a3_Zr empirical costant for Zr distribution coeff - Natarajan et al 2012 /0»

.4853/

49 a1_Ru empirical costant for Ru distribution coeff - Natarajan et al 2012 /-»
0.0691/

50 a2_Ru empirical costant for Ru distribution coeff - Natarajan et al 2012 /0.»
8356/

51 a3_Ru empirical costant for Ru distribution coeff - Natarajan et al 2012 /-»
2.3672/

52 a4_Ru empirical costant for Ru distribution coeff - Natarajan et al 2012 /0»
.9165/

53 MW(comp) MW for metals

54 sumC0_metals sum of initial concentration of all metals

55 cm3h_to_tonsyr2 scaling factor

56 C_H20_org organic concentration of water [M] from Chen 2016 "Development and»
Validation of a Flowsheet Simulation Model for Neptunium Extraction in an Ad»
vanced PUREX Process" /0.42/

57 KII_org 1st order kinetic constant for hydrolysis rate in organic phase - Vla»
dimirova et al 92 - @ 25C from Arrenhius plot [h-1] /6.97e-6/

58 KZr_org 1st order kinetic constant for hydrolysis rate in organic phase - Vla»
dimirova et al 92 - @ 25C from Arrenhius plot [h-1] /2.05e-3/

59 KIII_org 1st order kinetic constant for hydrolysis rate in organic phase - Vl»
adimirova et al 92 - for [H+]org calculation [h-1]

60 KIII 2nd order kinetic constant for hydrolysis rate in the two-phase - Vladim»
irova et al 92 - @ 25C from Arrenhius plot [h mol-1 L-1]

61 K_Np_for1(step) kinetic constant Np(V) oxidation - by Koltunov see Chen 2019

62 K_Np_for2(step) kinetic constant Np(V) oxidation - by Koltunov see Chen 2019

63 K_Np_rev1(step) kinetic constant Np(VI) reduction - by Koltunov see Chen 2019

64 K_Np_rev2(step) kinetic constant Np(VI) reduction - by Koltunov see Chen 2019

65 K_Np_IV_for(step) kinetic constant Np(V) reduction to Np(IV) - from Tachimori»
- k19 p.35 - eq. 2.5-19 p. 31 [units are mol - L - s]

66 K_Np_IV_rev(step) kinetic constant Np(IV) oxidation- from Tachimori - k6 p.35»
- eq. 2.5-9 p. 30 [units are mol - L - s]

67 K_Pu_ox_aq(step) kinetic constant Pu III oxidation - from Tachimori - k4 p35 »
- eq. 2.5-4 p. 30 [units are mol - L - s]

68 K_Pu_ox_org(step) kinetic constant Pu III oxidation - organic phase - from Go»
nda [units are mol - L - s]

69 K_U_ox_aq kinetic constant U IV oxidation - aqueous phase - from Gonda [unit»
s are mol - L - s] for [H+]<0.8 M

70 K_U_ox_org kinetic constant U IV oxidation - organic phase - from Gonda [un»
its are mol - L - s] for [H+]<0.34 M

71 K_NO2_scav_aq(step) kinetic constant for NO2 scavenge by N2H5 - aqueous phase»
- from Gonda [units are mol - L - s]

72 K_Pu_red_N2H5(step) kinetic constant Pu IV reduction by N2H5 - aqueous phase
»
- from Tachimori - k3 p.35 - eq. 2.5-3 p. 30 [units are mol - L - s]

73 K_Np_VI_red_N2H5(step) kinetic constant Pu IV reduction by N2H5 - aqueous
pha»
se - from Tachimori - k8 p.35 - eq. 2.5-8 p. 30 [units are mol - L - s]

74 K_Pu_red_HAN kinetic constant Pu IV reduction by HAN - aqueous phase - from
T»
achimori - k2 p.35 - eq. 2.5-2 p. 30 [units are mol - L - s]

75 K_Np_red_HAN kinetic constant Np VI reduction by HAN - aqueous phase - from
T»
achimori - k11 p.35 - eq. 2.5-14 p. 31 [units are mol - L - s]

76 K_NO2_HAN kinetic constant for NO2 scavenge by HAN - aqueous phase - from Go»
nda [units are mol - L - s]

77 K_Pu_red_U_aq(step) kinetic constant for Pu IV reduction by U(IV) - aqueous »
phase - from Tachimori - k1 p.35 - eq. 2.5-1 p. 31 [units are mol - L - s]

78 K_Pu_red_U_org(step) kinetic constant for Pu IV reduction by U(IV) - organic»
phase - from Tachimori - k'1 p.38 - eq. 2.5-1 p. 31 [units are mol - L - s]

79 K_NpIV_red_U(step) kinetic constant Np VI reduction by U(IV) - aqueous phase»
- from Tachimori - k9 p.35 - eq. 2.5-12 p. 31 [units are mol - L - s]

80 K_NpV_red_U(step) kinetic constant Np V reduction by U(IV) - aqueous phase -»
from Tachimori - k10 p.35 - eq. 2.5-13 p. 31 [units are mol - L - s]

81 C0_DBP inlet DBP + MBP concentration [mol m-3] /0/

82 cm3h_to_tonsyr scaling factor to convert [cm3 h-1] to [ton year-1 of U]

83 cm3h_to_m3s scaling factor to convert [cm3 h-1] to [m3 s-1]

84 h_to_s scaling factor from hours to seconds /3600/

85 h_to_yr scaling factor from hours to year /8760/

86 kinf infinite multiplication factor - considering 0.268 g cm-3 4ue from ARH-600 /1.01/

87 m2 migration area - considering 0.268 g cm-3 41/

88 delta extrapolation distance for migration area approximation - 6 cm as rule » of thumbs [cm] /6/

89 g gravitational acceleration m s-2 /9.81/

90 s_to_h scaling factor from hours to seconds /3600/

91 z_disp(step) constant to select the disperse phase - 1 if organic is contin» uous and aquoeus is dispersed - 0 otherwise (disp organic and cont aqueous)

92 Rho_cont(step) mass density continuous phase [SI]

93 Rho_disp(step) mass density dispersed phase [SI]

94 Mu_cont(step) viscosity continuous phase [SI]

95 mu_DP(i,step) viscosity for DP calculations [Pa s]

96 z_extr(step) 1 if extraction - 0 if stripping

97 V_feed(k2) Volumetric feed to be reprocessed [L h-1]

98 z_inlet(k2,step) 1 if the inlet is a new stream - 0 if it comes from the prev» ious unit operation

99 C0(k2,comp) initial concentrations

100 z_feed(step) 1 for the first step - 0 otherwise

101 z_recycle(step) 1 if any stream is recycled - 0 otherwise - for C inlet calc» ulation

102 z_HNO3(k2,comp,step) 1 for HNO3 - 0 for other comps

103 Diff_cont(comp,step) diffusivity coefficients continuous phase

104 Diff_disp(comp,step) diffusivity coefficients dispersed phase

105 z_step_initial(step) parameter to initialiase - to set equal to zero the mor» e nonlinear eq in the first optimisations

106 scal_Zr(step) parameter to scale distr coeff of Zr - too high otherwise » in some equations

107 z_inlet_fresh(k2,step) 1 if the inlet is a new stream - 0 if it comes from th» e previous unit operation

108 z_new_step(step) parameter used for initialisation - 1 if a new step is inse» rted in the flowsheet but not connected to the previous ones yet

109 z_reac_UIV(step) 1 if reactions of U(IV) are considered - 0 otherwise

110 z_reac_PuIII_ox(step) 1 if reactions of Pu(III) are considered - 0 otherwise

111 z_reac_N2H5(step) 1 if reactions of N2H5 are considered - 0 otherwise

112 z_red(k2,comp,step) 1 if reductants are considered - 0 otherwise

113 z_scav(k2,comp,step) 1 if nitrite scavenger is considered - 0 otherwise

114 z_co_strip(step) 1 for co strip step - 0 otherwise

115 z_step_ru(step) 1 if Ru is considered - 0 otherwise

116 z_step_zr(step) 1 if Ru is considered - 0 otherwise

117 z_step_NpV(step) 1 if Np(V) is considered - 0 otherwise

118 z_step_NpVI(step) 1 if Np(VI) is considered - 0 otherwise

119 z_step_NpIV(step) 1 if Np(IV) is considered - 0 otherwise

120 z_inlet_comp(comp,step) 1 if inlet concentrations are parameters - 0 otherwi»
se - for initialisation

121 z_scrub_hno3(step) 1 if HNO3 is scrubbed - 0 otherwise

122 z_E_Ru_step(step) 1 if E Ru is calculated - 0 otherwise - for initialis»
ation

123 z_reac_Pu_IV_ox(step) 1 if oxidation to Pu(IV) is considered - 0 otherwise »
- for initialisation

124 z_no_Np(step) 1 if there is Np - 0 otherwise

125 z_step_IS(step) 0 if the step is disabled - 1 otherwise - for initialis»
ation

126

127 ;

128 z_step_IS(step)=1;

129 z_new_step(step)=0;

130 z_new_step('u_strip')=1;

131 z_co_strip(step)=0;

132 z_co_strip('co_strip')=1;

133 z_scrub_hno3(step)=0;

134 z_scrub_hno3('scrub1_codec')=1;

135 z_scrub_hno3('u_strip')=1;

136 z_no_Np(step)=1;

137 z_reac_Pu_IV_ox(step)=0;

```
138 z_reac_Pu_IV_ox('co_strip')=1;
139 z_step_ru(step)=1;
140 z_step_ru('co_strip')=0;
141 z_step_ru('u_strip')=0;
142 z_step_zr(step)=1;
143 z_step_zr('co_strip')=0;
144 z_step_zr('u_strip')=0;
145 z_step_NpV(step)=1;
146 z_step_NpVI(step)=1;
147 z_step_NpIV(step)=1;
148 z_red(k2,comp,step)=0;
149 z_scav(k2,comp,step)=0;
150 z_red('aq','U_iv','Co_strip')=1;
151 z_scav('aq','n2h5','Co_strip')=1;
152 z_reac_UIV(step)=0;
153 z_reac_PuIII_ox(step)=0;
154 z_reac_N2H5(step)=0;
155 z_reac_UIV('co_strip')=1;
156 z_reac_PuIII_ox('co_strip')=1;
157 z_reac_N2H5('co_strip')=1;
158 z_reac_UIV('u_strip')=1;
159 z_reac_PuIII_ox('u_strip')=1;
160 scal_Zr(step)=1;
161 scal_Zr('Co_strip')=1e5;
162 scal_Zr('U_strip')=1e5;
163 z_inlet_fresh(k2,step)=1;
164 z_inlet_fresh(k2,'main_extr_codec')=0;
165 z_inlet_fresh('org','scrub1_codec')=0;
166 z_inlet_fresh('aq','comp_extr_codec')=0;
167 z_inlet_fresh('org','co_strip')=0;
168 z_inlet_fresh('org','U_strip')=0;
169 z_recycle(step)=0;
170 z_recycle('main_extr_codec')=1;
```

```
171 z_HNO3(k2,comp,step)=0;
172 z_HNO3('aq','HNO3',step)=1;
173 z_feed(step)=0;
174 z_feed('main_extr_codec')=1;
175 z_extr(step)=1;
176 z_extr('main_extr_codec')=1;
177 z_extr('scrub1_codec')=0;
178 z_extr('Co_strip')=0;
179 z_extr('u_strip')=0;
180 z_disp(step)=1;
181 z_disp('U_strip')=0;
182 T(step)=298;
183 T('u_strip')=323;
184 tau_T(step)=1/T(step)-1/298;
185 K_Pu_ox_org(step)= 9/3600;
186 K_NpV_red_U(step)=2.25/60;
187 K_NpIV_red_U(step)=7/60;
188 K_Pu_red_U_aq(step)=5000/60;
189 K_Pu_red_U_org(step)=50/60;
190 K_NO2_HAN=1.92e4/3600;
191 K_Np_red_HAN=92.1/60;
192 K_Pu_red_HAN=.732/60;
193 K_Np_VI_red_N2H5(step)=8.3/60;
194 K_Pu_red_N2H5(step)=0.038/60;
195 K_NO2_scav_aq(step)=2.22e4/3600;
196 K_U_ox_aq=1.5/3600;
197 K_U_ox_org=0.96/3600;
198 K_Pu_ox_aq(step)=6.25/60;
199 K_Np_IV_for(step)=8e-4/60;
200 K_Np_IV_rev(step)=2.5/60;
201 K_Np_for1(step)=2.884e11*exp(-9922/T(step));
202 K_Np_for2(step)=5.405e12*exp(-10031/T(step));
203 K_Np_rev1(step)=2*6.928e10*exp(-7505/T(step));
```

```
204 K_Np_rev2(step)=2*2.497e12*exp(-7806/T(step));
205 K_Pu_ox_org('u_strip')=7.46E-03;
206 K_NpV_red_U('u_strip')=1.32E-01;
207 K_Pu_red_U_aq('u_strip')=2.15E+03;
208 K_Pu_red_U_org('u_strip')=2.15E+01;
209 K_Pu_ox_aq('u_strip')=3.11E-01;
210 K_Np_IV_for('u_strip')=1.14E-04;
211 K_Np_IV_rev('u_strip')=1.04E+00;
212 MW('U_VI')=238;
213 MW('Pu_IV')=244;
214 MW('HNO3')=0;
215 MW('HNO3_2')=0;
216 MW('TBP')=0;
217 MW('Zr')=91;
218 MW('Ru')=101;
219 MW('Tc')=98;
220 MW('Np_V')=237;
221 MW('Np_VI')=237;
222 MW('Np_IV')=237;
223 MW('U_IV')=0;
224 MW('Pu_III')=244;
225 MW('HAN')=0;
226 MW('N2H5')=0;
227 C0_org(comp,'u_strip')=0;
228 C0_org('TBP','u_strip')=F0*rho_TBP/MW_TBP*sf;
229 C0_aq(comp,'u_strip')=0;
230 C0_aq('U_VI','u_strip')=1050.42;
231 C0_aq('Pu_IV','u_strip')=11.65;
232 C0_aq('Pu_III','u_strip')=0;
233 C0_aq('HNO3','u_strip')=3000;
234 C0_aq('Zr','u_strip')=12.99;
235 C0_aq('Ru','u_strip')=7.6;
236 C0_aq('Tc','u_strip')=2.77;
```

237 C0_aq('Np_VI','u_strip')=0;

238 C0_aq('Np_V','u_strip')=0.64;

239 *HNO2 is produced by HNO3 radiolysis, 9.71 mol/,m3 from Chen 2016 (NaNO2 tota»
l concentration in the

240 C0_aq('HNO2','u_strip')=9.71;

241 C0_aq('U_IV','u_strip')=0;

242 C0_aq('N2H5','u_strip')=0;

243 C0_aq('HAN','u_strip')=0;

244   sumC0_metals=sum(comp,C0_aq(comp,'u_strip'))-C0_aq('HNO3','u_strip')-C0_aq('H»
NO2','u_strip')-C0_aq('N2H5','u_strip')-C0_aq('HAN','u_strip')-C0_aq('U_IV','»
u_strip');

245 MW_av=sum(comp,MW(comp)*C0_aq(comp,'u_strip')/sumC0_metals);

246 cm3h_to_tonsyr=1/1000000*365*24*(MW_av)/1000/1000;

247 cm3h_to_m3s=1/1000000/3600;

248 cm3h_to_m3s=1/1000000/3600;

249 KIII_org=70*KII_org;

250 KIII=KIII_org/(F0*rho_TBP/MW_TBP*sf/sf);

251 rho('aq',step)=1070;

252 rho('org',step)=828;

253 rho('mix',step)=rho('org',step);

254 mu('aq',step)= 0.001;

255 mu('org',step)=1.8E-03;

256 mu('aq','u_strip')=0.00055;

257 mu('org','u_strip')=9.4E-04;

258 mu('mix',step)=mu('org',step);

259 rho_2('aq',step)=rho('aq',step);

260 rho_2('org',step)=rho('org',step);

261 mu_2('aq',step)= mu('aq',step);

262 mu_2('org',step)=mu('org',step);

263 mu_DP('disp',step)=mu('aq',step)*z_disp(step)+mu('aq',step)*(1-z_disp(step));

264 mu_DP('cont',step)=mu('org',step)*z_disp(step)+mu('org',step)*(1-z_disp(step)»
);

265 Mu_cont(step)=mu_DP('cont',step);

266 Rho_cont(step)=rho('org',step)*z_disp(step)+rho('org',step)*(1-z_disp(step));

267 Rho_disp(step)=rho('aq',step)*z_disp(step)+rho('aq',step)*(1-z_disp(step));

268 Diff(k2,comp)=1e-6;

269 Diff('aq',comp)=4.5e-6;

270 Diff('org',comp)=2.5e-6;

271 *from Knoch 2.5-3 M HNO3 (Zotero), similar by Ondecjn, Physical properties of»
uranium process solutions

272 Diff('aq','U_VI')=4.5e-6;

273 *from Friehemlt, He, Yang, Marx, The diffusion coefficients and viscosities o»
f the UO2(NO3)22TBP complex

274 Diff('org','U_VI')=2.5e-6;

275 *assumed equal to U_VI

276 Diff('aq','Pu_IV')=4.5e-6;

277 *from Knoch 2.5-3 M HNO3 (Zotero)

278 Diff('org','Pu_IV')=2.5e-6;

279 *from Perry's Handbook 8th ed, tab 2-325 Diffusivies in Liquids (25 C)- Trans»
port properties 2-457

280 Diff('aq','HNO3')=3e-5;

281 *assumed equal to U_VI

282 Diff('org','HNO3')=2.5e-6;

283 Diff('aq','HNO3_2')=Diff('aq','HNO3');

284 Diff('org','HNO3_2')=Diff('org','HNO3');

285 Diff('aq','HNO2')=Diff('aq','HNO3');

286 Diff('org','HNO2')=Diff('org','HNO3');

287 Diff('aq','Pu_III')=Diff('aq','Pu_IV');

288 Diff('org','Pu_III')=Diff('aq','Pu_IV');

289 C0('aq',comp)=C0_aq(comp,'u_strip');

290 C0('org',comp)=C0_org(comp,'u_strip');

291 V_feed('aq')=ann_throughput*1e6/MW_av/((sumC0_metals)/1000)/(24*365);

292 V_feed('org')=0;

293

294 * Other parameters

295 Parameters

296 z_scale(scale) parameter for Fd calculations - 1 for 1st scale 0 for others

297 psi_c singularity due to contraction - for DP manifolds (Pan et al 2009) /0.5»
/

298 psi_s singularity due to splitting - for DP manifolds - assumption /1/

299 psi_t singularity due to turning - for DP manifolds (Pan et al 2009 delta=90»
E=W) /1.2/

300 psi_m singularity due to combining - for DP manifolds - assumption /1/

301 psi_e singularity due to increase in section area - for DP manifolds (Pan et »
al 2009) /1/

302 N_ch number of channel per manifold /100/

303 N_discr number of finite elements for L - equal to set h length /50/

304 mu_sep(sep,step) viscosity for deltaP calculation in the separator

305 rho_man(k_man) mass density [kg m-3]

306 mu_man(k_man) viscosity [Pa s]

307 Lmax upper bound for the length of the channel [m] /.5/

308 theta contact angle Teflon-[C4mim][Ntf2]-Deionised Water [degree] /70/

309 costDP(i) constant for DP calculation ratio Lphases over Lunitcell

310 costheta cos(theta) used for DP calculations - to be replaced in the apposite»
equation

311 constant_a,constant_b,constant_c,constant_d constants for the mass transfer c»
oefficient correlation

312 const1 const for mass transf correlation

313 L L channel [m] - sometimes used as parameter for initialisation /.1/

314 z2(j), z3(j) constants for the calculation of the inlet concentration

315 Cost_coeff1 first coeff capital cost rotary pupm from Process Equipment Cost»
Estimation /0.205/

316 Cost_coeff2 second coeff capital cost rotary pupm from Process Equipment Cost»
Estimation /2.972/

317 cm3h_to_gpm scaling factor from c3 h-1 to gpm

318 Luc length unit cell assumed constant - average value from D.Tsaoulidis pag 1»
73 [mm] /3.95e-3/

319 Const_DP_Y angular coefficient DP Y junction 45Âř sq velocity ciclohecane (con»

t)- water (disp) from Kashir and Agar 2007 (DP in kPa) /4.82/

320 z4(h) to calculate C along L - at each finite element

321 tub_cost tubing price - average value from Eduardo [£m-1] /9/

322 interv length interval[m]

323 cost_A(mater) 1st cost parameter for polymeric channels

324 cost_B(mater) 2nd cost parameter for polymeric channels

325 scale4_on_off(scale) 1 if the scale 4 is off - 0 otherwise

326 Tee_cost_single cost of a single tee junction from data by Eduardo /31.78/

327 Teflon_cost_corr correction factor for PTFE cost

328 singular(scale) 1 if singularity DP is considered in that scale 0 otherwise

329 transf_org(comp) array to be used in the RK calculations for mass transfer

330 transf_aq(comp) array to be used in the RK calculations for mass transfer

331 equil_HNO3(comp) array to be used for equilibrium concentrations (since HNO3»
has two forms in the organic phase)

332 equil_TBP(comp) array to be used for TBP equilibrium concentration

333 equil_HAN(comp) array to be used for HAN and N2H5 equilibrium concentration

334 equil_HNO3_2(comp) array to be used for HNO2 equilibrium concentration

335

336 ;

337

338

339

340 equil_HNO3_2(comp)=0;

341 equil_HNO3_2('HNO3_2')=1;

342 equil_HAN(comp)=0;

343 equil_HAN('HAN')=1;

344 equil_HAN('N2H5')=1;

345 equil_HNO3(comp)=0;

346 equil_HNO3('HNO3')=1;

347 equil_TBP(comp)=0;

348 equil_TBP('TBP')=1;

349 transf_org(comp)=0;

350 transf_org('HNO3_2')=1;

```
351 transf_aq(comp)=1;
352 transf_aq('HNO3_2')=0;
353 transf_aq('TBP')=0;
354 transf_aq('HAN')=0;
355 transf_aq('N2H5')=0;
356 transf_org('HAN')=0;
357 transf_org('N2H5')=0;
358 transf_org('TBP')=0;
359 singular(scale)=0;
360 singular('1')=1;
361 Teflon_cost_corr=1.013/10.36;
362 scale4_on_off(scale)=1;
363 scale4_on_off('4')=1;
364 cost_A('poly') =2618;
365 cost_B('poly')=5.119;
366 cost_A('SS')=100879;
367 cost_B('SS')=4.326;
368 z_scale(scale)=0;
369 z_scale('1')=1;
370 interv=L/N_discr;
371 costheta=cos(theta*pi/180);
372 constant_a= 0.88;
373 constant_b= -0.09;
374 constant_c= -0.09;
375 constant_d= -0.1;
376 cm3h_to_m3s=1/1000000/3600;
377 costDP('disp')=1/1.45;
378 costDP('cont')=costDP('disp');
379 mu_sep('main',step)=mu_DP('cont',step);
380 mu_sep('side',step)=mu_DP('disp',step);
381 rho_man('org')=rho('org','u_strip');
382 rho_man('aq')=rho('aq','u_strip');
383 mu_man('org')=mu('org','u_strip');
```

384 mu_man('aq')=mu('aq','u_strip');
385 z2(j)=0;
386 z2('1')=1;
387 z3(j)=0;
388 z3('6')=1;
389 z4(h)=0;
390 z4('1')=1;
391 cm3h_to_gpm=1/(1000*3.758*60);
392 costheta=cos(theta*pi/180);
393 C0_org(comp,'main_extr_codec')=0;
394 C0_org('TBP','main_extr_codec')=F0*rho_TBP/MW_TBP*sf;
395 C0_aq(comp,'main_extr_codec')=0;
396 C0_aq('U_VI','main_extr_codec')=1050.42;
397 C0_aq('Pu_IV','main_extr_codec')=11.65;
398 C0_aq('Pu_III','main_extr_codec')=0;
399 C0_aq('HNO3','main_extr_codec')=3000;
400 C0_aq('Zr','main_extr_codec')=12.99;
401 C0_aq('Ru','main_extr_codec')=7.6;
402 C0_aq('Tc','main_extr_codec')=2.77;
403 C0_aq('Np_VI','main_extr_codec')=0;
404 C0_aq('Np_V','main_extr_codec')=0.64;
405 *HNO2 is produced by HNO3 radiolysis, 9.71 mol/,m3 from Chen 2016 (NaNO2 tota»
l concentration in the
406 C0_aq('HNO2','main_extr_codec')=9.71;
407 C0_aq('U_IV','main_extr_codec')=0;
408 C0_aq('N2H5','main_extr_codec')=0;
409 C0_aq('HAN','main_extr_codec')=0;
410 const1(step)=constant_a*(4/3.14)**(1+constant_b+constant_c)*(mu_DP('cont',ste»
p)/gamma)**constant_b*((Rho_cont(step))/Mu_cont(step))**constant_c;
411
412
413 binary variable
414 z(j,step) 1 for each stage added - otherwise 0 - the sum is equal to N

415 ;

416 z.l(j,step)=1;

417 z.l('5',step)=0;

418 z.l('6',step)=0;

419

420 integer variables

421 N_elem_IS(scale,step) number of elements in each scale of the manifold

422 N_IS(step) number of stages

423 ;

424

425 N_elem_IS.up(scale,step)=100;

426 N_elem_IS.lo(scale,step)=1;

427 N_elem_IS.lo('4',step)=0;

428 N_elem_IS.up('4',step)=1;

429 N_elem_IS.up('3',step)=80;

430 N_IS.lo(step)=2;

431 N_IS.up(step)=7;

432 N_IS.l(step)=4;

433

434

435 Positive variables

436 F volumetric TBP percentage

437 C_fresh_costrip(j,comp,step) inlet concentration in the co strip step

438 C_fresh_Ustrip(j,comp,step) inlet concentration in the U strip step

439 V_fresh_costrip(j,step) inlet volumetric rate in the co strip step

440 Units_is2(j,step) number of parallel small channels required

441 a_IS(j,step) coefficient for RK calculations - mass transfer

442 b_IS(j,h,comp,step) coefficient for RK calculations - mass transfer

443 E_IS(comp,step) extraction efficiency

444 keff_IS(step) effective multiplication factor for nuclear cri»
ticality safety

445 buck_IS(step) buckling considering delta- for nuclear crit sa»
fety

446 L_discr(h) Length of interval

447 C_DBP_IS(j,h,step) DBS concentration [mole m-3] - from TBP degrad»
ation

448 C_DBP_in_IS(j,h,step) DBP inlet conc [mole m-3]

449 Re_IS(scale,k_man,step) Reynolds number

450 r_forw_Np_V_RK1(j,h,step) rate reaction for oxidation Np_V to Np_VI for R»
unge-Kutta method - concentrations in [M]

451 r_back_Np_V_RK1(j,h,step) rate reaction for reduction Np_VI to Np_V for R»
unge-Kutta method - concentrations in [M]

452 r_forw_Np_V_RK2(j,h,step) rate reaction for oxidation Np_V to Np_VI for R»
unge-Kutta method - concentrations in [M]

453 r_back_Np_V_RK2(j,h,step) rate reaction for reduction Np_VI to Np_V for R»
unge-Kutta method - concentrations in [M]

454 a_Fd(scale,k_man,step) coefficient for flow maldistribution regression

455 b_Fd(scale,k_man,step) coefficient for flow maldistribution regression

456 I_S_IS(j,h,step) ionic strength for equilibrium calculations [M]

457 C_NO3_IS(j,h,step) nitrate concentration [mol m-3]

458 Vdot_IS(j,k,step) volumetric flowrate within channels [cm3 h-1]

459 vel_IS(j,k,step) velocity of fluid [m s-1]

460 Vdot_scale_IS(scale,k_man,step) volumetric flowrate within flow network sca»
le [cm3 h-1]

461 L_scale_IS(scale,k_man,step) length of elements in each scale and phase [m]

462 W_scale_IS(scale,k_man,step) width of elements in each scale and phase [m]

463 Sigma_Vdot_IS(scale,k_man,step) sum of volume flow rate for DP calculations»
in manifolds [cm3 h-1]

464 C_aq_IS(j,h,comp,step) concentrations in aq phase [mol m-3]

465 C_org_IS(j,h,comp,step) concentrations in org phase [mol m-3]

466 C_aq_eq_IS(j,h,comp,step) equilibrium comp concentrations aq phase [m»
ol m-3]

467 C_org_eq_IS(j,h,comp,step) equilibrium comp concentrations org phase [»
mol m-3]

468 m_IS(j,h,comp,step) distribution coefficients - C org over C aq

469 K_eq_IS(j,h,comp,step) equilibrium constant

470 C_aq_in_IS(j,h,comp,step) inlet aq concentration [mol m-3]

471 C_org_in_IS(j,h,comp,step) inlet org concentration [mol m-3]

472 DP_IS(scale,k_man,step) total pressure drop in each scale [kPa]

473 DP_fr_IS(scale,k_man,step) frictional pressure drop in each scale [kPa»
]

474 DP_sin_IS(scale,k_man,step) singularities pressure drop in each scale [»
kPa]

475 R_sin_IS(scale,k_man,step) singularities hydraulic resistances in each»
scale and phase [Pa s m-3]

476 R_IS(scale,k_man,step) hydraulic resistances in each scale and pha»
se [Pa s m-3]

477 R_ratio_IS(scale,k_man,step) resistance ratio

478 R_eq_IS(scale,k_man,step) equivalent hydraulic resistances in each s»
cale and phase [Pa s m-3]

479 Fd_IS(scale,k_man,step) flow maldistribution in each scale

480 Fdtot_IS(k_man,step) total flow maldistribution

481 L_scale_min_IS(scale,k_man,step) minimum length of elements in each scale an»
d phase [m]

482 Kla_IS(j,step) overall volumetric mass transfer coefficien»
t [m s-1]

483 q_corr_IS(j,step) correction factor to include the flow ratio»
effect on Kla - from Tsaoulidis experimental data

484 q_IS(j,step) flow ratio aq over org phase

485 DP_sep_IS(sep,step) frictional pressure drop in the separator [»
kPa]

486 D_IS(step) channel diameter [m]

487 L_IS(step) channel length [m]

488 D_sep_IS(sep,step) separator diameter [m]

489 L_sep_IS(sep,step) separator length [m]

490 DP_Ch_Y_IS(step) total pressure drop within channel + at Y j»
unction [kPa]

491 DP_fr_Ch_IS(i,step) frictional pressure drop within channel [kP»
a]

492 DP_int_IS(step) interfacial pressure drop within channel [k»
Pa]
493 DP_Y_IS(step) local pressure drop at Y junction [kPa]
494 const_mass_tr_IS(step) coefficient for mass transfer calc - Kashid»
eq
495 Vdot_sep_IS(sep,step) volume flow rate within separator [cm3 hr-1»
]
496 vel_scale_IS(scale,k_man,step) superficial velocity in each scale [m s-1]
497 D_Tc0_IS(j,h,step) coeffcient for Tc distribution coeff calcul»
ation - Tc conc dependence
498 D_U_IS(j,h,step) coeffcient for Tc distribution coeff calcul»
ation - U conc dependence
499 D_Pu_IS(j,h,step) coeffcient for Tc distribution coeff calcul»
ation - Pu conc dependence
500 D_Zr_IS(j,h,step) coeffcient for Tc distribution coeff calcul»
ation - Zr conc dependence
501 A_Scheiff_IS coeff for separator calcuation
502 H_org_IS(j,h,step) H+ cations in organic phase - Vladimirova et al [mol»
m-3] - for TBP degradation
503 phi_IS(j,step) aqueous phase holdup
504
505 ;
506
507
508 *starting points and bounds
509 F.l=0.3;
510 F.up=0.9;
511 F.lo=0.1;
512 L_IS.lo(step)=L;
513 a_Fd.l(scale,k_man,step)=.001;
514 a_Fd.up(scale,k_man,step)=.5;
515 b_Fd.l(scale,k_man,step)=.03;
516 b_Fd.up(scale,k_man,step)=1;

```
517 b_Fd.up('1',k_man,step)=9e9;
518 C_aq_IS.up(j,h,'Np_V',step)=50;
519 C_aq_IS.up(j,h,'Np_VI',step)=50;
520 C_aq_IS.up(j,h,'HNO2',step)=50;
521 phi_IS.up(j,step)=1;
522 phi_IS.l(j,step)=.25;
523 C_NO3_IS.l(j,h,step)=5000;
524 Fdtot_IS.up(k_man,step)=10;
525 A_Scheiff_IS.up(step)=10;
526 DP_fr_IS.up(scale,k_man,step)=100;
527 DP_sin_IS.up(scale,k_man,step)=100;
528 vel_scale_IS.lo(scale,k_man,step)=1e-5 ;
529 DP_fr_IS.up(scale,k_man,step)=10;
530 DP_sin_IS.up(scale,k_man,step)=1;
531 R_IS.lo(scale,k_man,step)=0;
532 R_IS.up(scale,k_man,step)=1e8;
533 R_eq_IS.lo(scale,k_man,step)=0;
534 R_eq_IS.up(scale,k_man,step)=1e8;
535 Fd_IS.lo(scale,k_man,step)=0;
536 Fd_IS.up(scale,k_man,step)=10;
537 L_scale_IS.up('1',k_man,step)=.3;
538 L_scale_IS.up('2',k_man,step)=1;
539 L_scale_IS.up('3',k_man,step)=3;
540 L_scale_IS.up('4',k_man,step)=6;
541 W_scale_IS.lo(scale,k_man,step)=1e-3;
542 W_scale_IS.up(scale,k_man,step)=10;
543 W_scale_IS.up('1',k_man,step)=.003;
544 W_scale_IS.up('2',k_man,step)=.05;
545 W_scale_IS.up('3',k_man,step)=.5;
546 W_scale_IS.up('4',k_man,step)=5;
547 R_ratio_IS.lo(scale,k_man,step)=2500;
548 R_ratio_IS.up(scale,k_man,step)=18000;
549 R_ratio_IS.lo('1',k_man,step)=1;
```

550 R_ratio_IS.L('1',k_man,step)=1;

551 R_ratio_IS.up('1',k_man,step)=1;

552 a_IS.up(j,step)=100;

553 q_corr_IS.lo(j,step)=.3;

554 q_corr_IS.up(j,step)=1.6;

555 *bounds achieved using [HNO3]=5 M, 30556 K_eq_IS.up(j,h,'U_VI',step)=100000;

557 K_eq_IS.up(j,h,'Pu_IV',step)=100000;

558 K_eq_IS.up(j,h,'HNO3',step)=10;

559 K_eq_IS.up(j,h,'HNO3_2',step)=10;

560 K_eq_IS.l(j,h,'Zr',step)=45;

561 K_eq_IS.l(j,h,'Ru',step)=3.5;

562 m_IS.up(j,h,comp,step)=50;

563 m_IS.up(j,h,'U_VI',step)=50;

564 m_IS.up(j,h,'Pu_IV',step)=50;

565 m_IS.up(j,h,'HNO3',step)=1;

566 m_IS.up(j,h,'HNO3_2',step)=1;

567 m_IS.l(j,h,'Zr',step)=.2;

568 m_IS.l(j,h,'Ru',step)=.01;

569 m_IS.l(j,h,'Tc',step)=1.53;

570 D_Tc0_IS.l(j,h,step)= 1.28E-04;

571 D_U_IS.l(j,h,step)=0.180542862;

572 D_Pu_IS.l(j,h,step)= 4.8638E-05;

573 D_Zr_IS.l(j,h,step)=1.34490002;

574 I_S_IS.up(j,h,step)=C0_aq('HNO3','U_strip')*2/1000;

575 I_S_IS.lo(j,h,step)=1e-3;

576 I_S_IS.l(j,h,step)=(C0_aq('HNO3','U_strip')+C0_aq('U_VI','U_strip'))/1000;

577 keff_IS.up(step)=1;

578 buck_IS.up(step)=10;

579 L_discr.up(h)=0.5;

580 q_IS.lo(j,step)=.2;

581 q_IS.up(j,step)=3;

582 vel_IS.lo(j,'aq',step)=0.001;

583 vel_IS.lo(j,'org',step)=0.001;

584 vel_IS.lo(j,'mix',step)=.01;
585 vel_IS.up(j,k,step)=0.06;
586 Vdot_IS.lo(j,k,step)=15;
587 Vdot_IS.up(j,k,step)=500;
588 E_IS.up(comp,step)=100;
589 kla_IS.lo(j,step)=.1;
590 Kla_IS.up(j,step)=.4;
591 const_mass_tr_IS.lo(step)=1e-8;
592 const_mass_tr_IS.up(step)=1e-5;
593 C_org_eq_IS.up(j,h,comp,step)=F0*rho_TBP/MW_TBP*1000*1.1;
594 C_org_eq_IS.up(j,h,'TBP',step)=F0*rho_TBP/MW_TBP*1000;
595 C_aq_eq_IS.up(j,h,'U_VI',step)=C0_aq('U_VI','U_strip')*2;
596 C_aq_eq_IS.up(j,h,'Pu_IV',step)=C0_aq('Pu_IV','U_strip')*2;
597 C_aq_eq_IS.up(j,h,'HNO3',step)=C0_aq('HNO3','U_strip')*2;
598 C_aq_eq_IS.up(j,h,'HNO3_2',step)=0;
599 C_aq_eq_IS.up(j,h,'TBP',step)=0;
600 C_aq_IS.up(j,h,'U_VI',step)=C0_aq('U_VI','U_strip')*2;
601 C_aq_IS.up(j,h,'U_IV',step)=C0_aq('U_IV','U_strip')*2;
602 C_aq_IS.up(j,h,'Pu_IV',step)=C0_aq('Pu_IV','U_strip')*2;
603 C_aq_IS.up(j,h,'Pu_III',step)=C0_aq('Pu_IV','U_strip')*2;
604 C_aq_IS.up(j,h,'HNO3',step)=C0_aq('HNO3','U_strip')*2;
605 C_aq_IS.up(j,h,'HNO3_2',step)=0;
606 C_aq_IS.up(j,h,'TBP',step)=0;
607 C_org_IS.up(j,h,comp,step)=F0*rho_TBP/MW_TBP*500*1.2;
608 C_org_IS.up(j,h,'TBP',step)=F0*rho_TBP/MW_TBP*1000;
609 C_org_in_IS.up(j,h,comp,step)=F0*rho_TBP/MW_TBP*500*1.2;
610 C_org_in_IS.up(j,h,'TBP',step)=F0*rho_TBP/MW_TBP*1000;
611 DP_IS.up(scale,K_man,step)=10;
612 R_ratio_IS.lo('4',k_man,step)=0;
613 R_ratio_IS.up('4',k_man,step)=1e8;
614 vel_scale_IS.up(scale,k_man,step)=.1;
615 L_scale_IS.up('2',k_man,step)=.6;
616 L_scale_IS.up('3',k_man,step)=2;

```
617 L_scale_IS.up('4',k_man,step)=1;
618 W_scale_IS.up('2',k_man,step)=.3;
619 W_scale_IS.up('3',k_man,step)=1;
620 W_scale_IS.up('4',k_man,step)=1;
621 vel_scale_IS.up('4',k_man,step)=1;
622 Re_IS.up(scale,k_man,step)=2000;
623 R_IS.up('3',k_man,step)=1000;
624 R_IS.up('4',k_man,step)=100;
625 W_scale_IS.lo('4',k_man,step)=0;
626 vel_scale_IS.lo('4',k_man,step)=0;
627 D_sep_IS.lo(sep,step)=.0005;
628 D_sep_IS.up(sep,step)=.002;
629 L_sep_IS.lo(sep,step)=.01;
630 L_sep_IS.up(sep,step)=.5;
631
632 Variables
633 obj objective function
634 log_Kla_IS(j,step)
635 extr_Pu(j,h)
636 C_Pu_III(j,h)
637 k0_IS(j,h,comp,step)
638 k1_IS(j,h,comp,step)
639 k2_IS(j,h,comp,step)
640 k3_IS(j,h,comp,step)
641 k0_r_IS(k_man,j,h,comp,step)
642 k1_r_IS(k_man,j,h,comp,step)
643 k2_r_IS(k_man,j,h,comp,step)
644 k3_r_IS(k_man,j,h,comp,step)
645 k0_red_IS(k_man,j,h,comp,red,step)
646 k1_red_IS(k_man,j,h,comp,red,step)
647 k2_red_IS(k_man,j,h,comp,red,step)
648 k3_red_IS(k_man,j,h,comp,red,step)
649 Reac_IS(k_man,j,h,comp,step)
```

650 Extr_IS(j,h,comp,step)

651 Reac_red_IS(k_man,j,h,comp,red,step)

652 ;

653

654 Reac_red_IS.l(k_man,j,h,comp,red,step)=.1;

655 k0_red_IS.up(k_man,j,h,comp,red,step)=1e5;

656 k1_red_IS.up(k_man,j,h,comp,red,step)=1e5;

657 k2_red_IS.up(k_man,j,h,comp,red,step)=1e5;

658 k3_red_IS.up(k_man,j,h,comp,red,step)=1e5;

659 D_IS.lo(step)=0.0005;

660 D_IS.up(step)=2.5e-3;

661 log_kla_IS.lo(j,step)=-1.3;

662 log_kla_IS.up(j,step)=.3;

663 R_IS.l('2',k_man,step)= 822.47895203874;

664 q_IS.l(j,step)= 0.455632867283152;

665 vel_IS.l(j,'mix',step)= 0.0177560483551909;

666 W_scale_IS.l('2','aq',step)= 0.0096667425416197;

667 W_scale_IS.l('2','org',step)= 0.0111969123431518 ;

668 W_scale_IS.l('3','aq',step)= 0.0270129274510062;

669 W_scale_IS.l('3','org',step)= 0.0393239611901497;

670 W_scale_IS.l('4','aq',step)= 0.0329378671227223 ;

671 W_scale_IS.l('4','org',step)= 0.0478093311395163;

672 L_scale_IS.l('2','aq',step)= 0.252;

673 L_scale_IS.l('2','org',step)= 0.252;

674 L_scale_IS.l('3','aq',step)= 1.16000910499436;

675 L_scale_IS.l('3','org',step)= 1.34362948117821;

676 L_scale_IS.l('4','aq',step)= 0.0810387823530185 ;

677 L_scale_IS.l('4','org',step)= 0.117971883570449;

678

679

680

681 Positive variable

682 C_in_HNO3_stage(j,comp,step) HNO3 concentration in the interstage streams

683 C_in(k2,comp,step) Inlet concentration in the step

684 C_out(k2,comp,step) Outlet concentration from the step

685 Vdot_IS2(j,k2,step) volume flow rate [L h-1]

686 units2(step) number of parallel small extractors required

687 V_fresh(k2,step) volume flow rate of new streams [L h-1]

688 ;

689

690

691

692 Equation

693 Eq_vel1_IS(j,step)

694 Eq_vel2_IS(j,step)

695 Eq_vel3_IS(j,step)

696 Eq_flowrate1_IS(j,step)

697 Eq_flowrate3_IS(j,step)

698 Eq_L_discr(h)

699 Eq_m_U_IS(j,h,step)

700 Eq_m_Pu_IS(j,h,step)

701 Eq_m_H1_IS(j,h,step)

702 Eq_m_H2_IS(j,h,step)

703 Eq_K_U_Rich_IS(j,h,step)

704 Eq_K_Pu_Rich_IS(j,h,step)

705 Eq_K_H1_Rich_IS(j,h,step)

706 Eq_K_H2_Rich_IS(j,h,step)

707 Eq_m_Zr_IS(j,h,step)

708 Eq_K_Zr_IS(j,h,step)

709 Eq_m_Ru_IS(j,h,step)

710 Eq_K_Ru_IS(j,h,step)

711 Eq_D_Tc0_IS(j,h,step)

712 Eq_D_U_IS(j,h,step)

713 Eq_D_Zr_IS(j,h,step)

714 Eq_D_Pu_IS(j,h,step)

715 Eq_m_Tc_IS(j,h,step)

716 Eq_k0_r_Np_V(j,h,step)

717 Eq_k1_r_Np_V(j,h,step)

718 Eq_k2_r_Np_V(j,h,step)

719 Eq_k3_r_Np_V(j,h,step)

720 Eq_m_Np_V_IS(j,h,step)

721 Eq_m_Np_VI_IS(j,h,step)

722 Eq_r_forw_Np_V_RK1(j,h,step)

723 Eq_r_back_Np_V_RK1(j,h,step)

724 Eq_r_forw_Np_V_RK2(j,h,step)

725 Eq_r_back_Np_V_RK2(j,h,step)

726 Eq_m_HNO2_IS(j,h,step)

727 Eq_Reac_Np_IS(j,h,step)

728 Eq_Reac_Np_org_IS(j,h,step)

729 Eq_k0_r_org_Np_V(j,h,step)

730 Eq_k1_r_org_Np_V(j,h,step)

731 Eq_k2_r_org_Np_V(j,h,step)

732 Eq_k3_r_org_Np_V(j,h,step)

733 Eq_hydrol_org_IS(j,h,step)

734 Eq_hydrol_IS(j,h,step)

735 Eq_protons_org_IS(j,h,step)

736 Eq_k0_r_TBP(j,h,step)

737 Eq_k1_r_TBP(j,h,step)

738 Eq_k2_r_TBP(j,h,step)

739 Eq_k3_r_TBP(j,h,step)

740 Eq_C_DBP_IS(j,h,step)

741 Eq_C_DBP_in_IS(j,h,step)

742 Eq_m_Np_IV_IS(j,h,step)

743 Eq_Reac_Np_IV_IS(j,h,step)

744 Eq_k0_r_aq_Np_IV(j,h,step)

745 Eq_k1_r_aq_Np_IV(j,h,step)

746 Eq_k2_r_aq_Np_IV(j,h,step)

747 Eq_k3_r_aq_Np_IV(j,h,step)

748 Eq_m_U_IV_IS(j,h,step)

749 Eq_m_Pu_III_IS(j,h,step)
750 Eq_Reac_Pu_ox_IS(j,h,step)
751 Eq_k0_r_aq_Pu_ox(j,h,step)
752 Eq_k1_r_aq_Pu_ox(j,h,step)
753 Eq_k2_r_aq_Pu_ox(j,h,step)
754 Eq_k3_r_aq_Pu_ox(j,h,step)
755 Eq_Reac_U_ox_aq_IS(j,h,step)
756 Eq_k0_r_aq_U_ox(j,h,step)
757 Eq_k1_r_aq_U_ox(j,h,step)
758 Eq_k2_r_aq_U_ox(j,h,step)
759 Eq_k3_r_aq_U_ox(j,h,step)
760 Eq_Reac_NO2_scav_IS(j,h,step)
761 Eq_k0_r_aq_N2H5(j,h,step)
762 Eq_k1_r_aq_N2H5(j,h,step)
763 Eq_k2_r_aq_N2H5(j,h,step)
764 Eq_k3_r_aq_N2H5(j,h,step)
765 Eq_Reac_Pu_N2H5_IS(j,h,step)
766 Eq_k0_r_aq_Pu_N2H5(j,h,step)
767 Eq_k1_r_aq_Pu_N2H5(j,h,step)
768 Eq_k2_r_aq_Pu_N2H5(j,h,step)
769 Eq_k3_r_aq_Pu_N2H5(j,h,step)
770 Eq_Reac_Np_VI_red_N2H5_IS(j,h,step)
771 Eq_k0_r_aq_Np_VI_red_N2H5(j,h,step)
772 Eq_k1_r_aq_Np_VI_red_N2H5(j,h,step)
773 Eq_k2_r_aq_Np_VI_red_N2H5(j,h,step)
774 Eq_k3_r_aq_Np_VI_red_N2H5(j,h,step)
775 Eq_Reac_Pu_U_aq_IS(j,h,step)
776 Eq_k0_red_Pu_U_aq(j,h,step)
777 Eq_k1_red_Pu_U_aq(j,h,step)
778 Eq_k2_red_Pu_U_aq(j,h,step)
779 Eq_k3_red_Pu_U_aq(j,h,step)
780 Eq_Reac_Pu_U_org_IS(j,h,step)
781 Eq_k0_red_Pu_U_org(j,h,step)

191

782 Eq_k1_red_Pu_U_org(j,h,step)

783 Eq_k2_red_Pu_U_org(j,h,step)

784 Eq_k3_red_Pu_U_org(j,h,step)

785 Eq_Reac_NpVI_U_aq_IS(j,h,step)

786 Eq_k0_red_NpVI_U_aq(j,h,step)

787 Eq_k1_red_NpVI_U_aq(j,h,step)

788 Eq_k2_red_NpVI_U_aq(j,h,step)

789 Eq_k3_red_NpVI_U_aq(j,h,step)

790 Eq_Reac_NpV_U_aq_IS(j,h,step)

791 Eq_k0_red_NpV_U_aq(j,h,step)

792 Eq_k1_red_NpV_U_aq(j,h,step)

793 Eq_k2_red_NpV_U_aq(j,h,step)

794 Eq_k3_red_NpV_U_aq(j,h,step)

795 Eq_I_S_IS(j,h,step)

796 Eq_C_NO3_IS(j,h,step)

797 Eq_C_aq_in_IS(j,h,comp,step)

798 Eq_C_org_in_IS(j,h,comp,step)

799 Eq_C_aq_in_IS(j,h,comp,step)

800 Eq_C_org_in_IS(j,h,comp,step)

801 Eq_a_IS(j,step)

802 Eq_b_IS(j,h,comp,step)

803 Eq_C_aq_U_IS(j,h,step)

804 Eq_C_aq_Pu_IS(j,h,step)

805 Eq_C_aq_HNO3_IS(j,h,step)

806 Eq_C_aq_HNO3_2_IS(j,h,step)

807 Eq_C_aq_TBP_IS(j,h,step)

808 Eq_C_aq_Zr_IS(j,h,step)

809 Eq_C_aq_Ru_IS(j,h,step)

810 Eq_C_aq_Tc_IS(j,h,step)

811 Eq_C_aq_Np_V_IS(j,h,step)

812 Eq_C_aq_Np_VI_IS(j,h,step)

813 Eq_C_aq_Np_IV_IS(j,h,step)

814 Eq_C_aq_HNO2_IS(j,h,step)

815 Eq_C_aq_Pu_III_IS(j,h,step)

816 Eq_C_aq_U_IV_IS(j,h,step)

817 Eq_C_aq_N2H5_IS(j,h,step)

818 Eq_C_aq_HAN_IS(j,h,step,step)

819 Eq_C_org_U_IS(j,h,step)

820 Eq_C_org_Pu_IS(j,h,step)

821 Eq_C_org_HNO3_IS(j,h,step)

822 Eq_C_org_HNO3_2_IS(j,h,step)

823 Eq_C_org_Zr_IS(j,h,step)

824 Eq_C_org_Ru_IS(j,h,step)

825 Eq_C_org_Tc_IS(j,h,step)

826 Eq_C_org_Np_V_IS(j,h,step)

827 Eq_C_org_Np_IV_IS(j,h,step)

828 Eq_C_org_Np_VI_IS(j,h,step)

829 Eq_C_org_HNO2_IS(j,h,step)

830 Eq_C_org_Pu_III_IS(j,h,step)

831 Eq_C_org_U_IV_IS(j,h,step)

832 Eq_C_org_TBP_IS(j,h,step)

833 Eq_Kla_IS(j,step)

834 Eq_k0_2(j,h,comp,step)

835 Eq_k1_2(j,h,comp,step)

836 Eq_k2_2(j,h,comp,step)

837 Eq_k3_2(j,h,comp,step)

838 Eq_mass_Eq_aq_IS(j,h,comp,step)

839 Eq_mass_Eq_org_IS(j,h,comp,step)

840 Eq_E_U_IS(step)

841 Eq_E_Pu_IS(step)

842 Eq_E_HNO3_IS(step)

843 Eq_E_Zr_IS(step)

844 Eq_E_Ru_IS(step)

845 Eq_E_Tc_IS(step)

846 Eq_E_HNO2_IS(step)

847 Eq_E_Np_IS(step)

848 eq_phi_IS(j,step)

849 Eq_Extr_IS(j,h,comp,step)

850 Eq_q_corr(j,step)

851 Eq_Reac_U_ox_org_IS(j,h,step)

852 Eq_k0_r_org_U_ox(j,h,step)

853 Eq_k1_r_orgU_ox(j,h,step)

854 Eq_k2_r_org_U_ox(j,h,step)

855 Eq_k3_r_org_U_ox(j,h,step)

856 Eq_C_org_N2H5_IS(j,h,step)

857 Eq_C_org_HAN_IS(j,h,step,step)

858 eq_N(step)

859

860 ;

861

862 eq_N(step)..N_IS(step)=e=sum(j,z(j,step))*z_step_IS(step);

863 eq_phi_IS(j,step)..phi_IS(j,step)=e=((q_IS(j,step)/(1+q_IS(j,step)))*z_disp(s»
tep)+ (1-z_disp(step))*(1-(q_IS(j,step)/(1+q_IS(j,step)))*z_disp(step)))*z_s»
tep_IS(step);

864 Eq_q_corr(j,step)..q_corr_IS(j,step)=e=((-0.511*log(q_IS(j,step))+0.9702)*z_d»
isp(step)+(1-z_disp(step))*((-0.511*log(1/q_IS(j,step))+0.9702)));

865

866 *concentrations from mass balance

867 Eq_C_aq_U_IS(j,h,step)..C_aq_IS(j,h,'U_VI',step)=e=(C_aq_in_IS(j,h,'U_VI',ste»
p)+interv/6*(k0_IS(j,h,'U_VI',step)+2*k1_IS(j,h,'U_VI',step)+2*k2_IS(j,h,'U_V»
I',step)+k3_IS(j,h,'U_VI',step))+Reac_IS('aq',j,h,'U_IV',step)+0.5*Reac_red_I»
S('aq',j,h,'Pu_IV','U_IV',step)+0.5*Reac_red_IS('aq',j,h,'Np_VI','U_IV',step)»
+0.5*Reac_red_IS('aq',j,h,'Np_V','U_IV',step))*z_step_IS(step);

868 Eq_C_aq_Pu_IS(j,h,step)..C_aq_IS(j,h,'Pu_IV',step)=e=(C_aq_in_IS(j,h,'Pu_IV',»
step)+interv/6*(k0_IS(j,h,'Pu_IV',step)+2*k1_IS(j,h,'Pu_IV',step)+2*k2_IS(j,h»
,'Pu_IV',step)+k3_IS(j,h,'Pu_IV',step)) +Reac_IS('aq',j,h,'Pu_III',step)-Rea»
c_IS('aq',j,h,'Pu_IV',step)-Reac_red_IS('aq',j,h,'Pu_IV','U_IV',step))*z_s»
tep_IS(step);

869 Eq_C_aq_HNO3_IS(j,h,step)..C_aq_IS(j,h,'HNO3',step)=e=(C_aq_in_IS(j,h,'HNO3',»

step)+interv/6*(k0_IS(j,h,'HNO3',step)+2*k1_IS(j,h,'HNO3',step)+2*k2_IS(j,h,'»
HNO3',step)+k3_IS(j,h,'HNO3',step))-4*Reac_IS('aq',j,h,'Np_IV',step)+1.5*Reac»
_IS('aq',j,h,'Np_V',step)+Reac_IS('aq',j,h,'N2H5',step)-4*Reac_IS('aq',j,h,'N»
p_IV',step)+Reac_IS('aq',j,h,'Pu_IV',step)+Reac_IS('aq',j,h,'Np_VI',step)+2*R»
eac_red_IS('aq',j,h,'Pu_IV','U_IV',step)+2*Reac_red_IS('aq',j,h,'Np_VI','U_IV»
',step)-2*Reac_red_IS('aq',j,h,'Np_V','U_IV',step))*z_step_IS(step);
870 Eq_C_aq_HNO3_2_IS(j,h,step)..C_aq_IS(j,h,'HNO3_2',step)=e=0;
871 Eq_C_aq_TBP_IS(j,h,step)..C_aq_IS(j,h,'TBP',step)=e=0;
872 Eq_C_aq_Zr_IS(j,h,step)..C_aq_IS(j,h,'Zr',step)=e=(C_aq_in_IS(j,h,'Zr',step)+»
interv/6*(k0_IS(j,h,'Zr',step)+2*k1_IS(j,h,'Zr',step)+2*k2_IS(j,h,'Zr',step)+»
k3_IS(j,h,'Zr',step)))*z_step_IS(step)*z_step_zr(step);
873 Eq_C_aq_Ru_IS(j,h,step)..C_aq_IS(j,h,'Ru',step)=e=(C_aq_in_IS(j,h,'Ru',step)+»
interv/6*(k0_IS(j,h,'Ru',step)+2*k1_IS(j,h,'Ru',step)+2*k2_IS(j,h,'Ru',step)+»
k3_IS(j,h,'Ru',step)))*z_step_IS(step)*z_step_ru(step);
874 Eq_C_aq_Tc_IS(j,h,step)..C_aq_IS(j,h,'Tc',step)=e=(C_aq_in_IS(j,h,'Tc',step)+»
interv/6*(k0_IS(j,h,'Tc',step)+2*k1_IS(j,h,'Tc',step)+2*k2_IS(j,h,'Tc',step)+»
k3_IS(j,h,'Tc',step)))*z_step_IS(step);
875 Eq_C_aq_Np_V_IS(j,h,step)..C_aq_IS(j,h,'Np_V',step)=e=(C_aq_in_IS(j,h,'Np_V',»
step)+Reac_IS('aq',j,h,'Np_V',step)+Extr_IS(j,h,'Np_V',step)-2*Reac_IS('aq',j»
,h,'Np_IV',step)+Reac_IS('aq',j,h,'Np_VI',step)+Reac_red_IS('aq',j,h,'Np_VI',»
'U_IV',step)-Reac_red_IS('aq',j,h,'Np_V','U_IV',step))*z_step_IS(step)*z_step»
_NpV(step);
876 Eq_C_aq_Np_VI_IS(j,h,step)..C_aq_IS(j,h,'Np_VI',step)=e=(C_aq_in_IS(j,h,'Np_V»
I',step)+Extr_IS(j,h,'Np_VI',step)+Reac_IS('aq',j,h,'Np_IV',step)-Reac_IS('aq»
',j,h,'Np_V',step)-Reac_IS('aq',j,h,'Np_VI',step)-Reac_red_IS('aq',j,h,'Np_VI»
','U_IV',step) +Reac_red_IS('aq',j,h,'Np_V','U_IV',step))*z_step_IS(step)*z_s»
tep_NpVI(step);
877 Eq_C_aq_Np_IV_IS(j,h,step)..C_aq_IS(j,h,'Np_IV',step)=e=0;
878 *(C_aq_in_IS(j,h,'Np_IV',step)+Reac_IS('aq',j,h,'Np_IV',step)+Extr_IS(j,h,'Np»
_IV',step)+Reac_red_IS('aq',j,h,'Np_V','U_IV',step))*z_step_IS(step)*z_step_N»
pIV(step);
879 Eq_C_aq_HNO2_IS(j,h,step)..C_aq_IS(j,h,'HNO2',step)=e=C_aq_in_IS(j,h,'HNO2',s»
tep)+interv/6*(k0_IS(j,h,'HNO2',step)+2*k1_IS(j,h,'HNO2',step)+2*k2_IS(j,h,'H»

195

NO2',step)+k3_IS(j,h,'HNO2',step))-0.5*Reac_IS('aq',j,h,'Np_V',step)-Reac_iS(»
'aq',j,h,'N2H5',step);

880 Eq_C_aq_Pu_III_IS(j,h,step)..C_aq_IS(j,h,'Pu_III',step)=e=(C_aq_in_IS(j,h,'Pu»
_III',step)+interv/6*(k0_IS(j,h,'Pu_III',step)+2*k1_IS(j,h,'Pu_III',step)+2*k»
2_IS(j,h,'Pu_III',step)+k3_IS(j,h,'Pu_III',step)) -Reac_IS('aq',j,h,'Pu_III',»
step)+Reac_IS('aq',j,h,'Pu_IV',step)+Reac_red_IS('aq',j,h,'Pu_IV','U_IV',step»
))*z_step_IS(step);

881 Eq_C_aq_U_IV_IS(j,h,step)..C_aq_IS(j,h,'U_IV',step)=e=(C_aq_in_IS(j,h,'U_IV',»
step)+interv/6*(k0_IS(j,h,'U_IV',step)+2*k1_IS(j,h,'U_IV',step)+2*k2_IS(j,h,'»
U_IV',step)+k3_IS(j,h,'U_IV',step)) -Reac_IS('aq',j,h,'U_IV',step)-0.5*Reac_r»
ed_IS('aq',j,h,'Pu_IV','U_IV',step)-0.5*Reac_red_IS('aq',j,h,'Np_VI','U_IV',s»
tep))*z_step_IS(step);

882 Eq_C_aq_N2H5_IS(j,h,step)..C_aq_IS(j,h,'N2H5',step)=e=(C_aq_in_IS(j,h,'N2H5',»
step)-Reac_IS('aq',j,h,'N2H5',step)-Reac_IS('aq',j,h,'Pu_IV',step)-Reac_IS('a»
q',j,h,'Np_VI',step))*z_step_IS(step);

883 Eq_C_aq_HAN_IS(j,h,step,step)..C_aq_IS(j,h,'HAN',step)=e=0;

884 *(C_aq_in_IS(j,h,'HAN',step) -Reac_red_IS('aq',j,h,'Pu_IV','HAN',step))*z_s»
tep_IS(step);

885 *-Reac_red_IS('aq',j,h,'HNO2','HAN',step)-Reac_red_IS('aq',j,h,'Np_VI','HAN',»
step);

886 Eq_C_org_U_IS(j,h,step)..C_org_IS(j,h,'U_VI',step)=e=(C_org_in_IS(j,h,'U_VI',»
step)-q_IS(j,step)*interv/6*(k0_IS(j,h,'U_VI',step)+2*k1_IS(j,h,'U_VI',step)+»
2*k2_IS(j,h,'U_VI',step)+k3_IS(j,h,'U_VI',step)) +0.5*Reac_red_IS('org',j,h,'»
Pu_IV','U_IV',step)+Reac_IS('org',j,h,'U_IV',step))*z_step_IS(step);

887 Eq_C_org_Pu_IS(j,h,step)..C_org_IS(j,h,'Pu_IV',step)=e=(C_org_in_IS(j,h,'Pu_I»
V',step)-q_IS(j,step)*interv/6*(k0_IS(j,h,'Pu_IV',step)+2*k1_IS(j,h,'Pu_IV',s»
tep)+2*k2_IS(j,h,'Pu_IV',step)+k3_IS(j,h,'Pu_IV',step)) -Reac_red_IS('org',j,»
h,'Pu_IV','U_IV',step)-Reac_red_IS('org',j,h,'Pu_IV','U_IV',step))*z_step_IS(»
step);

888 Eq_C_org_HNO3_IS(j,h,step)..C_org_IS(j,h,'HNO3',step)+C_org_IS(j,h,'HNO3_2',s»
tep)=e=(C_org_in_IS(j,h,'HNO3',step)+C_org_in_IS(j,h,'HNO3_2',step)-q_IS(j,st»
ep)*interv/6*(k0_IS(j,h,'HNO3',step)+2*k1_IS(j,h,'HNO3',step)+2*k2_IS(j,h,'HN»
O3',step)+k3_IS(j,h,'HNO3',step)) +1.5*Reac_IS('org',j,h,'Np_V',step) + 2*R»

196

eac_red_IS('org',j,h,'Pu_IV','U_IV',step)-Reac_IS('org',j,h,'U_IV',step))*z_s»
tep_IS(step);
889 Eq_C_org_HNO3_2_IS(j,h,step)..C_org_IS(j,h,'HNO3_2',step)=e=((C_org_in_IS(j,h»
,'HNO3_2',step)+interv/6*(k0_IS(j,h,'HNO3_2',step)+2*k1_IS(j,h,'HNO3_2',step)»
+2*k2_IS(j,h,'HNO3_2',step)+k3_IS(j,h,'HNO3_2',step)))))*z_step_IS(step);
890 Eq_C_org_Zr_IS(j,h,step)..C_org_IS(j,h,'Zr',step)=e=(C_org_in_IS(j,'1','Zr',s»
tep)+q_IS(j,step)*(C_aq_in_IS(j,'1','Zr',step)-C_aq_IS(j,h,'Zr',step)))*z_ste»
p_IS(step)*z_step_zr(step);
891 Eq_C_org_Ru_IS(j,h,step)..C_org_IS(j,h,'Ru',step)=e=(C_org_in_IS(j,'1','Ru',s»
tep)+q_IS(j,step)*(C_aq_in_IS(j,'1','Ru',step)-C_aq_IS(j,h,'Ru',step)))*z_ste»
p_IS(step)*z_step_ru(step);
892 Eq_C_org_Tc_IS(j,h,step)..C_org_IS(j,h,'Tc',step)=e=(C_org_in_IS(j,'1','Tc',s»
tep)+q_IS(j,step)*(C_aq_in_IS(j,'1','Tc',step)-C_aq_IS(j,h,'Tc',step)))*z_ste»
p_IS(step);
893 Eq_C_org_Np_V_IS(j,h,step)..C_org_IS(j,h,'Np_V',step)=e=C_org_in_IS(j,h,'Np_V»
',step)-q_IS(j,step)*(Extr_IS(j,h,'Np_V',step))+Reac_IS('org',j,h,'Np_V',step»
)*z_step_NpV(step);
894 Eq_C_org_Np_IV_IS(j,h,step)..C_org_IS(j,h,'Np_IV',step)=e=0;
895 *(C_org_in_IS(j,h,'Np_IV',step)-q_IS(j,step)*(Extr_IS(j,h,'Np_IV',step)))*z_s»
tep_IS(step)*z_step_NpIV(step);
896 Eq_C_org_Np_VI_IS(j,h,step)..C_org_IS(j,h,'Np_VI',step)=e=(C_org_in_IS(j,h,'N»
p_VI',step)-q_IS(j,step)*(Extr_IS(j,h,'Np_VI',step))-Reac_IS('org',j,h,'Np_V'»
,step))*z_step_IS(step)*z_step_NpIV(step);
897 Eq_C_org_HNO2_IS(j,h,step)..C_org_IS(j,h,'HNO2',step)=e=(C_org_in_IS(j,h,'HNO»
2',step)-q_IS(j,step)*(interv/6*(k0_IS(j,h,'HNO2',step)+2*k1_IS(j,h,'HNO2',st»
ep)+2*k2_IS(j,h,'HNO2',step)+k3_IS(j,h,'HNO2',step)))-0.5*Reac_IS('org',j,h,'»
Np_V',step)+Reac_IS('org',j,h,'U_IV',step))*z_step_IS(step);
898 Eq_C_org_Pu_III_IS(j,h,step)..C_org_IS(j,h,'Pu_III',step)=e=(C_org_in_IS(j,h,»
'Pu_III',step)-q_IS(j,step)*interv/6*(k0_IS(j,h,'Pu_III',step)+2*k1_IS(j,h,'P»
u_III',step)+2*k2_IS(j,h,'Pu_III',step)+k3_IS(j,h,'Pu_III',step)) +Reac_red_I»
S('org',j,h,'Pu_IV','U_IV',step))*z_step_IS(step);
899 Eq_C_org_U_IV_IS(j,h,step)..C_org_IS(j,h,'U_IV',step)=e=(C_org_in_IS(j,h,'U_I»
V',step)-q_IS(j,step)*(interv/6*(k0_IS(j,h,'U_IV',step)+2*k1_IS(j,h,'U_IV',st»

197

ep)+2*k2_IS(j,h,'U_IV',step)+k3_IS(j,h,'U_IV',step)))-0.5*Reac_red_IS('org',j»
,h,'Pu_IV','U_IV',step)-Reac_IS('org',j,h,'U_IV',step))*z_step_IS(step);
900 Eq_C_org_TBP_IS(j,h,step)..C_org_IS(j,h,'TBP',step)=e=(F*rho_TBP/MW_TBP*sf-
2*»
C_org_IS(j,h,'U_VI',step)-2*C_org_IS(j,h,'Pu_IV',step)-C_org_IS(j,h,'HNO3',st»
ep)-2*C_org_IS(j,h,'HNO3_2',step)-2*C_org_IS(j,h,'Zr',step)-2*C_org_IS(j,h,'R»
u',step)-3*C_org_IS(j,h,'Tc',step)-2*C_org_IS(j,h,'NP_VI',step)-2*C_org_IS(j,»
h,'HNO2',step)-4*C_org_IS(j,h,'U_IV',step)-3*C_org_IS(j,h,'Pu_III',step))*z_s»
tep_IS(step);
901 Eq_C_org_N2H5_IS(j,h,step)..C_org_IS(j,h,'N2H5',step)=e=0;
902 Eq_C_org_HAN_IS(j,h,step,step)..C_org_IS(j,h,'HAN',step)=e=0;
903 Eq_C_aq_in_IS(j,h,comp,step)..C_aq_in_IS(j,h,comp,step)=e=(z4(h)*C_in_HNO3_st»
age(j,comp,step)+(1-z4(h))*C_aq_IS(j,h-1,comp,step))*z_scrub_hno3(step)*(1-z_»
co_strip(step))+(z2(j)*z4(h)*C_in('aq',comp,step)+(1-z4(h))*C_aq_IS(j,h-1,com»
p,step)+z4(h)*(1-z2(j))*C_aq_IS(j-1,'50',comp,step))*(1-z_scrub_hno3(step))*(»
1-z_co_strip(step)) + (z2(j)*z4(h)*C_in('aq',comp,step)+(1-z4(h))*C_aq_IS(j»
,h-1,comp,step) +z4(h)*(1-z2(j))*(C_aq_IS(j-1,'50',comp,step)*(vdot_IS(j-1,»
'aq',step)+V_fresh_costrip(j-1,step)*z(j-1,step))+C_fresh_costrip(j,comp,step»
)*V_fresh_costrip(j,step)*z(j,step)) /(vdot_IS(j-1,'aq',step)+V_fresh_costrip»
(j-1,step)+V_fresh_costrip(j,step)*z(j,step)+1e-6))*(1-z_scrub_hno3(step))*z_»
co_strip(step);
904 Eq_C_org_in_IS(j,h,comp,step)..C_org_in_IS(j,h,comp,step)=e=(z3(j)*z4(h)*C_in»
('org',comp,step)+(1-z4(h))*C_org_IS(j,h-1,comp,step)+z4(h)*(1-z3(j))*C_org_I»
S(j+1,'50',comp,step))*z_step_IS(step);
905 Eq_C_NO3_IS(j,h,step)..C_NO3_IS(j,h,step)=e=((C_aq_in_IS(j,h,'HNO3',step)+2*C»
_aq_in_IS(j,h,'U_VI',step)+4*C_aq_in_IS(j,h,'Pu_IV',step) + 3*C_aq_in_IS(j,h,»
'Zr',step)+C_aq_in_IS(j,h,'Ru',step)+4*C_aq_in_IS(j,h,'U_IV',step)+3*C_aq_in_»
IS(j,h,'Pu_III',step)+C_aq_in_IS(j,h,'HAN',step)+C_aq_in_IS(j,h,'N2H5',step))»
*z_step_IS(step))*z_step_IS(step);
906
907 *reac rate mol/s/L for RK calculations - NpV-NpVI equilibrium Koltunov kine»
tic

908   Eq_r_forw_Np_V_RK1(j,h,step)..r_forw_Np_V_RK1(j,h,step)=e=
((K_Np_for1(step)*»
(C_aq_in_IS(j,h,'HNO3',step)/sf)**2*(C_NO3_IS(j,h,step)/sf)**.5)*z_step_IS(s»
tep))*z_step_IS(step);
909   Eq_r_forw_Np_V_RK2(j,h,step)..r_forw_Np_V_RK2(j,h,step)=e=
((K_Np_for2(step)*»
(C_aq_in_IS(j,h,'HNO3',step)/sf))*z_step_IS(step))*z_step_IS(step);
910   Eq_r_back_Np_V_RK1(j,h,step)..r_back_Np_V_RK1(j,h,step)=e=
((K_Np_rev1(step)*»
(C_aq_in_IS(j,h,'HNO3',step)/sf+1e-7)**(-1))*z_step_IS(step))*z_step_IS(ste»
p);
911 Eq_r_back_Np_V_RK2(j,h,step)..r_back_Np_V_RK2(j,h,step)=e=((K_Np_rev2(step)*
C_aq_in_IS(j,h,'HNO3',step)/sf+1e-7)**(-.5)*(C_NO3_IS(j,h,step)/sf+1e-7)**(-.»
5))*z_step_IS(step))*z_step_IS(step);
912
913 *TBP degradation product
914   Eq_C_DBP_IS(j,h,step)..C_DBP_IS(j,h,step)=e=((C_DBP_in_IS(j,h,step)-
Reac_IS('»
aq',j,h,'TBP',step))*z_step_IS(step))*z_step_IS(step);
915 Eq_C_DBP_in_IS(j,h,step)..C_DBP_in_IS(j,h,step)=e=((z3(j)*z4(h)*C0_DBP+(1-
z4(»
h))*C_DBP_IS(j,h-1,step)+z4(h)*(1-z3(j))*C_DBP_IS(j+1,'50',step))*z_step_IS(s»
tep))*z_step_IS(step);
916
917 *Pu(IV) reduction by U(IV) - aqueous phase
918 Eq_Reac_Pu_U_aq_IS(j,h,step)..Reac_red_IS('aq',j,h,'Pu_IV','U_IV',step)=e=(in»
terv/6*(k0_red_IS('aq',j,h,'Pu_IV','U_IV',step)+2*k1_red_IS('aq',j,h,'Pu_IV',»
'U_IV',step)+2*k2_red_IS('aq',j,h,'Pu_IV','U_IV',step)+k3_red_IS('aq',j,h,'Pu»
_IV','U_IV',step)))*z_step_IS(step)*z_reac_UIV(step)*z_reac_Pu_IV_ox(step);
919   Eq_k0_red_Pu_U_aq(j,h,step)..k0_red_IS('aq',j,h,'Pu_IV','U_IV',step)   *
(C_a»
q_in_IS(j,h,'HNO3',step)/sf +.05)**2=e=(K_Pu_red_U_aq(step)* (C_aq_in_IS»
(j,h,'Pu_IV',step)/sf) * (C_aq_in_IS(j,h,'U_IV',step)/sf)*sf*phi_»

IS(j,step)/vel_is(j,'aq',step)*z(j,step))*z_step_IS(step)*z_reac_UIV(step)*z_»
reac_Pu_IV_ox(step);

920   Eq_k1_red_Pu_U_aq(j,h,step)..k1_red_IS('aq',j,h,'Pu_IV','U_IV',step)   *
(C_aq»

_in_IS(j,h,'HNO3',step)/sf +.05)**2=e=(K_Pu_red_U_aq(step)* (C_aq_in_IS(»
j,h,'Pu_IV',step)/sf+interv/2*k0_red_IS('aq',j,h,'Pu_IV','U_IV',step)/sf) »

* (C_aq_in_IS(j,h,'U_IV',step)/sf)*sf*phi_IS(j,step)/vel_is(j,'aq',s»
tep)*z(j,step))*z_step_IS(step)*z_reac_UIV(step)*z_reac_Pu_IV_ox(step);

921   Eq_k2_red_Pu_U_aq(j,h,step)..k2_red_IS('aq',j,h,'Pu_IV','U_IV',step)   *
(C_aq»

_in_IS(j,h,'HNO3',step)/sf +.05)**2=e=(K_Pu_red_U_aq(step)* (C_aq_in_IS(»
j,h,'Pu_IV',step)/sf+interv/2*k1_red_IS('aq',j,h,'Pu_IV','U_IV',step)/sf) »

* (C_aq_in_IS(j,h,'U_IV',step)/sf)*sf*phi_IS(j,step)/vel_is(j,'aq',s»
tep)*z(j,step))*z_step_IS(step)*z_reac_UIV(step)*z_reac_Pu_IV_ox(step);

922   Eq_k3_red_Pu_U_aq(j,h,step)..k3_red_IS('aq',j,h,'Pu_IV','U_IV',step)   *
(C_aq»

_in_IS(j,h,'HNO3',step)/sf +.05)**2=e=(K_Pu_red_U_aq(step)* (C_aq_in_IS(»
j,h,'Pu_IV',step)/sf+interv/2*k2_red_IS('aq',j,h,'Pu_IV','U_IV',step)/sf) »

* (C_aq_in_IS(j,h,'U_IV',step)/sf)*sf*phi_IS(j,step)/vel_is(j,'aq',s»
tep)*z(j,step))*z_step_IS(step)*z_reac_UIV(step)*z_reac_Pu_IV_ox(step);

923

924 *Pu(IV) reduction by U(IV) - organic phase

925 Eq_Reac_Pu_U_org_IS(j,h,step)..Reac_red_IS('org',j,h,'Pu_IV','U_IV',step)=e=
»

(interv/6*(k0_red_IS('org',j,h,'Pu_IV','U_IV',step)+2*k1_red_IS('org',j,h,'Pu»
_IV','U_IV',step)+2*k2_red_IS('org',j,h,'Pu_IV','U_IV',step)+k3_red_IS('org',»
j,h,'Pu_IV','U_IV',step)))*z_step_IS(step)*z_reac_UIV(step)*z_reac_Pu_IV_ox(s»
tep);

926 Eq_k0_red_Pu_U_org(j,h,step)..k0_red_IS('org',j,h,'Pu_IV','U_IV',step) * (C»
_org_in_IS(j,h,'HNO3',step)/sf +.05)**2=e=(K_Pu_red_U_org(step)* (C_org_»
in_IS(j,h,'Pu_IV',step)/sf) * (C_org_in_IS(j,h,'U_IV',step)/sf)*s»
f*(1-phi_IS(j,step))/vel_is(j,'org',step)*z(j,step))*z_step_IS(step)*z_reac_U»
IV(step)*z_reac_Pu_IV_ox(step);

927 Eq_k1_red_Pu_U_org(j,h,step)..k1_red_IS('org',j,h,'Pu_IV','U_IV',step) * (C»
_org_in_IS(j,h,'HNO3',step))/sf +.05)**2=e=(K_Pu_red_U_org(step)* (C_org_»
in_IS(j,h,'Pu_IV',step)/sf+interv/2*k0_red_IS('org',j,h,'Pu_IV','U_IV',step)/»
sf) * (C_org_in_IS(j,h,'U_IV',step)/sf)*sf*(1-phi_IS(j,step))/vel»
_is(j,'org',step)*z(j,step))*z_step_IS(step)*z_reac_UIV(step)*z_reac_Pu_IV_ox»
(step);
928 Eq_k2_red_Pu_U_org(j,h,step)..k2_red_IS('org',j,h,'Pu_IV','U_IV',step) * (C»
_org_in_IS(j,h,'HNO3',step))/sf +.05)**2=e=(K_Pu_red_U_org(step)* (C_org_»
in_IS(j,h,'Pu_IV',step)/sf+interv/2*k1_red_IS('org',j,h,'Pu_IV','U_IV',step)/»
sf) * (C_org_in_IS(j,h,'U_IV',step)/sf)*sf*(1-phi_IS(j,step))/vel»
_is(j,'org',step)*z(j,step))*z_step_IS(step)*z_reac_UIV(step)*z_reac_Pu_IV_ox»
(step);
929   Eq_k3_red_Pu_U_org(j,h,step)..k3_red_IS('org',j,h,'Pu_IV','U_IV',step)   *
(C_»
org_in_IS(j,h,'HNO3',step))/sf +.05)**2=e=(K_Pu_red_U_org(step)* (C_org_i»
n_IS(j,h,'Pu_IV',step)/sf+interv/2*k2_red_IS('org',j,h,'Pu_IV','U_IV',step)/s»
f) * (C_org_in_IS(j,h,'U_IV',step)/sf)*sf*(1-phi_IS(j,step))/vel_»
is(j,'org',step)*z(j,step))*z_step_IS(step)*z_reac_UIV(step)*z_reac_Pu_IV_ox(»
step);
930
931 *Np(VI) reduction by U(IV)
932 Eq_Reac_NpVI_U_aq_IS(j,h,step)..Reac_red_IS('aq',j,h,'Np_VI','U_IV',step)=e=(»
interv/6*(k0_red_IS('aq',j,h,'Np_VI','U_IV',step)+2*k1_red_IS('aq',j,h,'Np_VI»
','U_IV',step)+2*k2_red_IS('aq',j,h,'Np_VI','U_IV',step)+k3_red_IS('aq',j,h,'»
Np_VI','U_IV',step)))*z_step_IS(step)*z_reac_UIV(step)*z_no_Np(step);
933 Eq_k0_red_NpVI_U_aq(j,h,step)..k0_red_IS('aq',j,h,'Np_VI','U_IV',step)=e=(
K»
_NpIV_red_U(step)* (C_aq_in_IS(j,h,'Np_VI',step)/sf) * (C_aq_i»
n_IS(j,h,'U_IV',step)/sf)*sf*phi_IS(j,step)/vel_is(j,'aq',step)*z(j,step))*z_»
step_IS(step)*z_reac_UIV(step) *z_no_Np(step);
934 Eq_k1_red_NpVI_U_aq(j,h,step)..k1_red_IS('aq',j,h,'Np_VI','U_IV',step)=e=(
K»
_NpIV_red_U(step)* (C_aq_in_IS(j,h,'Np_VI',step)/sf+interv/2*k0_red_IS('aq»

201

',j,h,'Np_VI','U_IV',step)/sf) * (C_aq_in_IS(j,h,'U_IV',step)/sf)»
*sf*phi_IS(j,step)/vel_is(j,'aq',step)*z(j,step))*z_step_IS(step)*z_reac_UIV(»
step)*z_no_Np(step);
935 Eq_k2_red_NpVI_U_aq(j,h,step)..k2_red_IS('aq',j,h,'Np_VI','U_IV',step)=e=(
K»
_NpIV_red_U(step)* (C_aq_in_IS(j,h,'Np_VI',step)/sf+interv/2*k1_red_IS('aq»
',j,h,'Np_VI','U_IV',step)/sf) * (C_aq_in_IS(j,h,'U_IV',step)/sf)»
*sf*phi_IS(j,step)/vel_is(j,'aq',step)*z(j,step))*z_step_IS(step)*z_reac_UIV(»
step)*z_no_Np(step);
936 Eq_k3_red_NpVI_U_aq(j,h,step)..k3_red_IS('aq',j,h,'Np_VI','U_IV',step)=e=(
K»
_NpIV_red_U(step)* (C_aq_in_IS(j,h,'Np_VI',step)/sf+interv/2*k2_red_IS('aq»
',j,h,'Np_VI','U_IV',step)/sf) * (C_aq_in_IS(j,h,'U_IV',step)/sf)»
*sf*phi_IS(j,step)/vel_is(j,'aq',step)*z(j,step))*z_step_IS(step)*z_reac_UIV(»
step)*z_no_Np(step);
937
938 *Np(V) reduction by U(IV)
939 Eq_Reac_NpV_U_aq_IS(j,h,step)..Reac_red_IS('aq',j,h,'Np_V','U_IV',step)=e=(in»
terv/6*(k0_red_IS('aq',j,h,'Np_V','U_IV',step)+2*k1_red_IS('aq',j,h,'Np_V','U»
_IV',step)+2*k2_red_IS('aq',j,h,'Np_V','U_IV',step)+k3_red_IS('aq',j,h,'Np_V'»
,'U_IV',step)))*z_step_IS(step)*z_reac_UIV(step)*z_no_Np(step);
940   Eq_k0_red_NpV_U_aq(j,h,step)..k0_red_IS('aq',j,h,'Np_V','U_IV',step)=e=(
K_N»
pV_red_U(step)* (C_aq_in_IS(j,h,'Np_V',step)/sf) * (C_aq_in_IS»
(j,h,'U_IV',step)/sf)* ((1.6*(C_aq_in_IS(j,h,'HNO3',step)/sf+1e7)**(-2) »
+1.42*C_aq_in_IS(j,h,'HNO3',step)/sf)) * sf*phi_IS(j,step)/vel_is(j»
,'aq',step)*z(j,step))*z_step_IS(step)*z_reac_UIV(step)*z_no_Np(step);
941   Eq_k1_red_NpV_U_aq(j,h,step)..k1_red_IS('aq',j,h,'Np_V','U_IV',step)=e=(
K_N»
pV_red_U(step)* (C_aq_in_IS(j,h,'Np_V',step)/sf+interv/2*k0_red_IS('aq',j,»
h,'Np_V','U_IV',step)/sf) * (C_aq_in_IS(j,h,'U_IV',step)/sf)* (»
(1.6*(C_aq_in_IS(j,h,'HNO3',step)/sf+1e7)**(-2) +1.42*C_aq_in_IS(j,h,'HNO3»
',step)/sf)) * sf*phi_IS(j,step)/vel_is(j,'aq',step)*z(j,step))*z_s»

tep_IS(step)*z_reac_UIV(step)*z_no_Np(step);

942   Eq_k2_red_NpV_U_aq(j,h,step)..k2_red_IS('aq',j,h,'Np_V','U_IV',step)=e=(
K_N»

pV_red_U(step)* (C_aq_in_IS(j,h,'Np_V',step)/sf+interv/2*k1_red_IS('aq',j,»

h,'Np_V','U_IV',step)/sf) * (C_aq_in_IS(j,h,'U_IV',step)/sf)* (»

(1.6*(C_aq_in_IS(j,h,'HNO3',step)/sf+1e7)**(-2) +1.42*C_aq_in_IS(j,h,'HNO3»

',step)/sf)) * sf*phi_IS(j,step)/vel_is(j,'aq',step)*z(j,step))*z_s»

tep_IS(step)*z_reac_UIV(step)*z_no_Np(step);

943   Eq_k3_red_NpV_U_aq(j,h,step)..k3_red_IS('aq',j,h,'Np_V','U_IV',step)=e=(
K_N»

pV_red_U(step)* (C_aq_in_IS(j,h,'Np_V',step)/sf+interv/2*k2_red_IS('aq',j,»

h,'Np_V','U_IV',step)/sf) * (C_aq_in_IS(j,h,'U_IV',step)/sf)* (»

(1.6*(C_aq_in_IS(j,h,'HNO3',step)/sf+1e7)**(-2) +1.42*C_aq_in_IS(j,h,'HNO3»

',step)/sf)) * sf*phi_IS(j,step)/vel_is(j,'aq',step)*z(j,step))*z_s»

tep_IS(step)*z_reac_UIV(step)*z_no_Np(step);

944

945 *Np(VI) reduction by N2H5

946 Eq_Reac_Np_VI_red_N2H5_IS(j,h,step)..Reac_IS('aq',j,h,'Np_VI',step)=e=(interv»

/6*(k0_r_IS('aq',j,h,'Np_VI',step)+2*k1_r_IS('aq',j,h,'Np_VI',step)+2*k2_r_IS»

('aq',j,h,'Np_VI',step)+k3_r_IS('aq',j,h,'Np_VI',step)))*z_step_IS(step)*z_re»

ac_N2H5(step);

947 Eq_k0_r_aq_Np_VI_red_N2H5(j,h,step)..k0_r_IS('aq',j,h,'Np_VI',step)=e=(K_Np_V»

I_red_N2H5(step)*C_aq_in_IS(j,h,'Np_VI',step)/sf*C_aq_in_IS(j,h,'N2H5',step)/»

sf*(C_aq_in_IS(j,h,'HNO3',step)/sf+1e-7)**(-1.3)*sf*phi_IS(j,step)/vel_is(j,'»

aq',step)*z(j,step))*z_step_IS(step)*z_reac_N2H5(step);

948 Eq_k1_r_aq_Np_VI_red_N2H5(j,h,step)..k1_r_IS('aq',j,h,'Np_VI',step)=e=(K_Np_V»

I_red_N2H5(step)*(C_aq_in_IS(j,h,'Np_VI',step)/sf+interv/2*k0_r_IS('aq',j,h,'»

Np_VI',step)/sf)*C_aq_in_IS(j,h,'N2H5',step)/sf*(C_aq_in_IS(j,h,'HNO3',step)/»

sf+1e-7)**(-1.3)*sf*phi_IS(j,step)/vel_is(j,'aq',step)*z(j,step))*z_step_IS(s»

tep)*z_reac_N2H5(step);

949 Eq_k2_r_aq_Np_VI_red_N2H5(j,h,step)..k2_r_IS('aq',j,h,'Np_VI',step)=e=(K_Np_V»

I_red_N2H5(step)*(C_aq_in_IS(j,h,'Np_VI',step)/sf+interv/2*k1_r_IS('aq',j,h,'»

Np_VI',step)/sf)*C_aq_in_IS(j,h,'N2H5',step)/sf*(C_aq_in_IS(j,h,'HNO3',step)/»

sf+1e-7)**(-1.3)*sf*phi_IS(j,step)/vel_is(j,'aq',step)*z(j,step))*z_step_IS(s»
tep)*z_reac_N2H5(step);
950 Eq_k3_r_aq_Np_VI_red_N2H5(j,h,step)..k3_r_IS('aq',j,h,'Np_VI',step)=e=(K_Np_V»
I_red_N2H5(step)*(C_aq_in_IS(j,h,'Np_VI',step)/sf+interv/2*k2_r_IS('aq',j,h,'»
Np_VI',step)/sf)*C_aq_in_IS(j,h,'N2H5',step)/sf*(C_aq_in_IS(j,h,'HNO3',step)/»
sf+1e-7)**(-1.3)*sf*phi_IS(j,step)/vel_is(j,'aq',step)*z(j,step))*z_step_IS(s»
tep)*z_reac_N2H5(step);
951
952 *Pu(IV) reduction by N2H5
953 Eq_Reac_Pu_N2H5_IS(j,h,step)..Reac_IS('aq',j,h,'Pu_IV',step)=e=(interv/6*(k0_»
r_IS('aq',j,h,'Pu_IV',step)+2*k1_r_IS('aq',j,h,'Pu_IV',step)+2*k2_r_IS('aq',j»
,h,'Pu_IV',step)+k3_r_IS('aq',j,h,'Pu_IV',step)))*z_step_IS(step)*z_reac_N2H5»
(step);
954 Eq_k0_r_aq_Pu_N2H5(j,h,step)..k0_r_IS('aq',j,h,'Pu_IV',step)=e=(K_Pu_red_N2H5»
(step)*(C_aq_in_IS(j,h,'Pu_IV',step)/sf*C_aq_in_IS(j,h,'N2H5',step)/sf)/(C_aq»
_in_IS(j,h,'HNO3',step)/sf+0.35)*sf*phi_IS(j,step)/vel_is(j,'aq',step)*z(j,st»
ep))*z_step_IS(step)*z_reac_N2H5(step);
955 Eq_k1_r_aq_Pu_N2H5(j,h,step)..k1_r_IS('aq',j,h,'Pu_IV',step)=e=(K_Pu_red_N2H5»
(step)*((C_aq_in_IS(j,h,'Pu_IV',step)/sf+interv/2*k0_r_IS('aq',j,h,'Pu_IV',st»
ep)/sf)*C_aq_in_IS(j,h,'N2H5',step)/sf)/(C_aq_in_IS(j,h,'HNO3',step)/sf+0.35)»
*sf*phi_IS(j,step)/vel_is(j,'aq',step)*z(j,step))*z_step_IS(step)*z_reac_N2H5»
(step);
956 Eq_k2_r_aq_Pu_N2H5(j,h,step)..k2_r_IS('aq',j,h,'Pu_IV',step)=e=(K_Pu_red_N2H5»
(step)*((C_aq_in_IS(j,h,'Pu_IV',step)/sf+interv/2*k1_r_IS('aq',j,h,'Pu_IV',st»
ep)/sf)*C_aq_in_IS(j,h,'N2H5',step)/sf)/(C_aq_in_IS(j,h,'HNO3',step)/sf+0.35)»
*sf*phi_IS(j,step)/vel_is(j,'aq',step)*z(j,step))*z_step_IS(step)*z_reac_N2H5»
(step);
957 Eq_k3_r_aq_Pu_N2H5(j,h,step)..k3_r_IS('aq',j,h,'Pu_IV',step)=e=(K_Pu_red_N2H5»
(step)*((C_aq_in_IS(j,h,'Pu_IV',step)/sf+interv/2*k2_r_IS('aq',j,h,'Pu_IV',st»
ep)/sf)*C_aq_in_IS(j,h,'N2H5',step)/sf)/(C_aq_in_IS(j,h,'HNO3',step)/sf+0.35)»
*sf*phi_IS(j,step)/vel_is(j,'aq',step)*z(j,step))*z_step_IS(step)*z_reac_N2H5»
(step);
958

959 *NO2 scavenge by N2H5

960 Eq_Reac_NO2_scav_IS(j,h,step)..Reac_IS('aq',j,h,'N2H5',step)=e=(interv/6*(k0_»
r_IS('aq',j,h,'N2H5',step)+2*k1_r_IS('aq',j,h,'N2H5',step)+2*k2_r_IS('aq',j,h»
,'N2H5',step)+k3_r_IS('aq',j,h,'N2H5',step)))*z_step_IS(step)*z_reac_N2H5(ste»
p);

961 Eq_k0_r_aq_N2H5(j,h,step)..k0_r_IS('aq',j,h,'N2H5',step)=e=(K_NO2_scav_aq(ste»
p)*(C_aq_in_IS(j,h,'HNO3',step)/sf*C_aq_in_IS(j,h,'N2H5',step)/sf*C_aq_in_IS(»
j,h,'HNO2',step)/sf)*sf*phi_IS(j,step)/vel_is(j,'aq',step)*z(j,step))*z_step_»
IS(step)*z_reac_N2H5(step);

962 Eq_k1_r_aq_N2H5(j,h,step)..k1_r_IS('aq',j,h,'N2H5',step)=e=(K_NO2_scav_aq(ste»
p)*(C_aq_in_IS(j,h,'HNO3',step)/sf*(C_aq_in_IS(j,h,'N2H5',step)/sf+interv/2*k»
0_r_IS('aq',j,h,'N2H5',step)/sf)*C_aq_in_IS(j,h,'HNO2',step)/sf)*sf*phi_IS(j,»
step)/vel_is(j,'aq',step)*z(j,step))*z_step_IS(step)*z_reac_N2H5(step);

963 Eq_k2_r_aq_N2H5(j,h,step)..k2_r_IS('aq',j,h,'N2H5',step)=e=(K_NO2_scav_aq(ste»
p)*(C_aq_in_IS(j,h,'HNO3',step)/sf*(C_aq_in_IS(j,h,'N2H5',step)/sf+interv/2*k»
1_r_IS('aq',j,h,'N2H5',step)/sf)*C_aq_in_IS(j,h,'HNO2',step)/sf)*sf*phi_IS(j,»
step)/vel_is(j,'aq',step)*z(j,step))*z_step_IS(step)*z_reac_N2H5(step);

964 Eq_k3_r_aq_N2H5(j,h,step)..k3_r_IS('aq',j,h,'N2H5',step)=e=(K_NO2_scav_aq(ste»
p)*(C_aq_in_IS(j,h,'HNO3',step)/sf*(C_aq_in_IS(j,h,'N2H5',step)/sf+interv/2*k»
2_r_IS('aq',j,h,'N2H5',step)/sf)*C_aq_in_IS(j,h,'HNO2',step)/sf)*sf*phi_IS(j,»
step)/vel_is(j,'aq',step)*z(j,step))*z_step_IS(step)*z_reac_N2H5(step);

965

966 *U(IV) oxidation - aqueous phase

967 Eq_Reac_U_ox_aq_IS(j,h,step)..Reac_IS('aq',j,h,'U_IV',step)=e=(interv/6*(k0_r»
_IS('aq',j,h,'U_IV',step)+2*k1_r_IS('aq',j,h,'U_IV',step)+2*k2_r_IS('aq',j,h,»
'U_IV',step)+k3_r_IS('aq',j,h,'U_IV',step)))*z_step_IS(step)*z_reac_UIV(step)»
;

968 Eq_k0_r_aq_U_ox(j,h,step)..k0_r_IS('aq',j,h,'U_IV',step)=e=((K_U_ox_aq*(C_aq_»
in_IS(j,h,'U_IV',step)/sf)*(C_aq_in_IS(j,h,'HNO2',step)/sf)**0.38*(C_aq_in_IS»
(j,h,'HNO3',step)/sf)**2.7)*sf*phi_IS(j,step)/vel_is(j,'aq',step)*z(j,step))*»
z_step_IS(step)*z_reac_UIV(step);

969 Eq_k1_r_aq_U_ox(j,h,step)..k1_r_IS('aq',j,h,'U_IV',step)=e=((K_U_ox_aq*(C_aq_»
in_IS(j,h,'U_IV',step)/sf+interv/2*k0_r_IS('aq',j,h,'U_IV',step)/sf)*(C_aq_in»

_IS(j,h,'HNO2',step)/sf)**0.38*(C_aq_in_IS(j,h,'HNO3',step)/sf)**2.7)*sf*phi_»
IS(j,step)/vel_is(j,'aq',step)*z(j,step))*z_step_IS(step)*z_reac_UIV(step);
970 Eq_k2_r_aq_U_ox(j,h,step)..k2_r_IS('aq',j,h,'U_IV',step)=e=((K_U_ox_aq*(C_aq_»
in_IS(j,h,'U_IV',step)/sf+interv/2*k1_r_IS('aq',j,h,'U_IV',step)/sf)*(C_aq_in»
_IS(j,h,'HNO2',step)/sf)**0.38*(C_aq_in_IS(j,h,'HNO3',step)/sf)**2.7)*sf*phi_»
IS(j,step)/vel_is(j,'aq',step)*z(j,step))*z_step_IS(step)*z_reac_UIV(step);
971 Eq_k3_r_aq_U_ox(j,h,step)..k3_r_IS('aq',j,h,'U_IV',step)=e=((K_U_ox_aq*(C_aq_»
in_IS(j,h,'U_IV',step)/sf+interv/2*k2_r_IS('aq',j,h,'U_IV',step)/sf)*(C_aq_in»
_IS(j,h,'HNO2',step)/sf)**0.38*(C_aq_in_IS(j,h,'HNO3',step)/sf)**2.7)*sf*phi_»
IS(j,step)/vel_is(j,'aq',step)*z(j,step))*z_step_IS(step)*z_reac_UIV(step);
972
973 *U(IV) oxidation - organic phase
974 Eq_Reac_U_ox_org_IS(j,h,step)..Reac_IS('org',j,h,'U_IV',step)=e=(interv/6*(k0»
_r_IS('org',j,h,'U_IV',step)+2*k1_r_IS('org',j,h,'U_IV',step)+2*k2_r_IS('org'»
,j,h,'U_IV',step)+k3_r_IS('org',j,h,'U_IV',step)))*z_step_IS(step)*z_reac_UIV»
(step);
975 Eq_k0_r_org_U_ox(j,h,step)..k0_r_IS('org',j,h,'U_IV',step)=e=((K_U_ox_org*(C_»
org_in_IS(j,h,'U_IV',step)/sf)*(C_org_in_IS(j,h,'HNO2',step)/sf)**0.49)*sf*ph»
i_IS(j,step)/vel_is(j,'org',step)*z(j,step))*z_step_IS(step)*z_reac_UIV(step)»
;
976 Eq_k1_r_orgU_ox(j,h,step)..k1_r_IS('org',j,h,'U_IV',step)=e=((K_U_ox_org*(C_o»
rg_in_IS(j,h,'U_IV',step)/sf+interv/2*k0_r_IS('org',j,h,'U_IV',step)/sf)*(C_o»
rg_in_IS(j,h,'HNO2',step)/sf)**0.49)*sf*phi_IS(j,step)/vel_is(j,'org',step)*z»
(j,step))*z_step_IS(step)*z_reac_UIV(step);
977 Eq_k2_r_org_U_ox(j,h,step)..k2_r_IS('org',j,h,'U_IV',step)=e=((K_U_ox_org*(C_»
org_in_IS(j,h,'U_IV',step)/sf+interv/2*k1_r_IS('org',j,h,'U_IV',step)/sf)*(C_»
org_in_IS(j,h,'HNO2',step)/sf)**0.49)*sf*phi_IS(j,step)/vel_is(j,'org',step)*»
z(j,step))*z_step_IS(step)*z_reac_UIV(step);
978 Eq_k3_r_org_U_ox(j,h,step)..k3_r_IS('org',j,h,'U_IV',step)=e=((K_U_ox_org*(C_»
org_in_IS(j,h,'U_IV',step)/sf+interv/2*k2_r_IS('org',j,h,'U_IV',step)/sf)*(C_»
org_in_IS(j,h,'HNO2',step)/sf)**0.49)*sf*phi_IS(j,step)/vel_is(j,'org',step)*»
z(j,step))*z_step_IS(step)*z_reac_UIV(step);
979

980 *reaction rate term in mol/m4

981 *Pu(III) auto-oxidation - aqueous phase

982 Eq_Reac_Pu_ox_IS(j,h,step)..Reac_IS('aq',j,h,'Pu_III',step)=e=(interv/6*(k0_r»
_IS('aq',j,h,'Pu_III',step)+2*k1_r_IS('aq',j,h,'Pu_III',step)+2*k2_r_IS('aq',»
j,h,'Pu_III',step)+k3_r_IS('aq',j,h,'Pu_III',step)))*z_step_IS(step)*z_reac_P»
uIII_ox(step);

983 Eq_k0_r_aq_Pu_ox(j,h,step)..k0_r_IS('aq',j,h,'Pu_III',step)=e=((K_Pu_ox_aq(st»
ep)*(C_aq_in_IS(j,h,'Pu_III',step)/sf)*(C_aq_in_IS(j,h,'HNO2',step)/sf)**0.5*»
(C_aq_in_IS(j,h,'HNO3',step)/sf)**0.5*(C_NO3_IS(j,h,step)/sf)**0.4)*sf*phi_IS»
(j,step)/vel_is(j,'aq',step)*z(j,step))*z_step_IS(step)*z_reac_PuIII_ox(step)»
;

984 Eq_k1_r_aq_Pu_ox(j,h,step)..k1_r_IS('aq',j,h,'Pu_III',step)=e=((K_Pu_ox_aq(st»
ep)*(C_aq_in_IS(j,h,'Pu_III',step)/sf+interv/2*k0_r_IS('aq',j,h,'Pu_III',step»
)/sf)*(C_aq_in_IS(j,h,'HNO2',step)/sf)**0.5*(C_aq_in_IS(j,h,'HNO3',step)/sf)*»
0.5(C_NO3_IS(j,h,step)/sf)**0.4)*sf*phi_IS(j,step)/vel_is(j,'aq',step)*z(j,»
step))*z_step_IS(step)*z_reac_PuIII_ox(step);

985 Eq_k2_r_aq_Pu_ox(j,h,step)..k2_r_IS('aq',j,h,'Pu_III',step)=e=((K_Pu_ox_aq(st»
ep)*(C_aq_in_IS(j,h,'Pu_III',step)/sf+interv/2*k1_r_IS('aq',j,h,'Pu_III',step»
)/sf)*(C_aq_in_IS(j,h,'HNO2',step)/sf)**0.5*(C_aq_in_IS(j,h,'HNO3',step)/sf)*»
0.5(C_NO3_IS(j,h,step)/sf)**0.4)*sf*phi_IS(j,step)/vel_is(j,'aq',step)*z(j,»
step))*z_step_IS(step)*z_reac_PuIII_ox(step);

986 Eq_k3_r_aq_Pu_ox(j,h,step)..k3_r_IS('aq',j,h,'Pu_III',step)=e=((K_Pu_ox_aq(st»
ep)*(C_aq_in_IS(j,h,'Pu_III',step)/sf+interv/2*k2_r_IS('aq',j,h,'Pu_III',step»
)/sf)*(C_aq_in_IS(j,h,'HNO2',step)/sf)**0.5*(C_aq_in_IS(j,h,'HNO3',step)/sf)*»
0.5(C_NO3_IS(j,h,step)/sf)**0.4)*sf*phi_IS(j,step)/vel_is(j,'aq',step)*z(j,»
step))*z_step_IS(step)*z_reac_PuIII_ox(step);

987

988 *Np(V)-Np(VI) equilibrium - aqueous phase

989 Eq_Reac_Np_IS(j,h,step)..Reac_IS('aq',j,h,'Np_V',step)=e=((interv/6*(k0_r_IS(»
'aq',j,h,'Np_V',step)+2*k1_r_IS('aq',j,h,'Np_V',step)+2*k2_r_IS('aq',j,h,'Np_»
V',step)+k3_r_IS('aq',j,h,'Np_V',step))))*z_step_IS(step) *z_no_Np(step);

990 Eq_k0_r_Np_V(j,h,step)..-k0_r_IS('aq',j,h,'Np_V',step)=e=((r_forw_Np_V_RK1(j,»
h,step)*(C_aq_in_IS(j,h,'HNO2',step)/sf)**.5*(C_aq_in_IS(j,h,'Np_V',step)/sf)»

+r_forw_Np_V_RK2(j,h,step)*(C_aq_in_IS(j,h,'HNO2',step)/sf)*(C_aq_in_IS(j,h,'»
Np_V',step)/sf)-r_back_Np_V_RK1(j,h,step)*(C_aq_in_IS(j,h,'Np_VI',step)/sf)*(»
C_aq_in_IS(j,h,'HNO2',step)/sf) -r_back_Np_V_RK2(j,h,step)*(C_aq_in_IS(j,h,'»
Np_VI',step)/sf)*(C_aq_in_IS(j,h,'HNO2',step)/sf)**1.5)*sf*phi_IS(j,step)/vel»
_is(j,'aq',step)*z(j,step))*z_step_IS(step) *z_no_Np(step);
991 Eq_k1_r_Np_V(j,h,step)..-k1_r_IS('aq',j,h,'Np_V',step)=e=((r_forw_Np_V_RK1(j,»
h,step)*(C_aq_in_IS(j,h,'HNO2',step)/sf)**.5*(C_aq_in_IS(j,h,'Np_V',step)/sf+»
interv/2*k0_r_IS('aq',j,h,'Np_V',step)/sf)+r_forw_Np_V_RK2(j,h,step)*(C_aq_in»
_IS(j,h,'HNO2',step)/sf)*(C_aq_in_IS(j,h,'Np_V',step)/sf+interv/2*k0_r_IS('aq»
',j,h,'Np_V',step)/sf)-r_back_Np_V_RK1(j,h,step)*(C_aq_in_IS(j,h,'Np_VI',step»
)/sf)*(C_aq_in_IS(j,h,'HNO2',step)/sf) -r_back_Np_V_RK2(j,h,step)*(C_aq_in_I»
S(j,h,'Np_VI',step)/sf)*(C_aq_in_IS(j,h,'HNO2',step)/sf)**1.5)*sf*phi_IS(j,st»
ep)/vel_is(j,'aq',step)*z(j,step))*z_step_IS(step) *z_no_Np(step);
992 Eq_k2_r_Np_V(j,h,step)..-k2_r_IS('aq',j,h,'Np_V',step)=e=((r_forw_Np_V_RK1(j,»
h,step)*(C_aq_in_IS(j,h,'HNO2',step)/sf)**.5*(C_aq_in_IS(j,h,'Np_V',step)/sf+»
interv/2*k1_r_IS('aq',j,h,'Np_V',step)/sf)+r_forw_Np_V_RK2(j,h,step)*(C_aq_in»
_IS(j,h,'HNO2',step)/sf)*(C_aq_in_IS(j,h,'Np_V',step)/sf+interv/2*k1_r_IS('aq»
',j,h,'Np_V',step)/sf)-r_back_Np_V_RK1(j,h,step)*(C_aq_in_IS(j,h,'Np_VI',step»
)/sf)*(C_aq_in_IS(j,h,'HNO2',step)/sf) -r_back_Np_V_RK2(j,h,step)*(C_aq_in_I»
S(j,h,'Np_VI',step)/sf)*(C_aq_in_IS(j,h,'HNO2',step)/sf)**1.5)*sf*phi_IS(j,st»
ep)/vel_is(j,'aq',step)*z(j,step))*z_step_IS(step) *z_no_Np(step);
993 Eq_k3_r_Np_V(j,h,step)..-k3_r_IS('aq',j,h,'Np_V',step)=e=((r_forw_Np_V_RK1(j,»
h,step)*(C_aq_in_IS(j,h,'HNO2',step)/sf)**.5*(C_aq_in_IS(j,h,'Np_V',step)/sf+»
interv/2*k2_r_IS('aq',j,h,'Np_V',step)/sf)+r_forw_Np_V_RK2(j,h,step)*(C_aq_in»
_IS(j,h,'HNO2',step)/sf)*((C_aq_in_IS(j,h,'Np_V',step)+interv/2*k2_r_IS('aq',»
j,h,'Np_V',step))/sf)-r_back_Np_V_RK1(j,h,step)*(C_aq_in_IS(j,h,'Np_VI',step)»
/sf)*(C_aq_in_IS(j,h,'HNO2',step)/sf) -r_back_Np_V_RK2(j,h,step)*(C_aq_in_IS»
(j,h,'Np_VI',step)/sf)*(C_aq_in_IS(j,h,'HNO2',step)/sf)**1.5)*sf*phi_IS(j,ste»
p)/vel_is(j,'aq',step)*z(j,step))*z_step_IS(step) *z_no_Np(step);
994
995 *Np(V)-Np(VI) equilibrium - org phase
996 Eq_Reac_Np_org_IS(j,h,step)..Reac_IS('org',j,h,'Np_V',step)=e=((interv/6*(k0_»
r_IS('org',j,h,'Np_V',step)+2*k1_r_IS('org',j,h,'Np_V',step)+2*k2_r_IS('org',»

j,h,'Np_V',step)+k3_r_IS('org',j,h,'Np_V',step))))*z_step_IS(step) ;

997 Eq_k0_r_org_Np_V(j,h,step)..-k0_r_IS('org',j,h,'Np_V',step)=e=((1.952e11*exp(»
-9008/T(step))*C_org_in_IS(j,h,'Np_V',step)/sf*((C_org_in_IS(j,h,'HNO3',step)»
+C_org_in_IS(j,h,'HNO3_2',step))/sf)**.5*(C_org_in_IS(j,h,'HNO2',step)/sf)**.»
5*C_H20_org**(-0.2))*sf*phi_IS(j,step)/vel_is(j,'org',step)*z(j,step))*z_step»
_IS(step) *z_no_Np(step);

998 Eq_k1_r_org_Np_V(j,h,step)..-k1_r_IS('org',j,h,'Np_V',step)=e=((1.952e11*exp(»
-9008/T(step))*(C_org_in_IS(j,h,'Np_V',step)/sf+interv/2*k0_r_IS('org',j,h,'N»
p_V',step)/sf)*((C_org_in_IS(j,h,'HNO3',step)+C_org_in_IS(j,h,'HNO3_2',step))»
/sf)**.5*(C_org_in_IS(j,h,'HNO2',step)/sf)**.5*C_H20_org**(-0.2))*sf*phi_IS(j»
,step)/vel_is(j,'org',step)*z(j,step))*z_step_IS(step) *z_no_Np(step);

999 Eq_k2_r_org_Np_V(j,h,step)..-k2_r_IS('org',j,h,'Np_V',step)=e=((1.952e11*exp(»
-9008/T(step))*(C_org_in_IS(j,h,'Np_V',step)/sf+interv/2*k1_r_IS('org',j,h,'N»
p_V',step)/sf)*((C_org_in_IS(j,h,'HNO3',step)+C_org_in_IS(j,h,'HNO3_2',step))»
/sf)**.5*(C_org_in_IS(j,h,'HNO2',step)/sf)**.5*C_H20_org**(-0.2))*sf*phi_IS(j»
,step)/vel_is(j,'org',step)*z(j,step))*z_step_IS(step) *z_no_Np(step);

1000 Eq_k3_r_org_Np_V(j,h,step)..-k3_r_IS('org',j,h,'Np_V',step)=e=((1.952e11*exp(»
-9008/T(step))*(C_org_in_IS(j,h,'Np_V',step)/sf+interv/2*k2_r_IS('org',j,h,'N»
p_V',step)/sf)*((C_org_in_IS(j,h,'HNO3',step)+C_org_in_IS(j,h,'HNO3_2',step))»
/sf)**.5*(C_org_in_IS(j,h,'HNO2',step)/sf)**.5*C_H20_org**(-0.2))*sf*phi_IS(j»
,step)/vel_is(j,'org',step)*z(j,step))*z_step_IS(step)*z_no_Np(step) ;

1001

1002 *Np(IV)-Np(V) equilibrium - aqueous phase NEGLIGIBLE

1003 Eq_Reac_Np_IV_IS(j,h,step)..Reac_IS('aq',j,h,'Np_IV',step)=e=0;

1004 *((interv/6*(k0_r_IS('aq',j,h,'Np_IV',step)+2*k1_r_IS('aq',j,h,'Np_IV',step)+»
2*k2_r_IS('aq',j,h,'Np_IV',step)+k3_r_IS('aq',j,h,'Np_IV',step))))*z_step_IS(»
step);

1005 Eq_k0_r_aq_Np_IV(j,h,step)..k0_r_IS('aq',j,h,'Np_IV',step)=e=0;

1006 *((K_Np_IV_for(step)*(C_aq_in_IS(j,h,'Np_V',step)/sf)**2*(C_aq_in_IS(j,h,'HNO»
3',step)/sf)**2-K_Np_IV_rev*(C_aq_in_IS(j,h,'Np_IV',step)/sf)*(C_aq_in_IS(j,h»
,'Np_VI',step)/sf)*(2.16+12.5*C_NO3_IS(j,h,step)/sf))*sf*phi_IS(j,step)/vel_i»
s(j,'aq',step)*z(j,step))*z_step_IS(step);

1007 Eq_k1_r_aq_Np_IV(j,h,step)..k1_r_IS('aq',j,h,'Np_IV',step)=e=0;

1008 *((K_Np_IV_for(step)*(C_aq_in_IS(j,h,'Np_V',step)/sf)**2*(C_aq_in_IS(j,h,'HNO»
3',step)/sf)**2-K_Np_IV_rev*(C_aq_in_IS(j,h,'Np_IV',step)/sf+interv/2*k0_r_IS»
('aq',j,h,'Np_IV',step)/sf)*(C_aq_in_IS(j,h,'Np_VI',step)/sf)*(2.16+12.5*C_NO»
3_IS(j,h,step)/sf))*sf*phi_IS(j,step)/vel_is(j,'aq',step)*z(j,step))*z_step_I»
S(step);
1009 Eq_k2_r_aq_Np_IV(j,h,step)..k2_r_IS('aq',j,h,'Np_IV',step)=e=0;
1010 *((K_Np_IV_for(step)*(C_aq_in_IS(j,h,'Np_V',step)/sf)**2*(C_aq_in_IS(j,h,'HNO»
3',step)/sf)**2-K_Np_IV_rev*(C_aq_in_IS(j,h,'Np_IV',step)/sf+interv/2*k1_r_IS»
('aq',j,h,'Np_IV',step)/sf)*(C_aq_in_IS(j,h,'Np_VI',step)/sf)*(2.16+12.5*C_NO»
3_IS(j,h,step)/sf))*sf*phi_IS(j,step)/vel_is(j,'aq',step)*z(j,step))*z_step_I»
S(step);
1011 Eq_k3_r_aq_Np_IV(j,h,step)..k3_r_IS('aq',j,h,'Np_IV',step)=e=0;
1012 *((K_Np_IV_for(step)*(C_aq_in_IS(j,h,'Np_V',step)/sf)**2*(C_aq_in_IS(j,h,'HNO»
3',step)/sf)**2-K_Np_IV_rev*(C_aq_in_IS(j,h,'Np_IV',step)/sf+interv/2*k2_r_IS»
('aq',j,h,'Np_IV',step)/sf)*(C_aq_in_IS(j,h,'Np_VI',step)/sf)*(2.16+12.5*C_NO»
3_IS(j,h,step)/sf))*sf*phi_IS(j,step)/vel_is(j,'aq',step)*z(j,step))*z_step_I»
S(step);
1013
1014 *extaction term - used in the Np mass balance to distinguish reactions and ma»
ss transfer terms
1015 Eq_Extr_IS(j,h,comp,step)..Extr_IS(j,h,comp,step)=e=(interv/6*(k0_IS(j,h,comp»
,step)+2*k1_IS(j,h,comp,step)+2*k2_IS(j,h,comp,step)+k3_IS(j,h,comp,step)))*z»
_step_IS(step);
1016
1017 *TBP DEGRADATION - neglected if it will not be compared with convent. tech.
1018 *this Reac('org',j,h,'TBP') is reaction rate - hydrolysis ONLY in organic con»
centration [mol m3-1 s-1]
1019 Eq_hydrol_org_IS(j,h,step)..Reac_IS('org',j,h,'TBP',step)=e=0;
1020 *((KII_org*(C_org_IS(j,h,'HNO3',step)+C_org_IS(j,h,'HNO3_2',step))/sf+KZr_org»
*C_org_IS(j,h,'Zr',step)/sf)/h_to_s*sf)*z_step_IS(step);
1021 Eq_protons_org_IS(j,h,step)..H_org_IS(j,h,step)=e=0;
1022 *(Reac_IS('org',j,h,'TBP',step)*h_to_s/KIII_org)*z_step_IS(step);
1023 *this Reac('aq',j,h,'TBP') is the term for TBP hydrolysis in the two-phase

210

1024 Eq_hydrol_IS(j,h,step)..Reac_IS('aq',j,h,'TBP',step)=e=0;
1025 *((interv/6*(k0_r_IS('aq',j,h,'TBP',step)+2*k1_r_IS('aq',j,h,'TBP',step)+2*k2»
_r_IS('aq',j,h,'TBP',step)+k3_r_IS('aq',j,h,'TBP',step))))*z_step_IS(step);
1026 Eq_k0_r_TBP(j,h,step)..-k0_r_IS('aq',j,h,'TBP',step)=e=0;
1027   *(KIII/h_to_s*(H_org_IS(j,h,step)/sf*C_org_IS(j,h,'TBP',step)/sf*sf*(1-phi_IS»
(j,step))/vel_IS('org',step)+q_IS(j,step)*C_aq_IS(j,h,'HNO3',step)/sf*TBP_sol»
/sf/MW_TBP*sf*phi_IS(j,step)/vel_IS('aq',step))*z(j,step))*z_step_IS(step);
1028 Eq_k1_r_TBP(j,h,step)..-k1_r_IS('aq',j,h,'TBP',step)=e=0;
1029 *(KIII/h_to_s*(H_org_IS(j,h,step)/sf*(C_org_IS(j,h,'TBP',step)/sf+interv/2*k0»
_r_IS('aq',j,h,'TBP',step)/sf)*sf*(1-phi_IS(j,step))/vel_IS('org',step)+q_IS(»
j,step)*C_aq_IS(j,h,'HNO3',step)/sf*TBP_sol/sf/MW_TBP*sf*phi_IS(j,step)/vel_I»
S('aq',step))*z(j,step))*z_step_IS(step);
1030 Eq_k2_r_TBP(j,h,step)..-k2_r_IS('aq',j,h,'TBP',step)=e=0;
1031 *(KIII/h_to_s*(H_org_IS(j,h,step)/sf*(C_org_IS(j,h,'TBP',step)/sf+interv/2*k1»
_r_IS('aq',j,h,'TBP',step)/sf)*sf*(1-phi_IS(j,step))/vel_IS('org',step)+q_IS(»
j,step)*C_aq_IS(j,h,'HNO3',step)/sf*TBP_sol/sf/MW_TBP*sf*phi_IS(j,step)/vel_I»
S('aq',step))*z(j,step))*z_step_IS(step);
1032 Eq_k3_r_TBP(j,h,step)..-k3_r_IS('aq',j,h,'TBP',step)=e=0;
1033 *(KIII/h_to_s*(H_org_IS(j,h,step)/sf*(C_org_IS(j,h,'TBP',step)/sf+interv/2*k2»
_r_IS('aq',j,h,'TBP',step)/sf)*sf*(1-phi_IS(j,step))/vel_IS('org',step)+q_IS(»
j,step)*C_aq_IS(j,h,'HNO3',step)/sf*TBP_sol/sf/MW_TBP*sf*phi_IS(j,step)/vel_I»
S('aq',step))*z(j,step))*z_step_IS(step);
1034
1035
1036 *terms for mass transfer calculations
1037 Eq_a_IS(j,step)..a_IS(j,step)=e=(Kla_IS(j,step)*q_corr_IS(j,step)/(vel_IS(j,'»
mix',step))*z(j,step))*z_step_IS(step);
1038 Eq_b_IS(j,h,comp,step)..b_IS(j,h,comp,step)=e=((Kla_IS(j,step)*q_corr_IS(j,st»
ep)/(vel_IS(j,'mix',step))*(C_aq_eq_IS(j,h,comp,step)*transf_aq(comp)+C_org»
_eq_IS(j,h,comp,step)*transf_org(comp)))*z(j,step))*z_step_IS(step);
1039   Eq_k0_2(j,h,comp,step)..k0_IS(j,h,comp,step)=e=((-a_IS(j,step)*(C_aq_in_IS(j,»

h,comp,step)*transf_aq(comp)+C_org_in_IS(j,h,comp,step)*transf_org(comp))+b_I»
S(j,h,comp,step))*z(j,step))*z_step_IS(step);

1040   Eq_k1_2(j,h,comp,step)..k1_IS(j,h,comp,step)=e=((-
a_IS(j,step)*((C_aq_in_IS(j»

,h,comp,step)*transf_aq(comp)+C_org_in_IS(j,h,comp,step)*transf_org(comp))+in»
terv/2*k0_IS(j,h,comp,step))+b_IS(j,h,comp,step))*z(j,step))*z_step_IS(step);

1041   Eq_k2_2(j,h,comp,step)..k2_IS(j,h,comp,step)=e=((-
a_IS(j,step)*((C_aq_in_IS(j»

,h,comp,step)*transf_aq(comp)+C_org_in_IS(j,h,comp,step)*transf_org(comp))+in»
terv/2*k1_IS(j,h,comp,step))+b_IS(j,h,comp,step))*z(j,step))*z_step_IS(step);

1042   Eq_k3_2(j,h,comp,step)..k3_IS(j,h,comp,step)=e=((-
a_IS(j,step)*((C_aq_in_IS(j»

,h,comp,step)*transf_aq(comp)+C_org_in_IS(j,h,comp,step)*transf_org(comp))+in»
terv/2*k2_IS(j,h,comp,step))+b_IS(j,h,comp,step))*z(j,step))*z_step_IS(step);

1043

1044

1045

1046 *Richardson calculations for distribution coefficients

1047 Eq_I_S_IS(j,h,step)..I_S_IS(j,h,step)=e=(C_aq_eq_IS(j,h,'HNO3',step)/sf+2*C_a»
q_eq_IS(j,h,'U_VI',step)/sf+4*C_aq_eq_IS(j,h,'Pu_IV',step)/sf + 3*C_aq_eq_IS(»
j,h,'Zr',step)/sf+C_aq_eq_IS(j,h,'Ru',step)/sf+0.5*C_aq_eq_IS(j,h,'Np_V',step»
)/sf+4*C_aq_eq_IS(j,h,'U_IV',step)/sf+3*C_aq_eq_IS(j,h,'Pu_III',step)/sf+C_aq»
_in_IS(j,h,'HAN',step)/sf+C_aq_in_IS(j,h,'N2H5',step)/sf)*z_step_IS(step)+(1-»
z_step_IS(step))*I_S_IS.lo(j,h,step);

1048 Eq_m_U_IS(j,h,step)..m_IS(j,h,'U_VI',step)=e=(K_eq_IS(j,h,'U_VI',step)*(C_org»
_eq_IS(j,h,'TBP',step)/sf)**2)*z_step_IS(step);

1049 Eq_m_Pu_IS(j,h,step)..m_IS(j,h,'Pu_IV',step)=e=(K_eq_IS(j,h,'Pu_IV',step)*(C_»
org_eq_IS(j,h,'TBP',step)/sf)**2)*z_step_IS(step);

1050 Eq_m_H1_IS(j,h,step)..m_IS(j,h,'HNO3',step)=e=(K_eq_IS(j,h,'HNO3',step)*C_org»
_eq_IS(j,h,'TBP',step)/sf)*z_step_IS(step);

1051 Eq_m_H2_IS(j,h,step)..m_IS(j,h,'HNO3_2',step)=e=(K_eq_IS(j,h,'HNO3_2',step)*(»
C_org_eq_IS(j,h,'TBP',step)/sf)**2)*z_step_IS(step);

1052 Eq_K_U_Rich_IS(j,h,step)..K_eq_IS(j,h,'U_VI',step)=e=((3.7*I_S_IS(j,h,step)**»

212

1.57+1.4*I_S_IS(j,h,step)**3.9+0.011*I_S_IS(j,h,step)**7.3)*(4*F**(-0.17)-3)*»
exp(2500*tau_T(step)))*z_step_IS(step);

1053 Eq_K_Pu_Rich_IS(j,h,step)..K_eq_IS(j,h,'Pu_IV',step)=e=(K_eq_IS(j,h,'U_VI',st»
ep)*(0.2+0.55*F**1.25+0.0074*I_S_IS(j,h,step)**2)*(4*F**(-0.17)-3)*exp(-200*t»
au_T(step)))*z_step_IS(step);

1054 Eq_K_H1_Rich_IS(j,h,step)..K_eq_IS(j,h,'HNO3',step)=e=((0.135*I_S_IS(j,h,step»
)**0.82+0.005*I_S_IS(j,h,step)**3.44)*(1-0.54*exp(-15*F))*exp(340*tau_T(step)»
))*z_step_IS(step);

1055 Eq_K_H2_Rich_IS(j,h,step)..K_eq_IS(j,h,'HNO3_2',step)=e=(K_eq_IS(j,h,'HNO3',s»
tep))*z_step_IS(step);

1056 Eq_K_Zr_IS(j,h,step)..K_eq_IS(j,h,'Zr',step)=e=(exp(a1_Zr*I_S_IS(j,h,step)**2»
+a2_Zr*I_S_IS(j,h,step)+a3_Zr))/scal_Zr(step)*z_step_IS(step);

1057 Eq_K_Ru_IS(j,h,step)..K_eq_IS(j,h,'Ru',step)=e=(exp(a1_Ru*I_S_IS(j,h,step)**3»
+a2_Ru*I_S_IS(j,h,step)**2+a3_Ru*I_S_IS(j,h,step)+a4_Ru))*z_step_IS(step);

1058

1059

1060

1061 *Np distr coeff from Benedict model, parameter re-calculated by Kumar e Kogan»
ti 2001

1062 Eq_m_Np_VI_IS(j,h,step)..m_IS(j,h,'Np_VI',step)=e=(0.52768*m_IS(j,h,'U_VI',st»
ep))*z_step_IS(step);

1063

1064 *Np(V) distr coeff as given by Tachimori, from Chen 2016

1065 Eq_m_Np_V_IS(j,h,step)..m_IS(j,h,'Np_V',step)=e=(0.01)*z_step_IS(step);

1066

1067 *Np(VI) distr coeff as given by Uchiyama, from Chen 2016

1068 Eq_m_HNO2_IS(j,h,step)..m_IS(j,h,'HNO2',step)=e=(25*C_org_eq_IS(j,h,'TBP',ste»
p)/sf)*z_step_IS(step);

1069

1070 *Np distr coeff from Benedict model, parameter re-calculated by Kumar e Kogan»
ti 2001

1071   Eq_m_Np_IV_IS(j,h,step)..m_IS(j,h,'Np_IV',step)=e=(1.109e-
7*exp(.29623*I_S_IS»

213

(j,h,step)+0.041519*T(step))*m_IS(j,h,'U_VI',step))*z_step_IS(step);

1072

1073 *distr coefficients by Geldard, from Kumar and Koganti

1074   Eq_m_Pu_III_IS(j,h,step)..m_IS(j,h,'Pu_III',step)=e=(1.138e-2*m_IS(j,h,'U_VI»

,step))*z_step_IS(step);

1075 Eq_m_U_IV_IS(j,h,step)..m_IS(j,h,'U_IV',step)=e=((0.0541+0.000658*I_S_IS(j,h,»

step)**2)*m_IS(j,h,'U_VI',step))*z_step_IS(step);

1076

1077 *distr coefficient for Tc

1078 Eq_D_Tc0_IS(j,h,step)..D_Tc0_IS(j,h,step)=e=(0.845*(C_org_eq_IS(j,h,'TBP',ste»

p)/sf)**(1.92*EXP(3300*tau_T(step)))*2.324*I_S_IS(j,h,step)**(0.848*EXP(230*t»

au_T(step)))*EXP(8070*tau_T(step))*EXP(-350*tau_T(step))/(1+0.157*I_S_IS(j,h,»

step)**(4.69*EXP(410*tau_T(step)))*EXP(324*tau_T(step))+1.72*I_S_IS(j,h,step)»

**(1.95*EXP(160*tau_T(step)))*EXP(3150*tau_T(step))))*z_step_IS(step);

1079 Eq_D_U_IS(j,h,step)..D_U_IS(j,h,step)=e=(0.331*(C_org_eq_IS(j,h,'U_VI',step)/»

sf)**2/((C_org_eq_IS(j,h,'U_VI',step)/sf)+(C_org_eq_IS(j,h,'Pu_IV',step)/sf))»

*(1+4.87*I_S_IS(j,h,step)**(-1.343)*EXP(980*tau_T(step)))*EXP(-1060*tau_T(ste»

p)))*z_step_IS(step);

1080 *the following term can be neglected

1081 Eq_D_Pu_IS(j,h,step)..D_Pu_IS(j,h,step)=e=0;

1082 *(3.31*I_S_IS(j,h,step)**(-0.707)*(C_org_eq_IS(j,h,'Pu_IV',step)/1000)**2/((C»

_org_eq_IS(j,h,'U_VI',step)/sf)+(C_org_eq_IS(j,h,'Pu_IV',step)/sf))*EXP(-1060»

*tau_T(step)))*z_step_IS(step);

1083 Eq_m_Tc_IS(j,h,step)..m_IS(j,h,'Tc',step)=e=(D_Tc0_IS(j,h,step)+D_U_IS(j,h,st»

ep)+D_Pu_IS(j,h,step)+D_Zr_IS(j,h,step))*z_step_IS(step);

1084

1085 *distr coeff for Ru and Zr

1086 Eq_D_Zr_IS(j,h,step)..D_Zr_IS(j,h,step)=e=(1670*(C_org_eq_IS(j,h,'Zr',step)/s»

f)*I_S_IS(j,h,step)**(-0.707)*EXP(2810*tau_T(step)))*z_step_IS(step);

1087 Eq_m_Zr_IS(j,h,step)..m_IS(j,h,'Zr',step)=e=(K_eq_IS(j,h,'Zr',step)*scal_Zr(s»

tep)*(C_org_eq_IS(j,h,'TBP',step)/sf)**2)*z_step_IS(step);

1088 Eq_m_Ru_IS(j,h,step)..m_IS(j,h,'Ru',step)=e=(K_eq_IS(j,h,'Ru',step)*(C_org_eq»

_IS(j,h,'TBP',step)/sf)**2)*z_step_IS(step);

1089

1090

1091 Eq_L_discr(h)..L_discr(h)=e=L_discr(h-1)+L/N_discr;

1092

1093 *nuclear subcriticality guaranteed - can be neglected in this case

1094 *Eq_keff_IS(step)..keff_IS(step)=e=(kinf/(1+m2*buck_IS(step)))*z_step_IS(step»
);

1095 *Eq_buck_IS(step)..buck_IS(step)=e=((2.405/(D_IS(step)/100/2+delta))**2+(3.14»
/(L_IS(step)/100+2*delta))**2)*z_step_IS(step);

1096

1097

1098 *FLOWRATES, VELOCITIES AND RESIDENCE TIMES

1099 Eq_vel1_IS(j,step)..vel_IS(j,'mix',step)*q_IS(j,step)=e=(vel_IS(j,'aq',step)*»
(1+q_IS(j,step)))*z_step_IS(step);

1100 Eq_vel2_IS(j,step)..vel_IS(j,'aq',step)=e=((Vdot_IS(j,'aq',step)+V_fresh_cost»
rip(j,step)*z(j,step))/((D_IS(step))**2*pi/4)*cm3h_to_m3s)*z_step_IS(step);

1101 Eq_vel3_IS(j,step)..vel_IS(j,'org',step)*(1+q_IS(j,step))=e=(vel_IS(j,'mix',s»
tep))*z_step_IS(step);

1102 Eq_flowrate1_IS(j,step)..Vdot_IS(j,'mix',step)*q_IS(j,step)=e=((Vdot_IS(j,'aq»
',step)+V_fresh_costrip(j,step)*z(j,step))*(1+q_IS(j,step)))*z_step_IS(step);

1103 Eq_flowrate3_IS(j,step)..Vdot_IS(j,'org',step)*q_IS(j,step)=e=((Vdot_IS(j,'aq»
',step)+V_fresh_costrip(j,step)*z(j,step)))*z_step_IS(step);

1104

1105 * Kla linearised if upper bound for D: 0.0025 m / coefficients from Excel fil»
es

1106 eq_kla_IS(j,step)..Kla_IS(j,step)=e=0.3184901+13.05809408*(Vel_IS(j,'mix',ste»
p)-0.02)-24.20524757*(D_IS(step)-0.0025);

1107

1108

1109 *equilibrium concentrations

1110 Eq_mass_Eq_aq_IS(j,h,comp,step)..C_aq_eq_IS(j,h,comp,step)*q_IS(j,step)+(C_or»
g_eq_IS(j,h,comp,step)+C_org_eq_IS(j,h,'HNO3_2',step)*equil_HNO3(comp))*trans»

f_aq(comp)=e=((C_org_in_IS(j,h,'HNO3_2',step)*equil_HNO3(comp)+C_org_in_IS(j,»
h,comp,step)+q_IS(j,step)*C_aq_in_IS(j,h,comp,step))*transf_aq(comp))*z_step_»
IS(step);
1111 Eq_mass_Eq_org_IS(j,h,comp,step)..C_org_eq_IS(j,h,comp,step)=e=(((C_aq_eq_IS(»
j,h,comp,step)*(1-equil_HNO3_2(comp))+C_aq_eq_IS(j,h,'HNO3',step)*equil_HNO3_»
2(comp))*m_IS(j,h,comp,step)* (1-equil_TBP(comp))+(F*rho_TBP/MW_TBP*1000-
2*C_»
org_eq_IS(j,h,'U_VI',step)-2*C_org_eq_IS(j,h,'Pu_IV',step)-C_org_eq_IS(j,h,'H»
NO3',step)-2*C_org_eq_IS(j,h,'HNO3_2',step)-2*C_org_eq_IS(j,h,'Zr',step)-2*C_»
org_eq_IS(j,h,'Ru',step)-3*C_org_eq_IS(j,h,'Tc',step)-2*C_org_eq_IS(j,h,'Np_V»
I',step)-2*C_org_eq_IS(j,h,'Np_IV',step)-2*C_org_eq_IS(j,h,'Np_V',step)-4*C_o»
rg_eq_IS(j,h,'U_IV',step)-3*C_org_eq_IS(j,h,'Pu_III',step))* equil_TBP(comp»
))*(1-equil_HAN(comp)))*z_step_IS(step);
1112
1113
1114
1115 *Efficiency of extraction
1116 Eq_E_U_IS(step)..E_IS('U_VI',step)*((C_aq_in_IS('1','1','U_VI',step)+C_aq_in_»
IS('1','1','U_IV',step))*z_extr(step)+(1-z_extr(step))*(C_org_in_IS('6','1','»
U_VI',step)+C_org_in_IS('6','1','U_IV',step)))=e=(((C_aq»
_in_IS('1','1','U_VI',step)-C_aq_IS('6','50','U_VI',step)+C_aq_in_IS('1','1',»
'U_IV',step)-C_aq_IS('6','50','U_IV',step)) *z_extr(step)+(1-z_extr»
(step))* (C_org_in_IS('6','1','U_VI',step)-C_org_IS('1','50','U_VI',st»
ep)+C_org_in_IS('6','1','U_IV',step)-C_org_IS('1','50','U_IV',step))) »
*100)*z_step_IS(step);
1117 Eq_E_Pu_IS(step)..E_IS('Pu_IV',step)*((C_aq_in_IS('1','1','Pu_IV',step)+C_aq_»
in_IS('1','1','Pu_III',step))*z_extr(step)+(1-z_extr(step))*(C_org_in_IS('6',»
'1','Pu_IV',step)+C_org_in_IS('6','1','Pu_III',step)))=e=((»
(C_aq_in_IS('1','1','Pu_IV',step)-C_aq_IS('6','50','Pu_IV',step)+C_aq_in_I»
S('1','1','Pu_III',step)-C_aq_IS('6','50','Pu_III',step)) *z_extr(s»
tep)+(1-z_extr(step))* (C_org_in_IS('6','1','Pu_IV',step)-C_org_IS('1»
','50','Pu_IV',step)+C_org_in_IS('6','1','Pu_III',step)-C_org_IS('1','50','Pu_»
III',step))) *100)*z_step_IS(step);

1118 Eq_E_HNO3_IS(step)..E_IS('HNO3',step)*(C_aq_in_IS('1','1','HNO3',step)*z_extr»
(step)+(1-z_extr(step))*(C_org_in_IS('6','1','HNO3',step)+C_org_in_IS('6','1'»
,'HNO3_2',step)))=e=(((C_aq_in_IS('1','1','HNO3',step)-C»
_aq_IS('6','50','HNO3',step)) *z_extr(step)+(1-z_extr(step))* »
(C_org_in_IS('6','1','HNO3',step)-C_org_IS('1','50','HNO3',step)+C_org_in_I»
S('6','1','HNO3_2',step)-C_org_IS('1','50','HNO3_2',step))) »
*100)*z_step_IS(step);
1119 Eq_E_Zr_IS(step)..E_IS('Zr',step)*((C_aq_in_IS('1','1','Zr',step)*z_extr(step»
))+(1-z_extr(step))*C_org_in_IS('6','1','Zr',step)))*z_step_zr(step) =e=(»
((C_aq_in_IS('1','1','Zr',step)-C_aq_IS('6','50','Zr',step)) »
z_extr(step)+(1-z_extr(step)) (C_org_in_IS('6','1','Zr',st»
ep)-C_org_IS('1','50','Zr',step))) *100)*z_step_IS(step)*z»
_step_zr(step);
1120 Eq_E_Ru_IS(step)..E_IS('Ru',step)*((C_aq_in_IS('1','1','Ru',step)*z_extr(step»
))+(1-z_extr(step))*C_org_in_IS('6','1','Ru',step)))*z_step_ru(step)=e=(»
((C_aq_in_IS('1','1','Ru',step)-C_aq_IS('6','50','Ru',step)) »
z_extr(step)+(1-z_extr(step)) (C_org_in_IS('6','1','Ru',ste»
p)-C_org_IS('1','50','Ru',step))) *100)*z_step_IS(step)*z_»
step_Ru(step);
1121 Eq_E_Tc_IS(step)..E_IS('Tc',step)*(C_aq_in_IS('1','1','Tc',step)*z_extr(step)»
+(1-z_extr(step))*C_org_in_IS('6','1','Tc',step))=e=(((C»
_aq_in_IS('1','1','Tc',step)-C_aq_IS('6','50','Tc',step)) *z_extr(s»
tep)+(1-z_extr(step))* (C_org_in_IS('6','1','Tc',step)-C_org_IS('1','5»
0','Tc',step))) *100)*z_step_IS(step);
1122 Eq_E_HNO2_IS(step)..E_IS('HNO2',step)*(C_aq_in_IS('1','1','HNO2',step)*z_extr»
(step)+(1-z_extr(step))*C_org_in_IS('6','1','HNO2',step))=e=((»
(C_aq_in_IS('1','1','HNO2',step)-C_aq_IS('6','50','HNO2',step)) »
z_extr(step)+(1-z_extr(step)) (C_org_in_IS('6','1','HNO2',step)-C»
_org_IS('1','50','HNO2',step))) *100)*z_step_IS(step);
1123 Eq_E_Np_IS(step)..E_IS('Np_V',step)*((C_aq_in_IS('1','1','Np_V',step)+C_aq_in»
_IS('1','1','Np_IV',step)+C_aq_in_IS('1','1','Np_VI',step))*z_extr(step)+(1-z»
_extr(step))*(C_org_in_IS('6','1','Np_V',step)+C_org_in_IS('6','1','Np_IV',st»
ep)+C_org_in_IS('6','1','Np_VI',step)))=e=(((C_aq_in_IS(»

'1','1','Np_V',step)-C_aq_IS('6','50','Np_V',step)+C_aq_in_IS('1','1','Np_IV'»
,step)-C_aq_IS('6','50','Np_IV',step)+C_aq_in_IS('1','1','Np_VI',step)-C_aq_I»
S('6','50','Np_VI',step)) *z_extr(step)+(1-z_extr(step))* (C»
_org_in_IS('6','1','Np_V',step)-C_org_IS('1','50','Np_V',step)+C_org_in_IS('6»
','1','Np_IV',step)-C_org_IS('1','50','Np_IV',step)+C_org_in_IS('6','1','Np_V»
I',step)-C_org_IS('1','50','Np_VI',step))) *100)*z_step_IS(»
step);

1124

1125

1126

1127 *further parameters implemented for the flowsheet

1128 parameter

1129 recycle_ratio_aq(k2) parameter for recycle of aqueous streams

1130 recycle_ratio_org(k2) parameter for recycle of organic streams

1131 recycle_org(k2) parameter for recycle of organic streams

1132 recycle_aq(k2) parameter for recycle of aqueous streams

1133 C0_scrub2(k2,comp) parameter used for initialisation

1134 recycle_ratio(k2) recycle ratio for mass balances in the flowsheet

1135 ;

1136

1137 recycle_ratio('aq')=1;

1138 recycle_ratio('org')=0;

1139 recycle_org(k2)=0;

1140 recycle_aq(k2)=0;

1141 recycle_org('org')=1;

1142 recycle_aq('aq')=1;

1143 recycle_ratio_org(k2)=0 ;

1144 recycle_ratio_org('org')=1 ;

1145 recycle_ratio_aq('aq')=1;

1146 recycle_ratio_aq('org')=0;

1147

1148

1149 *variables for flowsheet

1150

1151 Positive variable

1152 Vdot_out(k2,step) outlet volumetric flow rate

1153 chi recycle ratio

1154 psi(j,step) discharge ratio

1155 V_inlet_prev(k2,step) volume flow rate of streams coming from the previous»
unit operations (or fixed) [L hr-1]

1156 V_fresh(k2,step) volume flow rate of new streams [L h-1]

1157 C_fresh(k2,comp,step) new streams concentration - not valid for scrubbing »
sections - valid for main extr and costrip- see C_in_HNO3_stage [mol m-3]

1158 C_HNO3_fresh(step) new streams concentration - not valid for scrubbing »
sections - valid for main extr and costrip - see C_in_HNO3_stage [mol m-3]

1159 V_inlet_fresh(k2,step) fresh volume flow rate of streams [L hr-1]

1160 C_HAN_fresh(step) HAN concentration in the fresh solution

1161 C_U_IV_fresh(step) U(IV) concentration in the fresh solution

1162 C_N2H5_fresh(step) N2H5 concentration in the fresh solution

1163

1164 ;

1165

1166 *initial guesses and bounds

1167 C_fresh.lo(k2,comp,step)=0;

1168 C_fresh.l(k2,comp,step)=0;

1169 C_fresh.l(k2,'HNO3',step)=0;

1170 C_fresh.up(k2,'HNO3',step)=15000;

1171 C_HNO3_fresh.l(step)=1000;

1172 C_HNO3_fresh.lo(step)=500;

1173 C_HNO3_fresh.up(step)=3000;

1174 C_N2H5_fresh.lo(step)=0;

1175 C_N2H5_fresh.up(step)=100;

1176

1177

1178 Equation

1179 eq_c_out_aq(comp,step)

1180 eq_c_out_org(comp,step)

1181 Eq_C_fresh(k2,comp,step)

1182 eq_C_inlet_flowsheet(k2,comp,step)

1183 Eq_Vdot_IS2_aq(j,step)

1184 Eq_Vdot_IS2_org(j,step)

1185 Eq_C_fresh3

1186 eq_V_inlet_flowsheet(k2,step)

1187 Eq_Vdot_out_aq(step)

1188 Eq_Vdot_out_org(step)

1189 Eq_Vdot_IS2_aq2(j)

1190 Eq_Vdot_IS2_org2(j,step)

1191 eq_V_inlet_fresh(k2,step)

1192 Eq_unit_main(j)

1193 Eq_unit_comp(j)

1194 Eq_Vinlet_main

1195 Eq_Vinlet_main_org

1196 Eq_Vinlet_scrub1

1197 Eq_Vinlet_comp_extr

1198 Eq_Vinlet_costrip

1199 Eq_Vinlet_ustrip

1200 Eq_Vdot_IS2_aq3(j)

1201 Eq_vdotconst_main(j)

1202 ;

1203

1204 *mass balances in the flowsheet

1205 Eq_Vdot_out_aq(step).. Vdot_out('aq',step)=e= Vdot_IS2('3','aq',step)*(1-z_s»

crub_hno3(step))+(sum(j,Vdot_IS(j,'aq',step)*units_IS2(j,step)*psi(j,step)*z(»

j,step)/sf))*(z_scrub_hno3(step));

1206 Eq_Vdot_out_org(step).. Vdot_out('org',step)=e= Vdot_IS2('3','org',step);

1207 Eq_Vdot_IS2_aq(j,step)..z(j,step)*Vdot_IS2(j,'aq',step)=e=(Vdot_IS(j,'aq',ste»

p)+V_fresh_costrip(j,step)*z(j,step))*units_IS2(j,step)/sf*z(j,step);

1208 Eq_Vdot_IS2_aq2(j)..Vdot_IS(j,'aq','co_strip') =e=z2(j)*Vdot_IS('1','aq','co_»

220

strip') + (1-z2(j))*(Vdot_IS(j-1,'aq','co_strip')+V_fresh_costrip(j-1,'co_str»
ip')) ;
1209 Eq_Vdot_IS2_aq3(j)..Vdot_IS2(j,'aq','co_strip')=e=z2(j)*Vdot_IS2('1','aq','co»
_strip') + (1-z2(j))*((Vdot_IS2(j-1,'aq','co_strip')+V_fresh_costrip(j-1,'co_»
strip')*z(j-1,'co_strip')*units_IS2(j-1,'co_strip')/sf+V_fresh_costrip(j,'co_»
strip')*z(j,'co_strip')*units_IS2(j-1,'co_strip')/sf));
1210 Eq_Vdot_IS2_org(j,step)..Vdot_IS2(j,'org',step)*z(j,step)=e=Vdot_IS(j,'org',s»
tep)*units_IS2(j,step)/sf *z(j,step) ;
1211 Eq_Vdot_IS2_org2(j,step)..Vdot_IS2(j,'org',step)*z(j,step)=e=Vdot_IS2('3','or»
g',step)*z(j,step) ;
1212 eq_V_inlet_flowsheet(k2,step)..V_inlet_prev(k2,step)=e=z_feed(step)*V_feed(k2»
) +(1-z_feed(step))*(1-z_inlet_fresh(k2,step))*(Vdot_out(k2,step-1));
1213 eq_V_inlet_fresh(k2,step)..V_inlet_fresh(k2,step)=e= z_inlet_fresh(k2,step)*»
((1-z_feed(step)) *Vdot_out(k2,step)) ;
1214   Eq_vdotconst_main(j)..Vdot_IS2('1','aq','main_extr_codec')=e=
Vdot_IS2(j,'aq'»
,'main_extr_codec');
1215 Eq_unit_main(j)..units_IS2('3','main_extr_codec')*z(j,'main_extr_codec')=e=
»
units_IS2(j,'main_extr_codec') *z(j,'main_extr_codec');
1216   Eq_unit_comp(j)..units_IS2('3','comp_extr_codec')*z(j,'comp_extr_codec')
=e= »
units_IS2(j,'comp_extr_codec')*z(j,'comp_extr_codec');
1217 eq_C_inlet_flowsheet(k2,comp,step)..C_in(k2,comp,step)=e=((z_feed(step)*(»
((C0(k2,comp)*(1-z_HNO3(k2,comp,step))+z_HNO3(k2,comp,step)*C_HNO3_fresh(step»
))) *V_feed('aq')+C_out(k2,comp,'scrub1_codec')*chi*Vdot_out('aq','scrub1_c»
odec')*recycle_ratio_aq(k2))/(V_feed('aq')+chi*Vdot_out('aq','scrub1_codec')*»
recycle_ratio_aq(k2))* recycle_aq(k2)+(1-z_feed(step))*(1-z_inlet_fresh(k2,st»
ep))*C_out(k2,comp,step-1)+C_fresh(k2,comp,step)+ (C0(k2,comp)* »
(Vdot_out('org','main_extr_codec')-Vdot_out('org','comp_extr_codec')*r»
ecycle_ratio_org(k2)) +C_out('org',comp,'comp_extr_codec')*Vdot_out('org','»
comp_extr_codec')*recycle_ratio_org(k2))/Vdot_out('org','main_extr_codec')*r»
ecycle_org(k2)*z_feed(step)) * (1-z_co_strip(step)) +z_co_strip(step)*((1-»

z_inlet_fresh(k2,step))*C_out(k2,comp,step-2) +z_HNO3(k2,comp,step)*C_HNO3_f»
resh(step)+z_red(k2,comp,step)*C_U_IV_fresh(step)+z_scav(k2,comp,step)*C_N2H5»
_fresh(step))) ;

1218   Eq_C_fresh(k2,comp,step)..C_fresh(k2,comp,step)=e=(1-
z_feed(step))*z_HNO3(k2,»
comp,step)*C_HNO3_fresh(step)*z_inlet_fresh(k2,step)+(1-z_feed(step))*(1-z_HN»
O3(k2,comp,step))*0;

1219 Eq_C_fresh3..C_HNO3_fresh('u_strip')=e=C_in_HNO3_stage('4','HNO3','u_strip');

1220 Eq_Vinlet_main..Vdot_out('aq','main_extr_codec')=e=V_feed('aq')+(Vdot_out('aq»
','scrub1_codec')*chi);

1221 Eq_Vinlet_main_org..Vdot_out('org','main_extr_codec')=e=V_inlet_fresh('org','»
main_extr_codec')+V_inlet_fresh('org','comp_extr_codec');

1222 Eq_Vinlet_scrub1.. Vdot_out('org','scrub1_codec')=e=V_inlet_prev('org','scrub»
1_codec');

1223 Eq_Vinlet_comp_extr..Vdot_out('aq','comp_extr_codec')=e=V_inlet_prev('aq','co»
mp_extr_codec')* (1-chi);

1224 Eq_Vinlet_costrip..Vdot_out('org','Co_strip')=e= V_inlet_prev('org','Co_stri»
p');

1225 Eq_Vinlet_ustrip..Vdot_out('org','u_strip')=e= V_inlet_prev('org','u_strip');»
;

1226 eq_c_out_aq(comp,step)..C_out('aq',comp,step)=e=C_aq_IS('6','50',comp,step)*(»
1-z_scrub_hno3(step))+sum(j,(C_aq_IS(j,'50',comp,step)*z(j,step)*Vdot_IS2(j,'»
aq',step)*psi(j,step)))/ (1e-4+ sum(j,(z(j,step)*Vdot_IS2(j,'aq',step)*psi(j»
,step))))*z_scrub_hno3(step) ;

1227 eq_c_out_org(comp,step)..C_out('org',comp,step)=e=C_org_IS('1','50',comp,step»
);

1228
1229 *used in case of initialisation to set the inlet concentration as parameters
1230 C0_scrub2('aq',comp)=0;
1231 C0_scrub2('org',comp)=0;
1232
1233
1234 variable

1235 tot_atc annualised total cost for all plant - million £per year

1236 Pu_U_ratio Pu U concentration ratio in the MOX product

1237 ;

1238

1239 equations

1240 eq_Pu_U_ratio

1241 ;

1242

1243 eq_Pu_U_ratio..Pu_U_ratio=e=(C_out('aq','Pu_III','co_strip')+C_out('aq','Pu_I»
V','co_strip'))/(C_out('aq','U_VI','co_strip')+C_out('aq','U_IV','co_strip'))»
;

1244

1245

1246 *initial guesses and bounds

1247 C_HNO3_fresh.l('scrub1_codec')=1500;

1248 C_HNO3_fresh.lo('scrub1_codec')=500;

1249 C_HNO3_fresh.up('scrub1_codec')=3000;

1250 C_HNO3_fresh.lo('U_strip')=1000 ;

1251 C_HNO3_fresh.up('U_strip')=11000 ;

1252 C_aq_IS.up(j,h,comp,step)=C0('aq',comp)*5;

1253 C_aq_IS.up(j,h,'N2h5',step)=2000;

1254 C_aq_IS.up(j,h,'HAN',step)=500;

1255 C_aq_IS.up(j,h,'Pu_III',step)=500;

1256 C_org_IS.up(j,h,comp,step)=C_aq_IS.up(j,h,comp,step);

1257 C_aq_IS.up(j,h,'U_VI',step)=1300;

1258 C_aq_IS.up(j,h,'U_IV',step)=C_aq_IS.up(j,h,'U_VI',step);

1259 C_aq_IS.up(j,h,'HNO3',step)=15000;

1260 C_aq_IS.up(j,h,'Np_V',step)=C0('aq','Np_V')*10;

1261 C_aq_IS.up(j,h,'Pu_IV',step)=C0('aq','Pu_IV')*10;

1262 C_aq_IS.up(j,h,'Pu_III',step)=100;

1263 C_org_IS.up(j,h,'Np_V',step)=C0('aq','Np_V')*10;

1264 C_org_IS.up(j,h,'U_VI',step)=1098;

1265 C_org_IS.up(j,h,'U_IV',step)=1098;

```
1266 C_org_IS.up(j,h,'HNO3',step)=1098;
1267 C_org_IS.up(j,h,'TBP',step)=1098;
1268 C_org_IS.up(j,h,'Pu_III',step)=1098/2;
1269 C_org_IS.up(j,h,'HNO3_2',step)=1098/2;
1270 C_org_IS.up(j,h,'N2H5',step)=0;
1271 C_org_IS.up(j,h,'HAN',step)=0;
1272 C_org_IS.up(j,h,'Np_VI',step)=C_org_IS.up(j,h,'Np_V',step) ;
1273 C_org_IS.up(j,h,'Np_IV',step)=C_org_IS.up(j,h,'Np_V',step) ;
1274 C_aq_IS.up(j,h,'Np_VI',step)=C_aq_IS.up(j,h,'Np_V',step) ;
1275 C_aq_IS.up(j,h,'Np_IV',step)=C_aq_IS.up(j,h,'Np_V',step) ;
1276 C_aq_eq_IS.up(j,h,comp,step)=C_aq_IS.up(j,h,comp,step);
1277 C_aq_in_IS.up(j,h,comp,step)=C_aq_IS.up(j,h,comp,step);
1278 C_org_in_IS.up(j,h,comp,step)=C_org_IS.up(j,h,comp,step);
1279 C_out.up('aq',comp,step)=C_aq_IS.up('1','1',comp,step);
1280 C_out.up('org',comp,step)=C_org_IS.up('1','1',comp,step);
1281 m_IS.up(j,h,'HNO3',step)=1;
1282 m_IS.up(j,h,'HNO3_2',step)=1;
1283 m_IS.up(j,h,'U_VI',step)=100;
1284 m_IS.up(j,h,'Np_VI',step)=100;
1285 m_IS.up(j,h,'Np_IV',step)=10;
1286 m_IS.up(j,h,'Zr',step)=50;
1287 m_IS.up(j,h,'Ru',step)=10;
1288 m_IS.up(j,h,'Tc',step)=50;
1289 m_IS.up(j,h,'HNO2',step)=50;
1290 D_Zr_IS.up(j,h,step)=15;
1291 C_NO3_IS.up(j,h,step)=13000;
1292 I_S_IS.up(j,h,step)=13;
1293 K_eq_IS.up(j,h,'U_VI',step)=1e7;
1294 K_eq_IS.up(j,h,'Pu_IV',step)=1e7;
1295 K_eq_IS.up(j,h,'HNO3_2',step)=10;
1296 K_eq_IS.up(j,h,'Zr',step)=100;
1297 K_eq_IS.up(j,h,'Ru',step)=10;
1298 K_eq_IS.up(j,h,'HNO3_2',step)=1000;
```

```
1299 K_eq_IS.up(j,h,'HNO3',step)=100;
1300 K_eq_IS.up(j,h,'zr',step)=1e10;
1301 m_IS.up(j,h,'Zr',step)=1e6;
1302 I_S_IS.up(j,h,step)=12 ;
1303 m_IS.up(j,h,'Zr',step)=1e7;
1304 k_eq_IS.up(j,h,'Zr',step)=1e10;
1305 m_IS.up(j,h,'Ru',step)=10;
1306 kla_IS.up(j,step)=.4;
1307 C_NO3_IS.up(j,h,'U_strip')=13000;
1308 I_S_IS.up(j,h,'U_strip')=13;
1309 K_eq_IS.up(j,h,'U_VI','U_strip')=1e7;
1310 K_eq_IS.up(j,h,'Pu_IV','U_strip')=1e7;
1311 K_eq_IS.up(j,h,'HNO3_2','U_strip')=10;
1312 K_eq_IS.up(j,h,'Zr','U_strip')=100;
1313 K_eq_IS.up(j,h,'Ru','U_strip')=10;
1314 K_eq_IS.up(j,h,'HNO3_2','U_strip')=1000;
1315 K_eq_IS.up(j,h,'HNO3','U_strip')=100;
1316 K_eq_IS.up(j,h,'zr','U_strip')=1e10;
1317 m_IS.up(j,h,'Zr','U_strip')=1e6;
1318 I_S_IS.up(j,h,'U_strip')=12 ;
1319 m_IS.up(j,h,'Zr','U_strip')=1e7;
1320 k_eq_IS.up(j,h,'Zr','U_strip')=1e10;
1321 m_IS.up(j,h,'Ru','U_strip')=10;
1322 C_NO3_IS.up(j,h,'comp_extr_codec')=13000;
1323 I_S_IS.up(j,h,'comp_extr_codec')=13;
1324 K_eq_IS.up(j,h,'U_VI','comp_extr_codec')=1e7;
1325 K_eq_IS.up(j,h,'Pu_IV','comp_extr_codec')=1e7;
1326 K_eq_IS.up(j,h,'HNO3_2','comp_extr_codec')=10;
1327 K_eq_IS.up(j,h,'Zr','comp_extr_codec')=100;
1328 K_eq_IS.up(j,h,'Ru','comp_extr_codec')=10;
1329 K_eq_IS.up(j,h,'HNO3_2','comp_extr_codec')=1000;
1330 K_eq_IS.up(j,h,'HNO3','comp_extr_codec')=100;
1331 K_eq_IS.up(j,h,'zr','comp_extr_codec')=1e10;
```

```
1332 m_IS.up(j,h,'Zr','comp_extr_codec')=1e6;
1333 I_S_IS.up(j,h,'comp_extr_codec')=12 ;
1334 m_IS.up(j,h,'Zr','comp_extr_codec')=1e7;
1335 k_eq_IS.up(j,h,'Zr','comp_extr_codec')=1e10;
1336 m_IS.up(j,h,'Ru','comp_extr_codec')=10;
1337 *————————————————————————————
1338 E_IS.lo('HNO3',step)=-1000;
1339 E_IS.lo('HNO2',step)=-1000;
1340 *————————————————————————————
1341
1342
1343
1344 variable
1345
1346 DF(comp) decontamination factors in codecontamination
1347 Extract(comp) extraction in codecontamination
1348 Rec_HLW(comp) recovery of contaminants in codecontamination
1349 ;
1350
1351 equations
1352
1353 eq_DF_Zr
1354 eq_DF_Tc
1355 eq_DF_Ru
1356 eq_DF_Np
1357 eq_Extract_U
1358 eq_Extract_Pu
1359 Eq_Rec_HLW_Zr
1360 Eq_Rec_HLW_Ru
1361 Eq_Rec_HLW_Tc
1362 Eq_Rec_HLW_Np
1363
1364 ;
```

1365

1366 eq_DF_Zr..DF('Zr')*((C_out('org','Zr','scrub1_codec'))*Vdot_out('org','scrub1»
_codec'))=e=C0('aq','Zr')*V_feed('aq'));

1367 eq_DF_Tc..DF('Tc')*((C_out('org','Tc','scrub1_codec'))*Vdot_out('org','scrub1»
_codec'))=e=C0('aq','Tc')*V_feed('aq'));

1368 eq_DF_Ru..DF('Ru')*((C_out('org','Ru','scrub1_codec'))*Vdot_out('org','scrub1»
_codec'))=e=C0('aq','Ru')*V_feed('aq'));

1369 eq_DF_Np..DF('Np_V')*((C_out('org','Np_V','scrub1_codec')+C_out('org','Np_VI'»
,'scrub1_codec')+C_out('org','Np_IV','scrub1_codec'))*Vdot_out('org','scrub1_»
codec'))=e=C0('aq','Np_V')*V_feed('aq'));

1370 Eq_Extract_U..Extract('U_VI')*(C0('aq','U_VI')*V_feed('aq'))=e=C_out('org','U»
_VI','scrub1_codec')*Vdot_out('org','scrub1_codec')*100;

1371 Eq_Extract_Pu..Extract('Pu_IV')*(C0('aq','Pu_IV')*V_feed('aq'))=e=C_out('org'»
,'Pu_IV','scrub1_codec')*Vdot_out('org','scrub1_codec')*100;

1372 Eq_Rec_HLW_Zr..Rec_HLW('zr')*(C0('aq','zr')*V_feed('aq'))=e=(C_out('aq','zr',»
'main_extr_codec')*Vdot_out('aq','main_extr_codec')+C_out('aq','zr','comp_ext»
r_codec')*Vdot_out('aq','comp_extr_codec') + sum(j,(C_aq_IS(j,'50','zr','scru»
b1_codec')*z(j,'scrub1_codec')*Vdot_IS2(j,'aq','scrub1_codec')*(1-psi(j,'scru»
b1_codec')))))*100;

1373 Eq_Rec_HLW_Ru..Rec_HLW('Ru')*(C0('aq','Ru')*V_feed('aq'))=e=(C_out('aq','Ru',»
'main_extr_codec')*Vdot_out('aq','main_extr_codec')+C_out('aq','Ru','comp_ext»
r_codec')*Vdot_out('aq','comp_extr_codec') + sum(j,(C_aq_IS(j,'50','ru','scru»
b1_codec')*z(j,'scrub1_codec')*Vdot_IS2(j,'aq','scrub1_codec')*(1-psi(j,'scru»
b1_codec')))))*100;

1374 Eq_Rec_HLW_Tc..Rec_HLW('Tc')*(C0('aq','Tc')*V_feed('aq'))=e=(C_out('aq','Tc',»
'main_extr_codec')*Vdot_out('aq','main_extr_codec')+C_out('aq','Tc','comp_ext»
r_codec')*Vdot_out('aq','comp_extr_codec') + sum(j,(C_aq_IS(j,'50','tc','scru»
b1_codec')*z(j,'scrub1_codec')*Vdot_IS2(j,'aq','scrub1_codec')*(1-psi(j,'scru»
b1_codec')))))*100;

1375 Eq_Rec_HLW_Np..Rec_HLW('Np_V')*(C0('aq','Np_V')*V_feed('aq'))=e=((C_out('aq'»
'Np_V','main_extr_codec')+C_out('aq','Np_VI','main_extr_codec')+C_out('aq','N»
p_IV','main_extr_codec'))*Vdot_out('aq','main_extr_codec')+(C_out('aq','Np_V'»
,'comp_extr_codec')+C_out('aq','Np_VI','comp_extr_codec')+C_out('aq','Np_IV',»

227

'comp_extr_codec'))*Vdot_out('aq','comp_extr_codec') + sum(j,(C_aq_IS(j,'50',»
'NP_IV','scrub1_codec')*z(j,'scrub1_codec')*Vdot_IS2(j,'aq','scrub1_codec')*(»
1-psi(j,'scrub1_codec')))) + sum(j,(C_aq_IS(j,'50','NP_V','scrub1_codec')*z(j»
,'scrub1_codec')*Vdot_IS2(j,'aq','scrub1_codec')*(1-psi(j,'scrub1_codec')))) »
+ sum(j,(C_aq_IS(j,'50','NP_VI','scrub1_codec')*z(j,'scrub1_codec')*Vdot_IS2(»
j,'aq','scrub1_codec')*(1-psi(j,'scrub1_codec')))))))*100;

1376
1377 *initial guesses and bounds
1378 DF.lo('Zr')=1e4;
1379 DF.lo('Ru')=1e4;
1380 extract.lo('U_VI')=99;
1381 extract.lo('Pu_IV')=99;
1382 q_IS.lo(j,'comp_extr_codec')=0.1;
1383 q_IS.up(j,'comp_extr_codec')=5;
1384 q_IS.lo(j,'scrub1_codec')=0.1;
1385 q_IS.up(j,'scrub1_codec')=5;
1386 q_IS.lo(j,'co_strip')=0.1;
1387 q_IS.up(j,'u_strip')=3;
1388 e_is.lo('Hno3',step)=-1000;
1389 E_IS.lo('HNO2',step)=-1000;
1390 C_HNO3_fresh.lo('U_strip')=50 ;
1391 C_HNO3_fresh.up('U_strip')=1000;
1392 vel_IS.lo(j,k,step)=0.0001;
1393 N_IS.up(step)=6;
1394 L_scale_IS.up('4',k_man,step)=2;
1395 E_IS.lo('u_vi',step)=0.01;
1396 L_scale_IS.up('4',k_man,step)=2;
1397 L_scale_IS.up('1',k_man,step)=.2;
1398 L_scale_IS.up('1',k_man,step)=.2;
1399 kla_is.up(j,step)=.8;
1400 n_elem_is.lo('1',step)= 30 ;
1401 n_elem_is.up('1',step)= 70 ;
1402 n_elem_is.lo('2',step)= 10 ;

1403 n_elem_is.up('2',step)= 50 ;

1404 n_elem_is.lo('3',step)= 2 ;

1405 n_elem_is.up('3',step)= 10 ;

1406 r_ratio_is.up(scale,k_man,step)=5e6;

1407 a_Fd.l(scale,k_man,step)=.001;

1408 a_Fd.up(scale,k_man,step)=5;

1409 b_Fd.l(scale,k_man,step)=.03;

1410 b_Fd.up(scale,k_man,step)=1;

1411 b_Fd.up('1',k_man,step)=9e9;

1412

1413

1414 *sbb as minlp solver

1415 option minlp=sbb;

1416 option optcr=0.01;

1417

1418 integer variables

1419 N_elem_IS2(j,scale,step) ;

1420

1421 *further variables, redefined to allow the cross flow configuration in the fl»
owsheet

1422 positive variables

1423 Vdot_scale_IS2(j,scale,k_man,step) volumetric flowrate within flow network »
scale [cm3 h-1]

1424 L_scale_IS2(j,scale,k_man,step) length of elements in each scale and pha»
se [m]

1425 W_scale_IS2(j,scale,k_man,step) width of elements in each scale and phas»
e [m]

1426 Sigma_Vdot_out(j,scale,k_man,step) sum of volume flow rate for DP calculati»
ons in manifolds [cm3 h-1]

1427 DP_IS2(j,scale,k_man,step) total pressure drop in each scale [kPa]

1428 DP_fr_IS2(j,scale,k_man,step) frictional pressure drop in each scale [»
kPa]

1429 DP_sin_IS2(j,scale,k_man,step) singularities pressure drop in each scal»

e [kPa]

1430 R_sin_IS2(j,scale,k_man,step) singularities hydraulic resistances in e»
ach scale and phase [Pa s m-3]

1431 R_IS2(j,scale,k_man,step) hydraulic resistances in each scale and »
phase [Pa s m-3]

1432 R_ratio_IS2(j,scale,k_man,step) resistance ratio

1433 R_eq_IS2(j,scale,k_man,step) equivalent hydraulic resistances in eac»
h scale and phase [Pa s m-3]

1434 Fd_IS2(j,scale,k_man,step) flow maldistribution in each scale

1435 L_scale_min_IS2(j,scale,k_man,step) minimum length of elements in each scale»
and phase [m]

1436 DP_sep_IS2(j,sep,step) frictional pressure drop in the separato»
r [kPa]

1437 D_sep_IS2(j,sep,step) separator diameter [m]

1438 L_sep_IS2(j,sep,step) separator length [m]

1439 DP_Ch_Y_IS2(j,step) total pressure drop within channel + at »
Y junction [kPa]

1440 DP_fr_Ch_IS2(j,i,step) frictional pressure drop within channel [kPa]

1441 DP_int_IS2(j,step) interfacial pressure drop within channel [kPa]

1442 DP_Y_IS2(j,step) local pressure drop at Y junction [kPa]

1443 Vdot_sep_IS2(j,sep,step) volume flow rate within separator [cm3 h»
r-1]

1444 vel_scale_IS2(j,scale,k_man,step) superficial velocity in each scale [m s-»
1]

1445 tee_cost_IS2(j,step) tee cost [£]

1446 ATC_IS2(j,step) Annualised Total Cost [£]

1447 Man_cost_IS2(j,step) estimation of manifolds cost [£]

1448 Ch_cost_IS2(j,step) estimation of channel cost [£]

1449 Oper_cost_IS2(j,step) operating cost [£]

1450 sep_cost_IS2(j,step) estimation of separator cost [£]

1451 A_Scheiff_IS2 coeff for separator calcuation

1452 Fdtot_IS2 total malflowdistribution

1453 a_Fd2(j,scale,k_man,step) coeff for maldistribution calculation

1454 b_Fd2(j,scale,k_man,step) coeff for maldistribution calculation
1455 Re_IS2(j,scale,k_man,step) Reynolds number in the manifold
1456 sep_cost_step(step) cost of separator
1457 tub_cost_step(step) cost of tubings
1458 man_cost_step(step) cost of manifolds
1459 oper_cost_step(step) operating cost
1460 ATC_cost_step(step) total annualised cost per step
1461 HNO3_fresh_scrub(j) fresh HNO3 conc in the scrubbing
1462 ;
1463
1464 variable
1465 total_ann_cost_plant total annualised cost of the plant
1466 ;
1467
1468 *intial guesses and bounds
1469 L_IS.lo(step)=L;
1470 a_Fd2.l(j,scale,k_man,step)=.001;
1471 a_Fd2.up(j,scale,k_man,step)=.02;
1472 b_Fd2.l(j,scale,k_man,step)=.03;
1473 b_Fd2.up(j,scale,k_man,step)=.3;
1474 b_Fd2.up(j,'1',k_man,step)=1e6;
1475 Fdtot_IS2.up(j,k_man,step)=10;
1476 A_Scheiff_IS2.up(j,step)=10;
1477 DP_fr_IS2.up(j,scale,k_man,step)=100;
1478 DP_sin_IS2.up(j,scale,k_man,step)=100;
1479 vel_scale_IS2.lo(j,scale,k_man,step)=1e-5 ;
1480 DP_fr_IS2.up(j,scale,k_man,step)=10;
1481 DP_sin_IS2.up(j,scale,k_man,step)=1;
1482 R_IS2.lo(j,scale,k_man,step)=0;
1483 R_IS2.up(j,scale,k_man,step)=1e8;
1484 R_eq_IS2.lo(j,scale,k_man,step)=0;
1485 R_eq_IS2.up(j,scale,k_man,step)=1e8;
1486 Fd_IS2.lo(j,scale,k_man,step)=0;

```
1487 Fd_IS2.up(j,scale,k_man,step)=10;
1488 L_scale_IS2.up(j,'1',k_man,step)=.3;
1489 L_scale_IS2.up(j,'2',k_man,step)=1;
1490 L_scale_IS2.up(j,'3',k_man,step)=3;
1491 L_scale_IS2.up(j,'4',k_man,step)=6;
1492 W_scale_IS2.lo(j,scale,k_man,step)=1e-3;
1493 W_scale_IS2.up(j,scale,k_man,step)=10;
1494 W_scale_IS2.up(j,'1',k_man,step)=.003;
1495 W_scale_IS2.up(j,'2',k_man,step)=.05;
1496 W_scale_IS2.up(j,'3',k_man,step)=.5;
1497 W_scale_IS2.up(j,'4',k_man,step)=5;
1498 R_ratio_IS2.lo(j,scale,k_man,step)=2500;
1499 R_ratio_IS2.up(j,scale,k_man,step)=18000;
1500 R_ratio_IS2.lo(j,'1',k_man,step)=1;
1501 R_ratio_IS2.L(j,'1',k_man,step)=1;
1502 R_ratio_IS2.up(j,'1',k_man,step)=1;
1503 DP_IS2.up(j,scale,K_man,step)=10;
1504 R_ratio_IS2.lo(j,'4',k_man,step)=0;
1505 R_ratio_IS2.up(j,'4',k_man,step)=1e8;
1506 vel_scale_IS2.up(j,scale,k_man,step)=.1;
1507 L_scale_IS2.up(j,'2',k_man,step)=.6;
1508 L_scale_IS2.up(j,'3',k_man,step)=2;
1509 L_scale_IS2.up(j,'4',k_man,step)=1;
1510 W_scale_IS2.up(j,'2',k_man,step)=.3;
1511 W_scale_IS2.up(j,'3',k_man,step)=1;
1512 W_scale_IS2.up(j,'4',k_man,step)=1;
1513 vel_scale_IS2.up(j,'4',k_man,step)=1;
1514 Re_IS2.up(j,scale,k_man,step)=2000;
1515 R_IS2.up(j,'3',k_man,step)=1000;
1516 R_IS2.up(j,'4',k_man,step)=100;
1517 W_scale_IS2.lo(j,'4',k_man,step)=0;
1518 vel_scale_IS2.lo(j,'4',k_man,step)=0;
1519 D_sep_IS2.lo(j,sep,step)=.0005;
```

1520 D_sep_IS2.up(j,sep,step)=.002;

1521 L_sep_IS2.lo(j,sep,step)=.01;

1522 L_sep_IS2.up(j,sep,step)=.5;

1523

1524

1525 equations

1526 Eq_N_2_IS2(j,step)

1527 Eq_N_3_IS2(j,step)

1528 Eq_N_4_IS2(j,step)

1529 Eq_DP_IS2(j,scale,k_man,step)

1530 Eq_DP_fr_IS2(j,scale,k_man,step)

1531 Eq_DP_sin_IS2(j,scale,k_man,step)

1532 Eq_R_IS2(j,scale,k_man,step)

1533 Eq_R_sin_IS2(j,scale,k_man,step)

1534 Eq_R_ratio_IS2(j,scale,k_man,step)

1535 Eq_R_eq_IS2(j,scale,k_man,step)

1536 Eq_W_IS2(j,k_man,step)

1537 Eq_Re_IS2(j,scale,k_man,step)

1538 Eq_Vdot_scale_1_aq_IS2(j,step)

1539 Eq_Vdot_scale_1_org_IS2(j,step)

1540 Eq_Vdot_scale_2_IS2(j,k_man,step)

1541 Eq_Vdot_scale_3_IS2(j,k_man,step)

1542 Eq_Vdot_scale_4_IS2(j,k_man,step)

1543 Eq_vel_scale_IS2(j,scale,k_man,step)

1544 Eq_L_scale_IS2(j,scale,k_man,step)

1545 Eq_L_scale_1_IS2(j,k_man,step)

1546 Eq_L_scale_min_IS2(j,scale,k_man,step)

1547 Eq_W_constr_IS2(j,scale,k_man,step)

1548 Eq_Sigma_Vdot_out(j,scale,k_man,step)

1549 Eq_N_el_contr_IS2(j,scale,step)

1550 Eq_sep_cost_IS2(j,step)

1551 Eq_ATC_IS2(j,step)

1552 Eq_tub_cost_IS2(j,step)

1553 Eq_tee_cost_IS2(j,step)

1554 Eq_man_cost_IS2(j,step)

1555 Eq_oper_cost_IS2(j,step)

1556 Eq_DP_Ch_Y_IS2(j,step)

1557 Eq_DP_fr_Ch_IS2(j,i,step)

1558 Eq_DP_int_IS2(j,step)

1559 Eq_DP_Y_IS2(j,step)

1560 Eq_sep_cost_step(step)

1561 Eq_tub_cost_step(step)

1562 Eq_man_cost_step(step)

1563 Eq_oper_cost_step(step)

1564 Eq_ATC_cost_step(step)

1565 Eq_total_ann_cost_plant

1566

1567 ;

1568

1569 *calculation of number of elements in levels 2, 3 and 4

1570 Eq_N_2_IS2(j,step)..(N_elem_IS2(j,'1',step)*N_elem_IS2(j,'2',step)*N_elem_IS2»
(j,'3',step))*z(j,step) =e=Units_IS2(j,step)*z(j,step);

1571 Eq_N_3_IS2(j,step)..N_elem_IS2(j,'3',step)=g=N_elem_IS2(j,'4',step)+1;

1572 Eq_N_4_IS2(j,step)..N_elem_IS2(j,'4',step)=e=1-(1-scale4_on_off('4'));

1573 Eq_N_el_contr_IS2(j,scale,step)..z(j,step)*N_elem_IS2(j,scale+1,step)=l=N_ele»
m_IS2(j,scale,step)*z(j,step);

1574

1575 *pressure drop calculations

1576   Eq_DP_IS2(j,scale,k_man,step)..DP_IS2(j,scale,k_man,step)=e=(
(DP_fr_IS2(j,sc»
ale,k_man,step)+DP_sin_IS2(j,scale,k_man,step)*singular(scale))*scale4_on_off»
(scale))*z_step_IS(step);

1577 Eq_DP_fr_IS2(j,scale,k_man,step)..DP_fr_IS2(j,scale,k_man,step)*(N_elem_IS2(j»
,scale-1,step)-1)=e=((N_elem_IS2(j,scale-1,step)-1)*z_scale(scale)*(sum(i,DP_»
fr_Ch_IS2(j,i,step))+0*2)+(1-z_scale(scale))*scale4_on_off(scale)*Sigma_Vdot_»
out(j,scale,k_man,step)/sf/sf/3600*R_IS2(j,scale,k_man,step))*z_step_IS(step)»

234

;

1578 Eq_DP_sin_IS2(j,scale,k_man,step)..DP_sin_IS2(j,scale,k_man,step)=e=(z_scale(»
scale)*(DP_int_IS2(j,step)+DP_Y_IS2(j,step))+(1-z_scale(scale))*scale4_on_off»
(scale)*(Vdot_scale_IS2(j,scale,k_man,step)/sf/sf/3600*R_sin_IS2(j,scale,k_ma»
n,step)))*z_step_IS(step);

1579 Eq_DP_Ch_Y_IS2(j,step)..DP_Ch_Y_IS2(j,step)=e=(sum(i,DP_fr_ch_IS2(j,i,step))+»
DP_int_IS2(j,step)+DP_Y_IS2(j,step))*z_step_IS(step);

1580 Eq_DP_fr_Ch_IS2(j,i,step)..DP_fr_ch_IS2(j,i,step)=e=((8*mu_DP(i,step)*vel_is(»
j,'mix',step)*costDP(i)*L)/(D_IS(step)/2)**2/sf)*z_step_IS(step);

1581 Eq_DP_int_IS2(j,step)..DP_int_IS2(j,step)=e=(gamma*costheta/(D_IS(step)/2)/sf»
*(2*L_IS(step)-Luc)/Luc)*z_step_IS(step);

1582 Eq_DP_Y_IS2(j,step)..DP_Y_IS2(j,step)=e=(0.5*rho_cont(step)*vel_is(j,'mix',st»
ep)**2*Const_DP_Y)*z_step_IS(step);

1583

1584 *hydraulic resistances and size of distributors

1585 Eq_R_IS2(j,scale,k_man,step)..z(j,step)*R_IS2(j,scale,k_man,step)*(sf*(W_scal»
e_IS2(j,scale,k_man,step)**4))=e=(z_scale(scale)*sf*(W_scale_IS2(j,scale,k_ma»
n,step)**4)*((DP_Ch_Y_IS2(j,step)+0*2)/(vdot_is(j,'mix',step)/1e6/3600))+(1-z»
_scale(scale))*(28.5*mu_man(k_man)*L_scale_IS2(j,scale,k_man,step))*scale4_on»
_off(scale))*z_step_IS(step)*z(j,step);

1586 Eq_R_sin_IS2(j,scale,k_man,step)..z(j,step)*R_sin_IS2(j,scale,k_man,step)*(2*»
W_scale_IS2(j,scale,k_man,step)**2)=e=((1-z_scale(scale))*scale4_on_off(scale»
)*(((psi_s+psi_c+psi_t)+(psi_m+psi_e+psi_t))*rho_man(k_man)*vel_scale_IS2(j,s»
cale,k_man,step)/sf))*z_step_IS(step)*z(j,step);

1587 Eq_R_ratio_IS2(j,scale,k_man,step)..z(j,step)*R_ratio_IS2(j,scale,k_man,step)»
*R_IS2(j,scale,k_man,step)=e=(z_scale(scale)*R_IS2(j,scale,k_man,step)+(1-z_s»
cale(scale))*scale4_on_off(scale)*R_eq_IS2(j,scale-1,k_man,step))*z_step_IS(s»
tep);

1588 Eq_R_eq_IS2(j,scale,k_man,step)..z(j,step)*R_eq_IS2(j,scale,k_man,step)*(Vdot»
_scale_IS2(j,scale,k_man,step)/1e6/3600)=e=(z_scale(scale)*(Vdot_scale_IS2(j,»
scale,k_man,step)/1e6/3600)*R_IS2(j,scale,k_man,step)+(1-z_scale(scale))*scal»
e4_on_off(scale)*(DP_IS2(j,scale,k_man,step)+DP_IS2(j,scale-1,k_man,step)+DP_»
IS2(j,scale-2,k_man,step)+DP_IS2(j,scale-3,k_man,step)))*z_step_IS(step)*z(j,»

step);

1589 Eq_W_IS2(j,k_man,step)..z(j,step)*W_scale_IS2(j,'1',k_man,step)=e=(D_IS(step)»
)*z_step_IS(step)*z(j,step);

1590 Eq_L_scale_1_IS2(j,k_man,step)..z(j,step)*L_scale_IS2(j,'1',k_man,step)=e=(L)»
*z_step_IS(step)*z(j,step);

1591 Eq_L_scale_min_IS2(j,scale,k_man,step)..z(j,step)*L_scale_min_IS2(j,scale,k_m»
an,step)=e=((z_scale(scale)*L+(1-z_scale(scale))*3*W_scale_IS2(j,scale-1,k_ma»
n,step)*(N_elem_IS2(j,scale-1,step)-1)))*z_step_IS(step)*z(j,step);

1592 Eq_W_constr_IS2(j,scale,k_man,step)..z(j,step)*W_scale_IS2(j,scale,k_man,step»
)=g=(W_scale_IS2(j,scale-1,k_man,step)*scale4_on_off(scale))*z_step_IS(step)*»
z(j,step);

1593

1594 *Reynolds number

1595 Eq_Re_IS2(j,scale,k_man,step)..z(j,step)*Re_IS2(j,scale,k_man,step)=e=(z_scal»
e(scale)*rho_cont(step)*vel_is(j,'mix',step)*D_IS(step)/mu_cont(step)+(1-z_sc»
ale(scale))*rho_man(k_man)*vel_scale_IS2(j,scale,k_man,step)*W_scale_IS(scale»
,k_man,step)/mu_man(k_man))*z_step_IS(step)*z(j,step);

1596

1597 *flow rates and velocities

1598 Eq_Vdot_scale_1_aq_IS2(j,step)..z(j,step)*Vdot_scale_IS2(j,'1','aq',step)=e=(»
vdot_is(j,'aq',step))*z_step_IS(step)*z(j,step);

1599 Eq_Vdot_scale_1_org_IS2(j,step)..z(j,step)*Vdot_scale_IS2(j,'1','org',step)=e»
=(vdot_is(j,'org',step)) *z_step_IS(step)*z(j,step);

1600 Eq_Vdot_scale_2_IS2(j,k_man,step)..z(j,step)*Vdot_scale_IS2(j,'2',k_man,step)»
=e=(Vdot_scale_IS2(j,'1',k_man,step)*N_elem_IS2(j,'1',step)) *z_step_IS(step)»
*z(j,step);

1601 Eq_Vdot_scale_3_IS2(j,k_man,step)..z(j,step)*Vdot_scale_IS2(j,'3',k_man,step)»
=e=(Vdot_scale_IS2(j,'2',k_man,step)*N_elem_IS2(j,'2',step)) *z_step_IS(step)»
*z(j,step);

1602 Eq_Vdot_scale_4_IS2(j,k_man,step)..z(j,step)*Vdot_scale_IS2(j,'4',k_man,step)»
=e=(Vdot_scale_IS2(j,'3',k_man,step)*N_elem_IS2(j,'3',step))*z_step_IS(step) »
*z(j,step);

1603 Eq_vel_scale_IS2(j,scale,k_man,step)..z(j,step)*vel_scale_IS2(j,scale,k_man,s»

tep)*(W_scale_IS2(j,scale,k_man,step)**2)=e=(Vdot_scale_IS2(j,scale,k_man,ste»
p)/1e6/3600)*z_step_IS(step)*z(j,step);

1604 Eq_L_scale_IS2(j,scale,k_man,step)..z(j,step)*L_scale_IS2(j,scale,k_man,step)»
=e=(L_scale_min_IS2(j,scale,k_man,step))*z_step_IS(step)*z(j,step);

1605 Eq_Sigma_Vdot_out(j,scale,k_man,step)..z(j,step)*Sigma_Vdot_out(j,scale,k_man»
,step)=e=(z_scale(scale)*0+(1-z_scale(scale))*Vdot_scale_IS2(j,scale,k_man,st»
ep)*(0.5*N_elem_IS2(j,scale-1,step)**2-0.5*N_elem_IS2(j,scale-1,step)))*z_ste»
p_IS(step)*z(j,step);

1606

1607 *costs / separator not considered

1608 Eq_sep_cost_IS2(j,step)..Sep_cost_IS2(j,step)=e=0;

1609   Eq_ATC_IS2(j,step)..ATC_IS2(j,step)=e=(oper_cost_IS2(j,step)   +
(Ch_cost_IS2(j»
,step) +Sep_cost_IS2(j,step) + Man_cost_IS2(j,step)) * int*(1+int)**n_y/((1+i»
nt)**n_y-1))*z_step_IS(step)*z(j,step);

1610 Eq_tub_cost_IS2(j,step)..Ch_cost_IS2(j,step)=e=(((cost_A('poly')*D_IS(step)+c»
ost_B('poly'))*Teflon_cost_corr*z_disp(step) + (cost_A('SS')*D_IS(step)+cost»
_B('SS'))*(1-z_disp(step)))*L_IS(step)*Units_IS2(j,step))*z_step_IS(step)*z»
(j,step);

1611 Eq_tee_cost_IS2(j,step)..tee_cost_IS2(j,step)=e=((N_elem_IS2(j,'3',step)+N_el»
em_IS2(j,'3',step)*N_elem_IS2(j,'2',step)+N_elem_IS2(j,'3',step)*N_elem_IS2(j»
,'2',step)*N_elem_IS2(j,'1',step))*Tee_cost_single*Teflon_cost_corr)*z_step_I»
S(step)*z(j,step);

1612 Eq_man_cost_IS2(j,step)..Man_cost_IS2(j,step)=e=(sum(subset_scale,sum(k_man,(»
(cost_A('poly')*W_scale_IS2(j,subset_scale,k_man,step)+cost_B('poly'))*L_scal»
e_IS2(j,subset_scale,k_man,step)))*N_elem_IS2(j,subset_scale,step))*Teflon_co»
st_corr +tee_cost_IS2(j,step))*z_step_IS(step)*z(j,step);

1613 Eq_oper_cost_IS2(j,step)..Oper_cost_IS2(j,step)=e=((sum(k_man,sum(scale,DP_IS»
2(j,scale,k_man,step))*units_IS2(j,step)*Vdot_scale_IS2(j,'1',k_man,step)))* »
sf/eta/sf*cm3h_to_m3s*Energy_price*h_to_yr)*z_step_IS(step)*z(j,step);

1614 Eq_total_ann_cost_plant..total_ann_cost_plant=e=sum(step,ATC_cost_step(step))»
/1e6;

1615 Eq_sep_cost_step(step)..sep_cost_step(step)=e=sum(j,Sep_cost_IS2(j,step));

1616 Eq_tub_cost_step(step)..tub_cost_step(step)=e=sum(j,Ch_cost_IS2(j,step));

1617 Eq_man_cost_step(step)..man_cost_step(step)=e=sum(j,Man_cost_IS2(j,step));

1618 Eq_oper_cost_step(step)..oper_cost_step(step)=e=sum(j,Oper_cost_IS2(j,step));

1619 Eq_ATC_cost_step(step)..ATC_cost_step(step)=e=sum(j,ATC_IS2(j,step));

1620

1621

1622

1623 Model super7 /all/;

1624

1625

1626 *initial guesses and bounds

1627 N_IS.lo('comp_extr_codec')=1;

1628 R_ratio_IS2.up(j,scale,k_man,step)= 1e8;

1629 L_scale_IS2.up(j,'1',k_man,step)= .2;

1630 L_scale_IS2.up(j,'2',k_man,step)=.6;

1631 L_scale_IS2.up(j,'3',k_man,step)=2;

1632 L_scale_IS2.up(j,'4',k_man,step)=2;

1633 C_fresh_ustrip.fx(j,comp,step)=0;

1634 C_fresh_ustrip.l(j,'HNO3',step)=C_aq_in_IS.l(j,'1','HNO3',step);

1635 C_fresh_ustrip.up(j,'HNO3',step)=8000;

1636 C_fresh_ustrip.lo(j,'HNO3',step)=50;

1637 C_in_HNO3_stage.fx(j,comp,step)=0;

1638 C_in_HNO3_stage.lo(j,'HNO3','u_strip') =10;

1639 C_in_HNO3_stage.up(j,'HNO3','u_strip') =1000;

1640 C_in_HNO3_stage.lo(j,'HNO3','scrub1_codec')=10;

1641 C_in_HNO3_stage.up(j,'HNO3','scrub1_codec')=8000;

1642 chi.up=0.95;

1643 chi.lo=0.00;

1644 df.lo('tc')=50;

1645 N_elem_IS2.l(j,scale,step) =10;

1646 vdot_is2.l(j,k2,step)=100;

1647 N_elem_IS2.up(j,'2',step)= 30 ;

1648 N_elem_IS2.up(j,'3',step)= 30 ;

```
1649 N_elem_IS2.lo(j,'2',step)= 2 ;
1650 N_elem_IS2.lo(j,'3',step)= 2 ;
1651 DP_sin_IS2.up(j,'4',k_man,step)=10;
1652 DF.lo('zr')=1e4;
1653 DF.up('tc')=100;
1654 DF.up('np_v')=100;
1655 E_IS.lo('u_vi','co_strip')=0;
1656 R_ratio_IS2.lo(j,'2',k_man,step)=10000;
1657 N_elem_IS2.up(j,'1',step)=70;
1658 R_ratio_IS2.lo(j,'3',k_man,step)=10000;
1659 E_IS.lo('u_vi','u_strip')=99;
1660 E_IS.lo('pu_iv','co_strip')=(99);
1661 Pu_U_ratio.lo=.1;
1662 C_fresh_costrip.lo(j,'HNO3','co_strip') =50;
1663 C_HNO3_fresh.lo('co_strip') =50;
1664 vel_IS.lo(j,k,step)=0.001;
1665 V_fresh_costrip.up(j,'co_strip') =50;
1666 C_fresh_costrip.up(j,'HNO3','co_strip') =2000;
1667 C_out.l('org',comp,'co_strip')=1;
1668 N_elem_IS2.up(j,'1',step)= 70;
1669 N_elem_IS2.lo(j,'1',step)= 60 ;
1670 N_elem_IS2.up(j,'2',step)= 30 ;
1671 N_elem_IS2.lo(j,'2',step)=5;
1672 N_elem_IS2.up(j,'3',step)= 5;
1673 N_elem_IS2.lo(j,'3',step)= 25;
1674 C_HNO3_fresh.up('scrub1_codec')=7000;
1675 N_elem_IS2.up(j,'2',step)= 40;
1676 N_elem_IS2.up(j,'3',step)= 40;
1677 C_HNO3_fresh.lo('main_extr_codec')= 2500 ;
1678 DF.up('tc')=1000;
1679
1680 *parameters
1681 z_step_zr('co_strip')=1;
```

```
1682 z_step_zr('u_strip')=0;
1683 z_step_ru('co_strip')=0;
1684 z_step_ru('u_strip')=0;
1685
1686 *load initialisation (needed for bounds)
1687 EXECUTE_LOADPOINT 'coex_novel_minlp6.gdx' ;
1688 N_elem_IS2.fx(j,scale,step)= N_elem_IS2.l(j,scale,step) ;
1689 z.fx(j,step)=z.l(j,step);
1690 V_fresh_costrip.fx(j,step) = 0;
1691 c_fresh_costrip.fx(j,comp,step) = 0;
1692 C0_scrub2('aq',comp)=0;
1693 C0_scrub2('org',comp)=0;
1694 C0_scrub2('org','U_Vi')= 295.546354982558 ;
1695 C0_scrub2('org','Pu_IV')= 4.94462918636543E-5;
1696 C0_scrub2('org','hno3')= 156.238131127856 ;
1697 C0_scrub2('org','hno3_2')= 33.9813539920522;
1698 C0_scrub2('org','zr')= 1.41958175646779E-6;
1699 C0_scrub2('org','Ru')=0;
1700 C0_scrub2('org','Tc')= 0.00210564852339331 ;
1701 C0_scrub2('org','Np_V')= 1.97627040801673E-6;
1702 C0_scrub2('org','Np_VI')= 0.00940561087499217;
1703 C0_scrub2('org','Np_IV')=0;
1704 C0_scrub2('org','hno2')=1.37918643304462;
1705 C0_scrub2('org','U_iV')=16.1111848794196;
1706 C0_scrub2('org','Pu_Iii')=0.0350416411564014;
1707 C0_scrub2('org',comp)=C_out.l('org',comp,'co_strip');
1708 psi.up(j,'scrub1_codec')=1;
1709 psi.lo(j,'scrub1_codec')=0;
1710 F.lo=0.23;
1711 F.up=0.6;
1712 D_is.up(step)=0.0025;
1713 N_IS.lo('u_strip')=1;
1714 q_corr_IS.up(j,step)=4;
```

```
1715 q_corr_IS.lo(j,step)=.05;
1716 q_IS.lo(j,step)=.05;
1717 q_IS.up(j,step)=10;
1718 C_In_HNO3_stage.lo(j,'HNO3','u_strip')=10;
1719 C_HNO3_fresh.lo('u_strip')=10;
1720 F.up=0.35;
1721 F.lo=0.26;
1722
1723 *load initialisation
1724 EXECUTE_LOADPOINT 'coex_novel_minlpF188_3.gdx' ;
1725
1726 f0=0.4;
1727 *change of bounds if initial TBP fraction changes (used if TBP fraction is c»
onstant and changed in a loop)
1728 C0_org('TBP',step)=f0*rho_TBP/MW_TBP*sf;
1729 C_org_eq_IS.up(j,h,comp,step)=f0*rho_TBP/MW_TBP*1000*1.1;
1730 C_org_eq_IS.up(j,h,'TBP',step)=f0*rho_TBP/MW_TBP*1000;
1731          C0_scrub2('org','TBP')=f0*973/266*1000-2*C0_scrub2('org','U_VI')-
2*C0_scrub2(»
'org','Pu_IV')-C0_scrub2('org','Hno3')-2*C0_scrub2('org','Hno3_2')-2*C0_scrub»
2('org','Zr')-2*C0_scrub2('org','Ru')-3*C0_scrub2('org','Tc')-2*C0_scrub2('or»
g','Np_VI')-2*C0_scrub2('org','Np_V')-2*C0_scrub2('org','Np_IV')-2*C0_scrub2(»
'org','HNO2')-4*C0_scrub2('org','U_IV')-3*C0_scrub2('org','Pu_III');
1732 C_org_IS.up(j,h,'U_VI',step)=C0_org('TBP',step);
1733 C_org_IS.up(j,h,'HNO3',step)=C0_org('TBP',step);
1734 C_org_IS.up(j,h,'TBP',step)=C0_org('TBP',step);
1735 C_org_IS.up(j,h,'Pu_III',step)=C0_org('TBP',step)/2;
1736 C_org_IS.up(j,h,'U_IV',step)=C0_org('TBP',step)/2;
1737 C_org_IS.up(j,h,'Pu_IV',step)=C0_org('TBP',step)/2;
1738 C_org_in_IS.up(j,h,comp,step)=C_org_IS.up(j,h,comp,step);
1739 C_out.up('org',comp,step)=C_org_IS.up('1','1',comp,step);
1740 C_in.up('org',comp,step)=C_org_IS.up('1','1',comp,step);
1741
```

```
1742 V_fresh_costrip.fx('1','co_strip')=0;
1743 V_fresh_costrip.fx('2','co_strip')=0;
1744 V_fresh_costrip.fx('6','co_strip')=0;
1745 *rminlp always vfreshcostrip=0
1746 V_fresh_costrip.fx(j,step)=0;
1747 N_elem_IS2.fx(j,'1',step)= 70;
1748 N_elem_IS2.up(j,'2',step)= 30;
1749 N_elem_IS2.lo(j,'2',step)= 4;
1750 N_elem_IS2.up(j,'3',step)= 30;
1751 N_elem_IS2.lo(j,'3',step)= 4;
1752
1753 *load initialisation
1754 EXECUTE_LOADPOINT '209_mm_minlp25.gdx' ;
1755 *variables fixed after first solution (in 209_mm_minlp25.gdx) to reduce compu»
tational times - same results or infeasible if not
1756 z.fx(j,step)=z.l(j,step);
1757 psi.fx(j,step)= psi.l(j,step) ;
1758 V_fresh_costrip.fx(j,step)= V_fresh_costrip.l(j,step) ;
1759
1760
1761
1762 option optcr=0.01;
1763
1764
1765
1766 *node limit
1767 Super7.nodlim=1e6;
1768 option optcr=.01;
1769
1770
1771 *according to the previous results (minlp and rminlp), bounds for the number »
of elements in each level, otherwise either infeasible or too long computatio»
nal times
```

1772 N_elem_IS2.lo(j,'1',step)= 10;
1773 N_elem_IS2.up(j,'2',step)= 30;
1774 N_elem_IS2.lo(j,'2',step)= 2;
1775 N_elem_IS2.up(j,'3',step)= 30;
1776 N_elem_IS2.lo(j,'3',step)= 2;
1777 N_elem_IS2.up(j,'1','main_extr_codec')= 70;
1778 N_elem_IS2.lo(j,'1','main_extr_codec')= 10;
1779 N_elem_IS2.lo(j,'2','main_extr_codec')= 2;
1780 N_elem_IS2.up(j,'2','main_extr_codec')= 15;
1781 N_elem_IS2.lo(j,'3','main_extr_codec')= 2;
1782 N_elem_IS2.up(j,'3','main_extr_codec')= 15;
1783 N_elem_IS2.up(j,'1','scrub1_codec')= 70;
1784 N_elem_IS2.lo(j,'1','scrub1_codec')= 10;
1785 N_elem_IS2.lo(j,'2','scrub1_codec')= 2;
1786 N_elem_IS2.up(j,'2','scrub1_codec')= 8;
1787 N_elem_IS2.lo(j,'3','scrub1_codec')= 2;
1788 N_elem_IS2.up(j,'3','scrub1_codec')= 8;
1789 N_elem_IS2.up(j,'1','comp_extr_codec')= 70;
1790 N_elem_IS2.lo(j,'1','comp_extr_codec')= 10;
1791 N_elem_IS2.lo(j,'2','comp_extr_codec')= 2;
1792 N_elem_IS2.up(j,'2','comp_extr_codec')= 6;
1793 N_elem_IS2.lo(j,'3','comp_extr_codec')= 2;
1794 N_elem_IS2.up(j,'3','comp_extr_codec')= 6;
1795 N_elem_IS2.up(j,'1','co_strip')= 70;
1796 N_elem_IS2.lo(j,'1','u_strip')= 10;
1797 N_elem_IS2.lo(j,'2','co_strip')=2;
1798 N_elem_IS2.up(j,'2','co_strip')= 6;
1799 N_elem_IS2.lo(j,'3','co_strip')= 2;
1800 N_elem_IS2.up(j,'3','co_strip')= 6;
1801 N_elem_IS2.up('4','1','u_strip')= 70;
1802 N_elem_IS2.lo('4','1','u_strip')= 10;
1803 N_elem_IS2.lo('4','2','u_strip')= 2;
1804 N_elem_IS2.up('4','2','u_strip')= 11;

```
1805 N_elem_IS2.lo('4','3','u_strip')= 2 ;
1806 N_elem_IS2.up('4','3','u_strip')= 11;
1807 N_elem_IS2.lo('6','2','u_strip')= 2;
1808 N_elem_IS2.up('6','2','u_strip')= 13;
1809 N_elem_IS2.lo('6','3','u_strip')= 2;
1810 N_elem_IS2.up('6','3','u_strip')= 13;
1811
1812
1813 solve Super7 using minlp minimizing total_ann_cost_plant;
1814 display psi.l, chi.l, C_in_HNO3_stage.l, total_ann_cost_plant.l, atc_cost_st»
ep.l, tub_cost_step.l, man_cost_step.l, oper_cost_step.l, Rec_HLW.l, Df.l, »
extract.l, Units_IS2.l, N_elem_IS2.l, v_inlet_fresh.l, v_inlet_prev.l, q_IS.l»
, Vdot_out.l, Vdot_IS2.l, c_fresh.l, C_in.l, C_out.l;
1815
```